A Comparison of the Biosynthesis of Indole-3-Acetic Acid and Phenylacetic Acid

by

Sam David Cook, Bsc (Hons.)

School of Biological Sciences

Submitted in fulfilment of the requirements for the degree Doctor of Philosophy

University of Tasmania November, 2017

Declaration of originality

This thesis contains no material which has been accepted for a degree or diploma by the University or any other institution, except by way of background information and duly acknowledged in the thesis, and to the best of my knowledge and belief no material previously published or written by another person except where due acknowledgement is made in the text of the thesis, nor does the thesis contain any material that infringes copyright.

Authority of access

This thesis may be made available for loan. Copying and communication of any part of this thesis is prohibited for two years from the date this statement was signed; after that time limited copying and communication is permitted in accordance with the Copyright Act 1968.

Statement of published works

The publishers of the papers comprising Chapter 3 hold the copyright for that content and access to the material should be sought from the respective journals. The remaining non-published content of the thesis may be made available for loan and limited copying and communication in accordance with the Copyright Act 1968.

Sam D. Cook
School of Biological Sciences
University of Tasmania
November 2017

List of published works

Cook SD, Nichols DS, Smith J, Chourey PS, McAdam EL, Quittenden L, Ross JJ (2016) Auxin Biosynthesis: Are the Indole-3-Acetic Acid and Phenylacetic Acid Biosynthesis Pathways Mirror Images? Plant physiology **171:** 1230-1241

Located in Chapter 3

S.D.C. conducted all experiments and interpreted the majority of the results, except for IAAld experiments; E.L.M. and L.Q. participated in *tar2-1* mutant experiments and conducted IAAld experiments; J.S. synthesized the D_5 phenylpyruvate; D.S.N. was responsible for the running and minor interpretation of UPLC-MS; P.S.C. provided material and contributed to maize-related results; S.D.C. and J.J.R. conceived the project and wrote the article with contributions from other authors.

Cook SD, Ross JJ (2016) The auxins, IAA and PAA, are synthesized by similar steps catalyzed by different enzymes. Plant Signaling & Behavior **11:** e1250993

Located in Chapter 3

S.D.C. and J.J.R. Contributed equally in the production of this short communication as an addendum to Cook et al (2016).

Statement of co-authorship

The following people and institutions contributed to the publication of work undertaken as part of this thesis:

Name and School: Sam D Cook, School of Biological Sciences
Name and institution: John J Ross, UTAS
Name and institution: David Nichols, UTAS (CSL)
Name and institution: Jason Smith, UTAS
Name and institution: Prem Chourey, U.S. Department of Agriculture
Name and institution: Erin McAdam, UTAS
Name and institution: Laura Quittenden, UTAS

Signed: _____

John J Ross
Supervisor
School of Biological Sciences
University of Tasmania

Signed: _____

Mark Hunt
Head of School
School of Biological Sciences
University of Tasmania

Acknowledgements

First and foremost, I would like to thank my supervisor and mentor, Adjunct Professor John J. Ross for his indefatigable support throughout this journey. Your attention to detail, ability to micro-manage, and your jolly, burning, and excitable nature have made my candidature one of the most exiting and fulfilling challenges I will ever experience. It has been a pleasure to learn from you.

Secondly I give my thanks to Dr Scott McAdam, whose research practices are inspiring and sometimes controversial, but never dull. Your passion for learning new things is second to none and your fire was essential to the completion of this thesis. My only regret is not engaging you sooner.

I would also like to extend my thanks to Associate Professor Jim Weller. While our collaboration didn't quite achieve fruition, it was a pleasure engaging with your brilliant regimented research style.

Perhaps most importantly I would like to thank my family, whose support has made this process bearable. Mum and Dad, I have not always been the easiest person to get along with, but know that I could never be who I am today without you. You support me unconditionally and I can never do enough to show you how much that means. Ellie and Sarah, whenever I was feeling down, I would always think of you two and it would smile. You are all more important to me than you know.

I also have to thank all of the friends that I have made over the past few years. The day-to-day support from those closest to you gives a sense of belonging and companionship and is the single most important thing for a successful PhD. Those from the crib table, from the gym, the bushwalks, the lunches, the nights on the town. Bryce, Tai, Sarah, Ariane, Louise, Chris, Freya, Alynn, Narissa, Kathi, Andrew, Jarrod, Franklin and everyone else. Thank you for your support and your distraction.

Thank you to those who have provided assistance in the lab and the glasshouse, as well as the office staff and those who have contributed to publications, Clancy, Jodie, Morgan, David, Noel, Stephen, Laura, Erin, Frances, Adam, Jackie, Jason, Michelle, Tracey and Jenny. Your assistance has been invaluable

Finally, I would like to thank the late Dr Sandra Davidson, for without her ‘cool’ attitude and remarkable patience, I would never have been inspired to pursue molecular biology. The world would be a better place if everyone saw it the way you did, Sandra. Rest in peace.

Abstract

The biosynthesis of the auxin, indole-3-acetic acid (IAA), has been well studied in recent years. It is now accepted that the indole-3-pyruvate (IPyA) pathway is the main IAA biosynthetic route and is responsible for the majority of IAA produced in plants. This pathway involves the transamination of the amino acid, tryptophan (Trp), to IPyA by the TAR (TRYPTOPHAN AMINOTRANSFERASE RELATED) enzymes, followed by the oxidative decarboxylation of IPyA to IAA by the YUCCA proteins.

Recently it has been suggested that the TARs and the YUCCAs are also responsible for the biosynthesis of a less well-studied auxin, phenylacetic acid (PAA). Specifically, it is proposed that the TARs convert a second amino acid, phenylalanine (Phe), to phenylpyruvate, and that the YUCCAs convert phenylpyruvate to PAA.

The work in this thesis addresses several aspects of the biosynthesis of PAA. Using isotopically labelled compounds, several techniques were developed and adapted to demonstrate isotopic labelling of putative PAA precursors. It is reported herein that Phe is metabolised to both phenylpyruvate and PAA in homogenised plant extracts as well as in intact plant systems, consistent with previous hypotheses.

Additional experiments also demonstrate that the putative intermediate, phenylpyruvate, can be converted to PAA, as well as back to Phe. These experiments couple the biosynthesis of amino acids (Phe) and auxins (PAA), which appear to share a common mechanism. The aromatic aminotransferases (ArATs) have been characterised in several genera and catalyse the reversible conversion of Phe to phenylpyruvate. Here, an ArAT sequence is isolated from the pea gene atlas as a candidate enzyme for the biosynthesis of PAA.

However, investigations into IAA biosynthetic mutants demonstrate that the TARs and the YUCs do not contribute significantly to PAA biosynthesis in pea, maize or *Arabidopsis*. These mutants display significantly altered IAA (or IPyA) levels, but the endogenous levels of PAA (or phenylpyruvate) are not different from their respective WTs. It is suggested that the conversion of Phe to PAA, via phenylpyruvate, may be functional in plants but is not catalysed by the enzymes of the IPyA pathway.

Analyses of the distribution of IAA and PAA in major land plant divisions suggest that both auxins are present in all land plants. Applying the above-mentioned metabolism experiments also reveals that the IPyA and phenylpyruvate pathways appear to be functional in all land plants. These findings are supported by genetic evidence from several gene databases, which demonstrate that the *TARs*, *YUCs* and *ArATs* are present in a range of these species. Additionally, investigations on the major IAA metabolic genes, the *DAOs*, the *GH3s* and the *UGTs*, reveals unique distributions across the land plants and suggests that the regulation of IAA content in derived species (e.g. angiosperms) is stronger than in members of basal lineages.

Finally, this thesis describes further characterisation of the *bushy* mutant of pea, which has reduced IAA and IPyA levels as well as a small reduction in endogenous phenylpyruvate level. In this thesis, the *bushy* locus is also mapped to the top of pea linkage group 1 where it is closely linked with (but not identical to) the genes encoding the aldehyde oxidases.

The culmination of this thesis demonstrates that the IAA biosynthetic machinery does not function extensively in the biosynthesis of PAA and that the two auxins have unique biosynthetic pathways that are conserved throughout the land plants.

Table of Contents

Chapter 1: An introduction to auxin biosynthesis and biology

1.1 The phytohormone auxin

Auxins are a class of phytohormones that are fundamentally required for growth and development of all plant species. Auxin biology has a long history extending back to the late 19th century. Auxins have, in some way, control over essentially all aspects of plant growth and development (Davies, 1995). On a cellular level, auxin regulates processes including growth, division, differentiation and meristematic activity. On a larger scale, auxin is required for development of regular shoot and root structures, floral development and patterning. It functions in tropisms, defence response, formation of symbioses and countless other processes.

There are currently three endogenous compounds classified as auxins; indole-3-acetic acid (IAA), 4-Cl-indole-3-acetic acid (4Cl-IAA), and 2-phenylacetic acid (PAA). In addition to these, several synthetic (halo- and nitro-) derivatives of these compounds also contain auxin activity (Pybus et al, 1959). The best-characterised auxin, IAA, is heavily regulated in plants by several key mechanisms; its biosynthesis (Korasick et al, 2013; Tivendale et al, 2014), the metabolism of IAA (including degradation/ conjugation) (Staswick et al, 2005; Korasick et al, 2013) and IAA transport (Zažímalová et al, 2010; Peer et al, 2011). Each of these regulatory mechanisms function together to maintain optimum auxin levels for plant growth and development.

This chapter describes the recent history of auxin biology, covering its biosynthesis, metabolism, and perception. In addition to IAA, background on the less well-characterised auxin, PAA is also presented here. The aim of this introduction is to provide the reader with a basic understanding of auxin

biology, which will be required to fully understand the concepts that underpin subsequent chapters.

1.2 Biosynthesis

Historically, it was thought that IAA was synthesised by any one of four proposed tryptophan- (Trp-) dependent pathways. Each of these is named after its primary intermediate, indole-3-pyruvate (IPyA), tryptamine (TAM), indole-3-acetamide (IAM), and indole-3-acetaldoxime (IAOx). The intricacies of these pathways are presented in Figure 1.1. While the IPyA pathway is now widely accepted as the predominant pathway in plants (Zhao et al, 2001; Mashiguchi et al, 2011; Won et al, 2011; Dai et al, 2013), there is still evidence that other pathways may contribute to IAA levels in specific tissues and species (Schmidt et al, 1996; Pollmann et al, 2003; Quittenden et al, 2009; Sugawara et al, 2009). Additionally, there is also evidence supporting a Trp-Independent pathway, which appears to function in Trp auxotrophs (Wright et al, 1991; Normanly et al, 1993) and which may play a large role in embryogenesis (Wang et al, 2015).

1.2.1 The IPyA pathway

The IPyA pathway is now regarded as the primary auxin biosynthetic route for all plants (Zhao, 2012; Tivendale et al, 2014). This two-step pathway involves the transamination of Trp to IPyA followed by the oxidative decarboxylation of IPyA to IAA. These two steps are catalysed by the TAA1 (Tryptophan aminotransferase of *Arabidopsis* 1) and YUC (YUCCA, named based on the overexpression phenotype) proteins respectively (Stepanova et al, 2008; Tao et al, 2008; Mashiguchi et al, 2011; Won et al, 2011). In early work, IPyA was proposed as a key component of auxin biosynthesis (Cooney and Nonhebel, 1991). However, the study of the IPyA pathway has been infamously difficult as this intermediate is known to be labile and readily breaks down to IAA at room temperature (Tam and Normanly, 1998). More recently, a combination of mutant, genetic, and molecular studies has shed light on the importance of this pathway in IAA biosynthesis.

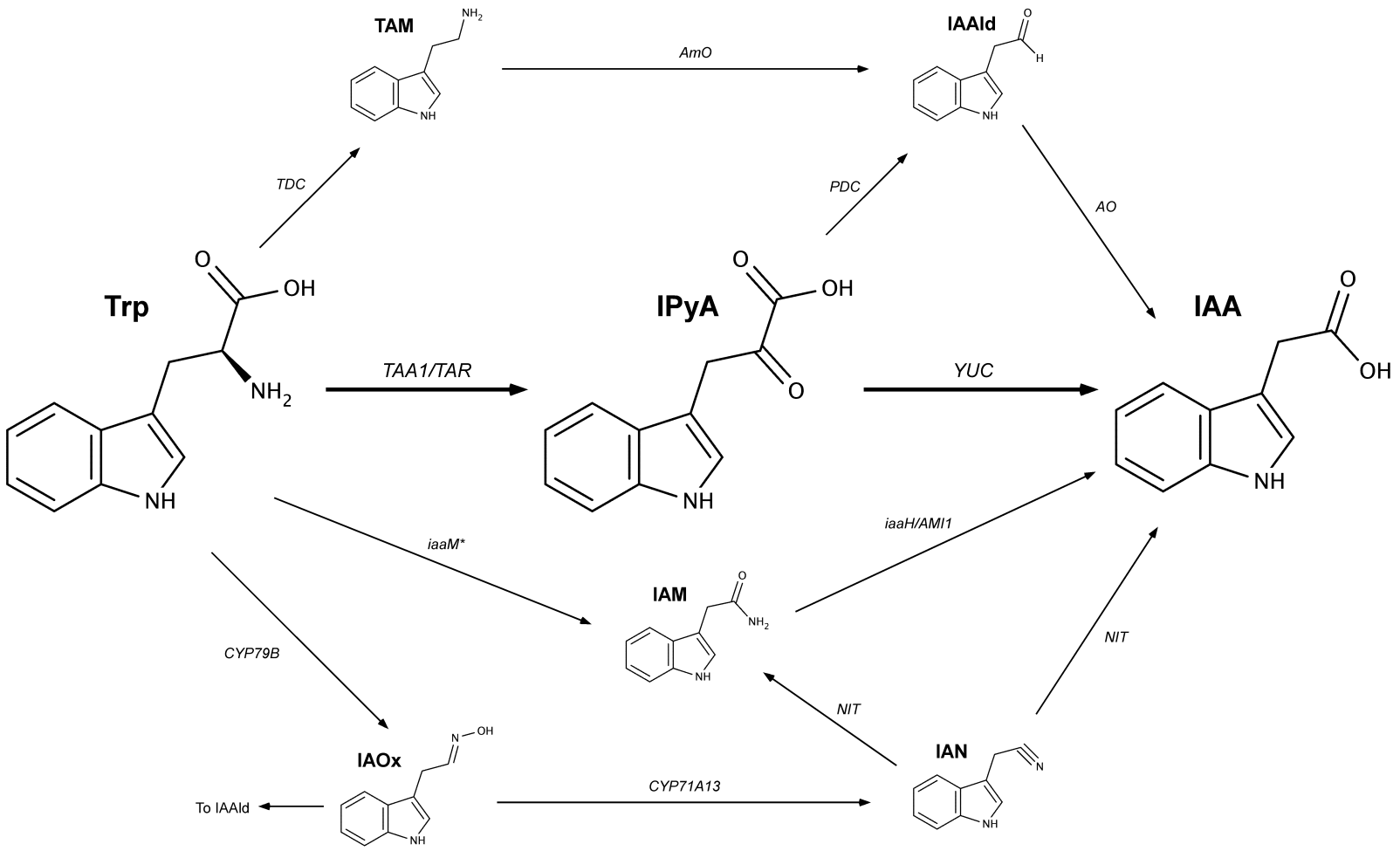

Figure 1.1 Tryptophan-dependent auxin biosynthetic pathways showing chemical abbreviations in bold: Trp (Tryptophan), TAM (Tryptamine), IAAld (indole-3-acetaldehyde), IPyA (indole-3-pyruvic acid), IAA (indole-3-acetic acid, IAM (indole-3-acetamide), IAOx (indole-3-acetaldoxime), and IAN (indole-3-acetonitrile). Genes encoding enzymatic proteins are presented in italics: *TDC* (Trp decarboxylase), *AmO* (amine oxidase), *TAA1/ TAR* (Trp aminotransferase), *PDC* (pyruvate decarboxylase), *YUC* (flavin monooxygenase), *iaaM* (Trp-2- monooxygenase), *iaaH/AMI1* (IAM hydrolase), *CYP79B/ CYP71A13* (Cytochrome P450 monooxygenase), and NIT (nitrilase). Arrows indicate primary reaction direction. * Indicates uncharacterised homologs in plants.

TAA1 was originally identified through analysis of the *Arabidopsis* shade avoidance mutant, *sav3* (*Shade Avoidance 3*)(Stepanova et al, 2008; Tao et al, 2008). The characterisation by Stepanova and Tao (2008) showed that Trp could be converted to IPyA by the *TAA1* gene product in vitro. These publications also identified four other members of this family, known as *Tryptophan Aminotransferase Related1-4* (*TAR1-TAR4*), although TAR3 and TAR4 are more closely related to alliinases (Stepanova et al, 2008; Tao et al, 2008). While this characterization is relatively recent, the inclusion of this specific step, the transamination of Trp to IPyA, was proposed much earlier (Cooney and Nonhebel, 1991). This step has also been confirmed in other species through in vitro studies in pea (PsTAR1 and PsTAR2) (Tivendale et al, 2012) and through mutant analyses in maize (Chourey et al, 2010; Phillips et al, 2011).

Single gene mutations in members of the *TAA1/ TAR* family do not always present obvious phenotypes (Stepanova et al, 2008). This can be attributed to the genetic redundancy in these gene families, which is understandable given the integral role that auxin plays in growth and development (Stepanova et al, 2008; Tivendale et al, 2012). In *Arabidopsis*, the *wei8-1* mutant (which is allelic to *sav3*) is mildly insensitive to ethylene in roots. However, when *AtTAR2* is also repressed on this background, the root meristem is completely lost (Stepanova et al, 2008). This is also manifest in the floral meristem, which prevents formation of normal reproductive tissue in these lines.

In pea, there are three characterized *TAR* genes, *PsTAR1-3* (Tivendale et al, 2012). Recent publication of the ‘Pea RNA-Seq gene atlas’ has also identified a fourth *TAR* in pea (*PsTAR4*, PsCam057706), although this is not yet annotated as such (Alves-Carvalho et al, 2015). *PsTAR2* is expressed specifically in seeds and the *tar2-1* mutation causes large reductions in the levels of both IAA and 4-Cl-IAA (Tivendale et al, 2012). These diminished auxin levels result in reduced seed size and cause a dimpled phenotype (McAdam et al, 2017a).

The second step in this pathway involves the oxidative decarboxylation of IPyA to IAA, catalysed by the YUC/ YUCCA proteins (Mashiguchi et al, 2011; Won et al, 2011; Dai et al, 2013). While YUCCA has been implicated in auxin biosynthesis for some time (Zhao et al, 2001), it was not until much later that the YUC enzymes were placed in the same pathway as the TARs (Strader and Bartel, 2008; Zhao, 2010; Stepanova et al, 2011). In fact, the *Zea mays vt2* (*vanishing tassel2*) *spi1* (*sparse inflorescence 1*) double mutant presented in Phillips et al (2011) was the first published TAR/ YUC double mutant. While the *vt2* and *spi1* mutations already cause large defects in maize development (Gallavotti et al, 2008; Phillips et al, 2011), the double mutant phenotype is similar to *vt2* and IAA levels are not further depleted. These analyses provided strong evidence that the TAR and YUC enzymes function in the same pathway.

Subsequent analyses involving the expression of single YUCs using recombinant protein expression systems have reportedly shown that both AtYUC2 and AtYUC6 are capable of converting IPyA to IAA in vitro (Mashiguchi et al, 2011; Dai et al, 2013). However, this function is still yet to be shown outside of *Arabidopsis*. Similar to the *TAA1/ TAR* mutants, individual *YUC* mutants do not produce obvious phenotypes (Cheng et al, 2006). In fact, only in high order loss-of-function mutants are phenotypes obvious (Cheng et al, 2006, 2007; Mashiguchi et al, 2011; Won et al, 2011; Dai et al, 2013). This is understandable, as the extent of redundancy in the *YUC* family is greater than that of *TAA1/ TAR*, with *Arabidopsis* containing 11 classified *YUC* genes with overlapping expression (Zhao et al, 2001; Cheng et al, 2006). Overexpression of *YUC* genes results in high auxin phenotypes in several species (Zhao et al, 2001; Tobeña-Santamaria et al, 2002; Cheng et al, 2006, 2007; Expósito-Rodríguez et al, 2007) and as such *YUC* mutants are commonly used in auxin research.

In other species, single *YUC* mutants confer a range of phenotypes. In maize, a reduction in the levels of IAA in the *de18* (*defective endosperm18*) mutant, which lacks functional ZmYUC1 protein, produces endosperm that is reduced in size and cell number (Bernardi et al, 2012). Inflorescence

development is also altered in the *spi1* mutants, which contain reduced branches and spikelets, which are also reduced in size (Gallavotti et al, 2008; Phillips et al, 2011). In *Petunia hybrida*, the *floozy* mutant displays retarded growth, leaf epinasty and reduced apical dominance (Tobeña-Santamaria et al, 2002). Similarly, in pea, the *crispoid-4* mutant contains altered leaf vasculature, similar to that of *floozy* (McAdam et al, 2017b) as well as altered floral patterning.

1.2.2 The TAM pathway

The TAM (tryptamine) pathway was characterised by the conversion of Trp to tryptamine (TAM) by a *Trp decarboxylase*, followed by conversion to n-hydroxyl-tryptamine (NHT) by the YUCCA proteins (Zhao et al, 2001; LeClere et al, 2010). NHT would then be converted directly to indole-3-acetaldehyde (IAAld) or to IAAld through indole-3-acetaldoxime (IAOx) via a series of unknown steps (Sugawara et al, 2009; LeClere et al, 2010). IAAld is subsequently converted to IAA by members of the *aldehyde oxidase* (*AO*) gene family, which also function in abscisic acid (ABA) biosynthesis (Sekimoto et al, 1998; Seo et al, 1998).

Early experiments in tomato (*Solanum lycopersicum*) investigated the metabolism of D_2O and the subsequent label dilution of the TAM pathway. These experiments showed that TAM continues to accumulate label despite diminishing accumulation in both Trp and IAA (Cooney and Nonhebel, 1991). This suggests that TAM is not intricately involved in IAA biosynthesis in this species. Similarly, overexpression of Trp decarboxylase in tobacco (*Nicotana tabacum*) produced large amounts of TAM in transformed lines (Songstad et al, 1990). However, even with this massive accumulation (250 times greater than the control), IAA levels were unchanged (Songstad et al, 1990). The TAM pathway also does not appear to function in pea seeds (Tivendale et al, 2010). Although, an amine oxidase has previously been characterised in the conversion of TAM to IAAld (McGowan and Muir, 1971), and metabolism of exogenously applied D_5 TAM results in dilution of the endogenous pools of IAAld and IAA in pea roots (Quittenden et al, 2009).

Prior to their inclusion in the IPyA pathway, the YUCCA proteins were implicated in the conversion of TAM to n-hydroxytryptamine (NHT)(LeClere et al, 2010). However, investigations in pea showed that NHT was not present in that species, despite label dilution of both TAM and IAA (Quittenden et al, 2009; Tivendale et al, 2010). The in vitro formation of NHT was also documented and proposed for maize (LeClere et al, 2010). However, as with Zhao et al (2001) this analysis lacked a comparable NHT standard, and subsequent analysis of authentic NHT found that the two spectra were not identical (Tivendale et al, 2010). When taken together, these results suggest that NHT is not involved in auxin biosynthesis, if present in plants at all.

The contribution of IAOx to this pathway also appears insignificant as metabolism experiments in *Arabidopsis* show that $^{15}N_2$ TAM was not converted to $^{15}N_2$ IAOx (Sugawara et al, 2009). Further investigations on the levels of IAOx in other species also suggest that IAOx is specific to the family Brassicaceae, as a precursor to the indole-glucosinolates (Mikkelsen et al, 2000). Since both of the proposed metabolites of TAM (NHT and IAOx) did not accumulate label, it is unlikely that this pathway functions in IAA biosynthesis in a significant way, although residual IAA may be synthesised through Trp → TAM → IAAld → IAA in some species (Quittenden et al, 2009).

1.2.3 The IAOx pathway

In the Brassicaceae, IAOx is a precursor to the indole-glucosinolates (Mikkelsen et al, 2000). It has been suggested that IAOx is converted to either IAAld (Rajagopal and Larsen, 1972) or indole-3-acetonitrile (IAN) (Helmlinger et al, 1985; Ludwig-Müller and Hilgenberg, 1990). IAAld and IAN would then be converted to IAA by the *AOs* (Sekimoto et al, 1998; Seo et al, 1998) and the *nitrilases* (*NIT1-3*) (Schmidt et al, 1996; Normanly et al, 1997), respectively.

The CYP79B2 and CYP79B3 proteins are able to catalyse the direct formation of IAOx from Trp in vitro (Hull et al, 2000; Mikkelsen et al, 2000).

Overexpression of these transcripts also results in a small accumulation of both IAA and its potential precursor, IAN (Zhao et al, 2002). However, while double *cyp79b2 cyp79b3* mutants do not produce detectable levels of IAOx (Sugawara et al, 2009), have reduced IAN, and almost no indolic glucosinolates (Zhao et al, 2002), the levels of IAA are not reduced in these lines (Sugawara et al, 2009).

Additionally, the *sur2* (*superroot 2*) mutant contains a non-functional CYP83B1 protein (Bak et al, 2001), responsible for directing IAOx towards the indole-glucosinolate pathway (Delarue et al, 1998). These mutants accumulate large levels of IAA and IAAld (Delarue et al, 1998; Barlier et al, 2000), presumably due to the redirection of IAOx towards IAA, and display high auxin phenotypes. This suggests that while IAOx is normally destined for the indole-glucosinolate pathway, metabolic flux can be directed towards IAA biosynthesis if indole-glucosinolate formation is blocked

Both IAN and IAAld levels can be altered in mutants when regular biological development is altered (Ludwig-Müller and Hilgenberg, 1990; Delarue et al, 1998; Barlier et al, 2000; Bak et al, 2001). A *CYP71A13* monooxygenase is responsible for the conversion of IAOx to IAN (Nafisi et al, 2007), although the enzymes required for the synthesis of IAAld (from IAOx) are unknown. While the conversion of these two compounds to IAA has been demonstrated (Schmidt et al, 1996; Normanly et al, 1997; Sekimoto et al, 1998), IAN is not readily detected outside of the Brassicaceae, similar to IAOx, and the *nitrilases* are also not widespread (Schmidt et al, 1996). While IAAld does appear to be ubiquitous, it is not clear whether it actually functions as an intermediate in any pathway, despite accumulating label from multiple sources in metabolism experiments (Quittenden et al, 2009; Mashiguchi et al, 2011).

Taken together, all of these investigations suggest that, even though IAOx is a potential route to IAA in the Brassicaceae, any IAOx-derived IAA is, at best, a minor component under normal growth conditions.

1.2.4 The IAM pathway

The IAM pathway was originally transposed to plants from a bacterial IAA biosynthetic pathway, as the intermediate, IAM, has been detected in numerous species (Pollmann et al, 2002; Sugawara et al, 2009; Lehmann et al, 2010). This two-step pathway involves conversion of Trp to IAM by a TRYPTOPHAN-2-MONOOXYGENASE (*iaaM*), followed by a conversion of IAM to IAA by an IAM HYDROLASE (*iaaH*)(Lehmann et al, 2010). Both *iaaM* and *iaaH* are widespread in bacteria, although no direct homologs of *iaaM* have been identified in plants and there are no known mutants with altered IAM levels (Spaepen et al, 2007; Lehmann et al, 2010).

In *Arabidopsis*, IAM is largely derived from IAOx (Sugawara et al, 2009), although this dependence would restrict the presence of IAM to the Brassicaceae. Contrary to this, IAM has been detected in a number of species (Sugawara et al, 2009), which suggests that alternative synthesis of IAM may occur, likely through a plant *iaaM-like* gene product. Enzymatic assays on purified plant extracts have shown that feeding deuterium labelled Trp can result in label dilution of IAM, although no *iaaM* homolog is known (Pollmann et al, 2009).

Interestingly, despite the absence of an obvious *iaaM* homolog in plants, the second step in this pathway, encoded by *iaaH*, shares homology with the *AMI1* (*AMIDASE1*) gene family, which appears to be widespread in the plant kingdom (Pollmann et al, 2003; Pollmann et al, 2006; Lehmann et al, 2010). Pollmann et al (2009) also conducted feeding studies using deuterium labelled IAM, and found significant dilution of endogenous IAA with the labelled species. This behaviour was attributed to an ‘IAA synthase’ which contains the function of both *iaaM* and *iaaH*. However, no enzyme was offered as a candidate for this role (Pollmann et al, 2009). Further, it was also found that IAM is not converted to IAA in pea seeds (Quittenden et al, 2009), and that the endogenous species was not detectable in this tissue. All of these results suggest that this pathway may function in *Arabidopsis* and the

Brassicaceae, but the enzymes involved, if they are present, do not contribute substantially to IAA production.

1.2.5 The tryptophan-independent pathway

Trp independent auxin biosynthesis has long been predicted in plants (Baldi et al, 1991; Wright et al, 1991; Michalczuk et al, 1992; Normanly et al, 1993; Rapparini et al, 1999; Epstein et al, 2002; Sztein et al, 2002). Early studies on the maize *orange pericarp1* (*orp1*), a Trp auxotroph deficient in *Trp synthase β* (*TSB*), revealed that these mutants accumulate total IAA despite being unable to synthesise Trp (Wright et al, 1991). This is also the case in *Arabidopsis*, where several mutants in Trp biosynthesis; *trp2-1* (*TSB*) and *trp3-1* (*Trp synthase α*, *TSA*) accumulated total IAA (Normanly et al, 1993). Although free levels were unaltered, and specific light conditions were required to elicit this effect, this suggests that the branch point for Trp independent synthesis lies upstream of the *TSB* and *TSA* gene products.

The *trp1-1* mutant (anthranilate phosphoribosyl transferase, *PAT*) blocks the initial conversion of anthranilate to indole-3-glycerol phosphate in the Trp biosynthetic pathway (Last and Fink, 1988; Ouyang et al, 2000). In these mutants, both IAA and Trp are decreased, suggesting that Trp-independent synthesis branches downstream of indole-3-glycerol. Indole synthase (*INS*) converts indole-3-glycerol to indole and has been suggested as the first step in the Trp-independent pathway (Wang et al, 2015). Interestingly, in the *ins-1* mutant, free IAA levels were depressed, which would indicate that Trp-independent IAA biosynthesis does contribute to endogenous IAA. Further, when the IPyA pathway is also repressed in the *ins-1 wei8-1* double mutant, the IAA reduction is greater than either single mutant (Wang et al, 2015). However, there is strong opposition to the role of *INS* in Trp-independent IAA biosynthesis, as *INS* is restricted to the Brassicaceae and a closely related sister clade (Nonhebel, 2015).

1.3 Auxin metabolism/ catabolism

Auxin levels are also controlled by their catabolism and conjugation through several interlinked pathways (Figure 1.2)(Staswick et al, 2005; Korasick et al,

2013; Stepanova and Alonso, 2016). Auxin conjugates exist in several different forms, with IAA being bound to sugars by ester linkages, or to amino acids by amide linkages (Jackson et al, 2001; Jackson et al, 2002; Tanaka et al, 2014). Alternatively, IAA catabolism also functions to regulate free levels directly through oxidation (Ray, 1958; Östin et al, 1998). Conjugates are thought to exist as storage products for IAA, which could be rapidly hydrolysed to increase free IAA levels when required (Cohen and Bandurski, 1982; Bandurski et al, 1995; Normanly et al, 1997). In this model, conjugation of IAA allows plants to bypass the (relatively) expensive process of de novo hormone synthesis. This also affords extensive control over the level of free IAA. There are three main enzymes by which free IAA levels are controlled, the *GH3s* (Hagen and Guilfoyle, 1985; Hagen and Guilfoyle, 2002), the *DAOs* (Mellor et al, 2016; Porco et al, 2016; Zhang et al, 2016) and the *UGTs* (Szerszen et al, 1994; Jackson et al, 2001). Each is discussed below.

1.3.1 Amide conjugation is catalysed by the GH3s

The *GH3s* were first characterised as auxin inducible genes that encode IAA amido synthetases, and are responsible for the amide conjugation of IAA to numerous amino acids (Hagen and Guilfoyle, 1985; Hagen and Guilfoyle, 2002; Rampey et al, 2004; Staswick et al, 2005). The *GH3s* (as well as the *SAURs* and *Aux/IAAs*) are known as early auxin response genes (Hagen and Guilfoyle, 2002). The transcription of these genes occurs within minutes of changes in auxin levels and provides plants with a rapid response system. The *GH3* family contains 19 members in *Arabidopsis*, of which seven show amido synthetase activity on IAA (Staswick et al, 2005). The remaining members appear to conjugate other phytohormones or currently have unknown functions (Staswick et al, 2002). Many of the IAA amide conjugates exist as storage forms and function in the homeostasis of free IAA levels through hydrolysis by amido hydrolases (LeClere et al, 2002).

While amide conjugation to most moieties is reversible (LeClere et al, 2002), none of the characterised amido-hydrolases use IAA- aspartate (Asp) or IAA-glutamate (Glu) as substrates (Rampey et al, 2004). This is consistent with evidence that IAA-Asp and IAA-Glu are components of an auxin catabolic

pathway (Normanly et al, 1997; Ljung et al, 2002; Staswick et al, 2005). Interestingly, IAA-Asp and IAA-Glu (as well as other amide conjugates) have highly variable profiles between species (Bajguz and Piotrowska, 2009). In *Arabidopsis*, these catabolites only account for 1% of total IAA levels (Tam et al, 2000), even though 90% of IAA is present in conjugated form (Tam et al, 2000; Ljung et al, 2002).

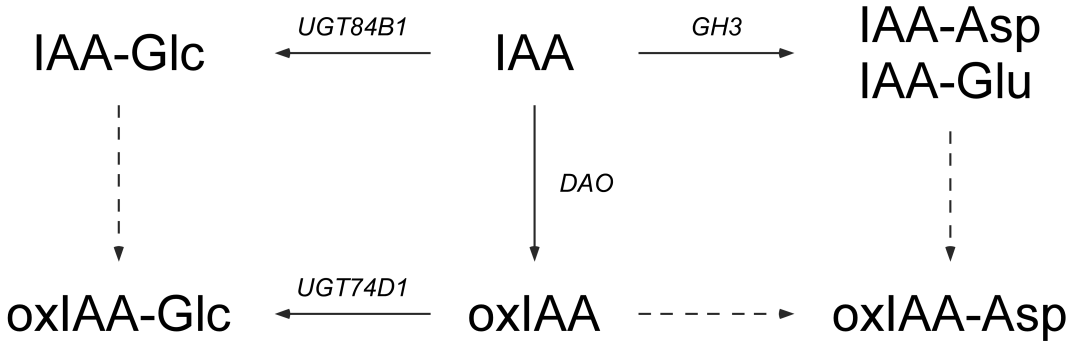

Figure 1.2 IAA metabolic pathways showing ester conjugation by the UGTs, amide conjugation by the GH3 amido synthetases and oxidation by the DAOs. oxIAA and IAA-Glc can be further converted to oxIAA-Glc by UGT74D1 and an as yet undiscovered mechanism, respectively. oxIAA and IAA-Asp can also be converted to oxIAA-Asp by unknown mechanisms. Arrows indicate direction of reactions and dashed lines indicate uncharacterised reactions.

1.3.2 The DAOs are responsible for IAA catabolism

It has been known for some time that the oxidation of IAA is the primary route of auxin catabolism (Ray, 1958), although these enzymes have only recently been identified (Mellor et al, 2016; Porco et al, 2016; Zhang et al, 2016). There are two characterised *DAO* (*DIOXYGENASE FOR AUXIN OXIDATION*) genes in *Arabidopsis,* which have distinct expression profiles (Zhang et al, 2016). The DAO proteins have been shown to convert IAA to oxIAA (2-oxoindole-3-acetic acid) (Zhao et al, 2013; Mellor et al, 2016; Porco et al, 2016; Zhang et al, 2016). Preventing the oxidation of IAA, as in the *dao1-1* mutant, causes a dramatic increase in the levels of IAA-Asp and IAA-Glu, yet, IAA levels remain normal, indicative of strong homeostatic control by the *GH3s* (Porco et al, 2016). Despite this, the *dao1-1* mutants still possess high auxin phenotypes such as increased hypocotyl length and

cotyledon size, increased lateral root density, and reduced fertility (Porco et al, 2016; Zhang et al, 2016). Interestingly, these plants have increased branching and reduced apical dominance, which are typically associated with low auxin.

1.3.3 Ester conjugation by the UGT gene family

The *UGTs* are a class of *UDP glucosyltransferases* that catalyse the conjugation of IAA to uridine 5'-diphosphate-glucose (UPG) forming the 1-O-indole acetyl glucose ester (IAA-Glc) (Szerszen et al, 1994; Jackson et al, 2001). There are between 107-120 UGTs in *Arabidopsis*, some of which catalyse the glucosylation of numerous plant hormones using UPG as a substrate (Jin et al, 2013; Tanaka et al, 2014). However, only *UGT84B1* appears to use IAA preferentially (Jackson et al, 2001; Jackson et al, 2002; Tanaka et al, 2014). This reaction is also likely to be reversible, with concentrations of either end product determining the direction of the reaction (Jackson et al, 2002). Another member of this family, *UGT74D1*, is reported to convert oxIAA to its glucosyl ester, although is also active on IAA (Tanaka et al, 2014). The exact role of the conjugates, beyond temporary storage is unclear. However, the genes for conjugation/ deconjugation have diverse expression and function, which suggests an important role in IAA homeostasis.

1.4 Auxin signalling/ perception

The auxin signalling and perception pathway is quite complex and involves gene families that are extensive and diverse (Quint and Gray, 2006). Auxin signalling is mediated by the E3 ubiquitin ligase complex, $SCF^{TIR1/\ AFB}$ (Zheng et al, 2002; Dharmasiri et al, 2005; Petroski and Deshaies, 2005). This complex contains several elements and targets Aux/IAA for degradation by the 26S proteasome (Gray et al, 2001; Quint and Gray, 2006). TIR1/ AFBs (*TRANSPORT INHIBITOR RESPONSE1/ AUXIN SIGNALLING F-BOX)*(Ruegger et al, 1998; Dharmasiri et al, 2005) are F-Box proteins responsible for the detection of particular residues on Aux/ IAA (Gray et al, 2001; Dharmasiri et al, 2005). The TIR1/ AFB F-Box proteins also interact with ASK1 (*ARABIDOPSIS SKP1-LIKE*), a structural component of the

$SCF^{TIR1/\ AFB}$ complex which itself binds to CUL1 (*CULLIN 1*) (Zheng et al, 2002). CUL1 is conjugated to the RUB1 (*Related to ubiquitin1)* E2 ligase (Del Pozo and Estelle, 1999; Dharmasiri et al, 2003) in an RBX1 (*RING BOX1 binding enzyme1*) dependent manner (Gray et al, 2002). This conjugation activates the E3 complex and ubiquitinates Aux/ IAAs for degradation (Gray et al, 2001; Gray et al, 2002).

The Aux/ IAAs, in the presence of low auxin, bind to particular residues of ARFs (Auxin Response Factors) (Guilfoyle and Hagen, 2007). ARFs themselves identify and bind to specific nucleotide sequences in promoter regions of auxin regulated genes (Dharmasiri et al, 2003; Kepinski and Leyser, 2005). There are numerous ARFs, which can be classed as either repressors or promoters of transcription (Ulmasov et al, 1999; Tiwari et al, 2003; Guilfoyle and Hagen, 2007). The regions that the ARFs bind to are known as AuxREs (Auxin Response Elements) and are highly conserved (Ulmasov et al, 1999). However, the N and C terminals of many ARFs vary considerably, which may suggest an extensive control network (Okushima et al, 2005).

1.5 Phenylacetic acid

Phenylacetic acid (PAA) is underwhelmingly characterised in plants, despite its wide distribution (Abe et al, 1974; Wightman et al, 1980; Wightman and Lighty, 1982; Schneider and Wightman, 1986; Korasick et al, 2013; Žižková et al, 2016). While PAA exhibits auxin activity (Abe et al, 1974; Milborrow et al, 1975), this is lower than IAA in many tissue types (Milborrow et al, 1975; Wightman and Lighty, 1982; Schneider et al, 1985; Ludwig-Müller and Cohen, 2002; Piotrowska-Niczyporuk and Bajguz, 2014; Sugawara et al, 2015). While the activity of PAA has not been as extensively tested as IAA, it is more effective at promoting growth in pea root primordia and lateral root induction (Wightman et al, 1980; Schneider et al, 1985). PAA is often present at higher levels than that of IAA, suggesting that it plays a physiologically relevant role in plant growth and development (Wightman and Lighty, 1982; Schneider et al, 1985; Schneider and Wightman, 1986; Sugawara et al,

2015). Despite decades of research on the biology of IAA, research on PAA is comparatively scant.

PAA biosynthesis has previously been suggested to occur through either transamination or decarboxylation of the amino acid Phe (Stafford and Lewis, 1979; Taylor and Wightman, 1987). The respective end products (phenylpyruvate and phenylethylamine) would then be converted to phenylacetaldehyde (PAAld) and then to the auxin PAA. The recent elucidation of the IAA biosynthetic pathway (Stepanova et al, 2008; Tao et al, 2008; Mashiguchi et al, 2011; Won et al, 2008) has stimulated interest in the biosynthesis of PAA (Sugawara et al, 2015). The precursor, phenylpyruvate, has been demonstrated as a substrate for *Arabidopsis* YUCCA proteins in vitro (Mashiguchi et al, 2011; Dai et al, 2013). In these experiments, phenylpyruvate was used as a substitute for the labile IPyA, which non-enzymatically degrades to IAA (Tam and Normanly, 1998). This has led to the proposition that YUCCA proteins may catalyse the conversion of phenylpyruvate to PAA, in addition to their role in IAA biosynthesis.

Interestingly when the TAA1 protein was characterised, in vitro assays also identified Phe as a substrate, even though its K_m (Michaelis constant) is more than 30 times that of Trp (Tao et al, 2008). Recent investigations on *wei8-1* (*taa1*) in *Arabidopsis* also show that PAA levels are reduced when the TAA1 protein is knocked out (Sugawara et al, 2015). However, this difference was relatively small when compared with the reduction in the levels of IAA.

Contrary to this, investigations on the level of PAA in high order *yuc1 yuc2 yuc6* mutants show no reductions in the levels of PAA, despite a 51% reduction of IAA in the absence of three *Arabidopsis* YUC proteins (Sugawara et al, 2015). However, in the same study, overexpression of YUC genes resulted in large accumulations of both IAA and PAA conjugates, suggesting some biological activity in vivo. Given the contradictory evidence presented on the role of TAA1/ TAR and YUC in PAA biosynthesis it is important to clarify these findings in auxin biosynthetic mutants from other species.

1.6 Overview

This thesis aims to provide an enhanced understanding of the biosynthesis of phenylacetic acid. The investigations within address several aspects of auxin biology and compare the well-characterised IAA biosynthetic pathway with that of PAA. These studies are an important step towards understanding how auxins, as a group, contribute towards the growth and development of all plants.

While *Arabidopsis* has been used extensively to develop our understanding of auxin biology, it is important to expand our knowledge to other species. To achieve this, Chapter 3 and Chapter 4 use the model species, *Pisum sativum*, to explore the effects of IAA biosynthetic mutations on the biosynthesis of PAA. The recent characterisation of *crd-4* (*crispoid-4*) as a mutation in the *PsYUC1* genetic sequence, and the mutant lines for *PsTAR1*, *PsTAR2* and *PsTAR3* enable analysis of auxin biosynthesis in pea.

It is also important to understand how auxin biosynthesis, as we know it, has come to be. Chapter 5 addresses the evolution of IAA and PAA, as well as their biosynthetic pathways and utilises representative species from all major divisions of the land plants. The presence of auxin biosynthesis is demonstrated through metabolism experiments and is correlated with a comprehensive analysis of auxin biosynthetic and metabolic gene families.

Finally, Chapter 6 attempts to map and characterise the *bushy* mutant in pea. The *bushy* locus is located in a region containing extensive signalling components, and using the strong synteny between pea and *Medicago truncatula*, several candidates are proposed that may explain the curious *bushy* phenotype. The *bushy* mutant is also used to understand the effects of mutations in auxin signalling and to demonstrate that the biosynthesis of PAA and IAA utilize separate mechanisms.

This thesis addresses several gaps in the literature. Since PAA biosynthesis has recently been re-addressed, it is important to authenticate suggestions

by other research groups on the mechanisms of PAA biosynthesis (Sugawara et al, 2015). It is also important to revise the evolutionary understanding of IAA biosynthesis and incorporate PAA into our explanations for the growth and development of land plants (Yue et al, 2014; Turnaev et al, 2015; Wang et al, 2016). Investigating PAA also provides a more holistic understanding of auxin biology and is essential to understand how auxin synthesis and metabolism is controlled in plants. These analyses will enhance our understanding of auxin biosynthesis for both IAA and PAA.

Chapter 2: General Materials and Methods

This Chapter outlines all materials and methods common to multiple experimental chapters. Specific adjustments to any of these processes are mentioned in their respective chapters.

2.1 Chemicals

The following standards were obtained from Sigma-Aldrich: $^{13}C_2$ phenylacetic acid, D_5 tryptophan, D_5 phenylalanine, phenylpyruvate, phenylethanol, phenylethylamine, phenylacetaldehyde and phenylacetonitrile. $^{13}C_6$ indole-3-acetic acid was obtained from Cambridge Isotope Laboratories, phenylacetamide was sourced through Santacruz biology, and D_2 tryptophol and D_4 4-Cl-indole-3-acetic acid were synthesised as previously described (Quittenden et al, 2009; Tivendale et al, 2012).

2.2 Metabolism experiments

For hydroponic experiments, pea seeds were sterilised briefly with 1% bleach and rinsed thoroughly with sterile distilled water. Seeds were planted in sterile gravel: vermiculite mix (50:50) topped with vermiculite. Seeds were watered daily with Milli-Q grade water and grown at 25°C with a 16 hour photoperiod. Six day old seedlings were transferred to 50 mL falcon tubes containing full strength MS (Sigma-Aldrich), supplemented with D_5 phenylalanine or D_5 tryptophan at concentrations of 0 mM, 10 mM, 50 mM, 100 mM. The falcon tubes were covered in black plastic to simulate dark, and the taproot of each seedling was inserted into a small 5 mm opening, up to the hypocotyl. Seedlings were grown for a further seven days under the same conditions with frequent wetting of the collar of the hypocotyl to prevent drying. Seedlings were removed from the solution and excess liquid was removed. Seedling fresh weight was recorded and hormones were extracted

as in Chapter 2.3. *m/z* values corresponding to deuterated (D_5) phenylpyruvate or D_5 PAA were selected and their products analysed following fragmentation. The spectra obtained were compared with those from D_5 phenylpyruvate and $^{13}C_2$ PAA standards.

For cell-free metabolism experiments, approximately 100 mg of tissue was harvested into 1.5 mL Eppendorf tubes containing a tungsten-carbide bead. Samples were frozen in liquid Nitrogen and tissue was homogenised using a Tissuelyser (Qiagen) at 30 frequency until homogenous. 1 mL of 100 µM D_5 Trp or 100 µM D_5 Phe in 50 mM sodium phosphate buffer (pH 7.0) was added to samples. Control reactions contained only 50 mM sodium phosphate buffer (pH 7.0). Reactions were incubated for 24 hours at room temperature after which the reaction mixture and any debris was transferred to a 15 mL falcon tube. Reactions were immediately terminated with the addition of 2 mL MeOH (final concentration 66% MeOH) and 500 µL aliquots were taken for stabilisation of labile precursors (Chapter 2.6). Remaining reaction mixtures were stored at -20ºC overnight, or until required for free (Chapter 2.4) or total (Chapter 2.5) hormone analyses.

2.3 Hormone Extraction

Whole tissue in excess of 200 mg was placed in 15-20 mL of 80% methanol with 250 mg L^{-1} of butylated hydroxytoluene (BHT) and homogenized using a Physcotron (Microtec). Alternatively, vegetative tissue or seeds weighing less than 200 mg were placed in 2 mL micro centrifuge tubes containing tungsten-carbide beads (Qiagen) and homogenized for two minutes at full speed with a Tissuelyser (Qiagen). Samples were then suspended in 1 mL of either 80% methanol or 65% isopropanol (with BHT) and homogenized for a further one minute. All homogenate was then stored overnight at 4°C then transferred to -20ºC until worked up. Hormones were always extracted at or in excess of a 1:5 (tissue: extraction solvent) ratio.

2.4 Quantification of hormones and precursors

Samples were centrifuged to pellet debris, and 1 mL aliquots from larger samples, or 250 mL aliquots from micro-extractions were taken and internal standards added. Organic solvent was removed using a sample concentrator and hormones were resuspended in 500 mL of 1% acetic acid in dH_2O. Samples were partitioned twice against 0.6 volumes of diethyl ether and the organic fractions were transferred to fresh tubes and evaporated under N_2 gas. Hormones were once again suspended in 1% acetic acid in dH_2O and centrifuged to clear extract. The resulting supernatant was transferred to auto-sample vials (Waters) and analysed by UPLC-MS (MRM, Chapter 2.7). All analyses were conducted in biological triplicate (n=3) with replicates from individual plants unless otherwise stated.

2.5 Preparation of total hormone levels

To determine total auxin levels in extracts, tissue was homogenized as above and extracted overnight. Internal standards were added to aliquots of extracts and taken to dryness with a sample concentrator. The first aliquot was prepared as above to determine free hormone levels. The second aliquot was taken up in 3 mL of 7 N NaOH and incubated at 100°C for 3 hours to hydrolyse ester and amide linkages. After three hours the samples were cooled to room temperature and the pH was reduced to <2.7 pH with 10 N HCl. Samples were partitioned as above (Chapter 2.4) with 0.6 volumes of diethyl ether. All samples were taken to dryness and resuspended in 1% acetic acid in dH_2O. To obtain conjugate/ derivative levels, levels of free auxins were deducted from total levels.

2.6 Stabilisation of labile intermediates

Volatile and labile intermediates were stabilized using cysteamine to produce thiazolidine- (TAZ-) derived species of phenylpyruvate (phenylpyruvate-TAZ), PAAld (PAAld-TAZ), IPyA (IPyA-TAZ), and IAAld (IAAld-TAZ) adapted from Novák et al (2012). Samples were prepared as above (Chapter 2.2-2.3). 500 µL aliquots were taken and added to 3 mL of 0.25 M cysteamine solution. Samples were incubated at room temperature for 1 hour with agitation and were reduced to pH 2.7 with 10 N HCl. Samples were purified by SPE using SepPak cartridges (Waters) preconditioned with 1 mL of methanol, 1 mL of dH_2O and 1 mL of sodium phosphate buffer (pH 2.7). The cartridges were washed with 2 mL of 5% methanol and eluted into round bottom flasks in 2 mL of 80% methanol. The eluate was taken to dryness by rotary evaporation and resuspended in 1% acetic acid as above.

2.7 UPLC-MS

Samples were analysed as previously (Tivendale et al, 2012) with a solvent combination of 1% (v/ v) acetic acid in water (solvent A) and acetonitrile (solvent B). The modified UPLC program was 95% A: 5% B to 50% A: 50% B at 4.5 min, followed by immediate re-equilibration to starting conditions for 3 min. The flow rate was 0.35 mL min^{-1} with the column held at 35°C, and the sample compartment was at 6°C.

The mass spectrometer was operated in positive and negative ion electrospray mode with a needle voltage of 2.8 kV, and MRM was used to detect all analytes (Table 2.1). The ion source temperature was 130°C, the desolvation gas was N_2 at 950 L per $hour^{-1}$, the cone gas flow was 100 L per $hour^{-1}$, and the desolvation temperature was 450°C. Data were processed using MassLynx software.

Table 2.1 MRM transition data for observed analytes. All analytes (Endogenous, deuterium ($^{2}H_x$) or $^{13}C_x$ species) were observed using either positive or negative ESI. Quantitation and qualification transitions and approximate retention times for each analyte are indicated as well as the cone voltage and collision energy for each species

Mode	Analyte	Primary Transition	Approximate RT (min)	Cone Voltage	Collision Energy (V)
+	Indole-3-acetic acid	176.2 ® 130.1 m/z	2.6	18	18
+	$^{13}C_6$ Indole-3-acetic acid	182.2 ® 136.1 m/z	2.6	18	18
+	D_5 Indole-3-acetic acid	181.2 ® 135.1/134.1 m/z	2.5	18	18
+	Indole-3-pyruvate	204.1 ® 130.1/158.1m/z	1.8	18	22
+	D_5 Indole-3-pyruvate	209.1 ® 134.1/135.1 m/z	1.8	18	22
+	Indole-3-pyruvate-TAZ	263.1 ® 132.1/ 88.0m/z	3.1	26	13
+	D_5 Indole-3-pyruvate-TAZ	268.1 ® 137.1/136.1m/z	3.1	26	13
+	Phenylacetaldehyde-TAZ	180.1 ® 135.1/91.0 m/z	2.2	18	18 / 28
+	D_5 Phenylacetaldehyde-TAZ	185.1 ® 140.1/139.1 m/z	2.2	18	28
+	Phenylacetamide	136.1 ® 91.0 / 65.0 m/z	2.5	37	14 / 29
-	Phenylacetic acid	135.1 ® 91.0 m/z	3.7	16	8
-	$^{13}C_2$ Phenylacetic acid	137.1 ® 92.0 m/z	3.7	16	8
-	D_5 Phenylacetic acid	140.1 ® 96.0 m/z	3.7	16	8

Continued over page

Table 2.1 continued

Mode	Analyte	Primary Transition	Approximate RT (min)	Cone Voltage	Collision energy (V)
+	Phenylacetonitrile	118.1 ® 86.0 / 101.1 m/z	1.1	35	16 / 12
+	Phenylalanine	166.1 ® 120.1 m/z	1.1	22	12
+	D_5-Phenylalanine	171.1 ® 125.1 m/z	1.1	22	12
+	Phenylethylamine	122.1 ® 105.1 / 79.0 m/z	2.4	27	12 / 19
-	Phenylpyruvate	163.1 ® 91.0 m/z	2.7	16	9
-	D_5 Phenylpyruvate	168.1 ® 96.0 m/z	2.7	16	9
+	Tryptophan	205.2 ® 188.1/146.1m/z	0.9	17	17
+	D_5 Tryptophan	210.2 ® 192.1/193.1 m/z	0.9	17	17
+	Tryptophol (IEt)	162.1 ® 144.1 m/z	2.6	18	14
+	D_2 Tryptophol (IEt)	164.1 ® 146.1 m/z	2.6	18	14
+	4-Cl-Tryptophol (4Cl-IEt)	196.1 ® 178.1 m/z	3.7	18	14

2.8 DNA extraction

All genomic DNA (gDNA) used in this thesis was obtained using a modified CTAB extraction protocol described by Murray and Thompson (1980).

Approximately 100 mg of unexpanded leaflet tissue was collected from each plant and added to a micro centrifuge tube containing a single tungsten carbide bead (Qiagen). Samples were frozen in liquid N_2 then Homogenized using a Tissuelyser (Qiagen) at 30 frequency for 2 minutes. 500 µL of extraction buffer (100 mM Tris-HCl pH 8.0, 1.4 M NaCl, 20 mM EDTA, 2% w/ v CTAB, 20 mM β-mercaptoethanol) was added to each tube and further homogenised for 1 minute. Homogenate was incubated at 60ºC for 10-15 minutes with gentle agitation. DNA was extracted twice (sequentially) with 500 µL of a 24:1 mix of chloroform and isoamyl-alcohol, vortexed well and centrifuged at 14,000 rpm for 1 minute. 1 mL of precipitation buffer (50 mM Tris-HCl pH 8.0, 10 mM EDTA, 1% w/ v CTAB) was added to each extract and incubated at room temperature for 5-10 minutes, followed by centrifugation at 14, 000 rpm for 10 minutes. The supernatant was discarded and remaining pellet dissolved in 300 µL of salt solution (1.5 M NaCl, supplemented with 1 µL of 25 mg mL^{-1} RNAseA [Qiagen]). Resuspended extracts were incubated for 1 hour at 50ºC. 600 µL of EtOH was added and samples were incubated for 10 minutes, followed by 10 minutes centrifugation at 14,000 rpm. Supernatant was removed and remaining pellet was washed with 200 µL of 70% EtOH. Samples were centrifuged at 14,000 rpm for 10 minutes and supernatant was removed. gDNA was air dried overnight and resuspended in 50 µL of dH_2O. Concentration was determined by spectrophotometry using a nanodrop (Thermo scientific) and diluted to 50 ng μL^{-1} with dH_2O.

2.9 RNA extraction and cDNA synthesis

RNA was extracted using an SV Total RNA Isolation Kit (Promega) according to the manufacturer's instructions. cDNA was synthesised using Tetro Reverse Transcriptase (Bioline). 1 µg of template was used in all synthesis

reactions. Template was denatured for 5 minutes at 70ºC, followed by 5 minutes incubation on ice. RNA was added to a synthesis buffer (5x Reaction buffer, 1 mM Oligo dT primer, 10 mM dNTPs and Tetro RT) and incubated for 30 minutes at 42ºC followed by 5 minutes at 95ºC. cDNA was diluted with 80 µL of DEPC-treated water and stored at -20ºC.

2.10 Genotyping by HRM

HRM (high resolution melt) analysis was conducted using a SensiFAST HRM Kit (Bioline). Each reaction contained 2 µL of sample gDNA (~ 50 ng μL^{-1}), 7.5 µL of Sensifast mix, 1.05 µL each of forward and reverse primer (10 mM, Chapter 2.12) and 3.4 µL of dH_2O. Reactions were assembled using a CAS-1200 liquid handling robot (Corbett) and amplified using a rotorgene Q real time PCR cycler (Qiagen). All PCR reactions were conducted as follows: 95ºC for 5 minutes, 50 cycles of (95ºC for 10 seconds, 60ºC for 30 seconds), 95ºC for 5 minutes, 50ºC for 5 minutes. HRM analysis for each marker was conducted over the following temperatures in increments of 0.1ºC per step (2 seconds) with a 90 second first step. AS2: 72ºC to 91ºC, NIN: 72ºC to 86ºC, MYB2: 72ºC to 83ºC, FRLb: 72ºC to 90ºC and PsTAR1: 70ºC to 85ºC.

2.11 Accession numbers

Accession numbers for the amino acid sequences of the pea enzymes utilized in this thesis are presented below.

Table 2.2 Accession numbers of pea enzymes from Pea RNA-Seq gene atlas and NCBI used in phylogenetic analyses (Chapter 5). Enzyme names are based on most similar *Arabidopsis* enzymes unless previously annotated. Names of mutants are also provided

Enzyme name	Accession	Enzyme name	Accession
Tryptophan aminotransferases		**IAA amido synthetases**	
PsTAR1 *(tar1-2)*	AFG31373	GH3.1-4 like	PsCam034040
PsTAR2 (*tar2-1*)	AFG31321	GH3.1-4 like	PsCam036984
PsTAR3 (*tar3*)	AFG31374	GH3.5-6 like	PsCam049973
PsTAR4	PsCam057706	GH3.5-6 like	PsCam044184
YUC flavin monooxygenases		GH3.5-6 like	PsCam037378
PsYUC1 (*crd-4*)	ADP88696	GH3.5-6 like	PsCam012882
YUC2/6 like	PsCam045906	GH3.5-6 like	PsCam016962
YUC2/6 like	PsCam036854	GH3.5-6 like	PsCam020871
YUC2/6 like	PsCam036728	GH3.5-6 like	PsCam037294
YUC3/5/7/8/9 like	PsCam038466	GH3.5-6 like	PsCam036898
YUC3/5/7/8/9 like	PsCam038241	GH3.5-6 like	PsCam036924
YUC3/5/7/8/9 like	PsCam034710	GH3.5-6 like	PsCam037341
YUC11/12 like	PsCam059460	GH3.5-6 like	PsCam012847
YUC11/12 like	PsCam039160	GH3.5-6 like	PsCam017652
YUC11/12 like	PsCam050635	GH3.9/17 like	PsCam000135
YUC11/12 like	PsCam000881	Jar1 like	PsCam037396
YUC11/12 like	PsCam038488	Jar1 like	PsCam037298
Aromatic aminotransferases		Jar1 like	PsCam006884
PsArAT	ANG65409	Jar1 like	PsCam026731
IAA glucosyltransferases		**IAA oxidase**	
UGT84 like	PsCam027195	DAO like	PsCam039164
UGT84 like	PsCam037917		
UGT84 like	PsCam045800		
UGT74 like	PsCam014158		

2.12 Primers

Several analyses throughout this thesis utilise primers for various purposes. Primers used throughout this thesis are presented in the following tables and are referred to in their respective chapters.

Table 2.3 Primer sequences used for quantitative PCR, sequencing and Protein expression via the Gateway system. Associated gene, primer function and name are provided (Chapter 3)

Gene	Primer name	Sequence (5' to 3')
PsTAR1 (Gateway)	PsTAR1_ENTR_F1	CACCATGGTGGTTGCTAGAGACGG
	PsTAR1_ENTR_R2	TCATTCTATTTTAGCATTTTCCAACCTTGTACA CAATTC
PsArAT (Gateway / Sequencing)	PsPheAT_ENTR_F2	CACCATGGAAAGTGGTGTTGG
	PsPheAT_ENRT_R2	TTACTGTTTTCTCGCGTGTCTTTG
PsTAR1 (qPCR)	qPsTAR-Mt5g90 F92	CCTTGCCAAAGTATCCATCCGCCTA
	qPsTAR-Mt5g90 r93	GCAGGATATTGCTCGGATATTTC
PsTAR3 (qPCR)	qPsTAR3 F85	GCAAACGTCTCGTGAAGGAA
	qPsTAR3 r85	GCCTTTGGATACTTGGTTACAGTG

Table 2.4 Primer sequences for HRM used to amplify the polymorphic region in the *tar1-2* mutant. (Chapter 4)

Gene	Primer name	Sequence (5' to 3')
PsTAR1 (HRM)	PsTAR1 1066gFW	CTGATGGAGAAGGGAATGTTG
	PsTAR1 1178gRev	GGTGCATTTGGAGAATGTGA

Table 2.5 Primer sequences for marker sequencing in L1794 and *bushy.* Associated gene, primer function and name are provided (Chapter 6)

Gene	Primer name	Sequence (5' to 3')
AS2 (sequencing)	AS2-F	CTAATCACACGTTTAGGACCGG
	AS2-R	CGAAATCCAAACCGAACCTAATCC
NIN (Sequencing)	NIN-F	CCATTGAGAAGTGTCTACACTGGC
	NIN-R	GATGCAGTAGTAGCAGCATCGG
MYB2 (Sequencing)	MYB2-1F	GGTGGACAGATGAAGAAC
	MYB2-1R	CTTCTGAGCATGACTTCG
FRLb (Sequencing)	FRLb-1F	CCAAGTTGGACTTTGGCTTT
	FRLb-1R	GCGGAAACTCAGAATCAAGG

Table 2.6 Sequences of primers used to genotype F_2 and F_3 mapping populations. Associated gene, primer function and name are provided (Chapter 6)

Gene	Primer name	Sequence (5' to 3')
AS2 (HRM)	AS2-4F	TGTGGCTAGAGATGCGATTG
	AS2-4R	TCCAAAACCAAAAATCCAAAA
NIN (HRM)	NIN-F	CCATTGAGAAGTGTCTACACTGGC
	NIN-2R	CAAGGGATAACGAGTTCAGCA
MYB2 (HRM)	MYB2-5F	AGAACATAAGAAGTTCCTTGAAGC
	MYB2-5R	AAATTCAACCTCTTTTGCAAGT
FRLb (HRM)	PsFRLb-2F	GCAATGCTTTTGGCCTGTAA
	PsFRLb-2R	GGGGAACTTATCCCCGAAAT
PsLip1 (CAPS)	Lip1_F3	CATCACTGGATCAGATTCAC
	Lip1_R3	GCTTATCTGCTGCTTGCC
AO1 (CAPS)	AO388re_F1	GTTCAAATTCCGCTATGCTATAACAT
	AO388re_R1	AAGGGTGGTTCACCAGATGCT

Table 2.7 Sequences of primers used in the amplification and sequencing of *PsAO* genes. Associated gene, primer function and name are provided (Chapter 6)

Gene	Primer name	Sequence (5' to 3')
PsAO1 (Amplification)	PsAO1_Nco1_F13	TTAGCCATGGATGGAAGTGAAGAATAATGAGAAT
	PsAO1_BamH1_R12	GCGGATCCCTGCTTTTTAACAAGACTCAA
PsAO1 (Forward Sequencing)	PsAO1_outer 216F	ATTTGTCTGAAATTGAAAATCAGTTATTG
	PsAO1_757F	GTTACCGACCGATTGCTGAT
	PsAO1_1389F	GCGGATTCAATGGTTCAAAT
PsAO1 (Reverse Sequencing)	PsAO1_484r	CAAGAGCTCGCGGTAAAATC
	PsAO1_2780r	TCCTCCATAACCTCCACCAA
	PsAO1_3428r	TGCAGCAGGTTTTACGTTCA
	PsAO1_outer 4509r	AATAAATCATGCAAGTTCCATTAAATAGC
PsAO2 (Amplification)	PsAO2 outer 35_F	TGAAGTATGGATGTGAAGAAGACTGAGAACCA
	PsAO2 outer 4271_r	TCCTCTCATATTTGTTCACCTGAGTTTGAGTGA
PsAO2 (Forward Sequencing)	js402_F1	TAAGTTGCCTCAATATGATCGTGA
	seq402_F2-4	GCTTTCCTTGTTCAGGTATCTTC
	js402_F3	TGCCGAAGATATTGCTAGATGTGT
PsAO2 (Reverse Sequencing)	PsAO2-SC-1R	GGGTGGATCTGGAGGATTG
	seq402-r2-4	ACTCAGGGCCTTGACTTGAC
	js402_r1	GCTTGCGTGGATGCCTGAA
PsAO3 (Amplification)	PsAO3_Nco1_F32	TTAGCCATGGATGGAAGTGAAGATGAGTGAGAAT
	PsAO3_BamH1_r32	AAGGATCCGACAGTATTACATGAAGTTCCA
PsAO3 (Forward Sequencing)	PsAO3 seq 717_F	TGGAGAAAGGGAGAGAGCAA
	PsAO3 seq 1336_F	GACCGCCATTAAGTTTGGAA
	PsAO3 seq 1952_F	GTCAGGAGCTGCCCTACAAG
	PsAO3 seq 2640_F	GGAGGAAAGGCCATAAAAGC
PsAO3 (Reverse Sequencing)	PsAO3 seq 479_r	AGCATGGAATCCAGCAAATC
	PsAO3 seq 3852_r	AACCCTGGACAAAAGCTCCT

Chapter 3: The biosynthesis of phenylacetic acid

3.1 Introduction

Recently, the predominant pathway for auxin biosynthesis in plants has been characterised, and it is now widely accepted that indole-3-acetic acid (IAA), the main auxin in plants, is primarily synthesised via a two-step pathway. This tryptophan (Trp)-dependent biosynthesis of IAA is reported to utilise indole-3-pyruvic acid (IPyA) as the sole intermediate (Mashiguchi et al, 2011; Won et al, 2011; Dai et al, 2013).

The initial conversion of Trp to IPyA is catalysed by the *TAA1* (*TRYPTOPHAN AMINOTRANSFERASE of ARABIDOPSIS*) gene family, which includes multiple members in *Arabidopsis* (Stepanova et al, 2008; Tao et al, 2008), maize (Chourey et al, 2010; Phillips et al, 2011), pea (Tivendale et al, 2012) and several other species (Chourey et al, 2010; Liu et al, 2012). Enzymatic assays on TAA family proteins have indicated that Trp is a preferred substrate for these enzymes (Stepanova et al, 2008; Tao et al, 2008).

The subsequent conversion of IPyA to IAA is catalysed by a group of enzymes known as YUCCAs (Mashiguchi et al, 2011; Dai et al, 2013). The *YUCCA (or YUC)* gene family is also quite extensive, with *Arabidopsis* possessing 11 annotated *YUC* genes (Cheng et al, 2007). Unfortunately, IPyA is prone to substantial non-enzymatic breakdown to IAA (Tam and Normanly, 1998), making quantification and analysis difficult. Nevertheless, YUCCA activity has been reported in vitro, in studies using recombinant YUC protein (Dai et al, 2013).

Such assays have been complemented by mutant studies, although in *Arabidopsis*, high order *yuc* mutants (triple or quadruple) are required to elicit a distinct phenotype (Cheng et al, 2007). However, in maize, single *YUC* knockouts can cause large reductions in IAA levels, resulting in severe alterations to vegetative and reproductive development (Gallavotti et al, 2008; Phillips et al, 2011; Bernardi et al, 2012).

Trp-independent synthesis may also contribute to the IAA pool in a range of species (Michalczuk et al, 1992; Rapparini et al, 1999; Epstein et al, 2002; Sztein et al, 2002). Recent evidence suggests that this pathway may be essential for embryo development (Wang et al, 2015), although this suggestion has been challenged (Nonhebel, 2015).

Phenylacetic acid (PAA) is an endogenous auxin that has received substantially less attention than that of IAA. PAA is present at physiologically similar levels to IAA and has been recorded at exceptionally high levels in some tissues (Schneider and Wightman, 1986; Sugawara et al, 2015). Although the auxin activity of PAA in wheat coleoptile and pea segment tests is not as strong as that of IAA (Wightman and Lighty, 1982), PAA is reportedly capable of eliciting a stronger response in initiation of root primordia (Wightman et al, 1980; Schneider et al, 1985).

Like IAA, PAA has been found in numerous genera, including bacteria, fungi, and some basal land plants (Abe et al, 1974; Kishore et al, 1976; Wightman and Lighty, 1982; Schneider and Wightman, 1986; Hwang et al, 2001; Kim et al, 2004; Sugawara et al, 2015). In fungi and bacteria, PAA is produced from the amino acid phenylalanine (Phe), via the intermediate phenylpyruvate (Kishore et al, 1976; Krings et al, 1996; Groot and de Bont, 1998; Somers et al, 2005). Bacterial phenylpyruvate is either converted directly to PAA by a phenylpyruvate decarboxylase or via an additional intermediate, phenylacetaldehyde (Somers et al, 2005; Spaepen et al, 2007).

It has been suggested that PAA biosynthesis in plants may also proceed through phenylpyruvate (Taylor and Wightman, 1987). Recently, It has been

proposed that the enzymes responsible for IAA biosynthesis are also involved in the conversion of Phe to PAA (Sugawara et al, 2015). *In vitro* assays support a TAA1-mediated conversion of Phe to phenylpyruvate (Tao et al, 2008). Although, the TAA1 enzyme possesses a Michaelis constant (K_m) for L-Phe that is more than 30 times that of L-Trp (Tao et al, 2008). There is also evidence for the conversion of phenylpyruvate to PAA by recombinant AtYUC2 and AtYUC6 *in vitro* (Dai et al, 2013; Sugawara et al, 2015). In fact, this reaction was used to identify the biochemical mechanism of the YUC flavin monooxygenases (Dai et al, 2013).

Phe is a precursor of many important compounds in plants, and its biosynthesis is well documented, although more than one biosynthetic pathway exists (Cho et al, 2007; Yamada et al, 2008; Tzin et al, 2009; Maeda et al, 2010; Yoo et al, 2013). The final product of the shikimate pathway, chorismate, is converted to prephenate, a branch point in Phe synthesis, by a chorismate mutase (Lee et al, 1995; Herrmann and Weaver, 1999). In some species, prephenate is then primarily directed towards arogenate by a prephenate aminotransferase. This is followed by conversion to Phe by an arogenate dehydratase (Siehl et al, 1986; Cho et al, 2007; Maeda et al, 2010; Maeda et al, 2011).

Alternatively, Phe biosynthesis may involve the conversion of prephenate to phenylpyruvate by a prephenate dehydratase (Maeda et al, 2010). Several arogenate dehydratases also possess this ability (Cho et al, 2007). Phenylpyruvate is subsequently converted to Phe by a phenylpyruvate aminotransferase (Tzin et al, 2009; Maeda et al, 2010; Yoo et al, 2013). This biosynthetic pathway is incongruous with the pathway proposed for PAA biosynthesis where phenylpyruvate exists only as a metabolite of phenylalanine, rather than a precursor (Sugawara et al, 2015). However, it should be noted that transamination is a reversible process (Jensen and Gu, 1996). Interestingly, the aminotransferases discussed in relation to Phe biosynthesis in petunia (*Petunia hybrida*)(Yoo et al, 2013) do not include TAA1 family proteins, nor their function on Trp.

Although Sugawara et al (2015) favour the TAA1/ YUC pathway for PAA biosynthesis; they do not identify or quantify phenylpyruvate in their model system, *Arabidopsis*. In fact, the quantification of this compound is thought to be problematic. Maeda et al (2010) reported that prephenate is subject to acid breakdown to phenylpyruvate during extraction procedures, casting doubt on identifications of phenylpyruvate that do not account for this possibility. In fact, after accounting for this conversion, Maeda et al (2010) reported undetectable levels of phenylpyruvate in petals of their model system, petunia. On the other hand, Manela et al (2015), have recently reported detection of phenylpyruvate in *Vitis vinifera* using GC-MS; although, no chromatograms were provided in this case.

In this chapter, it is demonstrated that PAA is derived from phenylpyruvate as suggested by Sugawara et al (2015). However, it is proposed that the enzymes involved are not those responsible for IAA biosynthesis. It is discussed here, that while IAA biosynthetic enzymes are capable of catalysing reactions involved in PAA synthesis *in vitro*, it is unlikely that this reflects the *in vivo* function of such enzymes. Further to this, an alternative candidate for the initial transamination reaction, identified here as *PsArAT* (PsCam000495_1), is presented.

3.2 Materials and Methods

3.2.1 Plant material

The *tar2-1* mutant line was previously obtained through Targeting Induced Local Lesions in Genomes (TILLING)(Dalmais et al, 2008) followed by at least eight generations of backcrossing against a cv. Caméor background (Tivendale et al, 2012). Non-mutant studies were conducted on cv. Torsdag unless otherwise stated. The maize (*Zea mays*) *de18* mutant and its wild type background, cv. B37, were the same as those in Bernardi et al (2012).

3.2.2 Expression and purification of functional proteins

Previously isolated *PsTAR1* sequence was amplified from *Pisum sativum* apex cDNA using primers containing a 5' CACC tag to facilitate directional cloning into a pENTR™ TOPO® vector (Invitrogen). *PsTAR1* containing constructs were verified by sequencing (Macrogen) and the gene was transferred into a pET-53-DEST vector using an LR clonase II reaction (Novagen) to produce PsTAR1-DEST. The expression construct was transformed into NOVA F- cells for selection, followed by transformation into the *E. coli* strain BL21 (DE3) for expression. Culture and Harvest of cells was conducted as in (Dai et al., 2013) followed by purification using Ni-NTA for metal chelation chromatography. Primer sequences are provided in Chapter 2.12).

3.2.3 Enzyme assay

Assays were conducted in 100 µL of 50 mM sodium phosphate buffer (pH 7.0) containing 4 µM PsTAR1 enzyme, 50 mM substrate, and 1 mM PLP and 50 mM sodium pyruvate as cofactors. Assays were incubated for 1 hour at 37°C and reactions were terminated with the addition of 5% acetic acid in methanol.

3.3 Results and Discussion

3.3.1 Phenylalanine can be converted to PAA *in vivo*

We sought to confirm that Phe is a precursor of PAA by investigating the metabolism of labelled (D_5) Phe in excised pea seeds (Figure 3.1A). Over the course of 16 hours, the substrate was metabolised, resulting in a clear dilution of the phenylpyruvate pool with deuterium (35%). PAA was also diluted by 18%, while the endogenous Phe pool was diluted by 44%. The identity of D_5 phenylpyruvate and D_5 PAA was confirmed by obtaining product scan spectra (Figure 3.2). These results are consistent with the proposition of a linear, two-step pathway (Sugawara et al, 2015).

It is known that different tissue types may possess alternative auxin synthetic pathways (Sugawara et al, 2009); therefore, to confirm this chemical pathway, we investigated PAA biosynthesis in vegetative tissue (Figure3.1B).

Germinating seedlings were hydroponically incubated in a solution containing D_5 Phe over a seven-day period. Following this, endogenous Phe was diluted in excess of 50% and PAA was labelled to a similar extent (49%; Figure 3.1B). This indicates that Phe can be an *in vivo* precursor to PAA in pea vegetative tissue. However, the major proposed intermediate, phenylpyruvate, was only diluted 5% with deuterium in this experiment (Figure 3.1B).

The low dilution may have been due to de novo synthesis of unlabelled phenylpyruvate from prephenate, or alternatively the conversion of unlabelled prephenate to phenylpyruvate in the acidic conditions used during purification (Hermes et al, 1984).

Further analysis of possible PAA intermediates identified a 10% dilution of the phenylacetaldehyde (PAAld) pool (following stabilisation to the thiazolidine-labelled derivative, PAAld-TAZ) in the homogenate of pea apical tissue (Figure 3.3G). This is consistent with previous studies on flavour volatiles in petunia where PAAld is an important metabolite of Phe (Boatright et al, 2004). While PAAld is absent from the proposed PAA biosynthetic scheme in plants (Sugawara et al, 2015), whether or not this exclusion is justified remains unclear.

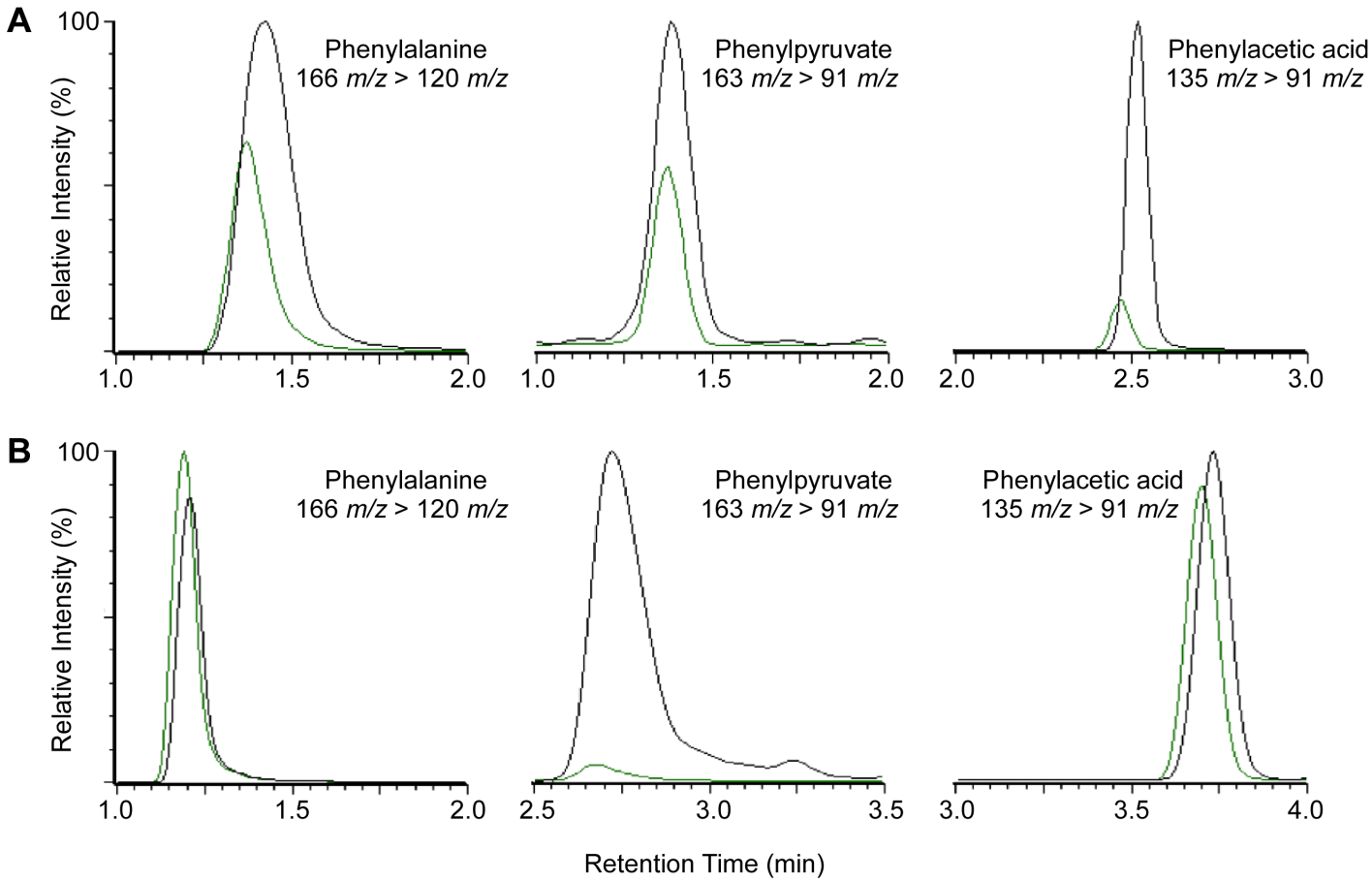

Figure 3.1 Representative UPLC-MS chromatograms showing dilution of Phe metabolic products after incubation with D_5 Phe in excised pea seeds (A) and seedlings (B). Peaks are relative intensities of deuterium labelled (green) and endogenous (black) species of Phe (approximate retention time: 1.11 min), phenylpyruvate (2.72 min), and phenylacetic acid (3.73 min). Retention times in A vary due to preparation under neutral pH conditions. Transitions indicated are for the endogenous species (all D5 transitions are m/z + 5).

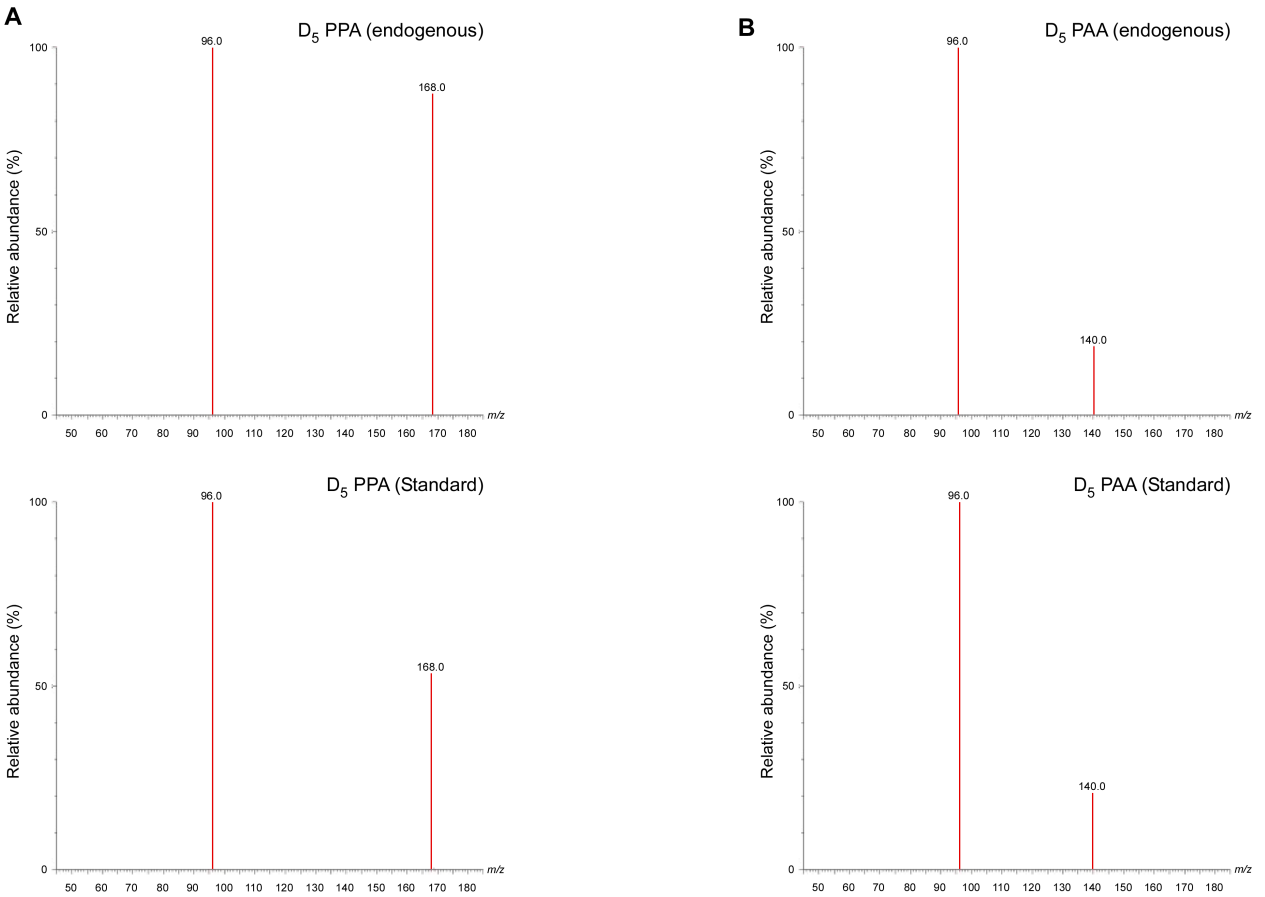

Figure 3.2 Product scan spectra of D_5 species of (A) phenylpyruvate (PPA) and (B) phenylacetic acid (PAA) showing relative abundance of major product ions from endogenous material incubated with D_5 Phe (top) and from a synthesised standard (Bottom). Retention time of major peaks for analytes is at 2.78 min for phenylpyruvate and 3.85 min for PAA.

The biosynthetic scheme for IAA presented by Sugawara et al (2009) includes several compounds from alternative IAA biosynthetic pathways as intermediates. We used this scheme to identify analogous compounds to determine if they are also intermediates in PAA biosynthesis. Phenylethylamine is a direct precursor to PAAld in other systems (Taylor and Wightman, 1987; Boatright et al, 2004; Tieman et al, 2006). However, despite its presence in petunia and tomato, we were unable to detect either the endogenous or labelled species of phenylethylamine in our feeding studies (Figure 3.3E-F). In *Tropaeolum*, phenylacetonitrile has previously been proposed as a possible intermediate between glucosinolates and PAA (Ludwig-Müller and Cohen, 2002). Here, we sought to determine if phenylacetonitrile and phenylacetamide, the remaining intermediate, were present in our system. However, we were unable to detect either of these compounds in either seeds or vegetative tissue of pea (Figure 3.3A-D). Based on the analogous IAA biosynthetic pathways (Sugawara et al, 2009), it is unlikely that either of these compounds are major intermediates involved in PAA biosynthesis in pea.

Our evidence from the labelling of Phe metabolites supports the theory that PAA is mainly synthesised through phenylpyruvate (Sugawara et al, 2015). However, labelling patterns similar to those in vegetative tissue (i.e. a small degree of dilution of endogenous phenylpyruvate, Figure 3.1B) have been previously used to exclude tryptamine from the IAA biosynthetic scheme in tomato (Cooney and Nonhebel, 1991). It is important to note that phenylpyruvate may be compartmentalised in the pea vegetative system, as reported for *Petunia hybrida* and *Atropa belladonna*, where phenylpyruvate is located in both the cytosol and in plastids (Yoo et al, 2013; Bedewitz et al, 2014). To explore these hypotheses further, it is important to examine individuals with mutations in putative PAA biosynthetic enzymes. However, there are currently no known mutants with a demonstrated reduction in the levels of endogenous PAA.

3.3.2 Phenylpyruvate can be converted to Phe *in vivo*

To further investigate the role of phenylpyruvate in our system, we incubated crude homogenates of pea apical tissue with synthesised D_5 phenylpyruvate (Chapter 3.5.2). In these experiments, the phenylpyruvate pool was diluted by an average of 32% with the labelled species following an overnight incubation (Figure 3.4). We found that label was heavily incorporated into PAA (Figure 3.4; in excess of 200%), supporting the suggestion that phenylpyruvate is a key intermediate in PAA biosynthesis (Sugawara et al, 2015). Although the degree of labelling of Phe was only 5-10%, this nevertheless indicates strong conversion of phenylpyruvate to Phe, given the abundance of this amino acid in the tissues concerned (up to 200 mg g^{-1} FW). PAAld was also labelled to a small extent (less than 1%; data not shown). The presence of label in Phe indicates that phenylpyruvate can be a precursor for Phe in our system.

3.3.3 Conversion of D_5 Tryptophan to D_5 IPyA *in vivo*

To confirm that labelled precursor metabolism studies are effective in the investigation of auxin synthetic pathways, we incubated pea seedlings with deuterated Trp to observe the fate of the deuterium label. In these experiments, deuterated IPyA was consistently detected, following conversion to the stable thiazolidine derivative with cysteamine (Figure 3.5)(Novák et al, 2012). To our knowledge, this is the first time that the conversion of labelled Trp to labelled IPyA has been directly demonstrated in plants, despite the fact that the IPyA pathway is now recognised as the main pathway in many species (Tivendale et al, 2014; Sugawara et al, 2015).

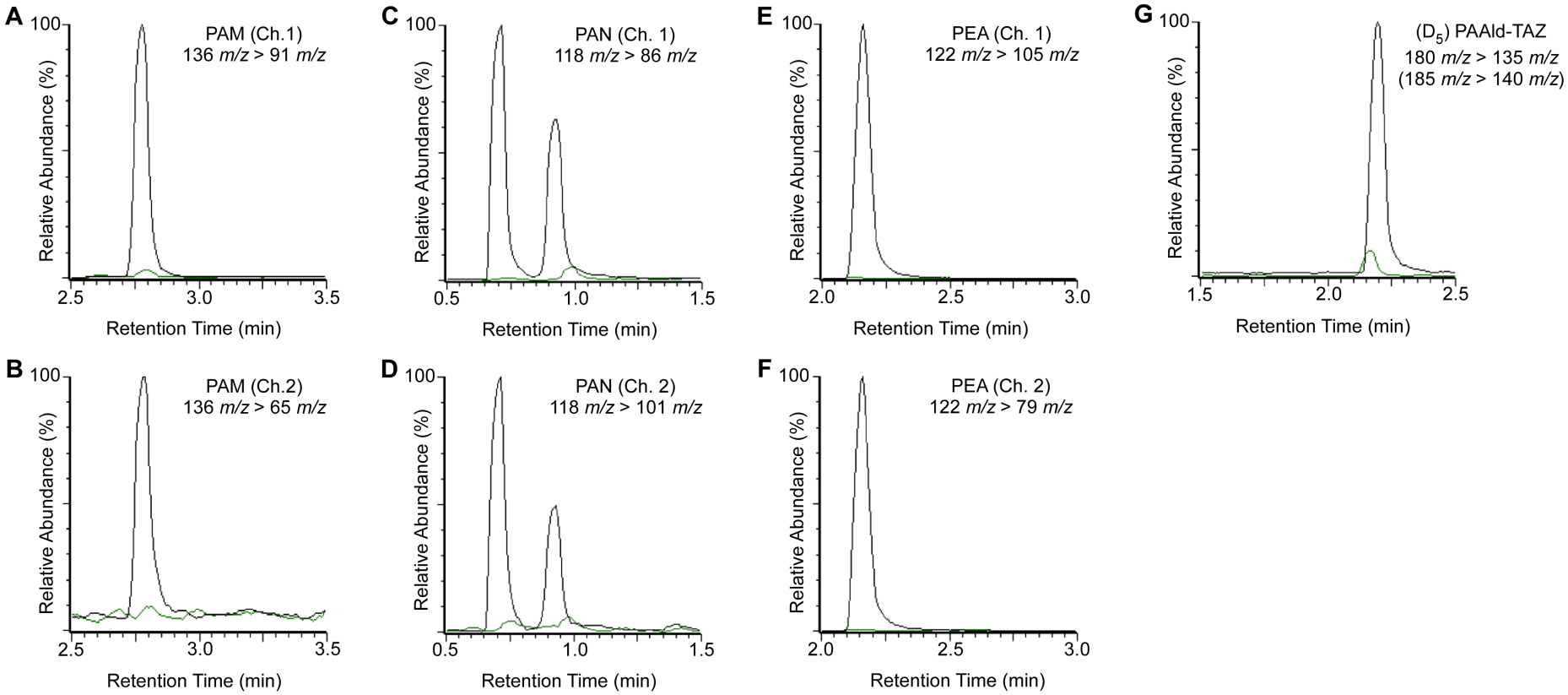

Figure 3.3 Representative UPLC-MS chromatograms of proposed PAA biosynthetic intermediates showing primary (Ch. 1) and secondary (Ch. 2) identification channels with standard (black) and endogenous (green) peaks. Chromatograms are as follows (A, B) phenylacetamide (PAM), (C, D) phenylacetonitrile (PAN), (E, F) phenylethylamine (PEA). Phenylacetaldehyde (PAAld-TAZ) levels (G) are endogenous (black) and D5 labelled (green) indicating the degree of label incorporation. Peak areas are relative abundances and mass transitions are indicated.

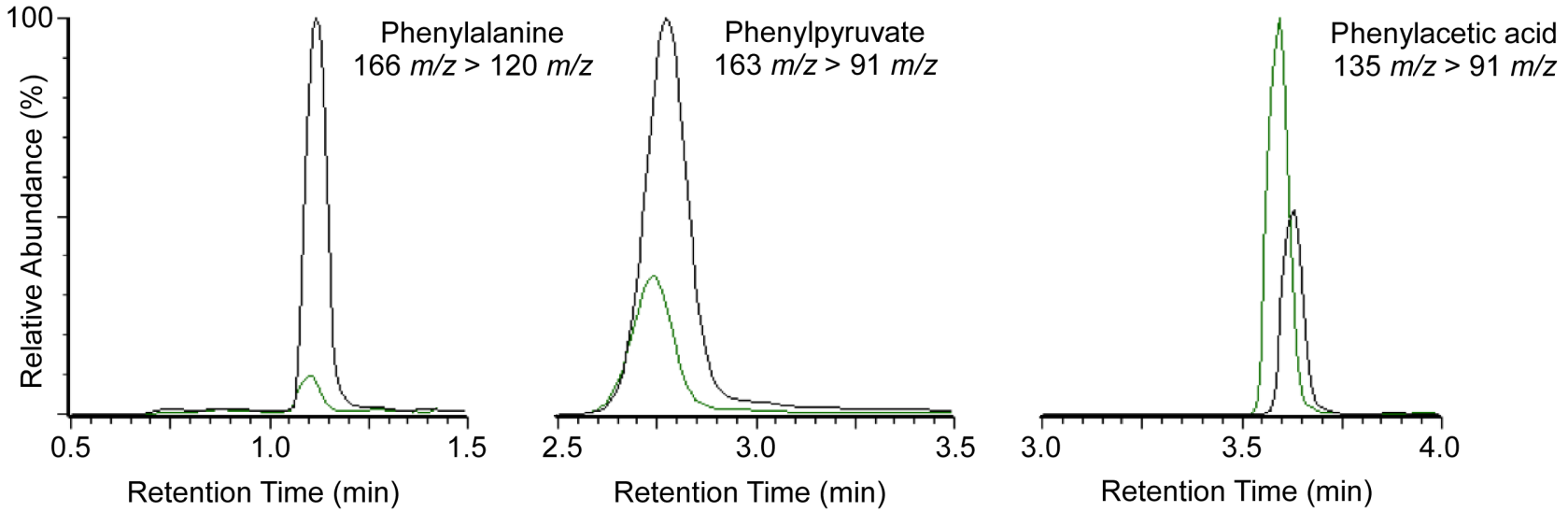

Figure 3.4 Representative UPLC-MS chromatograms from pea apical tissue incubated with labelled (D_5) phenylpyruvate for 16 h. Peaks are relative intensities of deuterium labelled (green) and endogenous (black) species of Phe (approximate retention time: 1.11 min), phenylpyruvate (2.78 min), and phenylacetic acid (3.63 min). Transitions indicated are for the endogenous species (all D_5 transitions are m/z +5).

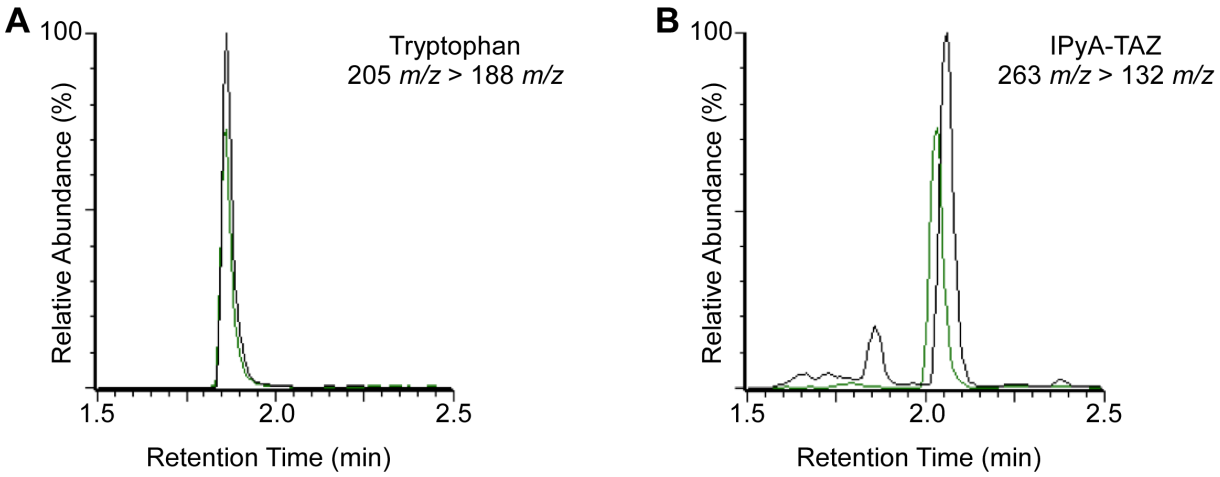

Figure 3.5 Representative UPLC-MS chromatograms showing incorporation of deuterium label in (A) Trp and (B) thiazolidine stabilised indole-3-pyruvate following incubation with D_5 Trp. Peak areas are relative abundance of D_5 (green) and endogenous (black) analytes and mass transitions are indicated (all D_5 transitions are m/z + 5).

3.3.4 ZmYUC1 is unlikely to play a role in PAA biosynthesis

It has been suggested that, *in vivo*, PAA is synthesised by the same enzymes involved in the synthesis of IAA (Sugawara et al, 2015). As there is currently no published *YUC* mutant in pea, we tested this suggestion by utilising an auxin mutant from maize. In the maize *defective endosperm18* mutant (*de18)*(Bernardi et al, 2012), the ZmYUC1 protein is truncated resulting in complete loss of enzyme function. This single mutation causes up to a 100-fold drop in the levels of free IAA in maize kernels throughout kernel maturation (Bernardi et al, 2012). Using mutant tissue, we sought to determine if a non-functional ZmYUC1 affected the levels of PAA. We found that, while IAA levels were reduced (Figure 3.6C), consistent with previous results (Bernardi et al, 2012), there was no reduction in free PAA content, compared with the WT, *B37* (Figure 3.6A).

To eliminate the possibility that altered conjugation of PAA was maintaining free auxin levels, samples were hydrolysed to release both ester and amide derivatives. The total PAA levels show no significant difference between the *de18* mutant and its corresponding WT, *B37* (Figure 3.6B). However, hydrolysis did reveal a more pronounced reduction in total IAA (0.3% of WT; Figure 3.6D) compared with that of free IAA (1.8% of WT; Figure 3.6C). These results suggest that ZmYUC1 does not play a role in PAA biosynthesis. In *Arabidopsis* also, there is no evidence that higher order YUC mutants (*yuc1yuc2yuc6*) affect PAA content, even though IAA levels were reduced in the triple mutant (Sugawara et al, 2015). Interestingly, two of the three enzymes concerned in that study (AtYUC2 and AtYUC6), have been shown to convert phenylpyruvate to PAA *in vitro* (Dai et al, 2013; Sugawara et al, 2015).

It has been suggested that other members of the *Arabidopsis* YUC family might contribute to PAA biosynthesis in the *yuc1yuc2yuc6* mutant (Sugawara et al, 2015), and the same may apply to the *de18* mutant. However, in maize endosperm, the *ZmYUC1*-like YUCs, *ZmYUC2* and *ZmYUC3*, are expressed

at exceptionally low levels (Bernardi et al, 2012), while another characterised *YUC*, *ZmSpi1* (Gallavotti et al, 2008), is not expressed. Based on additional expression data collected by Sekhon et al (2011), we sought to identify any other YUC sequences that were expressed at any stage in the maize endosperm. These data show that the only other gene with significant transcript levels (*GRMZM2G109515*) is expressed at a fraction of *ZmYUC1* levels (~7%) throughout endosperm development (Table 3.1). Given these expression patterns, it is possible that the protein encoded at the above locus may contribute to PAA biosynthesis; however, a substantial contribution appears unlikely.

Currently, the main *in vivo* evidence that YUCs are involved in PAA biosynthesis comes from overexpressing *AtYUC1*, *AtYUC2* and *AtYUC6* in *Arabidopsis*. This did appear to increase flux through the PAA biosynthesis pathway: in the overexpression lines, the level of the PAA conjugates PAA-Asp and PAA-Glu were elevated between 14-41 and 1.6-3.8 fold, respectively (Sugawara et al, 2015). However, the extent of up-regulation of the *YUC* genes was quite high: induction by β-estradiol resulted in overexpression of *YUC2* by 142- fold and *YUC6* by 29- fold (Sugawara et al, 2015). It is not unexpected that the elevated enzyme abundance can utilise endogenous phenylpyruvate, as this capacity has been shown *in vitro* (Dai et al, 2013; Sugawara et al, 2015). Furthermore, since overexpressing an enzyme that normally plays only a minor role in a pathway can dramatically affect flux in that pathway (Yoo et al, 2013), such overexpression studies are not necessarily definitive in themselves.

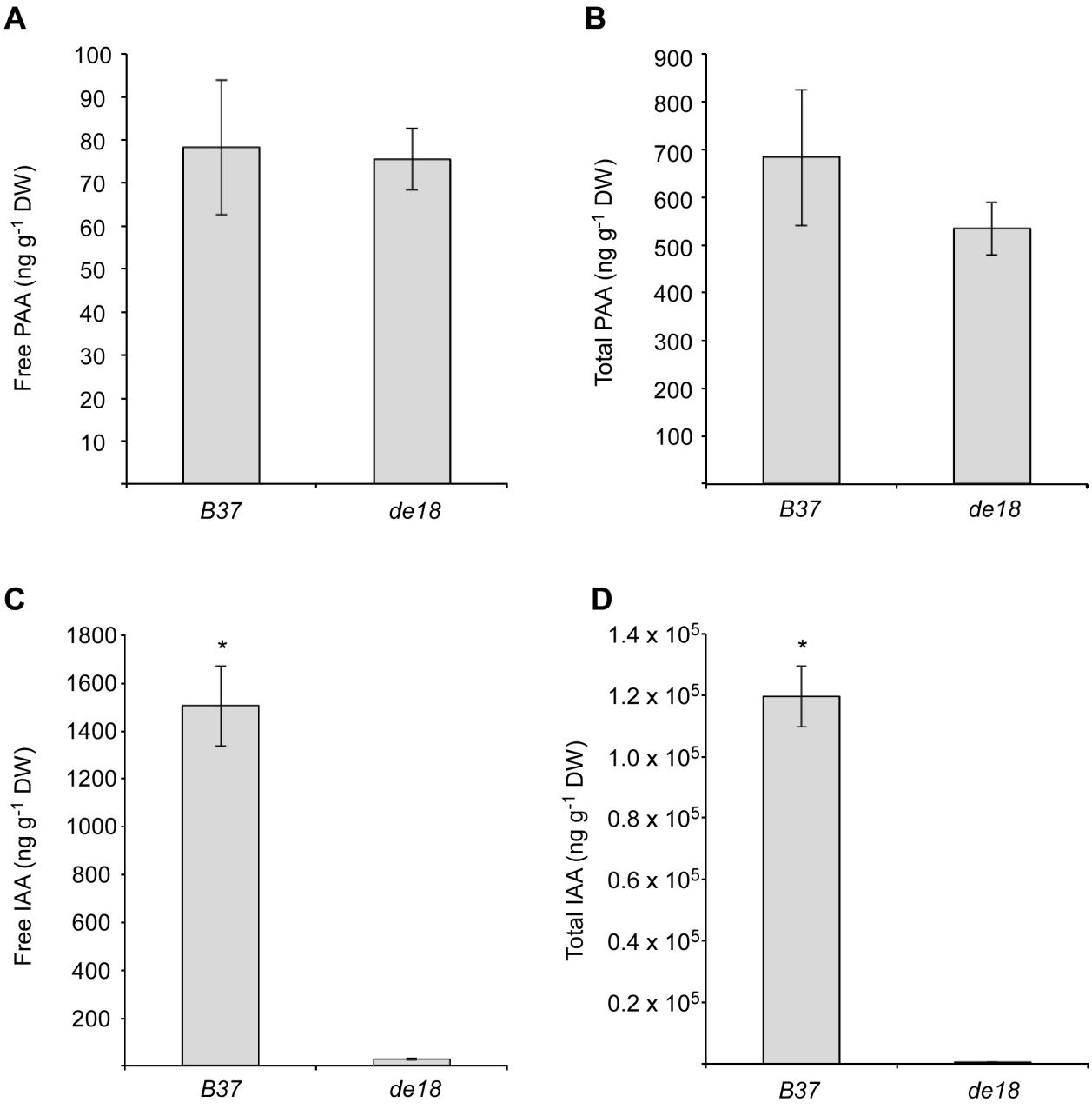

Figure 3.6 Effects of the maize *de18* mutation on the levels of free and total auxin in developing endosperm (16 d after pollination) compared to the corresponding wild type (B37). Data are means ± SE (ng g^{-1} dry weight [DW], n=3). * Indicates a significant difference at the 0.05 level. A, Free PAA; B total PAA; C, free IAA; D, total IAA.

Table 3.1 Relative expression of endosperm expressed YUC-like loci identified using the ZmYUC1 amino sequence as a probe. Data are relative expression compared with housekeeping genes listed in Sekhon et al (2011). Data are available from the maize genome database (http://www.maizegdb.org/)

	Endosperm (DAP)							Embryo (DAP)				
Loci / Gene	**12**	**14**	**16**	**18**	**20**	**22**	**24**	**16**	**18**	**20**	**22**	**24**
GRMZM2G091819 / *ZmYUC1*	3764	2312	1488	1602	2563	2291	2716	63.3	5.3	90.8	78.2	55.5
GRMZM2G019515 / No annotation	179.9	161.9	449.6	104.3	152.4	123.5	189	77.9	70.3	65	88.9	188.2
GRMZM2G017193 / No annotation	0.7	0	0	2.7	1.9	0	0	0	3.9	4.8	5.5	7.3
GRMZM2G011622 / No annotation	11.2	16.4	0	23.7	7.7	0	0	31.9	15.8	13.7	37.2	21.7
GRMZM2G159393 / *ZmYUC2*	0	0	0	0	0	0	0	6.5	5.3	7.1	7.0	18.4
GRMZM2G107761 / *ZmYUC3*	0.8	0	0	0	0	0	0	0	0	0	0	0
GRMZM2G025222 / *ZmSpi1*	0	0	0	0	0	0	0	138.4	65.2	28.7	33.8	55.8

3.3.5 A mutation in *PsTAR2* does not affect PAA levels despite drops in IAA, 4-Cl-IAA and their derivatives.

In maturing pea seeds, *PsTAR2* encodes the main enzyme for converting tryptophan and chlorinated tryptophan to IAA and chlorinated IAA, respectively (Tivendale et al, 2012). Here, we demonstrate that in addition to the reduced 4-Cl-IAA content in *tar2-1* seeds (Figure 3.7A), the levels of chlorinated IAA conjugates (including methyl esters) were also reduced (Figure 3.7B). We also report on strong reductions in the content of both IAA (Figure 3.7C) and IAA conjugates (Figure 3.7D) in mutant *tar2-1* seeds. These findings confirm that the vast majority of 4-Cl-IAA and IAA in maturing pea seeds is synthesised *via* the IPyA pathway. If this pathway made only a minor contribution, it is difficult to envisage how the *tar2-1* mutation could dramatically reduce the content of both free 4-Cl-IAA and 4-Cl-IAA derivatives.

However, the data in Figure 3.7E show no reduction in PAA in *tar2-1* seeds, and the level of PAA conjugates (putative end products) were also unaffected in the mutant (Figure 3.7F). The conjugate levels are in some ways more instructive than that of free PAA, since they provide a record of previous flux through the pathway. However, in both pea and maize, little is known about the specific nature of PAA conjugates. Our results indicate that TAR2 is unlikely to play a role in the synthesis of PAA in pea seeds. Interestingly, we did not detect chlorinated PAA in pea seeds, indicating some substrate specificity for the enzymes responsible for chlorination in these organs (Tivendale et al, 2012).

Sugawara et al (2015) reported a reduction in both IAA and PAA levels in dry seeds of the *TAA1* mutant (*wei8-1*) of *Arabidopsis*. However, the reduction in PAA was only 20% compared with 80% for IAA and no PAA conjugate data were provided. Sugawara et al (2015) also suggest that other TAA1-like enzymes may participate in the homeostatic regulation of PAA in the *wei8-1* mutant, thus explaining the weak reduction in PAA. However, in our system *PsTAR2* is strongly expressed from the middle to late stages of seed

development, while *PsTAR1* and *PsTAR3* are expressed at very low levels during this stage (Tivendale et al, 2012). In addition, expression of these genes was not altered in *tar2-1* seeds compared with the WT (Figure 3.8). We therefore conclude that the *TAR* genes, in general, do not appear to be involved in PAA biosynthesis in pea seeds.

We also exploited the *tar2-1* mutation to investigate the origin of (chlorinated) indole-3-acetaldehyde. The origin of this compound, and of the analogous PAAld, is relevant to the overall question of biosynthetic routes leading to auxins. The presence of some deuterium in PAAld after feeds of deuterated phenylpyruvate is consistent with phenylpyruvate being a precursor of PAAld. We found that in *tar2-1* seeds, the content of chlorinated indole-3-acetaldeyde was reduced (Figure 3.9); indicating that in pea seeds, chlorinated acetaldehyde originates mainly from the chlorinated IPyA pathway. This does not mean, however, that the acetaldehyde is further converted to 4-Cl-IAA in this system. Interestingly, in *Arabidopsis*, Mashiguchi et al (2011) concluded that indole-3-acetaldehyde does not originate from the IPyA pathway, possibly indicating a difference between the two species. The cause of any discrepancies between the two species is not currently known.

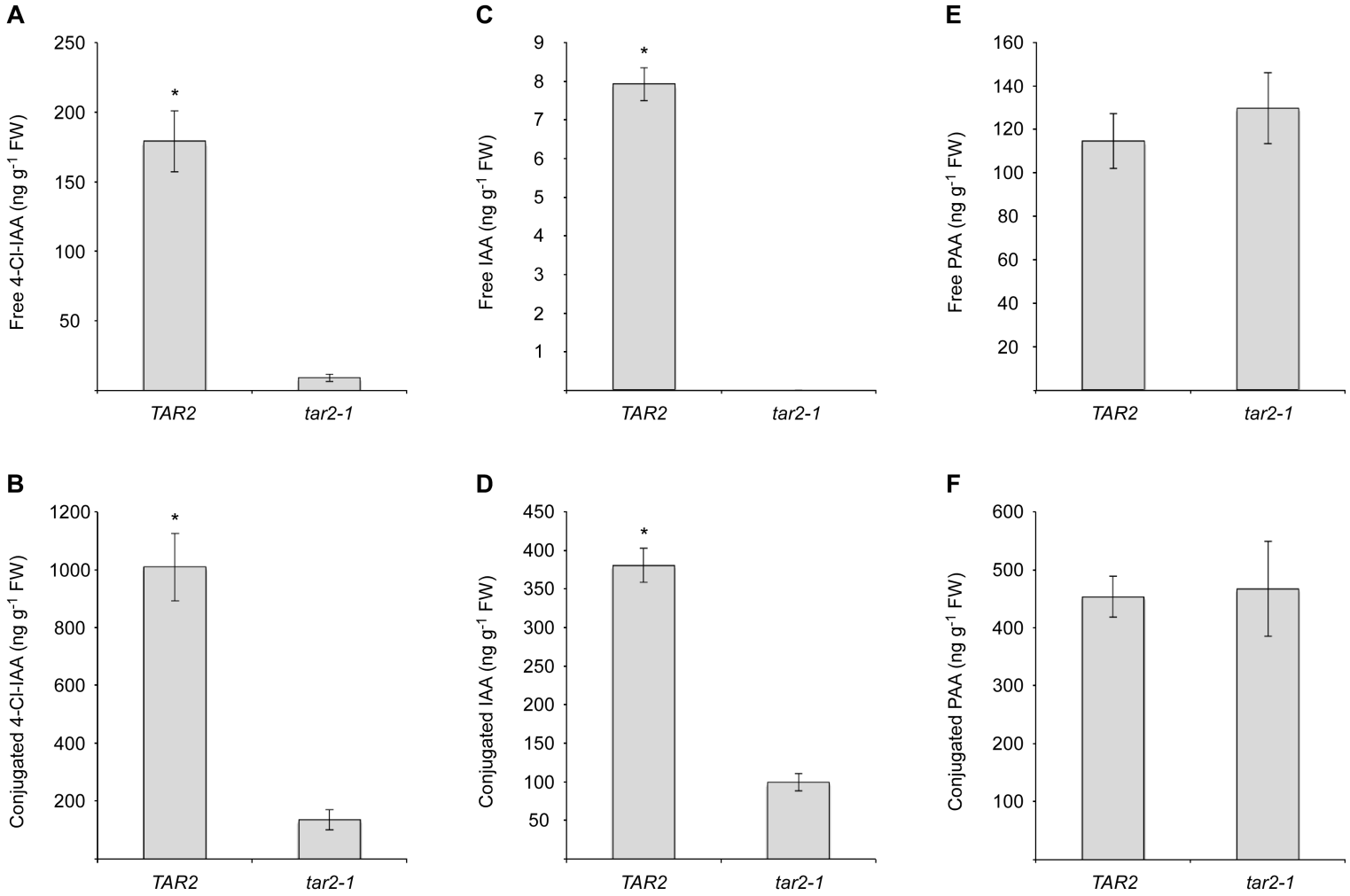

Figure 3.7 Effects of the pea *tar2-1* mutation on the levels of free auxins and auxin derivatives (including conjugates and methyl esters) in maturing seeds compared to the corresponding wild type (*TAR2*). Data are means ± SE (ng g^{-1} fresh weight [FW], n = 3-4). '*' Indicates a significant difference at the 0.05 level. (A) Free 4-Cl-IAA, (B) conjugated 4-Cl-IAA, (C), free IAA, (D) conjugated IAA, (E) free PAA and (F) conjugated PAA.

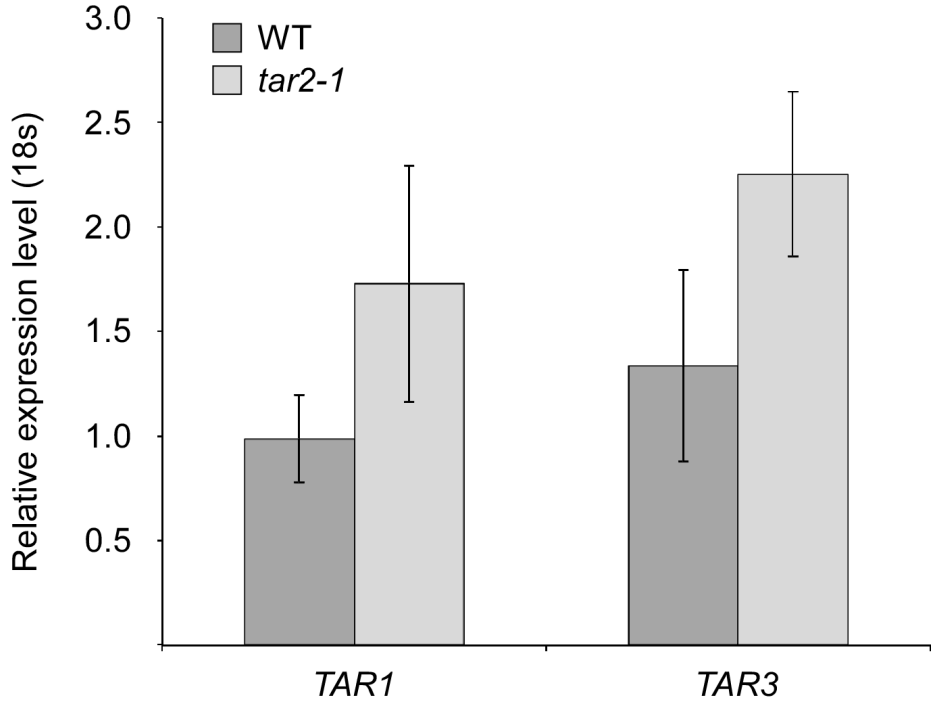

Figure 3.8 Effect of the *tar2-1* mutation on expression levels of *TAR1* and *TAR3* transcripts compared to WT. Levels are relative expression ± SE (n=4). Transcript expression was calculated in comparison to pea 18s ribosomal RNA levels in place of a housekeeper gene as described in Ozga et al (2003)

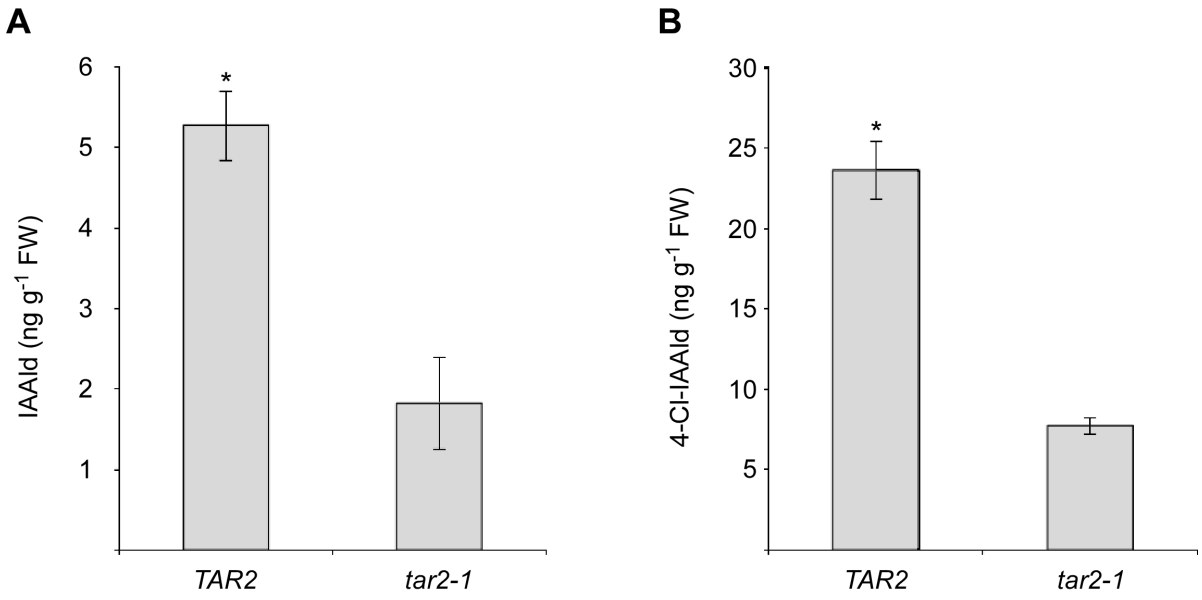

Figure 3.9 Effects of the *tar2-1* mutation on the levels of A: indole-3-acetaldehyde and B: 4-Cl-indole-3-acetaldehyde in maturing seeds. Data are technical means of pooled seeds ± SE (ng g^{-1} [FW], n=3). IAAld levels were obtained following conversion to tryptophol and 4-Cl-tryptophol.

3.3.6 PsTAR1 prefers Trp *in vitro*.

Another member of the pea *TAR* family, *PsTAR1,* is strongly expressed during the early stages of seed development (Tivendale et al, 2012). Since no *tar1* mutant is currently available, we instead expressed *TAR1* as a recombinant protein to test its functional activity in an enzymatic assay. Based on previous results in *Arabidopsis* (Tao et al, 2008), we sought to confirm if PsTAR1 was able to use a range of substrates *in vitro*.

As previously shown, PsTAR1 protein was able to convert Trp to IPyA *in vitro* (Tivendale et al, 2012). Following three hours incubation, more than 99% of the substrate was consumed (Figure 3.10A). Mass spectrometry identified significant amounts of IPyA in the reaction solution. As expected, large quantities of IAA were also present presumably due to the non-enzymatic degradation of IPyA to IAA (Tam and Normanly, 1998).

PsTAR1 also converted D_5 Phe to D_5 phenylpyruvate (Figure 3.10B), and D_5 PAA was also detected in the reaction mixture. However, the ratio of product to substrate was dramatically reduced for Phe, compared with Trp. Furthermore, less than half of the Phe substrate was consumed under identical conditions. These results show that PsTAR1 strongly prefers Trp to Phe, providing further evidence that TARs do not play a role in PAA biosynthesis in pea.

We also tested the ability of PsTAR1 to convert IPyA to Trp, given that transamination is reported to be a reversible reaction (Jensen and Gu, 1996). IPyA has previously been identified as a preferred substrate for AtTAA1 in in silico docking experiments (Tao et al, 2008), although to our knowledge this has not been confirmed in a functional assay. Here we report that PsTAR1 can catalyse the conversion of IPyA to Trp in vitro (Figure 3.10C). Consistent with IPyA as a preferred substrate (Tao et al, 2008), utilisation of D_5 Trp by PsTAR1 was reduced by 75% in the presence of IPyA (not shown). There is currently no evidence to suggest that the substrate preference of these enzymes is altered in vivo. As such, these results suggest that given the in

vitro substrate preference of TAR family proteins, it is unlikely that TARs play a major role in the PAA biosynthesis pathway in pea.

3.3.7 Alternative *aminotransferase* genes, separate from the *TAR* family, exist in the genome of pea.

Our results cast doubt on a role for *TAA1* or *YUC* in PAA biosynthesis, although they do suggest that PAA is synthesised from Phe through phenylpyruvate. Consequently, the question arises: are there alternative candidates for the enzymes that catalyse the conversion of Phe to PAA in pea? We therefore used a bioinformatics approach to identify enzymes that potentially play a role in PAA biosynthesis.

In petunia (*Petunia hybrida*), the conversion of phenylpyruvate to Phe can be catalysed by the phenylpyruvate aminotransferase, PhPPY-AT (Yoo et al, 2013). This reaction is reversible, and PhPPY-AT can also use Phe as a substrate (Yoo et al, 2013). In fact, this enzyme was initially identified using sequence information from an aminotransferase in *Cucumis melo*, which was also shown to utilize Phe *in vitro* (Gonda et al, 2010). Using these sequences we identified an aminotransferase (*PsCam000495_1*) in the pea gene atlas (Alves-Carvalho et al, 2015). We suggest that the encoded enzyme, a putative aromatic aminotransferase (PsArAT), is a strong candidate for the enzyme that converts Phe to phenylpyruvate in pea. PsArAT shares a strong similarity to the PhPPY-AT and CmArAT amino acid sequences (67% and 72% identity, respectively). Interestingly, there are no other similar sequences in pea, suggesting that PsArAT may be solely responsible for the transamination of Phe and phenylpyruvate in this species.

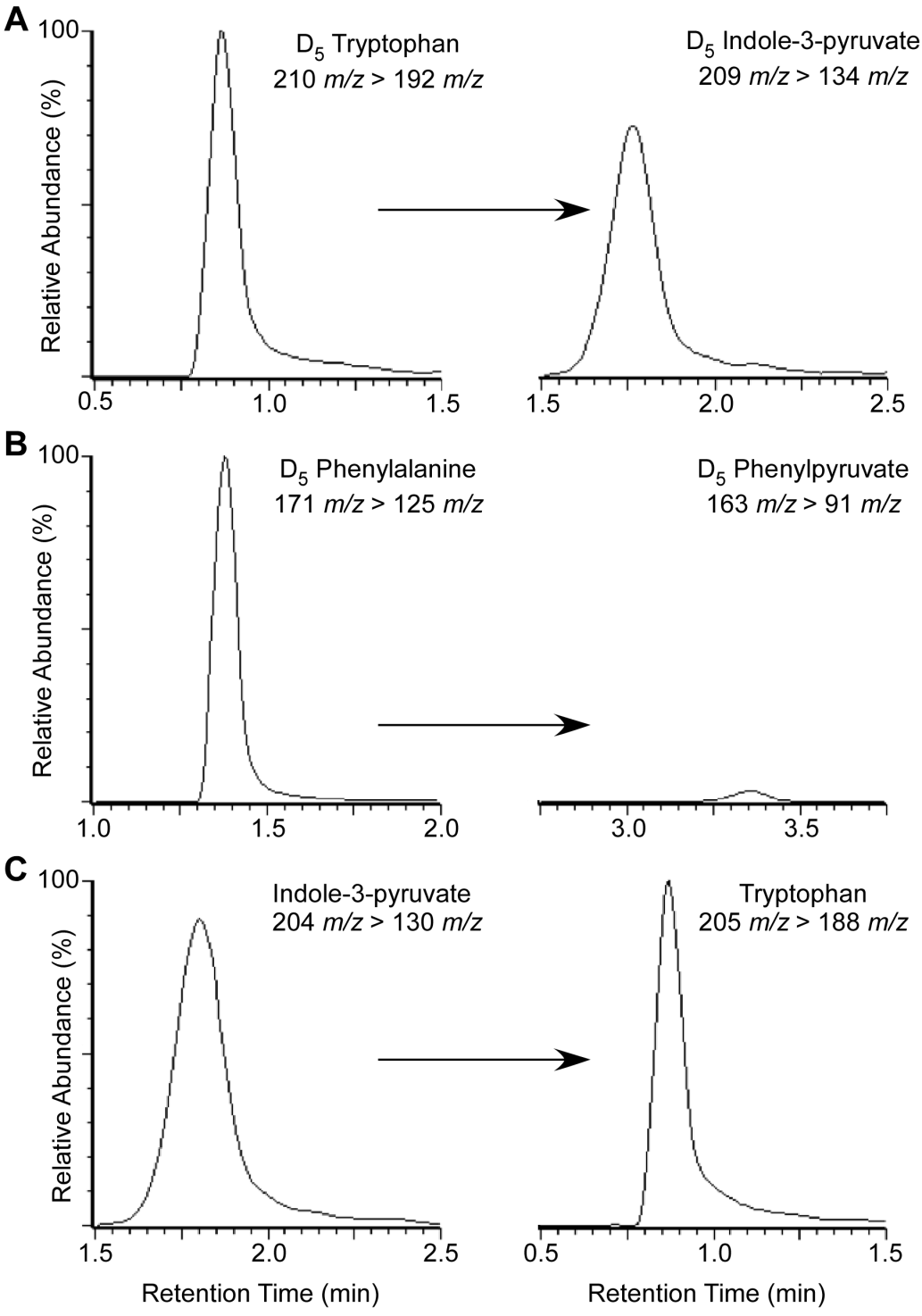

Figure 3.10. UPLC-MS chromatograms of in vitro enzyme assay products following incubation of recombinant PsTAR1 with D_5 Trp (to D_5 indole-3-phenylpyruvate; A), D_5 Phe (to D_5 phenylpyruvate; B), and indole-3-pyruvate (to Trp; C). Peaks are relative intensities accompanied by mass transitions. Arrows indicate the direction of reaction.

As transaminase activity for both CmArAT and PhPPY-AT has been demonstrated (Gonda et al, 2010; Yoo et al, 2013), we constructed a multiple sequence alignment (Figure 3.11) with these two sequences, and those of PsArAT and TcTAT (*Trypanosoma cruzi*), an aminotransferase on which x-ray crystallography has been conducted (Blankenfeldt et al, 1999). The PsArAT amino acid sequence contains conserved residues responsible for anchoring of the PLP co-factor as well as residues responsible for substrate binding (Blankenfeldt et al, 1999; Gonda et al, 2010). These residues are absolutely conserved across multiple lineages, including mammals and protozoans (Blankenfeldt et al, 1999), strongly supporting a potential role for PsArAT in the conversion of Phe to phenylpyruvate. However, the generation of a *PsArAT* mutant and subsequent enzymatic assays are required to demonstrate the biological function of this enzyme.

3.4 Conclusion

It is now widely accepted that for the biosynthesis of IAA, the IPyA pathway predominates in most, if not all, angiosperms (Zhao, 2012; Tivendale et al, 2014). Based on the chemical similarities of IAA and PAA, it has been suggested recently that the biosynthetic pathways for these two auxins are analogous, beginning from Trp and Phe, respectively (Sugawara et al, 2015). Here, using labelled compounds, we show that Phe can indeed be converted to phenylpyruvate, which can then be converted to PAA. However, while IAA biosynthesis appears to involve a simple 2-step pathway, it is possible that the intermediate phenylpyruvate is both a precursor and a metabolite of Phe. Consistent with its possible role as a Phe precursor, we show here that phenylpyruvate can be converted to Phe *in vivo*. An important difference between the analogous auxin pathways in plants is that, to our knowledge, IPyA is formed only from tryptophan whereas phenylpyruvate appears to be synthesised from both Phe and prephenate (Figure 3.12)(Cho et al, 2007; Maeda et al, 2010).

Our data from two *in vivo* systems indicate that the main enzymes for IAA biosynthesis are not the main enzymes for PAA biosynthesis. We

investigated the role of TAR and YUC in the synthesis of PAA by analysing hormone levels in hormone synthesis mutants. In both the pea *tar2-1* and the maize *de18* mutants, levels of IAA (and 4-Cl-IAA in pea) were dramatically reduced. Despite this, there were no consistent changes in the levels of PAA. We suggest that previous evidence (Sugawara et al, 2015) relies too heavily on gene overexpression, which results in accumulation of total PAA. However, overexpression of a gene that normally functions in a minor way can conceivably result in increased product levels, particularly when transcripts are elevated 100-fold. Based on our loss-of-function mutant data, it is unlikely that the very same TAA1 or YUC enzymes play a role in both IAA and PAA biosynthesis. Since other *TAR1*-like (pea) and *YUC*-like (maize) genes are only weakly expressed in the relevant tissues, we suggest that members of these families are not significantly involved in PAA biosynthesis. Additional work is required to definitively exclude either of these enzymes from the PAA biosynthetic pathway.

In order to explain the lack of effect of *TAA1* and *YUC* mutants on PAA content, Sugawara et al (2015) raised the possibility that quite different pathways might be involved in IAA and PAA synthesis. However, since sequence analysis of related aromatic aminotransferase proteins indicates enzymes with different functions in plants, we suggest that, while the biosynthetic pathways are analogous, the enzymes involved in these pathways belong to different gene families. We suggest that *in vivo*, there is a considerable degree of specificity for the aromatic aminotransferases, such that aminotransferases that utilise Trp do not use Phe to any great extent.

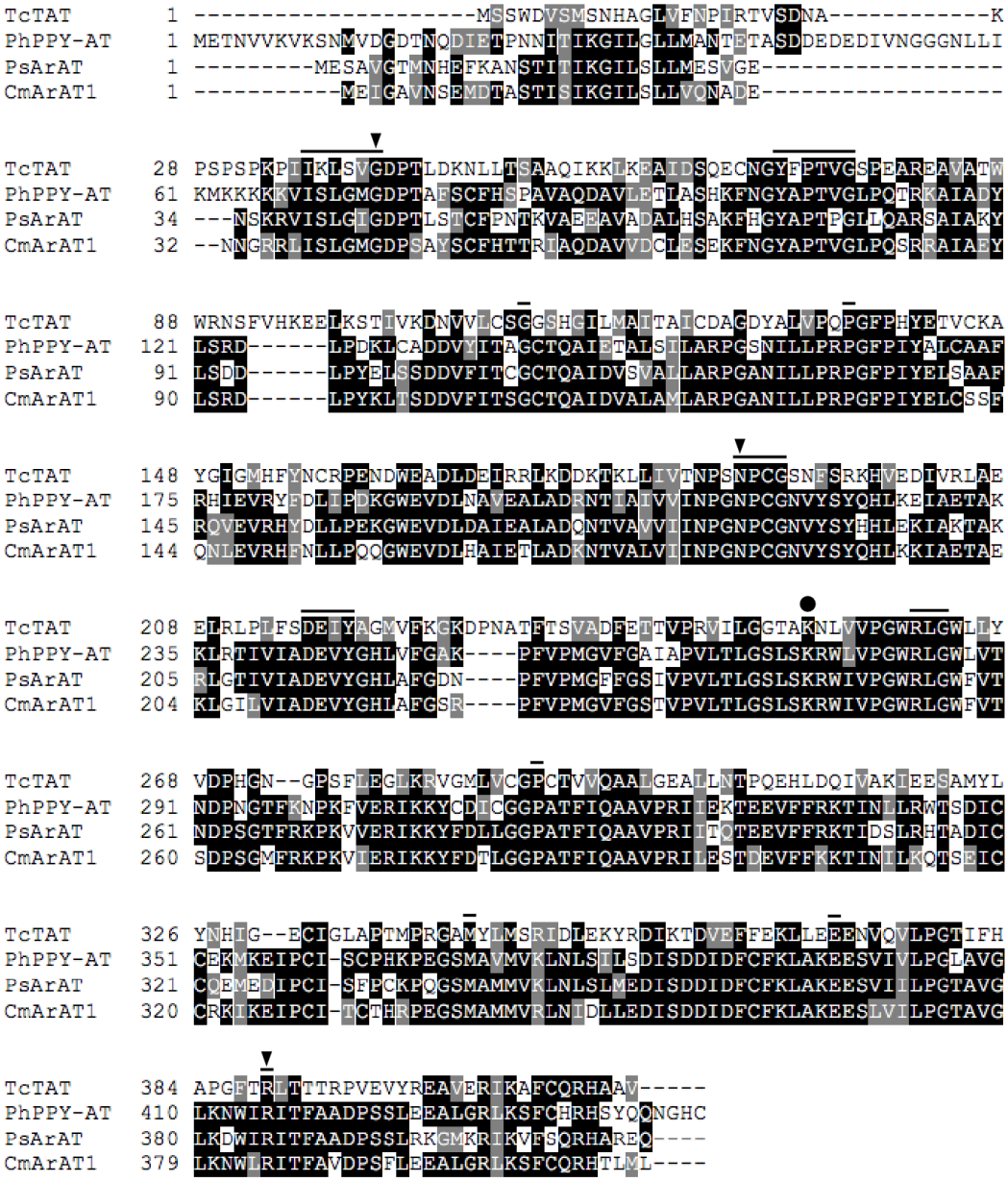

Figure 3.11. Multiple sequence alignment of aromatic aminotransferase proteins showing conserved amino acids in black and similarities in grey. The circle indicates the conserved lysine residue responsible for covalent bonding to the PLP co-factor and arrows indicate residues associated with substrate binding. Black bars indicate residues and motifs that are conserved across multiple genera as identified in Blankenfeldt et al (1999). Sequences included are CmArAT (NP_001284465), PsArAT (PsCam000495_1), PhPPY-AT (AHA62827) and TcTAT (P33447).

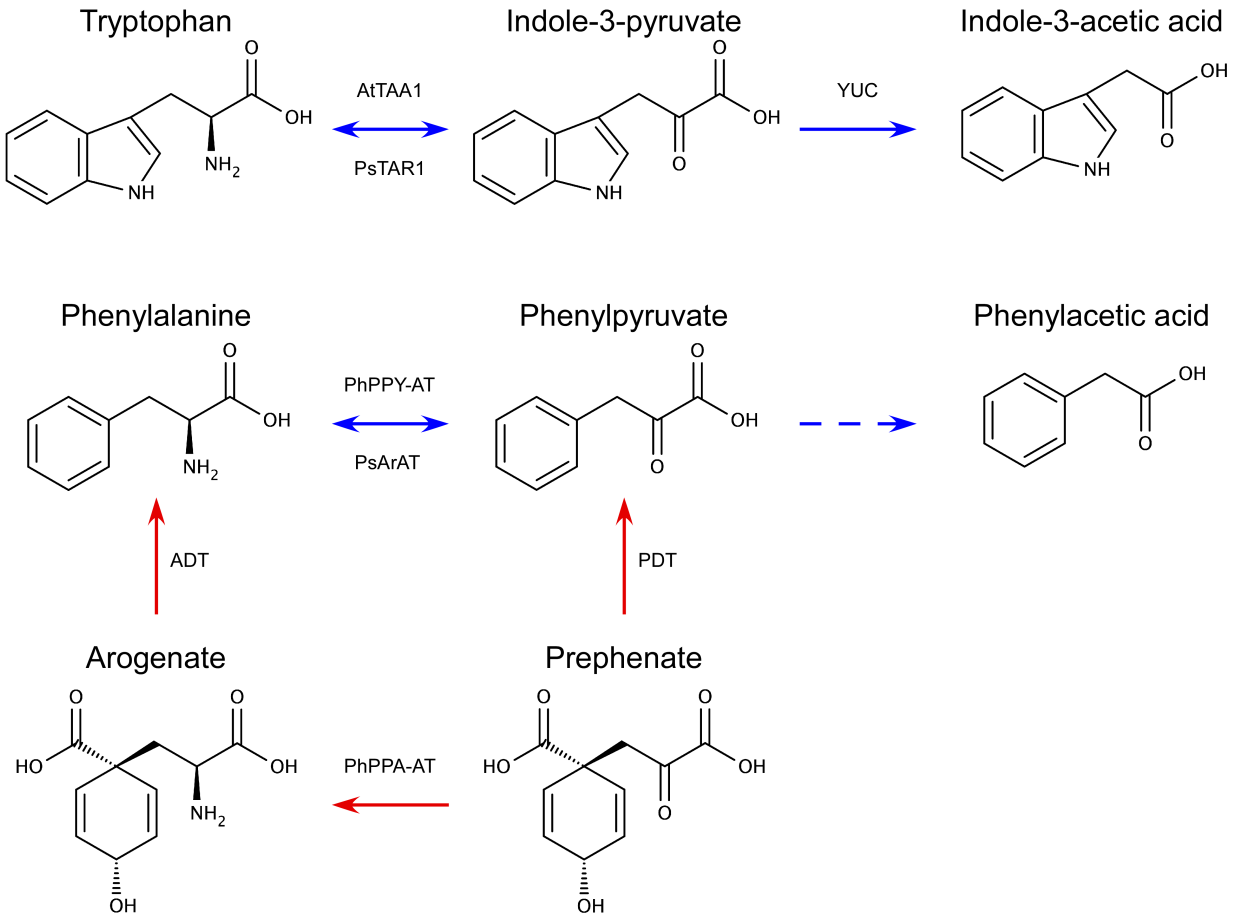

Figure 3.12. Comparison of the biosynthetic pathways for IAA and PAA (blue arrows) and Phe (red arrows). Catalytic enzymes are AtTAA1 and PsTAR1 (Trp aminotransferase related), YUC (flavin monooxygenase), PhPPY-AT and PsArAT (aromatic aminotransferase), ADT (arogenate dehydrogenase), PDT (prephenate dehydratase), and PhPPA-AT (prephenate aminotransferase). Arrows indicate direction of reaction, and the dashed line represents an as yet unknown catalytic mechanism.

3.5 Additional Materials and Methods

The following procedures were conducted by other researchers that have contributed to the generation of results presented in this chapter and in Cook et al (2016). Dr Erin McAdam and Dr Laura Quittenden conducted the quantitative real-time PCR and quantification of indole-3-acetaldehyde (and the 4-Cl- species) experiments. Dr Jason Smith synthesised the D_5 phenylpyruvate and its precursors, and Dr David Nichols developed of all novel UPLC-MS programs.

3.5.1 Quantitative real-time PCR

Mature green seeds of *TAR2* and *tar2-1* were harvested, and RNA extracted as before (Tivendale et al, 2012). Four replicates were taken for each genotype, each comprising one seed. cDNA was synthesized using random hexamers (Tetro cDNA synthesis kit, Bioline). First-strand cDNA was diluted 20 fold, with 1 µL used per 10 µL quantitative real-time PCR reaction using SYBR Green chemistry (SensiFAST™ SYBR® No-ROX Kit; Bioline). Samples were set up with a CAS-1200N robotic liquid-handling system (Corbett Research) and run for 50 or 55 cycles in a Rotor-Gene RG3000A Dual-Channel machine (Qiagen). Three technical replicates were performed for each biological replicate, and the concentrations were calculated relative to a curve containing seven serial dilutions (1/ 10) of original pooled cDNA taken equally from each replicate. Reaction efficiencies and correlation coefficients were as before (Tivendale et al, 2012). Pea 18s ribosomal RNA levels were utilized as before (Ozga et al, 2003), in place of a housekeeper gene. Primers used to amplify *TAR1* (JN990988.1) and *TAR3* (JN990990.1) were qPsTAR-Mt5g90 F92, qPsTAR-Mt5g90 r93 (*TAR1*) and qPsTAR3 F85, qPsTAR3 r85 (*TAR3*), respectively (Chapter 2.12).

3.5.2 Synthesis of D_5 phenylpyruvate

5.5.2.1 D_6 Azlactone

Ceric ammonium nitrate (55 g, 100.3 mmol) was dissolved in dilute nitric acid (3.5 M, 150 mL) and added to a solution of D_8-toluene (2.5 g, 2.5 mmol) in dilute nitric acid (3.5 M, 20 mL). The reaction mixture was heated at 80^{o}C for 2.5 hours before being cooled to room temperature and extracted with CH_2Cl_2 (3 x 75 mL). The combined organic extracts were washed with water (3 x 75 mL), dried over $MgSO_4$, filtered and evaporated to yield the crude D_6 benzaldehyde, which was added to acetylglycine (2.92 g, 25.4 mmol), sodium acetate (1.04 g, 12.7 mmol, 0.5 eq.) and acetic anhydride (5 mL, 43.1 mmol, 1.7 eq.). The mixture was refluxed for 1 hour before being removed from the heat and placed in a freezer overnight before collecting the D_6 azlactone by filtration (~50%).

3.5.2.2 D_6 Acetoaminocinnamic acid

D_6 azlactone (136 mg, 0.71 mmol) was refluxed in water (8 mL) and acetone (20 mL) for 4 hours before being cooled to room temperature. The acetone was removed under reduced pressure and the aqueous residue was extracted with ethyl acetate (3 x 20 mL). The combined organic extracts were washed with saturated NaCl (20 mL), dried, filtered and removed *in vacuo* to give the crude product (91 mg, 0.44 mmol).

3.5.2.3 D_5 Phenylpyruvate

D_5 acetoaminocinnamic acid (91 mg, 0.44 mmol) was refluxed in HCl (1 M, 10 mL) for 3 hours before being cooled to room temperature and extracted with ethyl acetate (2 x 20 mL). The combined extracts were dried over $MgSO_4$ and evaporated under reduced pressure to give crude D_5 phenylpyruvate as red brown crystals (55 mg, 0.33 mmol, 75%) 1H NMR (400 MHz) 4.22 (s, 3H), 8.5 (BS, 1H). e/z 169 (M+, 20%), 123 (60), 120(30), 118 (30), 110 (30), 96(100), 87(95), 82 (55).

3.5.3 Determination of indole-3-acetaldehyde and 4-Cl-indole-3-acetaldehyde

Seeds from *tar2-1* and *TAR2* lines were ground in liquid nitrogen and 600 µL of isopropanol was added. Following an overnight extraction, 2 ng and 10 ng of internal standard (D_2 tryptophol) was added to tryptophol and Indole-3-acetaldehyde (IAAld) samples, respectively. IAAld samples were further treated with sodium borohydride in 100 µL of 0.3 N NaOH and incubated for 1 hour at 35°C to stabilise IAAld as tryptophol. The pH of samples was reduced with 2 µL of 10 N HCl and isopropanol was evaporated under N_2 gas. Both IAAld and tryptophol samples were purified by SPE using SepPak cartridges (Waters) preconditioned with methanol and 1% acetic acid. Samples were eluted in 60% methanol and taken to dryness by rotary evaporation followed by re-suspension in 1% acetic acid for analysis by UPLC-MS. Levels of IAAld were calculated by subtracting endogenous tryptophol levels from tryptophol stabilised IAAld levels. 4-Cl-tryptophol levels were determined by comparison with added D_2 tryptophol internal standard.

Chapter 4: Further investigations of auxin biosynthesis in *Pisum sativum*

4.1 Introduction

There are three annotated *TAR* genes in pea (Tivendale et al, 2012), as well as a fourth in the pea gene atlas (PsCam057706)(Alves-Carvalho et al, 2015). In vitro activity for the *PsTAR1* and *PsTAR2* gene products has been demonstrated previously (Chapter 3)(Tivendale et al, 2012), although the expression pattern of these enzymes is only known for developing seeds (Tivendale et al, 2012). In this tissue, *PsTAR1* is highly expressed in early seed development and correlates with a peak in IAA levels. *PsTAR2* is expressed throughout seed development and is associated with the levels of 4-Cl-IAA (Tivendale et al, 2012). *PsTAR3* is also expressed in seeds, although its transcripts are at very low levels throughout development and maturation.

In pea, the *tar2-1* mutation causes a premature stop codon upstream of the PLP (pyridoxal ‘5 phosphate) binding domain essential for protein function (Tivendale et al, 2012). While, this mutation results in a reduction in the levels of both IAA and 4-Cl-IAA in developing seeds (Tivendale et al, 2012), the levels of PAA are normal in *tar2-1* seeds (Chapter 3). The reduction of IAA and 4-Cl-IAA is strongly correlated with a dimpled seed phenotype. However, *tar2-1* does not appear to directly alter vegetative development (McAdam et al, 2017a).

While the pea *tar2-1* mutation is relatively well characterised, little has been published on *PsTAR1* or *PsTAR3* (Tivendale et al, 2012), even though mutant lines for both of these genes have been produced by TILLING. Given

that auxin is abundant in seeds and its presence is essential for seed development, the polymorphisms in the *PsTAR1* and *PsTAR3* gene sequences and their respective effects on seeds are investigated here. Additionally, this chapter describes the development of a non-invasive technique for the introduction of auxin into seeds.

While there are currently no published *YUC* mutants in pea, recent characterisation of the *crispoid-4* (*crd-4*) mutation has identified a polymorphism in the *PsYUC1* gene sequence (McAdam et al, 2017b). The *crd-4* mutant was fortuitously identified and isolated from a population that contained a *PsTAR1* mutation, on the basis of the altered vascular development and crinkled leaf margins of the *crd-4* plants. In this chapter it is demonstrated that the *crd-4* mutant has altered IAA biosynthesis. It is further demonstrated that PsYUC1 does not affect the biosynthesis of PAA.

4.2 Materials and Methods

4.2.1 Plant material

All three mutations used were obtained through EMS mutagenesis of the Caméor line (TILLING)(Dalmais et al, 2008). Plants heterozygous for *TAR1*/*tar1-2* were obtained after backcrossing the initial line (TILLING line 2601) against Caméor six times. The *tar3* mutant (line 4005) was backcrossed to a similar extent although experiments were conducted on pure breeding mutants and WT plants grown on the same background. The *crd-4* line was isolated from TILLING line 905 and backcrossed to Caméor. Experiments on *crd-4* were conducted on segregating populations, which were screened for the presence of a WT copy of *TAR1*.

4.2.2 Genotyping by HRM

Genotyping of mutant *tar1-2* populations was conducted on gDNA extracted from developing leaflets as described in Chapter 2.8. HRM protocol is described in Chapter 2.10 using primers listed in Chapter 2.12

4.2.3 Application of 2,4-D

The synthetic hormone 2,4-D (2,4-dichlorophenoxyacetic acid, Sigma-Aldrich) was prepared as a solution containing 6 mg in 12 mL of 10% EtOH in dH_2O supplemented with 0.1% Tween20 (BioRad). Heterozygous plants segregating at the *TAR1* locus were grown for five weeks at which point they contained fully open flowers. 10 µL (5 µg), 50 µL (25 µg) and 100 µL (50 µg) of 2,4-D solution were applied to stipules subtending the open flowers (n=4). Superficial nicks were made to the stipules to facilitate uptake and a control solution of 10% EtOH in dH_2O was applied to control plants. Once pods had fully elongated, plants (n=2) were harvested to determine the presence of 2,4-D in pods and seeds. Seeds from remaining plants were harvested and planted once dry. The subsequent generation was grown until senescence and seeds from this generation were collected.

4.2.4 Phylogenetic analysis of the YUC family

The phylogenetic relationships between *YUCCA* family genes in *Arabidopsis thaliana*, *Medicago truncatula* and *P. sativum* were assessed using amino acid sequences obtained from Phytozome (phytozome.jgi.doe.gov; *A. thaliana* [TAIR release 10] and *M. truncatula* [Mt4.0v1]) and the *P. sativum* gene atlas (Alves-Carvalho et al, 2015). Additional sequences were obtained from GenBank (PhFLOOZY and ToFZY). Sequences were aligned using the Clustal Omega algorithm (Sievers et al, 2011) and phylogenies were reconstructed using an LG substitution model (Le and Gascuel, 2008) using the statistical analysis software ‘R’. The packages ‘*APE’* (Paradis et al, 2004) and ‘*phangorn’* (Schliep, 2011) were used for sequence management and modelling, and *‘ggtree’* was used for tree visualisation and manipulation.

4.3 Results

4.3.1 The synthetic auxin 2,4-D can be sequestered in seeds and affect the resulting seedlings

Initial analysis of the *tar1* mutation suggested that self-pollinated, heterozygous individuals are unable to produce homozygous mutant offspring (Adj Prof. J.J. Ross, pers. comm.). Phenotypically, all progeny resembled the WT, and genotyping of populations has previously used CAPS (Cleaved Amplified Polymorphic Sequence) markers to separate WT (*TAR1/ TAR1*) and heterozygous (*TAR1/ tar1*) individuals. However, at the stage when the current experimentation was conducted, this method was unable to identify mutants (*tar1/ tar1*) in segregating population screens. It was unclear whether the absence of homozygous mutants is a technical issue (i.e. poor CAPS resolution) or if there is a biological explanation for the absence of *tar1* mutants.

The HRM (High resolution Melt) analysis amplifies a small PCR product containing the polymorphism of the 2601 line (G599A, Figure 4.1). This polymorphism results in a premature stop codon at the W200 amino residue. As a result, the 2601 line lacks the absolutely conserved lysine residue (K221) required for aminotransferase activity in the *TARs* (Ferreira et al, 1993; Stepanova et al, 2008) as well as several conserved downstream residues (Figure 4.1). Similar to the CAPS markers, the HRM analysis was unable to clearly identify any homozygous mutants.

The PsTAR1 protein catalyses the reversible transamination of Trp to IPyA in vitro (Chapter 3)(Tivendale et al, 2012). As such, the absence of a WT *TAR1* allele in mutant plants might result in low IAA levels, and fertilisation (i.e. inviable pollen or ova) or seed development (i.e. early seed abortion) may be affected. This is demonstrated in other species, where auxin biosynthesis mutants often have irregular floral patterning and development, resulting in sterility (Nemhauser et al, 2000; Tobeña-Santamaria et al, 2002; Cheng et al, 2006; Gallavotti et al, 2008; Stepanova et al, 2008; Phillips et al, 2011).

Coincidentally, *PsTAR1* is strongly expressed during early seed development and, under normal conditions, is likely contributing significantly to the levels of IAA and 4-Cl-IAA in this tissue (Chapter 3)(Tivendale et al, 2012).

Since, at the time, the absence of homozygous *tar1-2* mutants might have been due to auxin deficiency, it was decided to support the system through the exogenous application of auxin. It was thought that application of endogenous auxins (IAA/ 4-Cl-IAA/ PAA) would be insufficient, as the plants would likely metabolise these compounds following application. It was also thought that the synthetic auxin, 2,4-D, would not be so easily metabolized. However, the application of 2,4-D, at this stage (to provide the system with an alternative auxin source) failed to produce any clear mutant plants when genotyped by HRM.

However, analysis of the treated plants showed that 2,4-D was indeed taken up into pods (Figure 4.2A) and developing seeds (Figure 4.2B). Interestingly, 2,4-D was also detected in germinating seedlings in the next generation (Figure 4.2C). Associated with this, there were obvious developmental defects in these individuals (at high doses only), which possessed narrow, elongated leaflets (Figure 4.3). However, these phenotypes were short-lived and normal leaf patterning resumed after node 4. Identical phenotypes were present in treated WT plants (not shown) and genotyping with HRM did not identify any homozygous *tar1* mutants. It appears that the leaf phenotype in the treated progeny was caused by the presence of 2,4-D during seedling germination.

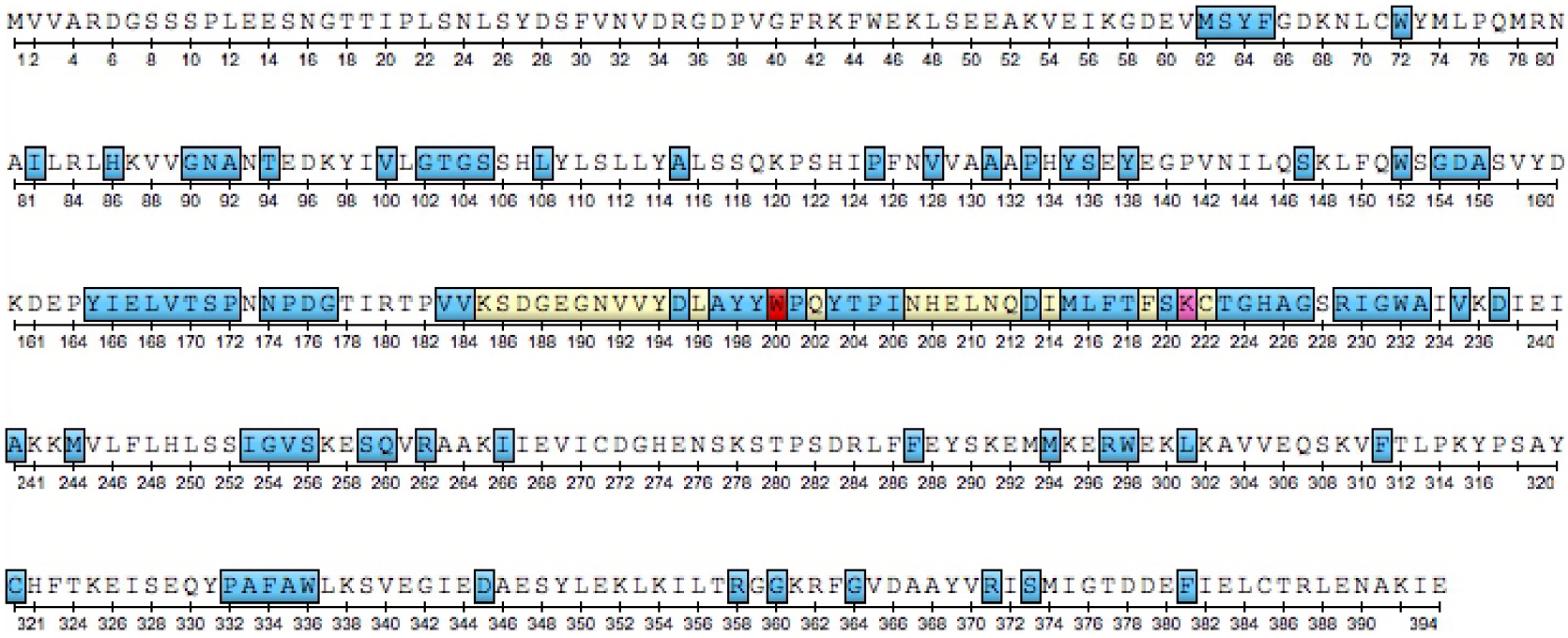

Figure 4.1 Amino acid sequence of the PsTAR1 protein showing the *tar1-2* polymorphism (red), conserved residues (blue), absolutely conserved lysine (pink) as well as the amplified HRM region (yellow). Residue positions are given below translated sequence.

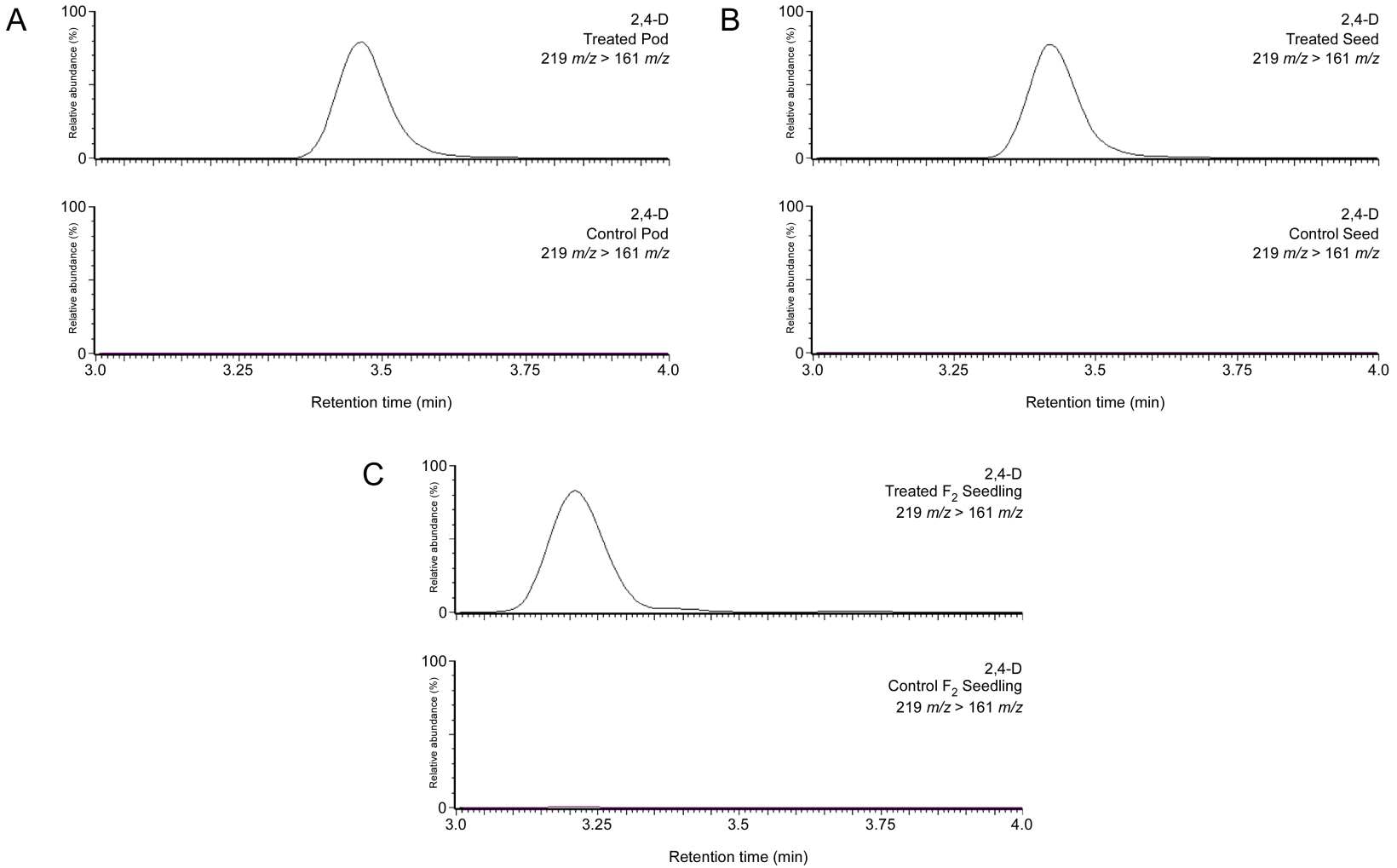

Figure 4.2 Representative UPLC-MS chromatograms showing presence and absence of 2,4-D in (A) pods, (B) seeds, and (C) seedlings from treated and untreated individuals, respectively. Peaks are relative intensities of the main 2,4-D transition (approximate retention time, 3.47 min). Retention time in (C) differed, due to preparation under neutral pH conditions.

Figure 4.3 Effect of 2,4-D application on the 14-day-old progeny from 5-week-old *tar1-2* individuals treated with 25 µg of 2,4-D (left) and control *tar1-2* individuals without 2,4-D application (right). Scale bar indicates 1 cm

4.3.2 PsTAR3 does not contribute significantly to auxin biosynthesis in pea seeds

The third tryptophan aminotransferase gene, *PsTAR3*, is expressed at low levels in developing seeds (Tivendale et al, 2012), and its transcripts are undetectable in whole shoots (Dr S.E. Davidson; pers. comm.). To determine if *tar3* mutants have altered hormone levels, three auxins (IAA, 4-Cl-IAA, and PAA) were measured in developing seeds over the course of three weeks.

Interestingly, the content of IAA was significantly elevated (~3000 ng g FW^{-1}, $P<0.05$) in 7 DAP seeds (Figure 4.4A), compared with the WT, but by 14 DAP, IAA levels were substantially lower (200-300 ng g FW^{-1}) and there was no difference between the mutant and WT. IAA content further diminished at 21 DAP, consistent with previous findings that 4-Cl-IAA replaces IAA as the most abundant auxin in pea seed development (Tivendale et al, 2012). However, the levels of 4-Cl-IAA were not altered by the *tar3* mutation at any time (Figure 4.4B), suggesting that the TAR3 protein does not contribute to 4-Cl-IAA biosynthesis to any great extent.

In Chapter 3 It is shown that the TAR2 enzyme does not contribute substantially to PAA biosynthesis, since the *tar2-1* mutation does not affect the levels of PAA. Similarly, the levels of PAA are not reduced in the *tar3* mutant (Figure 4.4C). If the TAR3 protein did contribute to PAA levels to any real extent, these levels should be reduced in the *tar3* mutant. However, even though IAA levels were unexpectedly elevated in 7 DAP seeds, the levels of PAA were unchanged. Preliminary analysis suggests that the TAR3 protein may contain activity on Trp in vitro (Cook, 2012), although its ability to use Phe as a substrate is yet to be determined. Additional enzymatic assays are required to determine the function of PsTAR3.

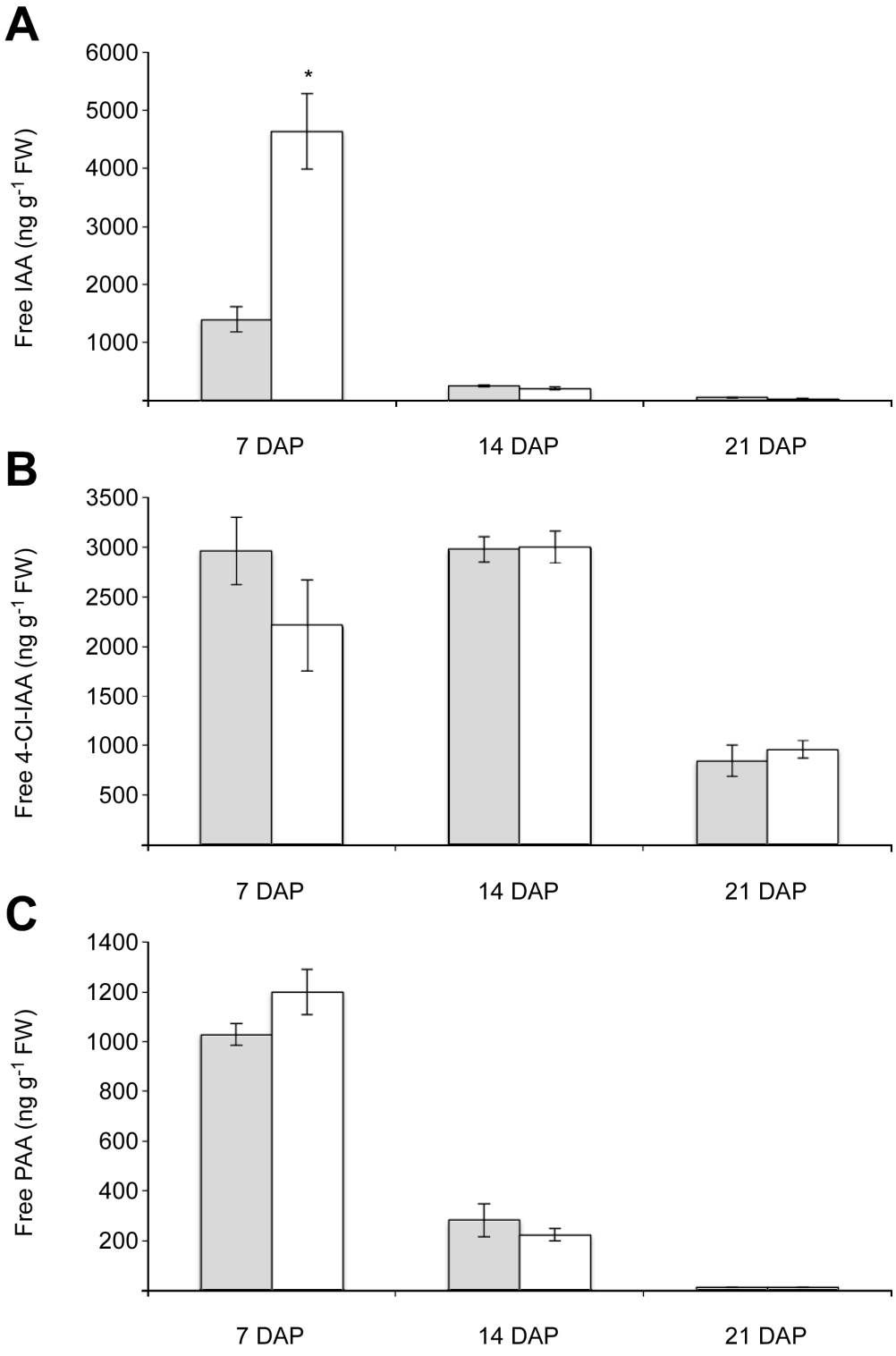

Figure 4.4 Effects of the *tar3* mutation on the endogenous levels of (A) IAA, (B) 4-Cl-IAA, and (C) PAA in pea seeds at 7, 14 and 21 DAP (days after pollination). Levels are ng g^{-1} fresh weight [FW] in both WT (grey) and *tar3* mutants (white). Data are means ± SE and an '*' indicates ($P<0.05$)

4.3.3 Auxin biosynthesis is altered in the *crd-4* mutant

The pea *crispoid-4* mutant has defective vegetative patterning, which manifests as a crinkling along the leaf margins. These mutants also possess altered vascular development, resulting in a 20% reduction in vein density (McAdam et al, 2017b). Similar phenotypes are seen in the petunia *floozy* mutant, which contains a mutation in a petunia ortholog of the *AtYUC1* gene (Tobeña-Santamaria et al, 2002). Genetic analysis of the *crd-4* mutant has identified a SNP in the *PsYUC1* coding sequence, which alters the intron splice receptor site, resulting in a non-sense C-terminus (Dr F Sussmilch; pers. comm.). Additional alleles for the *crispoid* locus have been identified and are explored in McAdam et al (2017b). While the *crd-4* mutation does not affect any of the conserved residues present in all flavin monooxygenases (Hou et al, 2011), it is appears that the C-terminus may be important for YUC function or stability.

To investigate whether a reduction in IAA levels causes the phenotype in the *crd-4* mutant, the levels of IAA were quantified in 2-week-old seedlings from *crd-4* and its WT. In this tissue the levels of IAA were not reduced (Figure 4.5B, $P > 0.05$). Interestingly, the *floozy* mutant in petunia also contains normal IAA levels (Tobeña-Santamaria et al, 2002). It has also been suggested that the YUC enzymes are responsible for the conversion of phenylpyruvate to PAA (Dai et al, 2013; Sugawara et al, 2015). However, the levels of PAA were also not reduced in 2-week-old *crd-4* seedlings (Figure 4.6B, $P > 0.05$). This is also the case with high order *YUC* mutants in *Arabidopsis,* which do not have reduced PAA content (Sugawara et al, 2015).

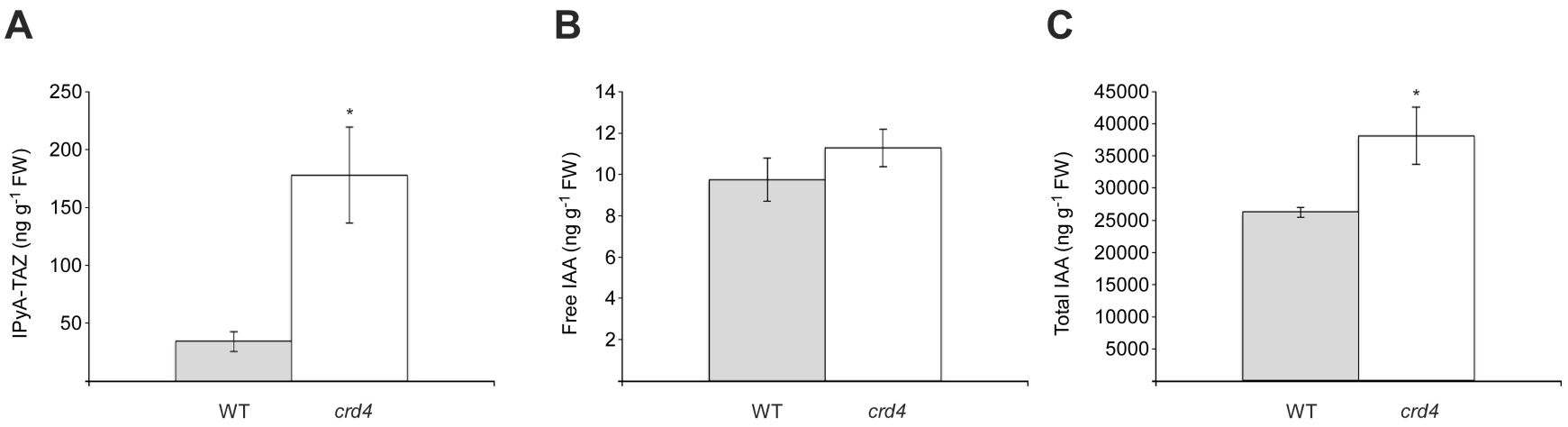

Figure 4.5 Effects of the *crd-4* mutation on the endogenous levels of (A) IPyA (TAZ labelled) in apical portions, (B) free IAA in 2-week-old seedlings, and (C) total IAA also in apical portions. Levels are ng g^{-1} fresh weight [FW] in both WT (grey) and *crd-4* mutants (white). Data are means + SE and an '*' indicates ($P \leq 0.05$)

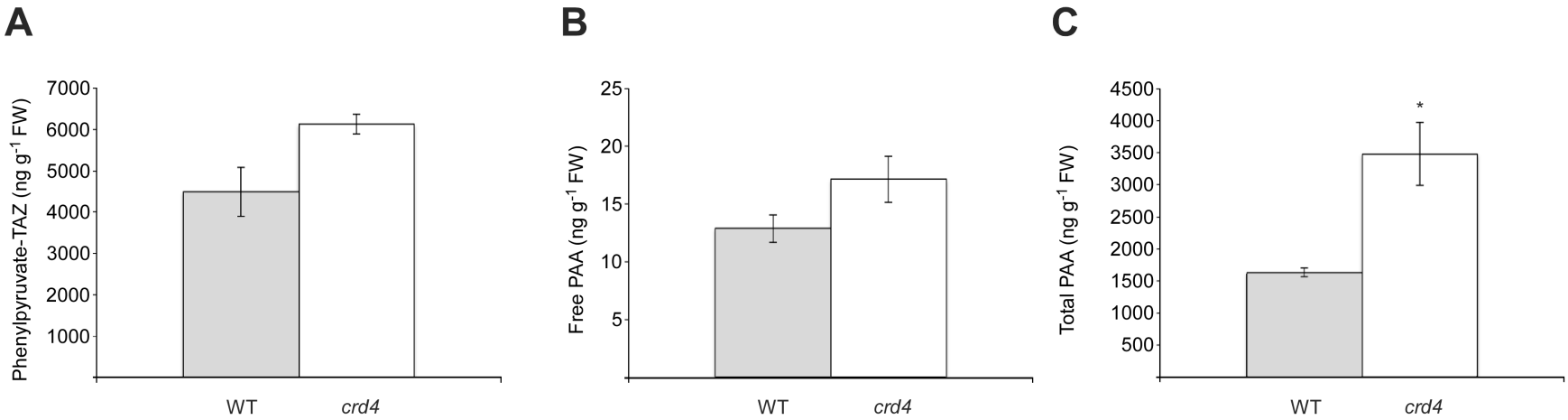

Figure 4.6 Effects of the *crd-4* mutation on the endogenous levels of (A) phenylpyruvate (TAZ labelled) in pea apical portions, as well as (B) free PAA, and (C) total PAA in 2-week-old seedlings. Levels are ng g^{-1} fresh weight [FW] in both WT (grey) and *crd-4* mutants (white). Data are means ± SE and an '*' indicates ($P<0.05$)

Further investigations were conducted on apical portions from the *crd-4* mutant as apices contain expanding leaves and the apical meristem, where *PsYUC1* transcripts should be highest (Tobeña-Santamaria et al, 2002; Cheng et al, 2006, 2007). Interestingly, the levels of IPyA (TAZ-labelled) showed a greater than 4-fold accumulation in mutant apex (Figure 4.5A, $P < 0.05$). However, the levels of phenylpyruvate were not elevated in this tissue (Figure 4.6A, $P > 0.05$), supporting the separate enzyme hypothesis (Chapter 3). Additionally, the levels of IAA conjugates were elevated in *crd-4* apex (Figure 4.5C, $P < 0.05$) and PAA conjugates were elevated in *crd-4* seedlings (Figure 4.6C, $P < 0.05$).

Phylogenetic trees depicting the relationship of auxin biosynthetic enzymes have been published extensively, although many of these early phylogenies use simple distance estimates to recreate tree topologies (Stepanova et al, 2008; Chourey et al, 2010; Tivendale et al, 2010; Mano and Nemoto, 2012; Tivendale et al, 2012). PsYUC1 was originally presented using a simple distance model (Tivendale et al, 2010). However, that reconstruction lacked many sequences now available from the Pea RNA-Seq gene atlas (Alves-Carvalho et al, 2015). While distance models are commonly used in auxin biology, maximum likelihood often produces more accurate and informative trees (Le and Gascuel, 2008). A phylogeny based on known protein sequences from *Arabidopsis*, *M. truncatula*, and pea, as well as *Petunia hybrida* (PhFLOOZY)(Tobeña-Santamaria et al, 2002), *Solanum lycopersicum* (ToFZY)(Expósito-Rodríguez et al, 2007) and a YUC sequence from *Klebsormidium flaccidum* (Turnaev et al, 2015) is presented in Figure 4.7.

PsYUC1 clusters with AtYUC1 and AtYUC4, which are expressed in vegetative and floral meristems, and in young leaf primordia (Cheng et al, 2006). Also in this clade is PhFLOOZY (Tobeña-Santamaria et al, 2002), which is phenotypically similar to the *Arabidopsis yuc1yuc4* double mutant (Cheng et al, 2006) and the *crd-4* mutant (McAdam et al, 2017b). Interestingly, PsYUC1 is the only pea YUC enzyme in the ‘floozy’ clade, despite the identification of 11 other *YUC* sequences in the pea gene atlas

(Alves-Carvalho et al, 2015). Three of these pea YUCs sit in the ‘reproductive development’ clade, which is sister to the ‘floozy’ YUCs. This sister clade has distinct, but overlapping expression with ‘floozy’ YUCs, but is primarily involved in reproductive development (Cheng et al, 2006).

Of the remaining pea YUCs, three sequences cluster with AtYUC3, AtYUC5, AtYUC7, AtYUC8 and AtYUC9, which are yet to be characterised in *Arabidopsis*. Three more cluster with AtYUC10 and AtYUC11, which are associated with embryogenesis (Cheng et al, 2006, 2007). The two remaining pea YUCs subtend this group, although may still be involved in embryogenesis.

4.4 Discussion

It is undeniable that auxin plays an important role in plant development as alterations to its synthesis, homeostasis, transport or perception can result in pronounced phenotypes (Woodward and Bartel, 2005; Quint and Gray, 2006; Guilfoyle and Hagen, 2007; Ludwig-Müller, 2011; Korasick et al, 2013). However, phenotypic effects do not always occur, and while the *tar1* and *tar3* mutations in pea do not produce any obvious developmental defects, similar to the *Arabidopsis taa1/ tar* mutants (Stepanova et al, 2008), the *crd-4* mutant confers obvious aberrant leaf and floral development (McAdam et al, 2017b).

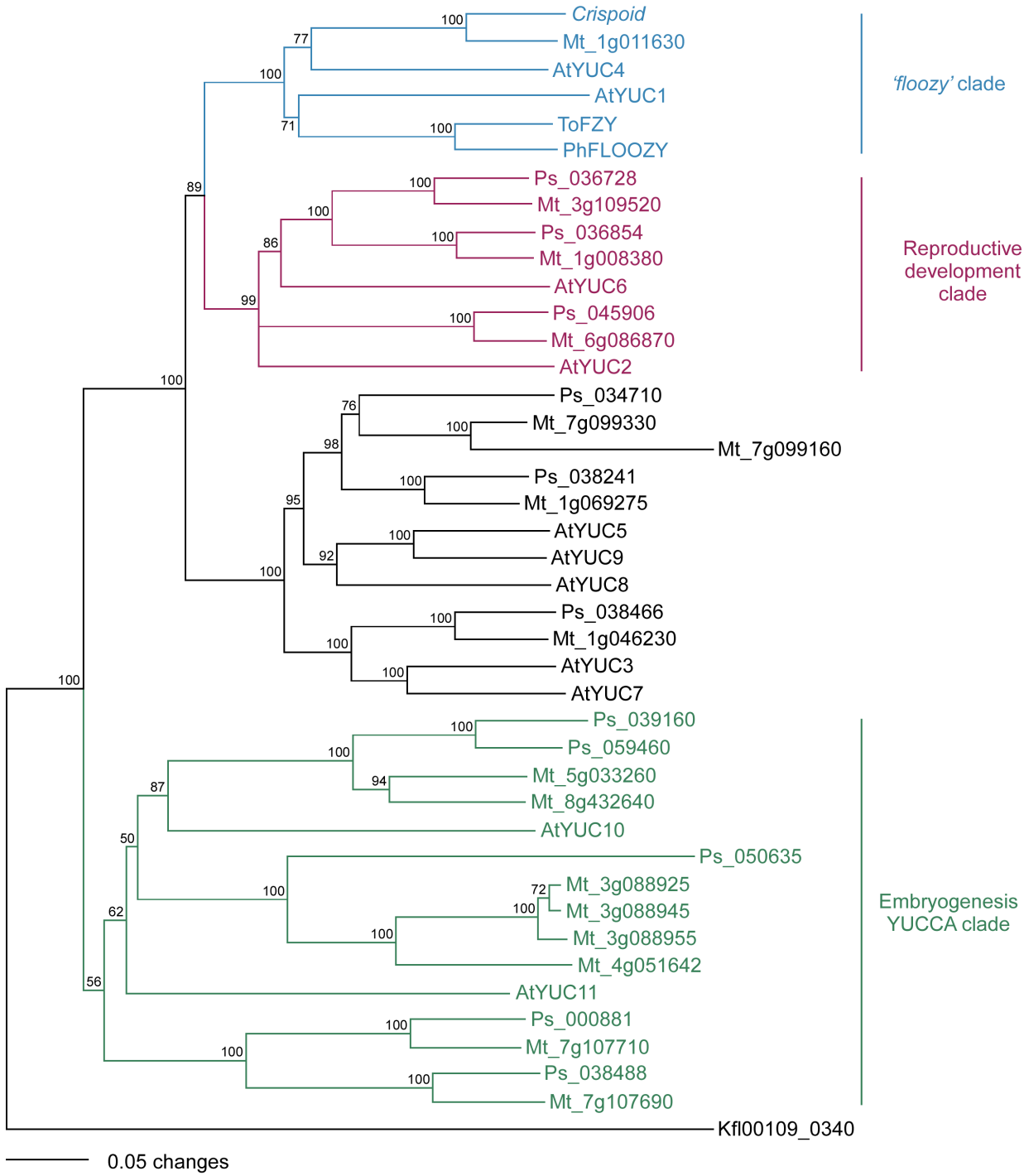

Figure 4.7 Phylogenetic reconstruction of the YUC protein family based on amino acid sequences. Tree contains sequences from pea (Ps), *Arabidopsis* (At), *Medicago truncatula (Mt), Petunia hybrida (*PhFLOOZY*), Solanum lycopersicum (*ToFZY*) and Klebsormidium flaccidum* (*Kfl*). Reconstruction utilised a LG model with optimised site variation and gamma distribution. Scale bar indicates changes per amino acid, and bootstrap values (from 1000 replicates) are presented adjacent to nodes. Distinct clades are highlighted blue 'floozy'; pink 'reproductive development' and green 'embryogenesis'.

4.4.1 The *tar1-2* mutant does not produce a phenotype and cannot be rescued by the application of 2,4-D

The *tar1-2* mutation in line 2601 involves the substitution of guanine to adenine (G599A), changing the tryptophan at residue 200 to a premature stop codon (Figure 4.1). A truncation of the protein at this site results in the loss of the absolutely conserved lysine residue (K221) required for binding to pyridoxal 5' phosphate (PLP)(Ferreira et al, 1993). PLP is an essential cofactor in all transaminase reactions and without the presence of the conserved lysine PLP is unable to form the Schiff base linkage required for aminotransferase activity (Ferreira et al, 1993; Liepman and Olsen, 2004). This residue has previously been shown to be essential for TAA1 activity in *Arabidopsis* (Stepanova et al, 2008). Recombinant proteins with a K217A substitution (which changes the conserved lysine) contained no aminotransferase activity despite substantial function in control reactions (Stepanova et al, 2008).

The absence of this residue in line 2601 should therefore result in complete loss of TAR1 function. In organs where *PsTAR1* is highly expressed, such as seeds during early development (Tivendale et al, 2012), the absence of a functional copy of this protein might result in a reduction of auxin levels and a distinct phenotype. This is demonstrated in the maize *vanishing tassel2* (*vt2*) mutant (Phillips et al, 2011). However, in *Arabidopsis*, the functional redundancy in the TAA family means that high order loss of function mutants are required to produce obvious phenotypes (Stepanova et al, 2008; Tao et al, 2008).

Since heterozygous plants are phenotypically identical to WT individuals, it is possible that either a single WT copy of *TAR1* is sufficient for regular IAA biosynthesis (i.e. the mutation is recessive), or that one of the other TAR enzymes can compensate for the loss of TAR1. In particular, PsTAR3 shares strong similarity with PsTAR1 (62% identity), although it is possible that any combination of TAR2, TAR3, and/ or the recently identified TAR4 (PsCam057706)(Alves-Carvalho et al, 2015) may compensate for the loss of

TAR1 function. However, HRM genotyping, using the techniques described here, failed to identify homozygous mutant individuals. The apparent absence of mutants here is a silent phenotype in itself, and suggests that development prior to seed maturation may be inhibited by local reductions of auxin levels. Additional work on seed abortion is required.

To alleviate the putative low auxin level in heterozygous plants, the synthetic auxin, 2,4-D (2,4-dichlorophenoxyacetic acid), was applied to heterozygous *TAR1/ tar1-2* plants. 2,4-D is not readily metabolised by plants, unlike IAA or 4-Cl-IAA, and is readily transported (in pea), at least from stipule to reproductive structures (Figure 4.2). Yet, despite the incorporation of 2,4-D into the developing seeds of both heterozygous and WT plants, no mutants were observed in the progeny of treated heterozygous plants.

It is unclear whether 2,4-D is capable of compensating for IAA levels in *tar1-2* mutants. However, 2,4-D was sequestered during seed maturation and was detectable in offspring from both heterozygous and WT plants (Figure 4.2C). The transmission of 2,4-D from parent to offspring has not been published previously and may be useful for studying the role of auxin in germination. The progeny of treated plants produced narrow epinastic leaves (Figure 4.3), a common high auxin phenotype (Zhao et al, 2001). The leaf phenotypes were most likely caused by the accumulation of 2,4-D, since untreated plants produced normal progeny. It is unclear whether this phenotype is produced during embryo development or during germination, although offspring did not display increased apical dominance at any point.

4.4.2 PsTAR3 does not contribute significantly to auxin biosynthesis

The function of the *PsTAR3* gene product is likely to be similar to that of *PsTAR1*, given their strong sequence similarity (Tivendale et al, 2012). Unfortunately, the functional activity of the TAR3 protein could not be demonstrated using in vitro assays due to complications during the

expression of the recombinant protein. However, TAR1 has been shown to possess transaminase activity and is able to convert Trp to IPyA in vitro (Chapter 3)(Tivendale et al, 2012). As such, mutations in *PsTAR3,* as with *PsTAR1*, might affect the biosynthesis of auxin in tissues where these transcripts are expressed.

Unlike the *tar2-1* mutant (Chapter 3)(Tivendale et al, 2012), which causes substantial reductions in the levels of IAA and 4-Cl-IAA in developing pea seeds, the levels of these two auxins, as well as PAA are not reduced in *tar3* mutant seeds. This is interesting, as IAA levels are reduced in several tissue types in the *Arabidopsis wei8-1* (Sugawara et al, 2015) and *wei8-1tar2-1* mutants (Stepanova et al, 2008). The *wei8-1* mutant in *Arabidopsis* also contains slightly reduced PAA levels in dry seeds (Sugawara et al, 2015). The *tar3* mutant does not produce a phenotype in either seeds or vegetative tissue, although due to the normal IAA levels detected in older seeds, this is unsurprising. It is possible, given the low expression of *PsTAR3* transcripts that this enzyme does not contribute to auxin biosynthesis in pea seeds.

It is curious that IAA levels were elevated in young *tar3* mutant seeds (in this experiment) as this enzyme is barely expressed compared to the other TAR enzymes (Tivendale et al, 2012). However, this elevation is short lived and levels are restored in 14 DAP seeds. The *tar3* mutant also contains normal PAA levels, which supports the two-enzyme hypothesis (Chapter 3). However, the levels of 4-Cl-IAA are also normal throughout seed development. Since PsTAR2 is the primary aminotransferase in seed development, normal 4-Cl-IAA levels are not surprising.

4.4.3 PsYUC1 is expressed in a spatiotemporal niche.

The *crd-4* mutant was recently isolated from a TILLING line that carried a mutation in *TAR1*. The *crd-4* mutant was identified as having altered leaf architecture, a typical phenotype of altered auxin biology (Tobeña-Santamaria et al, 2002; Cheng et al, 2006, 2007; Stepanova et al, 2008). The *crd-4* mutation co-segregated with *PsYUC1*, and sequencing of the *PsYUC1* loci has identified a SNP causing an alteration to the fourth intron splice site (McAdam et al, 2017b). This polymorphism results in complete mis-sense of the C-terminal of the PsYUC1 protein, although known conserved residues involved in binding are located upstream and are thus retained (Hou et al, 2011).

Single mutations in the *YUC* biosynthetic genes of *Arabidopsis* do not produce obvious phenotypes, unless other members of this family are also knocked out or down (Cheng et al, 2006, 2007; Sugawara et al, 2015). This speaks to the renowned functional redundancy and overlapping expression of these genes in *Arabidopsis* (Zhao et al, 2001; Cheng et al, 2006, 2007; Zhao, 2010; Sugawara et al, 2015). Interestingly, however, *YUC* single mutants in maize such as *spi1* (Gallavotti et al, 2008) and *de18* (Bernardi et al, 2012) produce obvious phenotypes and have markedly reduced IAA levels.

Similar to other *YUC* mutants in *Arabidopsis* and *Petunia hybrida* (Tobeña-Santamaria et al, 2002; Sugawara et al, 2015), the levels of IAA in *crd-4* are not reduced compared to the WT (Figure 4.5). However, unlike the single *Arabidopsis* mutants, *floozy* and *crd-4* produce clear phenotypes. While the IAA levels in *crd-4* whole seedlings were not reduced, the level of IPyA accumulated significantly in the *crd-4* apex (Figure 4.5). This four-fold increase in IPyA levels is consistent with a blockage in the conversion of IPyA to IAA, the step catalysed by the YUC enzymes (Mashiguchi et al, 2011; Won et al, 2011).

The normal IAA levels in *crd-4* shoots can be best explained through the expression of *PsYUC1* in a specific tissue at a specific developmental stage. In addition, the accumulation of IPyA can only be explained by the absence of a YUC with overlapping expression. This suggests that *PsYUC1* (and possibly the *P. hybrida* homolog) is expressed in a spatiotemporal niche. The YUC phylogenetic tree (Figure 4.7) shows that *PsYUC1* is the only pea YUC present in the 'floozy' clade, which also includes AtYUC1 and AtYUC4 from *Arabidopsis*, and *floozy* from petunia. It has been shown that both *AtYUC1* and *AtYUC4* have almost identical expression patterns, and knockout of both these genes results in obvious growth and developmental defects (Cheng et al, 2006). In fact, the phenotypes produced by the *Arabidopsis* double mutant (*yuc1yuc4*) strongly resemble those of *crd-4* and *floozy* (Tobeña-Santamaria et al, 2002).

The expression of members of the 'floozy' clade is highest in developing leaf margins and meristematic regions, as well as in vascular tissue (Tobeña-Santamaria et al, 2002; Cheng et al, 2006, 2007). However, the 'floozy' clade also shares overlapping expression with its sister clade, which contains *AtYUC2* and *AtYUC6*. Both of these YUCs are expressed slightly later in vegetative tissue and in reproductive tissue. The combination of either *yuc1* or *yuc4* with *yuc2* or *yuc6* produces a slight phenotype, and the additional loss of *yuc2* or *yuc6* on the *yuc1yuc4* background retards growth and development substantially (Cheng et al, 2006). The IAA levels in the *yuc1yuc2yuc6* triple mutant are also reduced when compared with the WT (Sugawara et al, 2015), indicating that a single member from both of these clades is required for normal plant development. In pea, the sister clade contains three YUC proteins (Figure 4.7). If the expression patterns of the 'floozy' and 'Reproductive development' clades are similar in pea, it is likely that the three sister YUCs would be able to quickly restore normal IAA levels in the *crd-4* mutant.

The IAA conjugates also accumulated slightly, compared with the WT, in the *crd-4* apical bud. This is interesting, as *GH3s* should be less active following a drop in IAA. This would result in reduced conjugation and conjugate levels

(Mellor et al, 2016). There is little known about the steps that occur following conjugation by GH3s, although it has been demonstrated that both IAA-Asp and IAA-Glu can be converted to oxIAA-Asp and oxIAA-Glu, respectively (Östin et al, 1998; Kai et al, 2007; Pěnčík et al, 2013). The mechanisms behind this oxidation are currently unknown, although in *Arabidopsis*, neither ^{14}C IAA-Asp nor ^{14}C IAA-Glu was metabolised within 24 hours of application to *Arabidopsis* plantlets (Pěnčík et al, 2013). As such, the slight elevation of bound IAA (and PAA) might be explained by the slow catabolism of IAA-Asp and IAA-Glu relative to the rapid conjugation of IAA by the GH3s (Hagen and Guilfoyle, 2002; Pěnčík et al, 2013).

4.4.4 PAA biosynthesis is unaffected by the absence of PsYUC1

It was recently suggested that the TAA1/ TAR and YUC enzymes might be responsible for the conversion of Phe to phenylpyruvate, and from phenylpyruvate to PAA (Sugawara et al, 2015). This hypothesis is challenged in Chapter 3, where it is suggested that the in vitro function of these enzymes does not necessarily equate to their role in vivo. It is also suggested that the ArATs may function instead of the TARs for the conversion of Phe to phenylpyruvate. It is important to determine if the YUC enzymes function in the conversion of phenylpyruvate to PAA and alter the levels of PAA and its precursors.

In two-week-old *crd-4* seedlings, the levels of endogenous PAA were not significantly different from the WT (Figure 4.6). This supports the hypothesis that an alternative mechanism may be responsible for the conversion of phenylpyruvate to PAA. However, the levels of free IAA were also normal in this tissue (Figure 4.5). On the other hand, while the level of IPyA was elevated in *crd-4* apical buds (Figure 4.5), the phenylpyruvate content was not different from that of the WT (Figure 4.6). The combination of these two results suggests that PsYUC1 is unlikely to be essential for the biosynthesis of PAA. Despite this, the levels of PAA conjugates were elevated in this tissue (Figure 4.6); the reason for this observation is not clear.

4.5 Conclusion

This chapter has further addressed components of the IPyA pathway in pea to better understand the contributions of the TARs and YUCs to auxin biosynthesis in this species. The expression of the *TAR* genes is well characterised in pea seeds (Tivendale et al, 2012), yet only the *tar2-1* mutant has been investigated to any extent. Similarly, the *crd-4* mutant has only recently been characterised as a mutation in the *PsYUC1* genetic sequence (McAdam et al, 2017b). The research presented in this chapter will serve to assist further investigations on auxin biosynthesis in pea.

It is interesting that heterozygous individuals for *tar1-2* (Line 2601) do not produce any progeny with a distinct phenotype. This mutation results in the complete loss of the absolutely conserved lysine and several other conserved residues (Figure 4.1). Under normal inheritance patterns, 25% of offspring should contain two copies of the mutant allele. The experimental application of 2,4-D was conducted on the assumption that localized low auxin levels might prevent the production of homozygous *tar1-2* mutants, since fertility is known to be affected in auxin mutants (Nemhauser et al, 2000; Tobeña-Santamaria et al, 2002; Cheng et al, 2006; Gallavotti et al, 2008; Stepanova et al, 2008; Phillips et al, 2011). The demonstration that 2,4-D moved from the leaf into developing seeds, and its “vertical transmission” to the resulting seedlings is a useful observation. This synthetic auxin is not completely broken down during seed filling and maturation in pea. 2,4-D has been used extensively as a tool in auxin related research and may prove to be effective for further analyses on the role of auxin in germination.

The *tar3* mutation does not produce an obvious vegetative or seed phenotype. This is not unexpected given that single mutants in *Arabidopsis* also lack a distinct phenotype under normal growth conditions (Stepanova et al, 2008; Tao et al, 2008). Quantification of PAA levels in the *tar3* mutant suggest that the *PsTAR3* gene product does not contribute significantly to its biosynthesis, although 4-Cl-IAA levels (and IAA in 14 and 21 DAP seeds)

were also normal throughout seed development. This suggests that PsTAR3 may not be functional in auxin biosynthesis, at least in pea seeds. The elevated IAA in 7DAP seeds was unexpected, although this result was only demonstrated in a single experiment. It is possible that the up regulation of other TARs, or any of the *YUCs*, may explain this accumulation.

The spatiotemporal expression of *YUC* genes is not a novel suggestion (Zhao et al, 2001; Cheng et al, 2006, 2007). This redundancy makes it difficult to present evidence that the IPyA pathway is altered in *YUC* mutants. In this chapter, it is demonstrated that a mutation in PsYUC1 results in an accumulation of IPyA, demonstrating a blockage of the oxidative decarboxylation of IPyA to IAA. The normal IAA levels in whole seedlings can be explained through the overlapping expression and functional redundancy of the *YUC* genes (Zhao et al, 2001).

As explained in Chapter 3, strong evidence indicates that the *YUC*s are not responsible for PAA biosynthesis. However, an alternative for the *YUC* genes is not so clear. The most logical alternative is that phenylpyruvate is converted to phenylacetaldehyde, a reaction that has been demonstrated previously (Chapter 3)(Boatright et al, 2004). Phenylacetaldehyde would then be converted to IAA by an as yet unknown mechanism. This pathway (phenylpyruvate → phenylacetaldehyde → phenylacetic acid) is functional in bacteria and fungi (Kishore et al, 1976; Somers et al, 2005; Spaepen et al, 2007) and may function in plants. Alternatively, phenylpyruvate may be converted to PAA by a non-YUC FMO (flavin-containing monooxygenase). However, more work is required to understand the biosynthesis of PAA.

Chapter 5: Evolution of auxin biosynthesis and metabolism

5.1 Introduction

Auxin biosynthesis has now been well characterised in the angiosperms (Chapter 1). Model species such as *Arabidopsis* (Stepanova et al, 2008; Tao et al, 2008; Mashiguchi et al, 2011; Won et al, 2011), maize (Gallavotti et al, 2008; Phillips et al, 2011) and pea (Chapter 3)(Tivendale et al, 2012), have been instrumental in elucidating the IPyA pathway and demonstrating its importance in IAA biosynthesis. However, the understanding of IAA biosynthesis in basal lineages has only limited experimental support (Jayaswal and Johri, 1985; Eklund et al, 2015) and typically relies on phylogenetic comparisons of gene families to imply function (Yue et al, 2014). There is evidence that the IPyA pathway is functional in the liverwort, *Marchantia polymorpha* (Eklund et al, 2015), and the moss, *Funaria hygrometrica* (Jayaswal and Johri, 1985). However, evidence for a functioning IPyA pathway in the hornworts, lycophytes, ferns and gymnosperms is lacking.

IAA is ubiquitous in land plants and its presence has also been demonstrated in both red (Ashen et al, 1999; Yokoya et al, 2010) and brown algae (Le Bail et al, 2010), as well as bacteria (Spaepen et al, 2007) and fungi (Reineke et al, 2008). The broad distribution of this phytohormone suggests that it is ancient in origin, although the specific origin of IAA biosynthesis in plants is heavily disputed (Lau et al, 2009; Huang et al, 2014; Wang et al, 2014; Yue et al, 2014; Turnaev et al, 2015; Wang et al, 2016).

Recently, Yue et al (2014) suggested that a horizontal gene transfer (HGT) event from bacteria to the most recent common ancestor (MRCA) of the land plants identifies a the origin of the IPyA pathway in land plants. These authors were unable to find any direct homologs of the YUCs in the

Characeae, the closest division to the land plants (Karol et al, 2001; Wickett et al, 2014). However, Wang et al (2014) present evidence that both TAA1- and YUC-related sequences are present in *Klebsormidium flaccidum*, a member of the Klebsormidiaceae, a higher charophyte. They also propose several, more complex, models whereby multiple HGT events have taken place; of note is the hypothesis that two separate HGT events, one to plants and one to algae, have occurred. In response to this, Huang et al (2014) suggest that multiple HGT events are not parsimonious as this implies that the charophytes and the land plants do not form a monophyletic group.

Turnaev et al (2015) conducted similar investigations but found that of the available charophyte databases, only *K. flaccidum* contains a *TAA1/ TAR* homolog. They show that the N-terminus of the *K. flaccidum* protein contains a region similar to *SYN1* from *Arabidopsis*, a protein involved in meiosis (Cai et al, 2003), whereas the C-terminus of the same construct contains strong similarities to the *TAA1/ TARs*. However, phylogenetic analysis showed that the *K. flaccidum TAA1/ TAR* region is more similar to the alliinases than to the core *TAA1/ TARs* (Turnaev et al, 2015). Both Turnaev et al (2015), and Wang et al (2016) present in silico support for the origin of IAA biosynthesis but neither provide any physicochemical evidence for their hypotheses. As such the origin of a functional IPyA pathway is still unclear.

Similar to IAA, PAA is present in numerous divisions of land plants (Wightman and Lighty, 1982; Schneider and Wightman, 1986; Ludwig-Müller and Cohen, 2002; Sugawara et al, 2015). However, identification of this auxin is lacking in the hornworts, lycophytes and gymnosperms. PAA is also present in brown (Abe et al, 1974) and green algae (Fries and Āberg, 1978), bacteria (Hwang et al, 2001; Kim et al, 2004; Somers et al, 2005; Spaepen et al, 2007) and fungi (Kishore et al, 1976). The wide distribution of this hormone also implies an ancient origin, similar to that of IAA.

In higher plants, it appears that PAA is synthesised via a pathway analogous to the IPyA pathway in *Arabidopsis*, pea and *Sorghum bicolor* (Chapter 3)(Stafford and Lewis, 1979; Sugawara et al, 2015). However, our

understanding of plant PAA biosynthesis is restricted to the angiosperms. It has been demonstrated that aromatic aminotransferases (ArATs) are responsible for the reversible transamination of Phe to phenylpyruvate (Chapter 3)(Yoo et al, 2013). It has also been suggested that the YUC enzymes involved in IAA biosynthesis may also convert phenylpyruvate to PAA (Dai et al, 2013; Sugawara et al, 2015). However, as discussed in Chapters 3 and 4, the levels of PAA are normal in all tested YUC mutants, including the *Arabidopsis yuc1yuc2yuc6* loss of function lines (Sugawara et al, 2015).

Auxin metabolism has been studied in the basal lineages, as well as in representatives from all major divisions of land plants (Sztein et al, 1995; Sztein et al, 1999; Sztein et al, 2000). In this work the levels of endogenous and bound auxin (IAA) were determined and three distinct modes of auxin metabolism were demonstrated. The first is present in the charophytes and liverworts, where free IAA is regulated through a balance of biosynthesis and degradation. The second strategy is utilised by the mosses and hornworts, where IAA is stored in small amounts as reversible conjugates. The third strategy is used by the tracheophytes, where large amounts of IAA are conjugated and the maintenance of IAA levels is controlled by extensive conjugation/ deconjugation (Sztein et al, 1995; Sztein et al, 1999; Sztein et al, 2000). Whilst comprehensive, these reports lacked genetic evidence to support the different metabolic strategies proposed therein. However, with the availability of genome databases for model species in each major division, it is important to augment these studies with genetic support.

This chapter presents an evolutionary perspective on IAA and PAA biosynthesis by demonstrating the presence/ absence of these auxins in each major evolutionary division. In addition, metabolism experiments show that the IPyA and phenylpyruvate pathways are functional in almost all of the representative species. The metabolism experiments are further supported by phylogenetic analyses comparing genomes of model species, the distribution of these species is presented in Figure 5.1. Finally, this chapter also addresses the distribution of the major auxin conjugation/ degradation

enzymes, the *UGTs*, *GH3s*, and the recently characterised *DAOs*, responsible for ester conjugation, amide conjugation and oxidation, respectively.

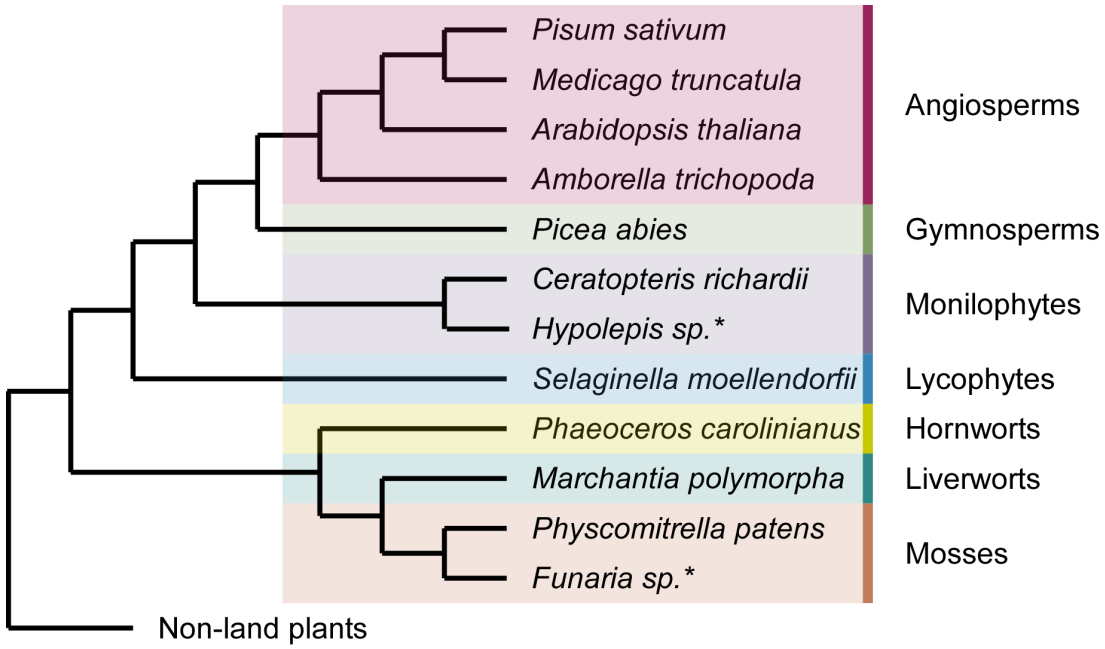

Figure 5.1 presents a cladogram of the current evolutionary distribution of major land plant divisions (shaded) and the approximate positions of species investigated within Chapter 5. * *Hypolepis sp.* and *Funaria sp.* were used in physicochemical analyses as substitutes for *C. richardii* and *P. patens*, respectively. *Hypolepis sp.* and *Funaria sp.* are not included in phylogenetic reconstructions.

5.2 Materials and methods

5.2.1 Plant materials

Physcomitrella patens plantlets (ecotype: Gransden) were obtained from the International Moss Stock Center (IMSC, Freiburg University) and maintained in axenic culture. *Hypolepis sp.* gametophytes were germinated from spores collected from adult plants and placed into axenic culture following surface sterilisation with 5% sodium hypochlorite. *Marchantia polymorpha* (Liverwort), *Funaria sp.* (Moss), *Phaeoceros carolinianus* (Hornwort), *Selaginella moellendorfii* (Lycophyte), *Hypolepis sp.* (Fern), *Picea abies* (Gymnosperm) and *Amborella trichopoda* (Angiosperm) were already present in our glasshouse facilities and were grown under glasshouse conditions. *Hypolepis sp.* gametophytes were grown at 25ºC in growth cabinets.

5.2.2 Phylogenetic analysis

Phylogenetic analysis was conducted on sequences obtained from Phytozome (*Arabidopsis thaliana*, *M. truncatula*, *A. trichopoda*, *S. moellendorfii*, *P. patens* and *M. polymorpha*), the pea gene atlas (*P. sativum*), Congenie (*P. abies*), and the *C. richardii* database (http://koke.asrc.kanazawa-u.ac.jp/Ceratopteris/blast.html). For all genetic analyses, *P. patens* was used in place of *Funaria sp.* and *C. richardii* was used in place of *Hypolepis sp.*.

The ‘ModelTest’ function in the R package ‘Phangorn’ was used to rank, statistically, all available models for reconstruction (Schliep, 2011). In each case, the model with the lowest Akaike Information Criterion (AIC) was selected and applied. An LG model (Le and Gascuel, 2008) with gamma distribution and invariable sites was used for all analyses, except for the UGT reconstruction, which used a JTT model (Jones et al, 1992). Both gamma and the proportion of invariant sites were calculated in situ.

5.3 Results and Discussion

5.3.1 Evidence that the hormones IAA and PAA are present in all land plants

In order to investigate the origin of auxin biosynthesis it is essential to first look at the endogenous levels of the two auxins in land plants. The levels of free IAA in the basal lineages were typically higher than100 ng g^{-1} FW (Figure 5.2). These levels decreased gradually through the tracheophytes and were around 50 ng g^{-1} FW in both *Picea abies* and *A. trichopoda*. Sztein et al (1999) found that the liverwort *Marchantia polymorpha* contained just 17 ng g^{-1} fresh weight, whereas levels of just over 2 ng have also been reported (Eklund et al, 2015). Interestingly, however, the experiments here indicate that endogenous IAA can be as high as 300 ng g^{-1} in this species (Figure 5.2).

Sztein et al (1999); Sztein et al (2000) found the levels of IAA in species from *Funaria* (8 ng g^{-1}), *Phaeoceros* (35 ng g^{-1}), and *Selaginella* (5 ng g^{-1}) to be substantially lower than the levels presented here, although the species used were not the same. It is also possible that some reproductive tissue may have been inadvertently included in this analysis, resulting in increase hormone levels. However, despite the elevated IAA in these representatives (liverwort, moss and hornwort), the levels of free IAA in the fern, *Hypolepis sp.* are similar to those recorded for *Matteucia struthiopteris* (Schneider and Wightman, 1986). It is possible that in addition to different species, a combination of tissue type and extraction technique may contribute substantially to deviations in the IAA levels determined by different laboratories.

It is interesting that despite the transition from a predominantly gametophytic life stage (*M. polymorpha*, *Funaria sp.*, and *Phaeoceros carolinianus*) to a sporophytic one (*S. moellendorfii*, *Hypolepis sp.*, *P. abies* and *A. trichopoda*); the levels of free IAA tend to decrease. This may indicate an increase in the

types and/ or number of enzymes responsible for the regulation of endogenous IAA levels in higher plant species.

Similar to IAA, the auxin PAA was present in all species tested. This is not entirely surprising given that PAA has been reported in *M. polymorpha*, *Physcomitrella patens*, *M. struthiopteris*, and many angiosperms previously (Chapter 3)(Wightman and Lighty, 1982; Schneider and Wightman, 1986; Sugawara et al, 2015). However, this may be the first documentation of this auxin in the hornwort, lycophyte and gymnosperm divisions, and the first comparative analysis of PAA levels in these species.

Unlike IAA, the levels of endogenous PAA were highly variable across throughout the land plants (Figure 5.3). The variation of PAA between the divisions suggests that the capacity to regulate endogenous PAA levels is not a strongly conserved trait. The PAA levels in *M. polymorpha* presented here are slightly higher than previously reported (~65 ng g^{-1}, Sugawara et al 2015), although like IAA, the levels of PAA in *Hypolepis sp.* are similar to those in *M. struthiopteris* (~379 ng g^{-1})(Schneider and Wightman, 1986).

Interestingly, PAA accumulated substantially in the lycophyte *S. moellendorfii* (just over 6000 ng g^{-1}). This was unexpected, although the tissue used in these experiments may have contained young reproductive strobili. It is known that auxins are typically higher in reproductive organs when compared with vegetative tissue (Sugawara et al, 2015). However, levels of PAA in *M. struthiopteris* were higher in developing pinnae, compared with fertile, spore-containing pinnae (Schneider and Wightman, 1986). That finding may suggest that high auxin content in reproductive structures is only common to the angiosperms. Despite these findings, preliminary experiments on the levels of endogenous PAA in the closely related lycophyte *Selaginella uncinata* suggests that *S. moellendorfii* may not be representative of the entire lycophyte division, as far as PAA biosynthesis is concerned.

5.3.2 Evidence that the IPyA and phenylpyruvate pathways are operative in all land plants.

In higher plants, the majority of IAA is largely synthesised from the amino acid Trp through the intermediate IPyA (Zhao, 2012). However, the operation of this pathway in basal species has only limited support (Jayaswal and Johri, 1985; Eklund et al, 2015). Since IAA is ubiquitous in land plants it was important to determine if this pathway is functional in each of the representative species. A key finding was that in a range of species, and using the techniques described here, deuterium labelled (D_5) Trp was metabolised to D_5 IAA, diluting the endogenous IAA pool (Figure 5.4). Suggesting that both the TAA1/ TAR and YUC enzymes are present in these species.

In Chapter 3 it was demonstrated that PAA could be synthesised from the amino acid Phe via phenylpyruvate. This pathway has also been proposed in *Arabidopsis* (Sugawara et al, 2015) and demonstrated in *Sorghum bicolor* (Stafford and Lewis, 1979). Similar to the D_5 Trp experiments, the provision of labelled D_5 Phe resulted in the dilution of the endogenous PAA pool with deuterated PAA, in all representative species (Figure 5.5). The amount of D_5 PAA synthesised in these experiments was higher than that of IAA in every species (2-16 fold), consistent with previous reports on endogenous levels of the two auxins (Wightman and Lighty, 1982; Sugawara et al, 2015).

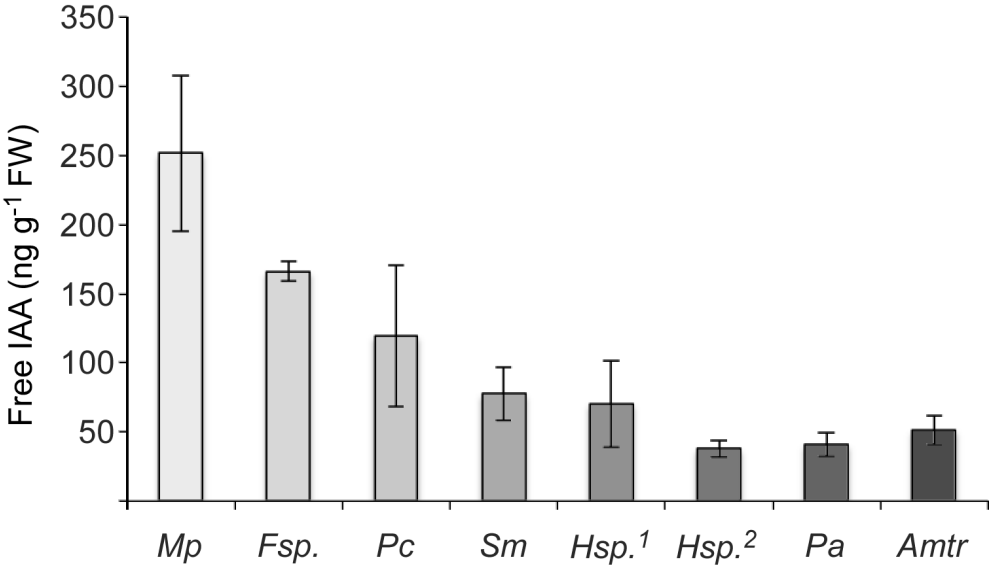

Figure 5.2 presents the endogenous levels of IAA in vegetative tissue from representative species of all major land plant divisions. Mp (*Marchantia polymorpha*; liverwort), Fsp. (*Funaria sp.*; moss), Pc (*Phaeoceros carolinianus*; hornwort), Sm (*Selaginella moellendorfii*; lycophyte), Hsp. (*Hypolepis sp.*; fern [^{1}gametophyte, ^{2}sporophyte]), Pa (*Picea abies*; gymnosperm), Amtr (*Amborella trichopoda*; angiosperm). Data are means ± SE, (ng g^{-1} FW n=4)

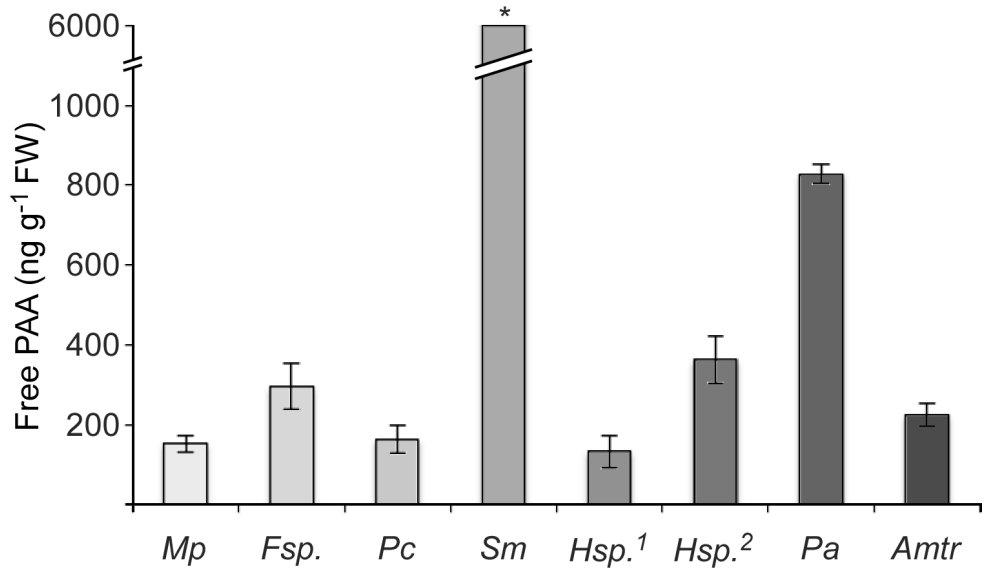

Figure 5.3 presents the endogenous levels of PAA in vegetative tissues from representative species of all major land plant divisions. Species abbreviations are given in Figure 5.1. Data are means ± SE, (ng g^{-1} FW n=4)

The results here also show that most of the major evolutionary groups can utilise the IPyA pathway for the biosynthesis of IAA (Figure 5.6, Table 5.1) and the phenylpyruvate pathway for the biosynthesis of PAA (Figure 5.7, Table 5.1). Unexpectedly, the endogenous and labelled species of IPyA were undetectable in *M. polymorpha*, *Funaria sp.* and *A. trichopoda* (Table 5.1). On the other hand previous experiments on *Funaria hygrometrica* reported the conversion of (^{3}H) Trp to (^{3}H) IPyA in chloronemal cultures (Jayaswal and Johri, 1985). Additionally, overexpression of a *YUC* homolog in *M. polymorpha* increased the levels of free IAA in transformed lines (Eklund et al, 2015). These results suggest that these species can use the IPyA pathway in the biosynthesis of IAA.

The presence of endogenous phenylpyruvate in the majority of the representative species suggests it is common to all land plants (Figure 5.7, Table 5.1). Consistent with this, the identification of labelled phenylpyruvate following incubation with deuterium labelled Phe suggests that phenylpyruvate is likely a key intermediate in Phe dependent PAA biosynthesis. However, the transitions for endogenous and labelled phenylpyruvate were not analysed in the *S. moellendorfii* extracts. It is assumed that this pathway is functional in this division as both the ferns and the hornworts, the major divisions on either side of the lycophytes, can utilise the phenylpyruvate pathway for PAA biosynthesis. Nonetheless, these results are the first to indicate that the phenylpyruvate pathway to PAA is functional in the majority of land plants.

Table 5.1 Presence/ absence of deuterium labelled intermediates IPyA and phenylpyruvate following 24-hour incubation with labelled (D_5) Trp or (D_5) Phe. ND: not detected, NA: not analysed

Division (Species)	D_5 IPyA-TAZ	D_5 phenylpyruvate
Liverwort (*Marchantia polymorpha*)	ND	Present
Moss (*Funaria sp.*)	ND	Present
Hornwort (*Phaeoceros carolinianus*)	Present	Present
Lycophyte (*Selaginella moellendorfii*)	Present	NA
Fern (*Hypolepis sp.*)	Present	Present
Gymnosperm (*Picea abies*)	Present	Present
Angiosperm (*Amborella trichopoda*)	ND	Present
Angiosperm (*Pisum sativum*)	Present	Present

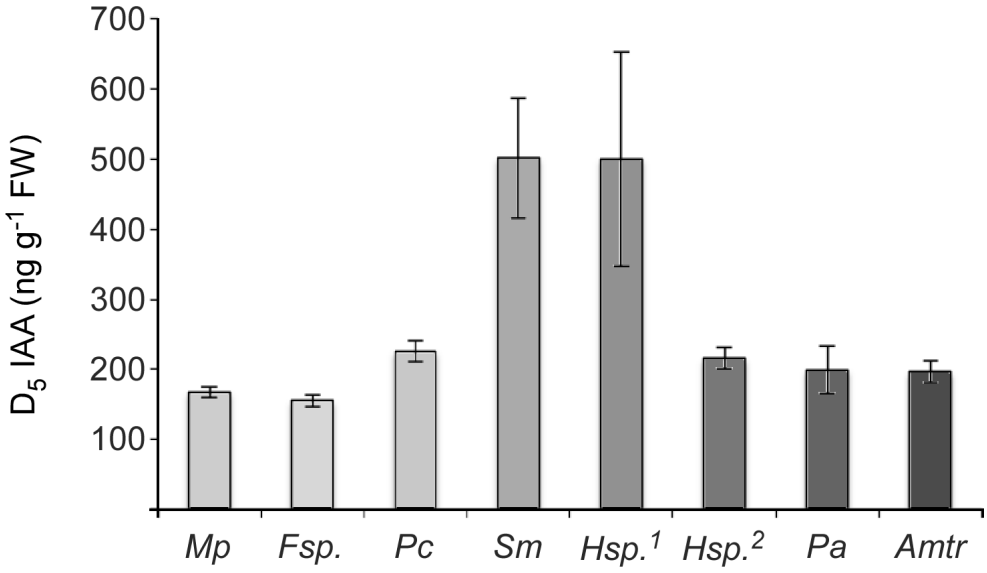

Figure 5.4 presents the levels of deuterium- (D_5) labelled IAA (de novo biosynthesis from D_5 Trp) over 24 hours in representative species from all major land plant divisions. Species abbreviations are given in Figure 5.1. Data are means ± SE, (ng g^{-1} FW n=4)

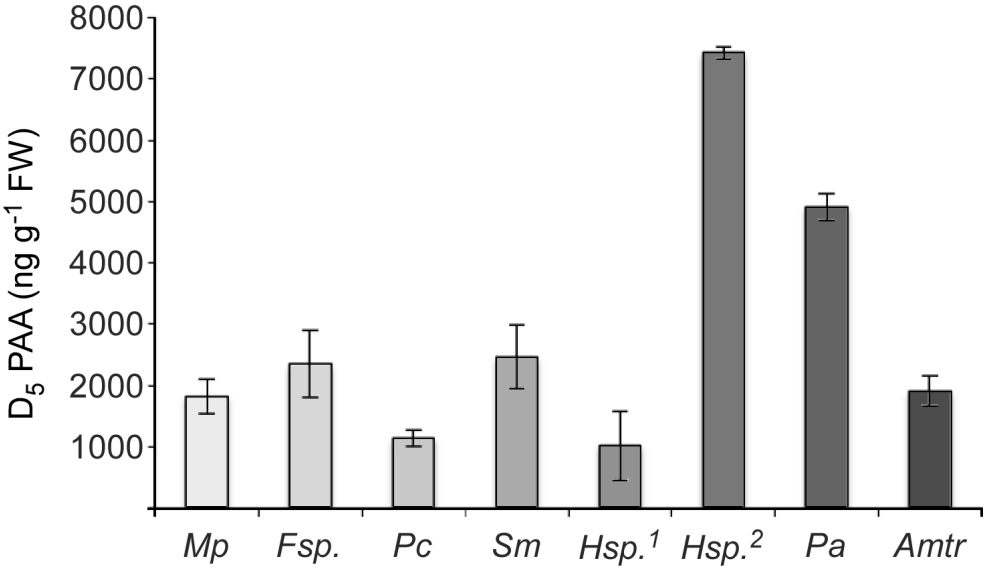

Figure 5.5 presents the levels of deuterium- (D_5) labelled PAA (de novo biosynthesis from D_5 Phe) over 24 hours in representative species from all major land plant divisions. Species abbreviations are given in Figure 5.1. Data are means ± SE, (ng g^{-1} FW n=4)

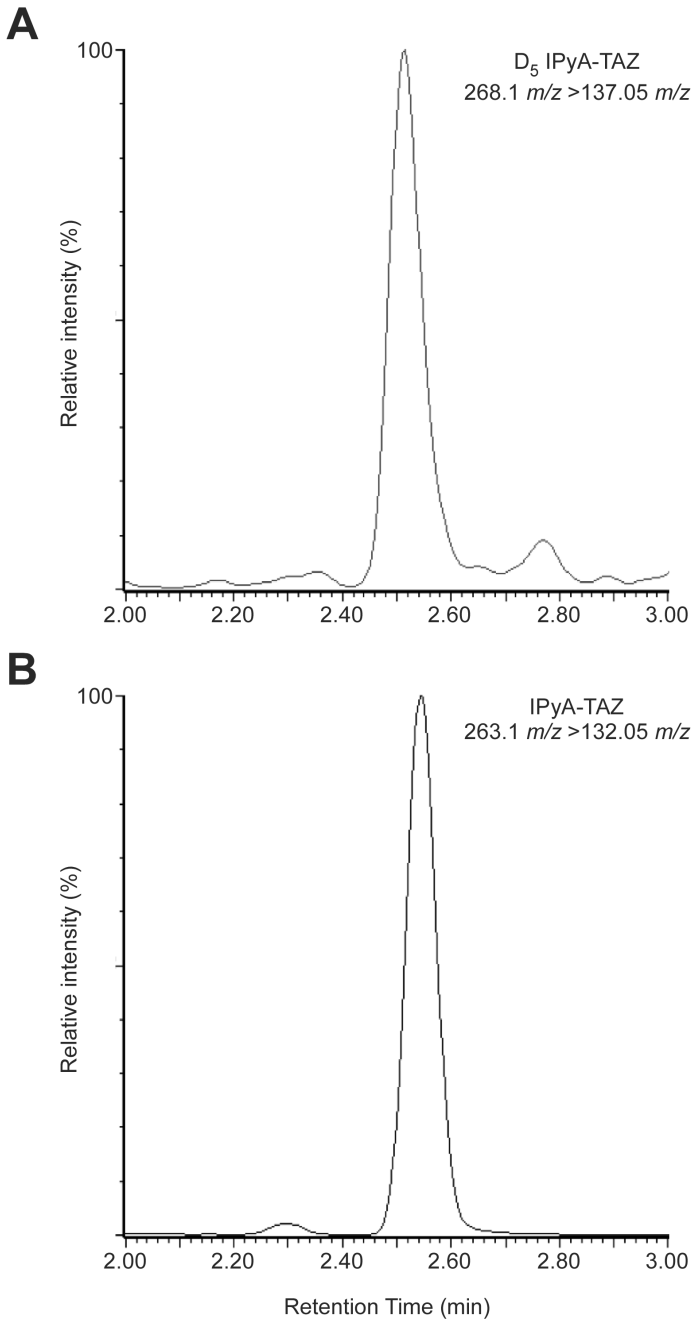

Figure 5.6 representative UPLC-MS chromatograms from metabolism experiments incubated with D_5 Trp showing (A) D_5 IPyA-TAZ and (B) endogenous IPyA-TAZ. Approximate retention time is 2.54 min and MRM transitions are provided.

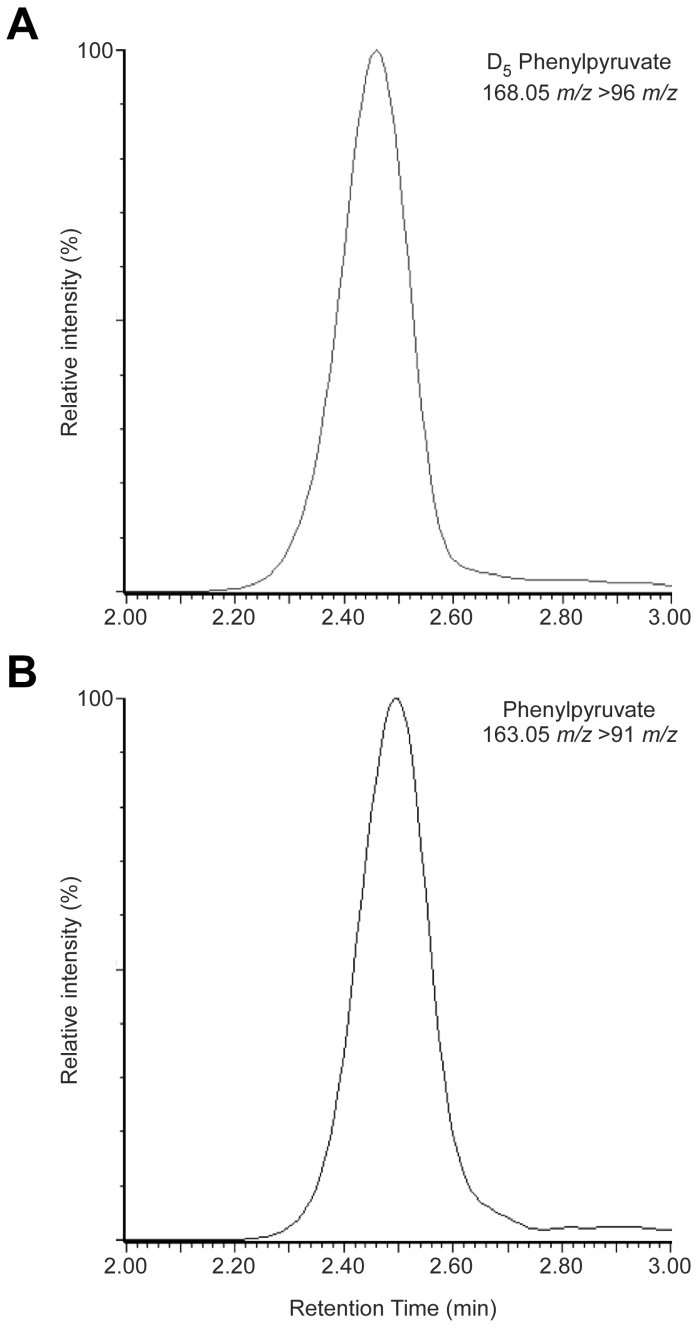

Figure 5.7 representative UPLC-MS chromatograms from metabolism experiments incubated with D_5 Phe showing (A) D_5 phenylpyruvate and (B) endogenous phenylpyruvate. Approximate retention time 2.5 min and MRM transitions are provided.

5.3.3 The *TAA1* gene family is ubiquitous in the land plants and evolutionarily distinct from the alliinases

Since the IPyA pathway is functional in many of the species tested (Table 5.1), it is important to confirm the distribution of the *TAA1* gene family in each major division. Similar to previous analyses on the Trp aminotransferases, the reconstructed *TAA1/ TAR* family tree (Figure 5.8) contains two distinct groups; the core *TARs* (*AtTAA1*, *AtTAR1* and *AtTAR2*), and the auxiliary *TARs* (*AtTAR3* and *AtTAR4*), which contain the EGF (epidermal growth factor) domain typical of alliinases (Stepanova et al, 2008) and indeed cluster more strongly with the similar Alliin C-S lyases (Mano and Nemoto, 2012). The reconstructed tree also largely conforms to the current understanding of the evolutionary progression of land plants; mosses and liverworts being basal to the lycophytes, ferns, gymnosperms and angiosperms, sequentially (Wickett et al, 2014).

The tree presented here confirms that the core *TARs* have been separated from the Alliin C-S lyases for at least 450 million years (Turnaev et al, 2015), since sequences belonging to each clade are present in both the mosses and liverworts. This raises the possibility that the *AtTAR3* and *AtTAR4* gene products may not function, primarily, as *TARs* in IAA biosynthesis. These genes, despite being annotated as TARs, are structurally divergent from the core group, and have yet to be screened for aminotransferase activity. Similarly, sequences from other species within the alliinase sister clade may not contribute to IAA biosynthesis, although additional experimental evidence is still required to rule out the contribution of these proteins.

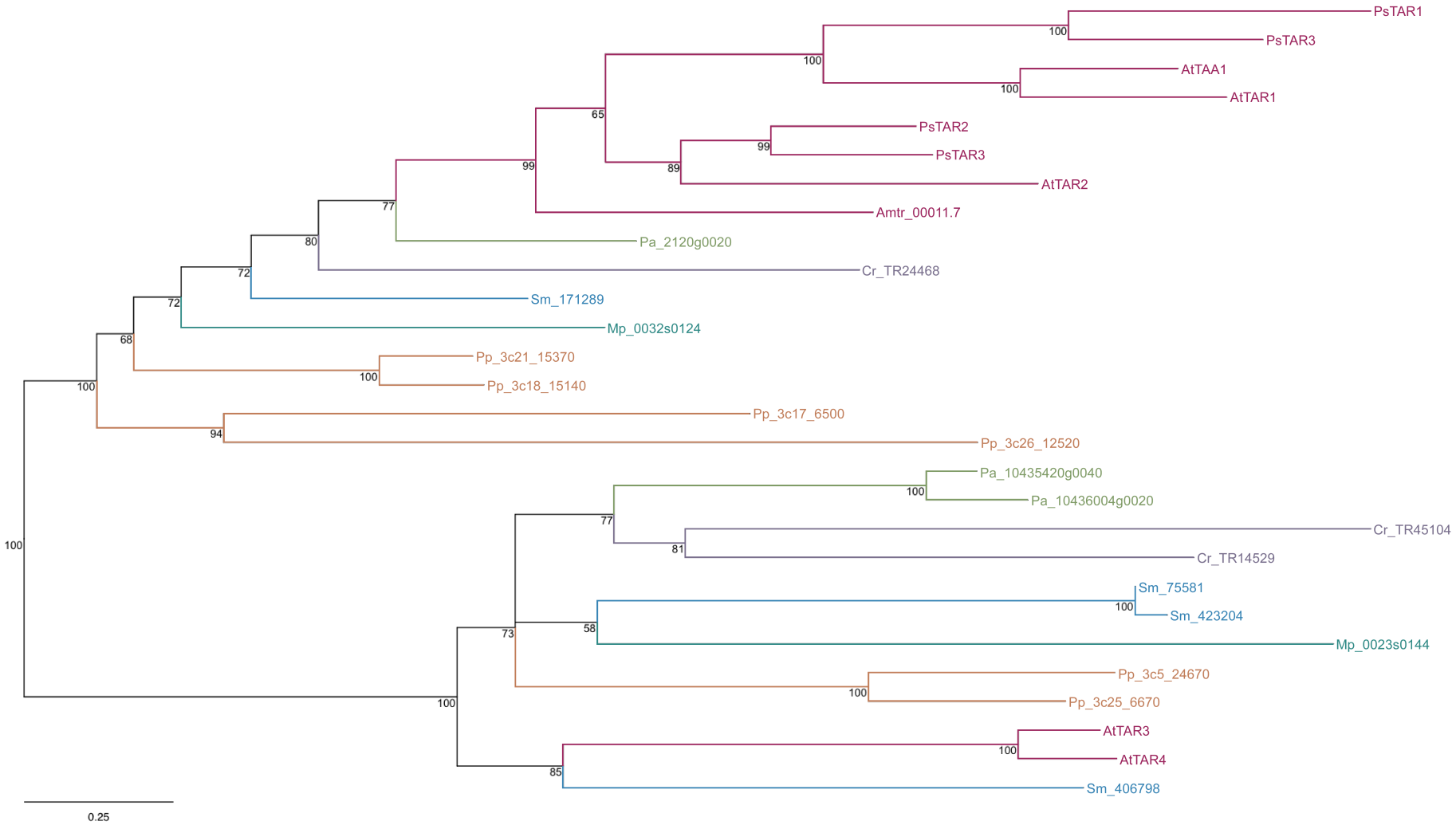

Figure 5.8 Phylogenetic reconstruction of the TAR protein family based on amino acid sequences. Tree contains sequences from pea (Ps), *Arabidopsis* (At), *A. trichopoda* (Amtr), *P. abies* (Pa), *C. richardii* (Cr), *S. moellendorfii* (Sm), *M. polymorpha* (Mp) and *P. patens* (Pp). Reconstruction utilised a LG model with optimised site variation and gamma distribution. Scale bar indicates evolutionary distance, and bootstrap values (from 1000 replicates) are presented adjacent to nodes

The function of the core *TARs* as Trp aminotransferases has been demonstrated in *Arabidopsis* and pea (Stepanova et al, 2008; Tao et al, 2008; Tivendale et al, 2012). This group has a single gene origin in *A. trichopoda,* which is preserved back to *P. patens* where there are multiple sequences that subtend the *TAR* clade. However, It may still be speculative to extrapolate TAR activity to all of the basal enzymes, even though the IPyA pathway is functional in each of these divisions, and all core *TAR* sequences contain the conserved lysine residue required for PLP binding and aminotransferase activity (Ferreira et al, 1993; Liepman and Olsen, 2004).

Further analysis of the conserved domains (Marchler-Bauer et al, 2014) in each of the core TARs shows that all lineages contain, in addition to the PLP binding site, several substrate-binding residues typical of aminotransferases (Ferreira et al, 1993; Stepanova et al, 2008). Unexpectedly, the core *TAR* sequences from *P. patens*, *M. polymorpha* and *C. richardii* also contain the N-terminal EGF domain common to the alliin C-S lyases in the sister group (Stepanova et al, 2008; Turnaev et al, 2015). Despite this, these enzymes are overall more similar to the core TARs in the reconstruction presented here (Figure 5.8). However, previous phylogenetic analyses have grouped the basal sequences from *P. patens* within the alliin C-S lyases (Phillips et al, 2011).

Interestingly, most of the divisions also contain an EGF/ C-S Alliin lyase. However, these are absent in the liverworts and in pea and *A. trichopoda*. It is possible that these *TARs* may retain some alliin lyase activity and that the retention of this domain is under some selection pressure. Given that the alliinase enzymes are involved in the production of volatile defence compounds (Kuettner et al, 2002), this is understandable. In vitro analyses on basal *TARs* (and the alliinases) would augment previous work and provide insight on how the *TAR* function may have changed over time, if at all.

It has been suggested that the charophyte *K. flaccidum* contains the ancestral form of the *TAR*/ *alliinase* gene (Turnaev et al, 2015). Structural analysis of this protein shows that both the *TAR* and *EGF alliinase* domains are present, although they are fused to an ortholog of *Arabidopsis SYN1*, which is involved in meiosis (Cai et al, 2003). Turnaev et al (2015) interpret the structure of this enzyme as the origin of the IPyA pathway in green plants, although none of the other charophytes examined in Huang et al (2014) appear to contain *TAR* homologs. Additionally, the Klebsormidales are positioned basal to other charophytes (from the Charales) in a broader evolutionary context (Wickett et al, 2014). If this reconstruction is correct, then *TAR* homologs must be present in all Charales. As such, the exact origin of the *TAR*s and the IPyA pathway remains unclear.

5.3.4 Distribution of the YUC gene family

The YUC family is extensive in higher plants with 11 members in *Arabidopsis* (Zhao et al, 2001) and 12 in pea (Chapter 4). *YUC* genes are present in all major divisions, supporting the conservation of the IPyA pathway in land plants (Figure 5.9). As described in Chapter 4, the YUC sequences form two large groups, one containing the ‘floozy’ and ‘reproductive development’ sister clades, as well as a subtending clade containing putative root expressed YUCs, and a second group containing YUC genes associated with embryogenesis (Cheng et al, 2007).

The pattern of radiation in the plant YUCs seems to indicate a selective pressure for a more complex regulation of IAA biosynthesis. Mutations in IAA biosynthetic genes that are expressed in niches (*PsTAR2* in pea seeds, *ZmYUC1* in maize endosperm) can have substantial effects on plant phenotypes (Bernardi et al, 2012; Tivendale et al, 2012). However, mutations in IAA biosynthetic genes that share overlapping expression produce comparatively mild phenotypes (Cheng et al, 2006, 2007). It is logical that the duplication of these genes not only affords enhanced evolutionary fitness, but also allows for the development of unique expression profiles, which can be correlated with increased body plan complexity.

In *Arabidopsis*, members of the 'floozy' clade (AtYUC1 and AtYUC4) are responsible for IAA biosynthesis in vegetative tissue. They are expressed primarily in meristematic regions, leaf margins and vascular tissue (Tobeña-Santamaria et al, 2002; Cheng et al, 2006, 2007). YUCs belonging to the 'reproductive development' clade (AtYUC2 and AtYUC6) are expressed primarily in reproductive structures, although they share expression with the 'floozy' YUCs (Cheng et al, 2006, 2007). The separation of these two groups is strongly supported in the angiosperms, and has been demonstrated in previous analyses (Cheng et al, 2006; Gallavotti et al, 2008; Mano and Nemoto, 2012).

These two groups are subtended by a clade containing AtYUC3, AtYUC7, AtYUC9, AtYUC5 and AtYUC8. These enzymes are likely expressed in root tissue as *FvYUC3* and *FvYUC7* from strawberry (*Fragaria vesca*), which are homologous to *AtYUC3* and *AtYUC7*, are most strongly expressed in strawberry roots and stolons (Liu et al, 2014). Interestingly, these three groups are all retained in *A. trichopoda*. This suggests that all angiosperms may contain YUCs with at least three unique expression profiles, although sequence radiation in the higher angiosperms has given rise to functional redundancy and unique distributions of these enzymes.

The angiosperm YUCs are subtended by a radiation of sequences in *P. abies*, which appear to have a single gene origin. This suggests that while YUCs in *P. abies* may have unique expression patterns, similar to the angiosperms, the MRCA of the seed plants only contained a single *YUC* gene responsible for non-embryo IAA biosynthesis. This is supported by sequence data from the *C. richardii* genome, which contains only a single YUC that clusters with this group.

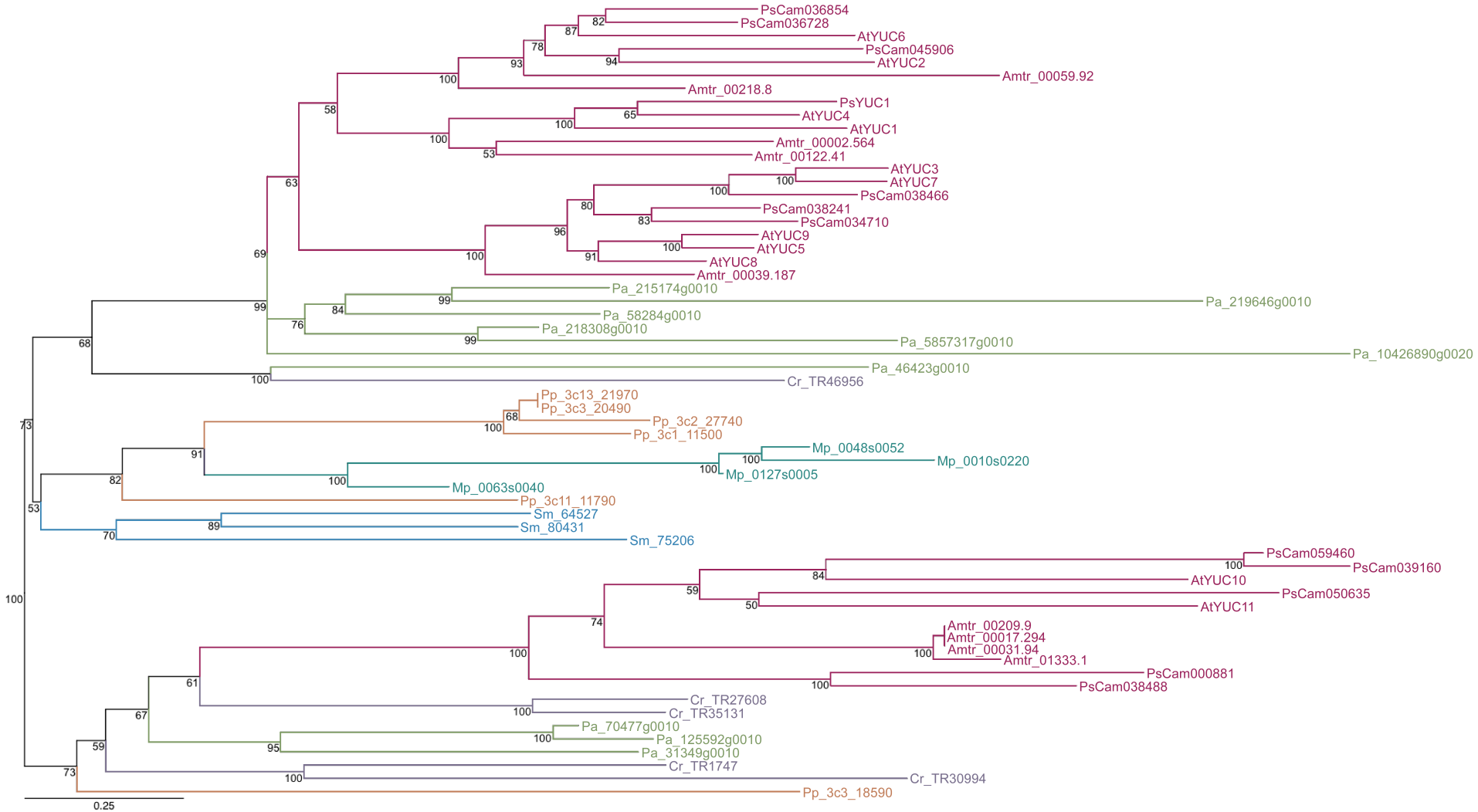

Figure 5.9 Phylogenetic reconstruction of the YUC protein family based on amino acid sequences. Tree contains sequences from pea (Ps), *Arabidopsis* (At), *A. trichopoda* (Amtr), *P. abies* (Pa), *C. richardii* (Cr), *S. moellendorfii* (Sm), *M. polymorpha* (Mp) and *P. patens* (Pp). Reconstruction utilised a LG model with optimised site variation and gamma distribution. Scale bar indicates evolutionary distance, and bootstrap values (from 1000 replicates) are presented adjacent to nodes

Interestingly, despite their simple body plan, there are sequence radiations in *P. patens*, *M. polymorpha* and *S. moellendorfii*, which all form a monophyletic group, sister to the higher tracheophytes. Within this, the *P. patens* and *M. polymorpha* sequences form a clade distinct from *S. moellendorfii,* in agreement with our current understanding of the evolutionary history of the basal lineages (Wickett et al, 2014). However, the formation of two sister groups at this junction is unexpected, but can largely be attributed to a lack of supporting sequences from the hornworts.

It is suggested that *AtYUC10* and *AtYUC11* are involved in embryogenesis, given their expression profiles (Cheng et al, 2007). This is also the case with *ZmYUC1* (*de18*), which is solely expressed in maize endosperm (Bernardi et al, 2012). This group of YUC enzymes also forms a monophyletic group with *A. trichopoda*, indicating conservation of embryogenesis associated YUCs in all angiosperms. However, the evolutionary history of this group in the basal lineages is not as clear, as the fern *C. richardii* contains sequences that are both basal and superior to those of *P. abies,* the gymnosperm. Similarly, there are no *M. polymorpha* sequences in this group, despite the presence of a YUC from *P. patens*. This is curious given that these two groups are closely related.

It is interesting that previous reconstructions of the YUC family tree have found that *P. abies*, *S. moellendorfii*, or *P. patens* do not contain orthologs of AtYUC10 or AtYUC11 (Gallavotti et al, 2008; Abu-Zaitoon et al, 2012). The reconstruction presented here shows that both *P. abies* and *P. patens* (as well as *C. richardii*), contain sequences that cluster in this group (Figure5.8). Similarly, other analyses have found that sequences from *P. patens* and *S. moellendorfii* cluster strongly with AtYUC10 and AtYUC11 (Yue et al, 2014). In fact, the reconstruction produced by Wang et al (2014) demonstrates that all angiosperm YUCs form a single monophyletic group superior to the basal species. The accuracy of these previous reconstructions is unclear as many of these analyses also included sequences from other kingdoms. While this provides evidence for the origin of the IPyA pathway, it comes at the expense of diminished resolution within the plant kingdom.

Interestingly, while Turnaev et al (2015) suggest that the origin of the TARs is in *Klebsormidium flaccidum* (Klebsormidiaceae), (Wang et al, 2014) demonstrate that *K. flaccidum* and the Charophyte, *Nitella hyalina*, both contain YUC homologs. Since *N. hyalina* (Characeae) is basal to the Klebsormidiaceae (Wickett et al, 2014), It is likely that the IPyA pathway has originated prior to *K. flaccidum*. For example, the brown alga, *Ectocarpus siliculosus,* also contains a YUC homolog (Le Bail et al, 2010), suggesting that the origin of the IPyA pathway could be as ancient as the MRCA of the brown and green alga. However, while biochemical analyses show *E. siliculosus* also contains approximately 3 ng g^{-1} of endogenous IAA, there are no TAR homologs in the *E. siliculosus* genome (Le Bail et al, 2010). As such, the IPyA pathway, as typified by the TARs and YUCs, has an origin somewhere between the brown and green algae, although extensive work is required to isolate the exact origin of this pathway.

5.3.5 The aromatic aminotransferases are widely distributed in land plants

It is suggested in Chapter 3 that an aromatic aminotransferase (ArAT), rather than the TAR/ TAA1 enzymes, may be involved in the biosynthesis of PAA. The ArATs are present in most lineages, including *K. flaccidum* from the Klebsormidiaceae (Figure 5.10). However, the ArATs are absent in the lycophyte, *S. moellendorfii*.

ArATs have been studied in several species, including *Cucumis melo* (Gonda et al, 2010), *Petunia hybrida* (Yoo et al, 2013), *Atropa belladonna* (Bedewitz et al, 2014), and *Arabidopsis* (Prabhu and Hudson, 2010). In *Arabidopsis*, these enzymes are annotated as TATs (Tyrosine aminotransferases)(Prabhu and Hudson, 2010), since they catalyse the reversible conversion of Tyr to hydroxyphenylpyruvate (HPP)(Riewe et al, 2012; Wang et al, 2016). The ArATs (and the TATs) are also capable of utilizing various aromatic substrates such as Phe and Trp, as well as their respective keto-acids (Prabhu and Hudson, 2010; Lee and Facchini, 2011; Riewe et al, 2012), although Tyr is often the preferred substrate for these enzymes.

The distribution of plant ArATs is similar to that of the YUCs in that the seed plants form a large monophyletic clade (Figure 5.10). Within the angiosperms, there are two groups; the first contains only *Arabidopsis* sequences with no substantial aminotransferase activity such as SUR1 (Mikkelsen et al, 2004), CORI3 (Lopukhina et al, 2001; Jones et al, 2003), and RSA1 (Rosas et al, 2013), as well as several unclassified 'TyrAT family proteins'. These enzymes have variable functions but largely appear to encode C-S lyases, which share overlapping domain architecture with aminotransferases (Marchler-Bauer et al, 2014).

The second group contains enzymes with confirmed ArAT activity and can be divided into two subgroups. The 'Specialized ArATs' include sequences from numerous species, *C. melo* (Gonda et al, 2010), *Arabidopsis* (Prabhu and Hudson, 2010), *P. hybrida* (Yoo et al, 2013), *A. belladonna* (Bedewitz et al, 2014), as well as pea and *M. truncatula*. These enzymes appear to largely function in the biosynthesis and metabolism of the amino acids Phe and Tyr. The second group composes the 'Generic ArATs' such as AtTAT2 from *Arabidopsis*, which has been shown to be active on numerous aromatic and aliphatic amino acids (Wang et al, 2016), as well as sequences from *A. trichopoda* and *M. truncatula*.

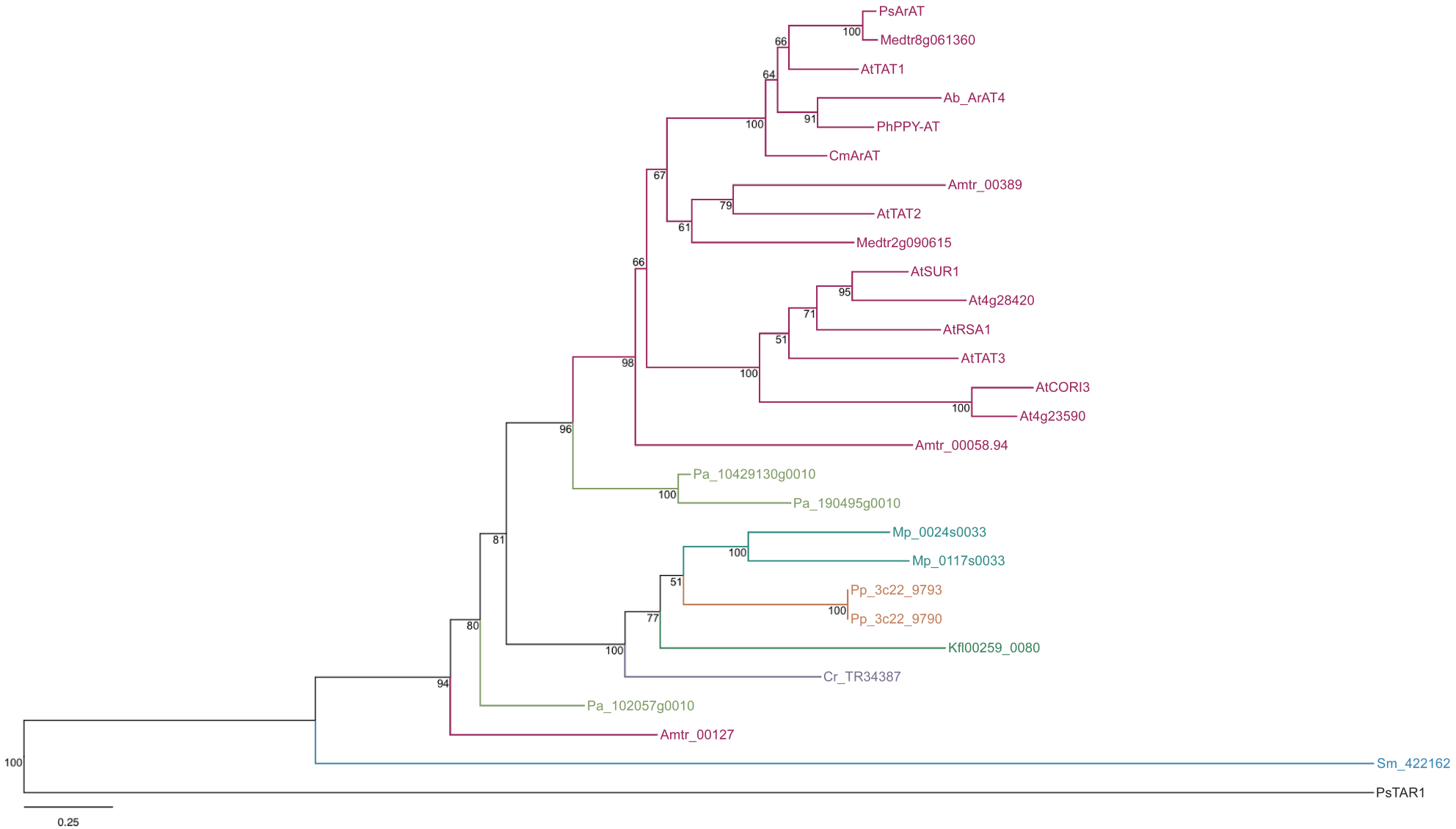

Figure 5.10 Phylogenetic reconstruction of the ArAT protein family based on amino acid sequences. Tree contains sequences from pea (Ps), *Arabidopsis* (At), *A. trichopoda* (Amtr), *P. abies* (Pa), *C. richardii* (Cr), *S. moellendorfii* (Sm), *M. polymorpha* (Mp) and *P. patens* (Pp). Reconstruction utilised a LG model with optimised site variation and gamma distribution. Scale bar indicates evolutionary distance, and bootstrap values (from 1000 replicates) are presented adjacent to nodes.

Previous work has demonstrated that AtTAT1, which belongs to the specialised ArAT clade, catalyses the reversible transamination of Tyr to HPP (Prabhu and Hudson, 2010; Riewe et al, 2012; Wang et al, 2016). This reaction (in *Arabidopsis* and other species) preferentially uses phenylpyruvate as an amino acceptor in the formation of the amino acid Phe (Prabhu and Hudson, 2010; Yoo et al, 2013; Wang et al, 2016). The Michaelis-Menten kinetics presented for this reaction show that the conversion of Tyr to HPP is 62 times more efficient than the reverse reaction, which deaminates Phe to phenylpyruvate (Wang et al, 2016). This is supported by work on *C. melo* and *P. hybrida* where these enzymes are responsible for the biosynthesis of Phe from phenylpyruvate (Gonda et al, 2010; Yoo et al, 2013).

Even though transamination is reversible, the enzyme kinetics are not congruent with the PAA biosynthetic pathway presented earlier (Chapter 3). However, research on other members of the specialised ArATs have shown that Ab_ArAT4 from *A. belladonna* preferentially catalyses the conversion of Phe to phenylpyruvate (Bedewitz et al, 2014). In this case, the catalytic efficiency for the conversion of Phe to phenylpyruvate was 250 fold higher than the reverse direction. This shows that while some members of the specialised ArATs prefer the conversion of phenylpyruvate to Phe, the reverse reaction can also be substantial.

Unlike the specific substrate preference of AtTAT1, AtTAT2 has been shown to use a broad range of amino acids as substrates (Wang et al, 2016), although its activity is highest with Met and Tyr. This function is more in line with that of the bacterial ArATs, which also possess broad substrate preferences (Berger et al, 2003). It is also interesting that a representative sequence from *A. trichopoda* is only present in the generic ArAT cluster. The distribution of the angiosperm sequences suggests that ArATs have undergone a recent duplication event, giving rise to the specialised ArATs. This is further supported by the recent characterisation of EsAroAT1 from *Ephedra sinica*, a shrubby gymnosperm (Kilpatrick et al, 2016). While EsAroAT1 prefers Tyr in vitro, similar to AtTAT1, this enzyme can also use

many keto acids as amino acceptors, a trait demonstrated by AtTAT2 (Kilpatrick et al, 2016). The combination of these two traits in a species that is basal to all angiosperms suggests that aromatic aminotransferases in land plants are likely to utilise a broad range of substrates, although there may be some preference for particular reactions.

The bryophytes and *C. richardii* form a sister clade to the spermatophytes, similar to the reconstruction of the YUC enzymes. However, the most similar *S. moellendorfii* sequence does not cluster with the other species and does not appear to be a canonical ArAT (Figure 5.10). Previous phylogenies looking at the distribution of the aromatic aminotransferases have shown that the same sequence in *S. moellendorfii* clusters with sequences encoding prephenate aminotransferases (Wang et al, 2016). These enzymes (at least in *Arabidopsis* and *P. hybrida*) are responsible for the conversion of prephenate to arogenate, an intermediate step in the biosynthesis of both Tyr and Phe (Maeda et al, 2011).

It is interesting that this sequence is absent in *S. moellendorfii*, given that PAA is extremely high in this species (Figure 5.3). Since the ArATs are responsible for the conversion of phenylpyruvate to Phe (Gonda et al, 2010; Prabhu and Hudson, 2010; Yoo et al, 2013) and since phenylpyruvate can also be a precursor to PAA, it is possible that the absence of an ArAT may cause the redirection of phenylpyruvate towards PAA (i.e. ArATs may act antagonistically in PAA biosynthesis under normal conditions).

Nonetheless, PAA biosynthesis (from Phe) occurs in all of the representatives analysed in this chapter, including *S. moellendorfii*. Additionally, labelling of the intermediate phenylpyruvate also suggests that PAA biosynthesis occurs through an initial transamination reaction. Since ArATs are able to use Phe as a substrate, and are present in all tested members of the green lineage (apart from the lycophyte *Selaginella*), it is possible that these enzymes function in the biosynthesis of PAA in all land plants.

5.3.6 DAOs are not conserved outside the angiosperms, despite widespread distribution of oxIAA

The catabolite oxIAA (2-oxindole-3-acetic acid) has been identified in most plant lineages, including mosses and liverworts (Drábková et al, 2015), hornworts (Sztein et al, 2000), ferns (Sztein et al, 1995), gymnosperms (Ernstsen et al, 1987) and angiosperms (Pěnčík et al, 2013). OxIAA has long been considered an important component of the IAA metabolic system (Ray, 1958; Östin et al, 1998), although only recently have the enzymes responsible for its biosynthesis been identified (Mellor et al, 2016; Porco et al, 2016; Zhang et al, 2016). The DAOs (DIOXYGENASE FOR AUXIN OXIDATION 1) convert IAA to oxIAA in vitro (Zhang et al, 2016) and mutant lines with compromised DAO activity accumulate significantly less oxIAA (Porco et al, 2016).

Zhang et al (2016) report on the DAO domain that separates these enzymes from the similar GA-2-oxidases (GA2ox), which catalyse gibberellin deactivation (Thomas et al, 1999; Schomburg et al, 2003). While the DAOs also contain conserved dioxygenase and 2OG Fe (II) oxygenase domains, they also possess an additional C-terminal motif (P_E_VD_EHPR), which is absent from the GA2ox enzymes (Zhang et al, 2016). This motif is conserved in rice (OsDAO), as well as in both AtDAOs, and has varying degrees of conservation within the *Viridiplantae*. Regardless of the conservation of the 2OG Fe (II) oxygenase and dioxygenase domains, Porco et al (2016), demonstrate that the DAOs are distinct from the GA2ox enzymes.

Sequence analysis of the DAOs presented here broadens the perspective of these analyses and demonstrates that the conserved DAO motif identified in these papers quickly degenerate outside of the angiosperms (Figure 5.11). While fractions of the DAO motif are present in the gymnosperms, ferns and lycophytes, the moss, *P. patens*, and the liverwort, *M. polymorpha*, are more similar to the GA2ox amino acid sequences. The GA2ox enzymes have not been reported to function in the oxidation of IAA, although many of these enzymes are uncharacterised. Additionally, oxIAA can be higher in mosses

(~350 ng g^{-1} FW in *Aulacomnium palustre)*(Drábková et al, 2015) than in *Arabidopsis* (~100 ng g^{-1} FW)(Porco et al, 2016). However, on average, the level of oxIAA in the bryophytes is much less (~28 ng g^{-1} FW)(Drábková et al, 2015).

These levels also correlate with reduced conservation in the DAO genetic sequence and suggest that DAO activity may not be as effective in the basal lineages. However, the DAO sequence from *M. polymorpha* contains 8 of the 11 residues in the DAO motif (Zhang et al, 2016), as opposed to two residues in the moss *P. patens*. Similarly, the DAO motif is also altered in the most similar pea sequence (54.54% similar, Figure 5.11). In the single pea sequence the glutamate (E) residue at position 8 of the pea DAO motif is substituted for aspartate (D). The same substitution of Glu with Asp (E8D) is also present in all five identified *M. truncatula* sequences (not shown). If the residues identified previously (Zhang et al, 2016) are important for DAO function, the concerted change in this residue may indicate that DAO function is reduced in the Fabaceae. However, glutamate and aspartate share similar structure and chemical properties (both are acidic and polar). It is interesting that unpublished work in pea suggests that oxIAA is not readily detectable in pea seeds (Adj Prof. J.J. Ross; pers. comm.), supporting at least partial loss of DAO activity when the motif is lost.

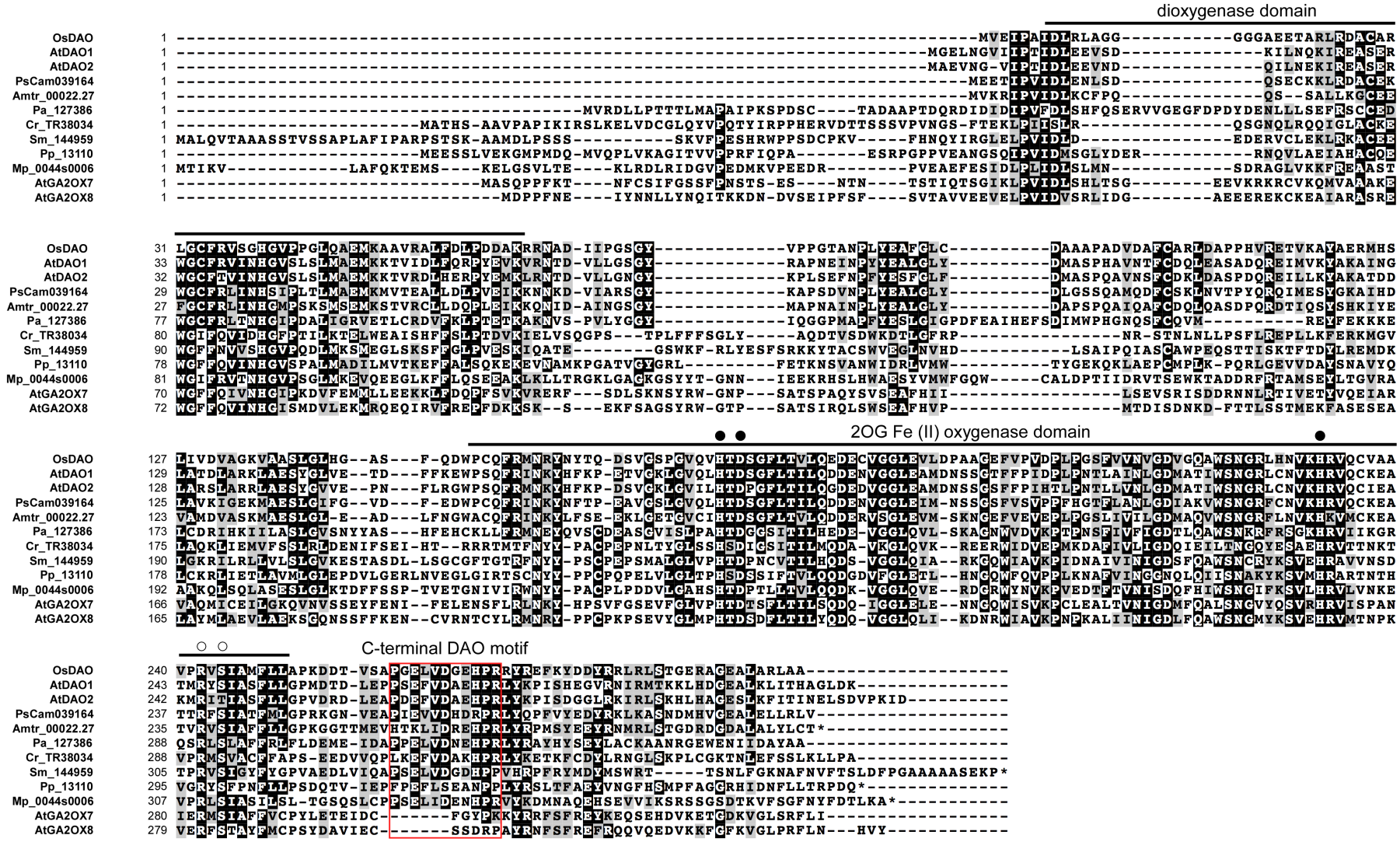

Figure 5.11 Multiple sequence alignment of DAO sequences from land plants as well as the similar GA2oxidases from *Arabidopsis*. Alignment shows conservation of the dioxygenase and 2OG Fe (II) oxygenase domains (black bars), Fe^{2+} binding residues (closed circles), OG binding residues (open circles) and the C-terminal DAO motif (red box). Sequence abbreviations are as follows; rice (Os) pea (Ps), *Arabidopsis* (At), *A. trichopoda* (Amtr), *P. abies* (Pa), *C. richardii* (Cr), *S. moellendorfii* (Sm), *M. polymorpha* (Mp) and *P. patens* (Pp).

It has been suggested that charophytes and liverworts utilise a biosynthetic/ catabolic mechanism to regulate free IAA levels, whereas the mosses and hornworts primarily use a conjugation/ deconjugation strategy to regulate free IAA (Sztein et al, 2000; Cooke et al, 2002). This makes sense given the lack of conservation in the DAO motif, although these studies were unable to detect oxIAA in species now known to contain this compound endogenously (Pěnčík et al, 2013; Drábková et al, 2015; Zhang et al, 2016).

Despite this, it is difficult to rationalise a complete loss of DAO activity in the basal lineages given the presence of oxIAA in these divisions (Drábková et al, 2015). Since the basal DAO sequences do not strongly resemble those from *Arabidopsis* or rice, yet basal species contain detectable amounts of oxIAA, it is possible that the conserved motifs identified by Zhang et al (2016) are not essential for the oxidation of IAA. However, this suggestion may implicate alternative methods by which plants oxidise IAA. This additional oxidative mechanism is supported in *Arabidopsis* since endogenous oxIAA levels in the *dao1-1* knockout mutant are still present in higher amounts than those reported endogenously for the bryophytes (Drábková et al, 2015; Porco et al, 2016). Additionally, in vitro assays on AtDAO1 contain detectable amounts of oxIAA in control reactions (Zhang et al, 2016).

Finally, an interesting observation regarding the DAOs is whether they can also utilise PAA as a substrate. In the conversion of IAA to oxIAA, oxygen is added to the indole backbone at the 2’ position, a site not available on the phenyl backbone of PAA. The aromatic nature of the phenyl structure is such that only a single bond can be shared between ring and the attaching oxygen, meaning that PAA is not likely to be catabolized through oxidation. Instead conjugation to amides or esters, or hydroxylation may be used. The inability for plants to break down PAA in this manner may explain why endogenous PAA levels are often higher than those of IAA.

5.3.7 Amide conjugation is an ancestral trait, but derived enzymes possess substrate specificity.

The GH3s are thought to be important for the regulation of endogenous IAA levels in plants. These enzymes function in the conjugation of IAA to various amino acids, which inhibits its biological activity. Previous work has demonstrated that the GH3s have a wide distribution in the angiosperms (Hagen and Guilfoyle, 1985; Zhang et al, 2009; Chen et al, 2010; Peat et al, 2012; Westfall et al, 2012). It is also suggested that these enzymes may function in all land plants, since homologs have been identified in the moss *P. patens* (Ludwig-Müller et al, 2009).

The GH3s from *Arabidopsis* can be divided into three distinct classes depending on their substrate preferences (Staswick et al, 2002). The enzymes responsible for the conjugation of IAA belong to the class II GH3s of which there are 8 members (Staswick et al, 2002; Staswick et al, 2005). Additionally, the class I GH3s, which include AtJAR1 (GH3.11), are responsible for the conjugation of jasmonic acid (Staswick et al, 2002; Staswick and Tiryaki, 2004). Finally, the class III GH3s conjugate amino acids to the benzoates, which are structurally similar to salicylic acid (SA) (Okrent et al, 2009). While the class II GH3s are chiefly responsible for IAA conjugation, both GH3.11 and GH3.12 reportedly have residual function on IAA (Staswick and Tiryaki, 2004; Staswick et al, 2005; Okrent et al, 2009). However, it is unclear if either of these enzymes can substantially conjugate IAA in vivo.

The class II GH3s can be divided into two groups, a core group containing GH3.1 to GH3.6, and a second group containing GH3.9 and GH3.17 (Figure 5.12). The core group is further subdivided into two distinct sister clades. The division of these three groups is supported by sequences in *A. trichopoda*, suggesting that the presence of three distinct groups of IAA amido-synthetases is conserved in all angiosperms. The first core can be further split into two sub-groups; the first, which includes GH3.1, GH3.2, GH3.3 and GH3.4, appears to be specific to the angiosperms. The second sub-group

contains GH3.5 and GH3.6 and is subtended by a radiation of sequences from *P. abies*. This whole core group is further subtended by sequences from both *C. richardii* and *S. moellendorfii*.

Previous work on these enzymes has demonstrated that the two sub-groups are differentially influenced by fluctuations in the levels of IAA (Hagen et al, 1984; Nakazawa et al, 2001; Tian et al, 2002; Staswick et al, 2005). Members of the first group are highly sensitive to changes in IAA levels and their transcripts are elevated substantially in the presence of IAA (Staswick et al, 2005). In the second group, GH3.5 and GH3.6 are regulated to a lesser extent in the presence of IAA, although all six of the core enzymes appear to preferentially conjugate IAA to Asp (Staswick et al, 2005).

The remaining class II enzymes, GH3.9 and GH3.17, form a monophyletic group sister to the core GH3s. This group also contains a sequence from *A. trichopoda*, as well as *P. abies* and *C. richardii*, suggesting that this group may have a separate function in all tracheophytes. It has been demonstrated that this group is insensitive to fluctuations in endogenous IAA, at least in *Arabidopsis* seedlings (Staswick et al, 2005). Previous work on GH3.17 also shows that while Glu is a preferred substrate for these enzymes, they are also capable of conjugating additional types of auxin-like compounds, including 4-Cl-IAA and tryptophan, unlike the core GH3s (Staswick et al, 2005).

Interestingly, GH3.12 also clusters within this group, although it is only distantly related to the class II GH3s, consistent with the residual activity this enzyme has on IAA. The tree presented here (Figure 5.12) shows that the class III GH3s are not widespread, even within the angiosperms. This is in agreement with previous findings that the class III GH3s have only been identified in *Arabidopsis* (Staswick et al, 2002; Staswick et al, 2005).

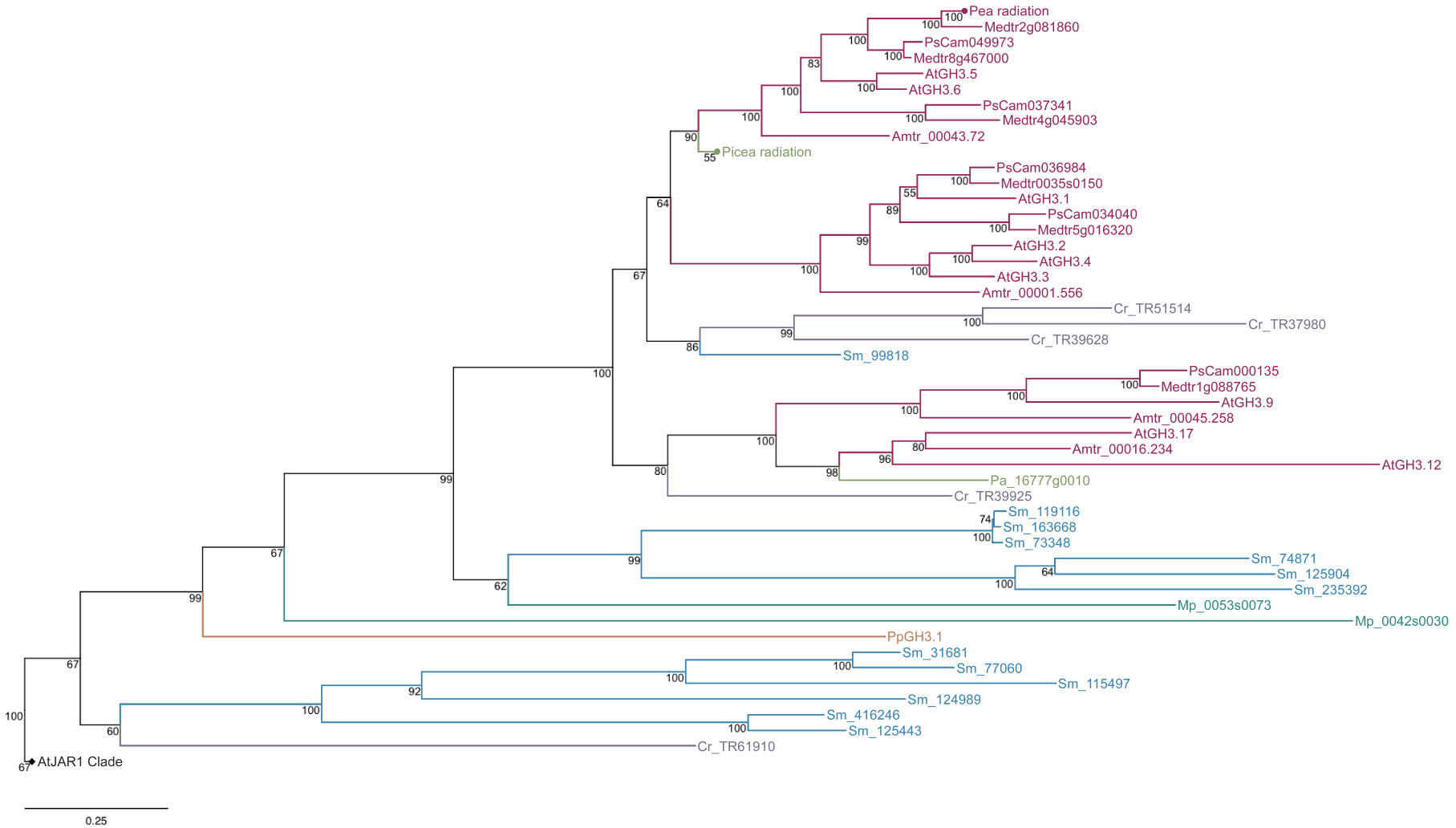

Figure 5.12 Phylogenetic reconstruction of the GH3 protein family based on amino acid sequences. Tree contains sequences from pea (Ps), *Arabidopsis* (At), *A. trichopoda* (Amtr), *P. abies* (Pa), *C. richardii* (Cr), *S. moellendorfii* (Sm), *M. polymorpha* (Mp) and *P. patens* (Pp). Reconstruction utilised a LG model with optimised site variation and gamma distribution. Scale bar indicates evolutionary distance, and bootstrap values (from 1000 replicates) are presented adjacent to nodes

While not expanded in Figure 5.12, the class I GH3s (AtJAR1 clade) contain sequences from all species, except *M. polymorpha*. This suggests that in addition to IAA amido-synthetase activity, most land plants can also conjugate jasmonic acid. Given their presence in the representative species, it is likely that all land plants posses this function. However, there are several sequences that do not cluster with either of these groups and the exact role they play in vivo is unclear.

Both *P. patens* and *M. polymorpha* contain two GH3 enzymes (Figure 5.12). While both *M. polymorpha* sequences belong to the class II GH3s, *P. patens* possesses a GH3 from both class I and class II. Previous work on the *P. patens* GH3s has shown that both are functional on IAA and JA (Ludwig-Müller et al, 2009). Interestingly PpGH3.1 only has weak IAA amido-synthetase activity, despite being more similar to the class II GH3s. The PpGH3.2 sequence groups with *AtJAR1* in the class I GH3s (collapsed in Figure 5.12). Previous work has shown that this enzyme is more efficient at conjugating IAA than PpGH3.1 (Ludwig-Müller et al, 2009). It is possible that previous annotations of these two genes have been reversed, since a third GH3 was also reported for *P. patens* (Bierfreund et al, 2004). However, this was later identified as a sequencing artefact.

Both GH3s in *P. patens* are able to use numerous substrates, similar to AtGH3.9 and AtGH3.17, and have unique conjugation profiles (Ludwig-Müller et al, 2009). While both of the PpGH3s are reportedly able to conjugate IAA to Asp in vitro (Ludwig-Müller et al, 2009), similar to the core class II GH3s in *Arabidopsis* (Staswick et al, 2002; Staswick et al, 2005), the IAA-Asp conjugate has not been detected in this species (Ludwig-Müller et al, 2009). This is also the case with the charophyte *Nitella sp.* and the hornwort *Phaeoceros carolinianus* which both lack IAA-Asp (Sztein et al, 2000). This suggests that the bryophytes (and green algae) do not utilise amide conjugation for the regulation of IAA.

Compared to IAA, very little is known of the metabolism of PAA. Sugawara et al (2015) report that PAA can be conjugated to both Asp and Glu, and that

overexpression of GH3.9 results in a substantial accumulation of both IAA-Glu and PAA-Glu amide conjugates. This makes sense since GH3.17, which is most similar to GH3.9 predominantly produces IAA-Glu, rather than IAA-Asp (Staswick et al, 2005). In fact, Staswick et al (2005) also found that GH3.2-GH3.6 and GH3.17 were all able to adenylate PAA, often to a greater extent than that of IAA, although this may be because PAA is typically present at higher levels than that of IAA in plant tissue (Sugawara et al, 2015). Despite this, it is likely that any GH3s with IAA amido synthetase activity also possess PAA amido synthetase activity and function in the concomitant degradation or storage of both endogenous auxins.

5.3.8 Ester conjugation

Another important component of the auxin metabolic scheme is the reversible ester conjugation of IAA to uridine 5'-diphosphate-glucose (UPG). It has been known for some time that this reaction is controlled by a reversible conversion of IAA to IAA-Glc by the IAA glucosyltransferases (UGTs)(Szerszen et al, 1994; Jackson et al, 2001). The UGT gene family is large in *Arabidopsis* (Li et al, 2001), although only one group (group ‘L’) has been demonstrated to have activity on IAA. Within this group, only UGT84B1 (Jackson et al, 2001) and UGT74D1 (Jin et al, 2013) appear to function appreciably in IAA conjugation, whereas other members of the group ‘L’ UGTs display limited or no function on IAA (Jackson et al, 2001). Instead, these enzymes appear responsible for the conjugation of other aromatic compounds (Lim et al, 2002; Meßner et al, 2003; Douglas Grubb et al, 2004).

The ester conjugate IAA-Glc is widely distributed in higher plants and has been detected in lycophytes and ferns as well as *Ginkgo biloba*, *Pinus thunbergiana* and several angiosperms (Sztein et al, 1995). However, these analyses failed to detect this compound in any of the bryophytes (Sztein et al, 1995; Sztein et al, 1999). IAA-Glc is considered a major conjugate in auxin biology, although its contribution to the total IAA pool varies depending on the species (Sztein et al, 1995). In order to better understand the distribution of the ester conjugates in the basal lineages, sequences from all representative species were compared with the *Arabidopsis* ‘group L’ UGTs,

as well as representatives from each of the other *Arabidopsis* UGT groups (A-K, Figure 5.13).

Interestingly, none of the identified sequences from the basal lineages were direct homologs of either UGT74D1 or UGT84B1, although sequences from pea (and *Medicago*) form separate monophyletic groups with both of these enzymes. Additionally, these groups include sequences from *A. trichopoda*, suggesting that ester conjugation of IAA by the UGT enzymes is present in all angiosperms. Further inspection of these relationships show that sequences from *P. abies* also belong to the group 'L' UGTs, although do not cluster with either of the two IAA glucosyltransferases.

Sequences from *C. richardii* and *S. moellendorfii* are also present in the UGT superfamily. However, the UGT from *C. richardii* is more similar to the Group 'H' and Group 'G' enzymes and the two *S. moellendorfii* sequences form a monophyletic group with the Group 'I' UGTs (Li et al, 2001). Neither of these groups possesses IAA glucosyltransferase activity. This is consistent with previous findings that *C. richardii* does not contain the IAA-Glc conjugate (Sztein et al, 1999). However, previous reports have detected IAA-Glc in *S. moellendorfii* (Sztein et al, 1995), even though the sequences from *S. moellendorfii* cluster with the group 'I' UGTs, which do not appear to conjugate IAA. This suggests that while particular group 'L' UGTs may be responsible for the conjugation of IAA in the angiosperms; similar enzymes from more basal species may exhibit more than one function.

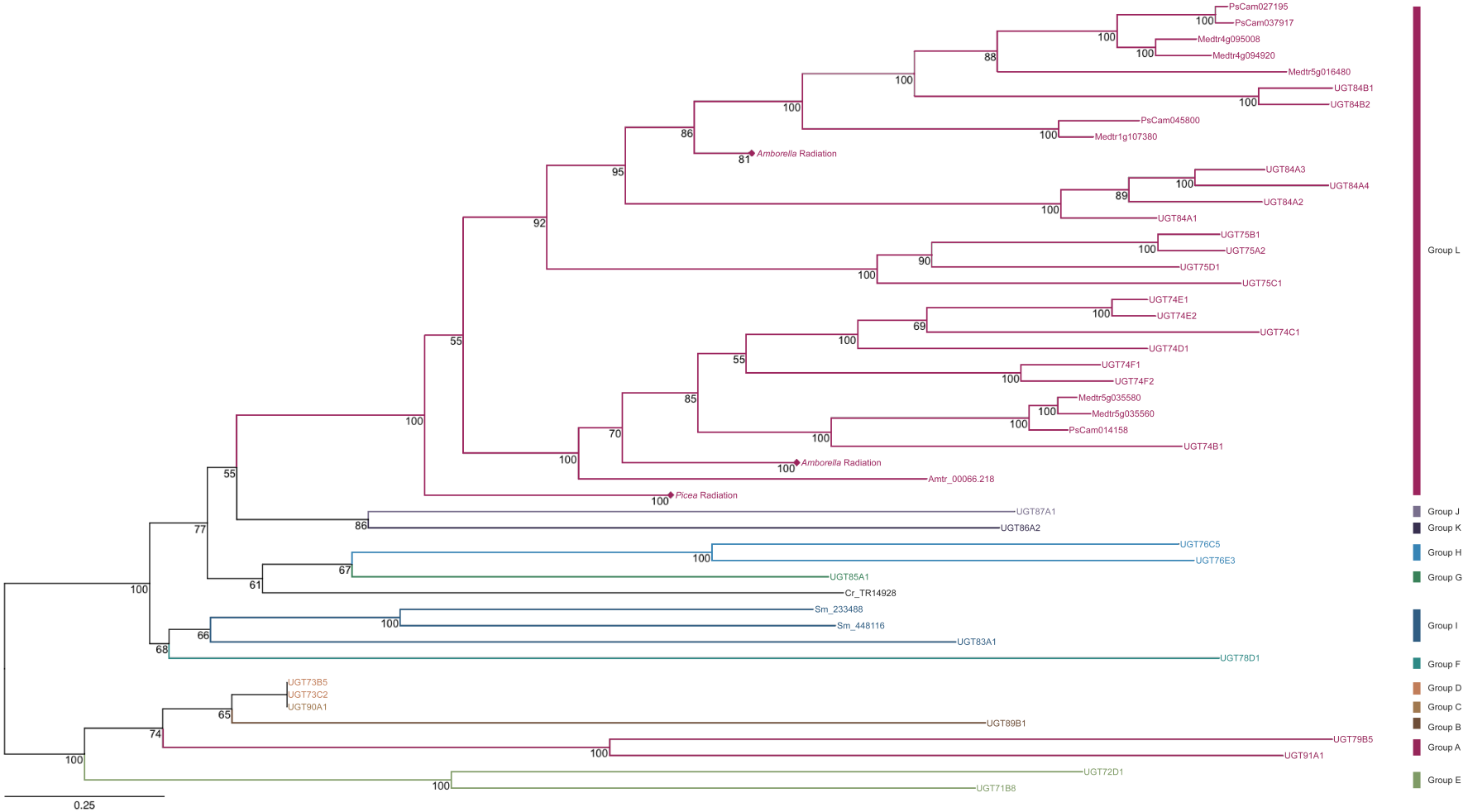

Figure 5.13 Phylogenetic reconstruction of the UGT protein family (groups are colour coded). Tree contains sequences from pea (Ps), *Arabidopsis* (At), *A. trichopoda* (Amtr), *P. abies* (Pa), *C. richardii* (Cr) and *S. moellendorfii* (Sm). Reconstruction is based on amino acid sequences and utilised a JTT model with optimised site variation and gamma distribution. Scale bar indicates evolutionary distance, and bootstrap values (from 1000 replicates) are presented adjacent to nodes

It has been suggested previously that sequence similarity is not an accurate predictor of function in this gene family (Jackson et al, 2001). This can be seen in UGT84B2, which lacks any IAA glucosyltransferase activity, even though its paralog, UGT84B1, appears to be responsible for the majority of this activity. The exact role of many of the UGTs is unclear since UGT74D1, which can also use IAA, preferentially conjugates oxIAA, an immediate catabolite of IAA, to oxIAA-Glc (Tanaka et al, 2014).

It was recently shown that members of the mosses and liverworts contain small amounts of the IAA glucose ester (Drábková et al, 2015). However, *M. polymorpha* and *P. patens* only contain sequences that are distantly similar to the UGTs from *Arabidopsis*. In a separate analysis, sequences from these two species were compared with representatives from all UGT groups (Figure 5.14). As expected, none of the *M. polymorpha* sequences clustered with the *Arabidopsis* UGTs, and formed a distant group with most of the sequences from *P. patens*. Interestingly, four sequences from P. patens clustered with the *Arabidopsis* UTGs, three in group ‘G’ and one group ‘E’. However, none of these sequences are strongly similar to the group ‘L’ UGTs.

These results support the absence of IAA-Glc in the bryophytes reported previously (Sztein et al, 1995). However, it is still unclear if the enzymes from *P. patens* are able to produce the glucose ester, since *S. moellendorfii*, but not *C. richardii*, is able to produce IAA-Glc, even though it lacks a group ‘L’ UGT. The identification of small amounts of IAA-Glc in other mosses and liverworts (Drábková et al, 2015) should not be discounted, since residual activity on IAA has been demonstrated in several group ‘L’ UGTs (Jackson et al, 2001). Similarly, Ludwig-Müller et al (2009) also detected ester-linked conjugates in *P. patens*, although IAA-Glc was not identified specifically. Despite this, it is suggested by these researchers that the UGTs in *P. patens* may be responsible for the ester conjugation.

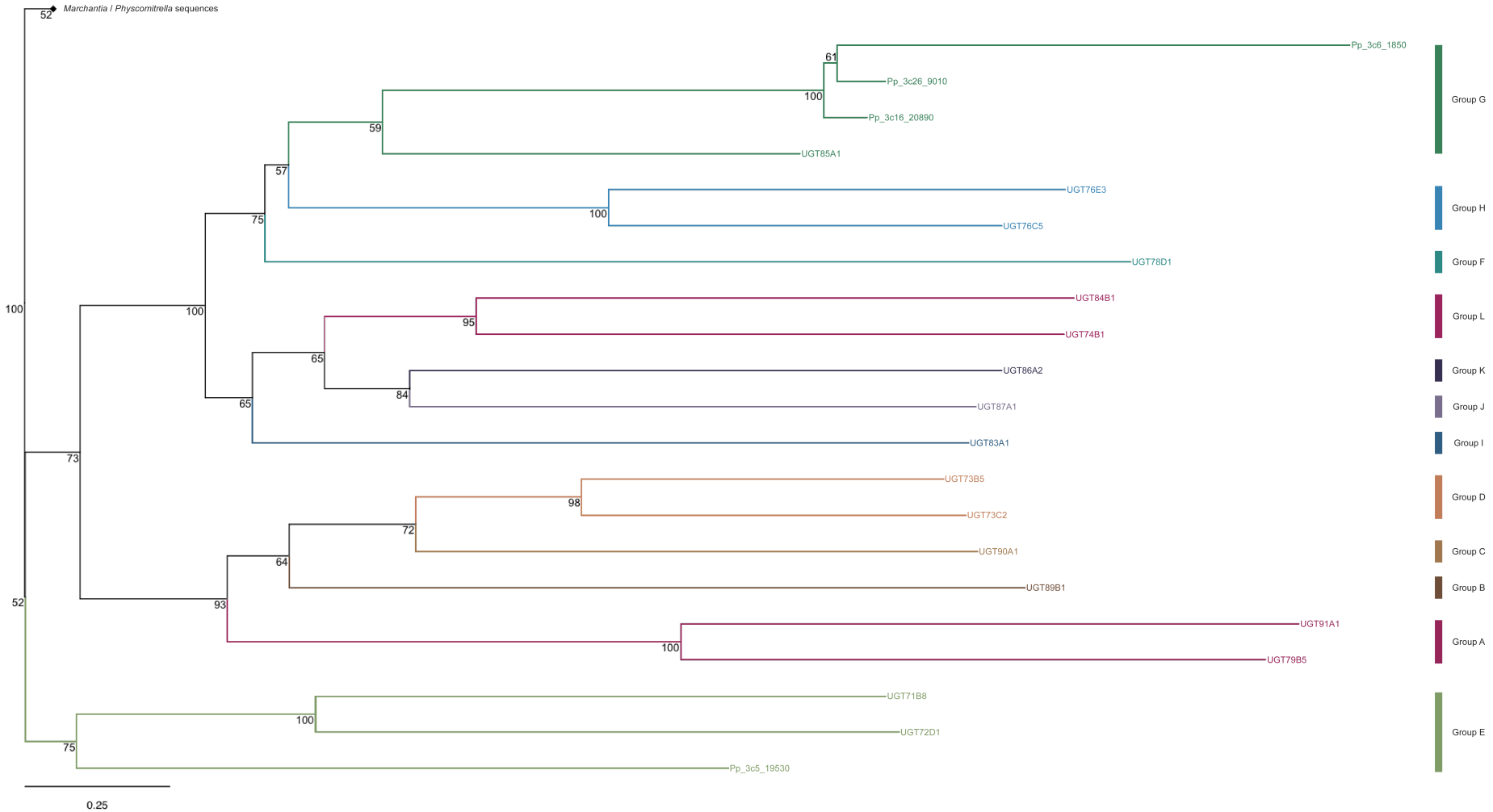

Figure 5.14 Phylogenetic reconstruction of all *Arabidopsis* UGT groups (colour-coded) and similar sequences from *P. patens* (Pp) and *M. polymorpha* (Mp). Reconstruction is based on amino acid sequences and utilised a JTT model with optimised site variation and gamma distribution. Scale bar indicates evolutionary distance, and bootstrap values (from 1000 replicates) are presented adjacent to nodes

It is unclear if the ester conjugation of PAA is analogous to IAA, although the UGTs may also function in the synthesis of PAA-Glc, similar to the dual role of the GH3s (Staswick et al, 2005). It has been demonstrated previously that UGT84B1 can utilise both IAA and PAA (Douglas Grubb et al, 2004). However, in identical reactions UGT74B1, which is not active on IAA, did not use PAA. This is consistent with previous findings within the group 'L' enzymes and suggests that the UGTs with IAA glucosyltransferase activity (84B1 and 74D1) may also function as PAA glucosyltransferases and that enzymes that cannot use IAA (such as 74B1) also cannot use PAA. As such, ester conjugation of PAA by the UGTs should be active, at least, in the majority of tracheophytes.

5.4 Conclusion

The recent interest in the biosynthesis of the auxin PAA (Chapter 3)(Sugawara et al, 2015) and discussion over the origins of the IPyA pathway (Yue et al, 2014; Turnaev et al, 2015; Wang et al, 2016) has inspired a comparative analysis of the biosynthetic pathways for both IAA and PAA. The evidence presented in this chapter supports the theory that the auxins, IAA and PAA, are ubiquitous in land plants. Previous work has also identified auxins in the green, red and brown algae (Abe et al, 1974; Fries and Āberg, 1978; Ashen et al, 1999; Le Bail et al, 2010; Yokoya et al, 2010) as well as bacteria (Hwang et al, 2001; Kim et al, 2004; Somers et al, 2005; Spaepen et al, 2007) and fungi (Kishore et al, 1976; Reineke et al, 2008). The distribution of both IAA and PAA in many organisms highlights its importance as a signalling molecule in the simpler forms of life as well as in complex higher plants.

In addition to the distribution of the two auxins, it is demonstrated in this chapter using deuterium labelled metabolism experiments that both the IPyA and phenylpyruvate pathways can be functional in representative species from most evolutionary divisions. These two pathways are augmented by phylogenetic studies demonstrating that the TAR, YUC and ArAT enzymes are present in all land plants, with the exception of the lycophyte *S.*

moellendorfii, which lacks an ArAT homolog. Despite this absence, *S. moellendorfii* accumulates substantial amounts of PAA, which suggests that the ArATs are not essential for the biosynthesis of PAA. However, It is also demonstrated in this chapter that D_5 Phe can be converted to D_5 PAA in all representative species. This prompts some interesting questions regarding the role that the ArATs play in PAA biosynthesis.

Since the biosynthesis of IAA and PAA is ubiquitous in land plants, it is important to understand if the metabolism of the two auxins is similar in all representative species. Previous investigations have suggested that land plants use one of three distinct conjugation patterns to regulate IAA (Sztein et al, 1995; Sztein et al, 1999; Sztein et al, 2000). The work presented in this chapter compares these findings with the distribution of three major metabolic enzymes; the DAOs, which convert IAA to oxIAA, the GH3s which conjugate IAA to amino acids, and the UGTs which catalyse the conversion of IAA to its glucose ester.

The work from this chapter shows that the conserved DAO motif identified by Zhang et al (2016) quickly breaks down outside of the angiosperms. Despite this, oxIAA has been detected in the bryophytes, albeit at much lower concentrations than the angiosperms (Drábková et al, 2015; Porco et al, 2016). It is likely then, that the while all land plants may catabolise IAA via oxIAA, the angiosperms have a much higher capacity to utilise this method. This is logical given that the moss and liverwort sequences are more similar to the GA2ox enzymes than the DAO proteins from *Arabidopsis*. Despite their function on IAA, these enzymes may not be able to utilise PAA as a substrate, since the phenyl backbone of this auxin lacks available sites to attach the free oxygen.

Similar to the IAA biosynthetic enzymes, the number of GH3s tends to increase towards the angiosperms. In fact, the class III enzymes are only present in *Arabidopsis*. This is consistent with the profile presented by Sztein et al (2000) who demonstrate increased amide conjugation in higher plants. The increase in the number of enzymes is correlated with divergent

sensitivities to endogenous IAA levels. It is also important to note that the enzymes from basal species appear to utilise several amino acids to similar extents. This is not necessarily the case with derived GH3s, which appear to prefer either Asp or Glu as substrates. This is consistent with (Sztein et al, 1995; Sztein et al, 1999) who failed to detect either of these conjugates in basal species.

The number of UGTs in *Arabidopsis* is also substantially higher than similar sequences in the basal lineages. These enzymes appear to have specific functions in *Arabidopsis*, since some, but not all, of the group 'L' UGTs are active on IAA. It is interesting that none of the sequences from the basal lineages cluster with the group 'L' UGTs, since IAA-Glu is present in these divisions. It is likely then, that many of the UGTs have become functionally specialized in higher species and can no longer function as IAA glucosyltransferases.

The mechanisms behind the metabolism of IAA are relatively well understood. However, our understanding of the catabolism of PAA is not. For the three major processes, there is evidence that PAA can potentially utilise two. It has been demonstrated recently that PAA can be conjugated to both Asp and Glu by the GH3s in *Arabidopsis* (Sugawara et al, 2015). Similarly, it appears that UGT84B1, which is active on IAA, can also use PAA as a substrate (Douglas Grubb et al, 2004). However, the putative end product of this reaction, PAA-Glu, has not been identified as yet. Given the distribution of these two gene families and their respective end products, it is likely that all land plants are able to synthesise both ester and amide PAA conjugates to some extent. Similar to IAA, it is also likely that the efficiency of these conversions is higher in the angiosperms.

Chapter 6: Mapping and characterisation of the *bushy* gene

6.1 Introduction

The *bushy* mutant is a single-gene semi-dominant pea mutant characterised by short, thin stems, small leaves and substantial basal branching, as reported by Symons et al (1999). Its potential as an auxin-related mutant was quickly realised and confirmed shortly after, through quantification of IAA, its 4-chlorinated form, as well as its ester, amide, and total conjugates (Symons et al, 2002). However, despite significant reductions in the levels of IAA and a striking phenotype, further research on this curious auxin mutant has been limited (Foo, 2013; Urquhart et al, 2015).

The phenotypic characterisation in Symons et al (1999) was extensive and made apt comparisons to the *rms* mutants, which also show increased branching (Arumingtyas et al, 1992). Yet, the phenotypes of all *rms* mutants are less severe than that of *bushy* and, unlike *bushy*, the *rms1-1*, *rms2-2*, and *rms3-2* mutants contain auxin levels up to 5-fold higher than their corresponding WT (Beveridge et al, 1994, 1996; Beveridge et al, 1997). It is now understood that most *rms* genes are involved in the biosynthesis and perception of the branching hormone strigolactone (Beveridge and Kyozuka, 2010). It is also interesting to note that the regulation of strigolactones appears to be controlled by elements of the auxin signal transduction pathway (Hayward et al, 2009), linking the two hormones.

Reproductive behaviour is also altered in the *bushy* mutant, which flowers about 32% later than the WT, and with flowers that are reduced to about 77% of the WT size (Symons et al, 1999). However, it is difficult to compare node of flower initiation as apical dominance is completely lost by the time the mutant plants flower. Pods are also reduced in size, but this has been attributed to a reduction in seed number (Symons et al, 1999). Pods on

bushy plants only produce 1-2 seeds (compared to 3-7 in the WT) that are around 70% of the dry weight of the WT.

Attempts at mapping the *bushy* loci in Symons et al (1999) did not reveal any linkage to the 20 scored markers across the linkage groups presented in Weeden (1998). However, subsequent analyses by the Hobart research group have suggested that *bushy* could potentially be linked to the *aldehyde oxidase* (*AO*) gene family (Dr S.E. Davidson; pers. comm.).

Aldehyde oxidases have previously been implicated in the oxidative hydroxylation of indole-3-acetaldehyde (IAAld) to IAA (Miyata et al, 1981; Koshiba et al, 1996; Seo et al, 1998). This could indicate that a mutation in one of the *AO* genes may be causing this phenotype. All three of the pea *AO's* share strong sequence similarity indicating a high degree of conservation or a very recent duplication event (Zdunek-Zastocka et al, 2004). At least one of the *AO's* is proposed to function specifically in the conversion of abscisic-aldehyde to abscisic acid (ABA), the final step in the biosynthesis of the hormone, ABA (Seo et al, 2000; Zdunek-Zastocka et al, 2004).

Previous work by Quittenden (2011) showed an accumulation of IAAld in the *bushy* mutant, consistent with a blockage of *AO* activity at this step. Yet in these experiments, the alternative end product, IEt (tryptophol), was not altered. One would expect a tandem increase in the level of IEt, should IAAld levels be increased. Further, the role of IAAld in auxin biosynthesis remains unclear, and based on the predominance of the IPyA pathway (Stepanova et al, 2008; Tao et al, 2008; Mashiguchi et al, 2011; Won et al, 2011), its contribution to the IAA pool is likely to be insubstantial (Mashiguchi et al, 2011; Tivendale et al, 2014; Sugawara et al, 2015).

Nonetheless, reduction of IAA levels in *bushy* is a curious feature of the mutant. Additional observations are that the WT phenotype cannot be completely restored by application of IAA (Symons et al, 2002). The metabolism of [^{3}H] IAA is also significantly altered in *bushy* where

radioactivity corresponding to IAA was reduced in the mutant when compared with the WT (indicating increased auxin metabolism). It is interesting to note that despite this increase, the levels of total IAA were not reduced in the *bushy* mutant, even though a major auxin conjugate in pea, IAA-Asp (aspartate), was lower (Symons et al, 2002). As IAA-Asp is only one part of the auxin catabolic/ conjugate system in other species (Staswick et al, 2005), this reduction may indicate an accumulation of other conjugates or metabolites.

Since exogenous application of IAA cannot reverse the *bushy* phenotype (Symons et al, 2002), and since *bushy* is a semi-dominant mutation, it is likely that the phenotype may be caused by a mutation in auxin signalling/ perception. There are many components involved in auxin signalling including ARFs, AUX/ IAA proteins, TIR1/ AFB, ASK1, Cullin and RBX (Chapter 1)(Guilfoyle and Hagen, 2007). Interestingly, auxin-signalling mutants are often characterised by reduced apical dominance, shorter internodes and smaller leaves, similar to the phenotype of *bushy*. However, the semi-dominant nature of *bushy* is unusual and may suggest that *bushy* is a “gain-of-function” mutant.

In this chapter I have investigated the physical location of the *bushy* locus and present evidence that it is linked to, but distinct from, the *AO* genes. In the process I have identified several candidate genes that may account for the *bushy* phenotype. In addition, I have further investigated the effect of *bushy* on the biosynthesis of IAA and PAA to improve our understanding of auxin biosynthesis/ metabolism.

6.2 Materials and Methods

6.2.1 Plant material

The populations studied in this chapter were derived from a cross of *bushy* (Hobart line 297H, paternal) to line 1794 (maternal), following emasculation. Pollen was collected from individuals that were heterozygous for *bushy* and was stored at 4°C as flowering times were not synchronised. Crosses were confirmed in the F_1 generation, which segregated roughly 1:1 (WT to Het).

Heterozygous phenotypes were obvious after three weeks, due to the fact that the *bushy* phenotype is not manifest immediately after germination. Heterozygous F_1 were self-pollinated to produce 67 segregating F_2 progeny, which displayed typical Mendelian inheritance (1:2:1) for the *bushy* phenotype. This population was used to generate a linkage map to confirm the position of the *bushy* loci, using JOINMAP (Kyazma). 140 F_3 seeds from all heterozygous individuals in the F_2 generation were planted to confirm marker positions, confirm heterozygous individuals and enhance the mapping of the *bushy* loci. Seeds harvested from F_2 plants were highly variable in number (from 2 to more than 10), but genetic material from all heterozygous lines was included. Healthier plants contributed no more than 8 seeds to the F_3 population. Developing leaflets for mapping populations was obtained after 3 weeks growth and gDNA was extracted as described in Chapter 2.8. All other analyses were conducted on 5-week-old apical portions from segregating progeny of selfed individuals from line 297H following at least ten generations of backcrossing.

6.2.2 Quantification and metabolism of auxin precursors in *bushy* apical tissue

Hormones were extracted and determined as described in Chapter 2.3-2.7. Metabolism experiments on *bushy* were conducted on apical portions of *bushy* mutants (and the segregating WT) obtained from 5-week-old plants grown in growth cabinets as described in Chapter 2.2.

6.2.3 HRM markers

High resolution melt markers were designed to span a large region on the top of pea linkage group I. Initial pea sequences for each marker were obtained for the lines L1794 and L297M using previously designed primers (Dr S Ridge) based on presumed orthologous genes in *Medicago*. Full-length sequences were obtained from Macrogen (Korea) and were screened for polymorphisms between the two lines. Primers were then designed to amplify regions containing identified polymorphisms.

The HRM markers *MYB2*, *NIN*, *AS2* and *FRLb* were tested using gDNA obtained from parent lines (1794 and 297M) and a mixture of the two in various ratios (50:50, 60:40, 40:60) to simulate heterozygous controls. High-resolution analysis of all melt curves allowed clear separation of all three genotypes.

6.2.4 CAPS markers

Previously designed CAPS markers (Dr S.E. Davidson) were applied to both the F_2 and subsequent F_3 populations. *AO1* was passed on both F_2 and F_3, and *Lip1* (*PsCOP1*) was passed on the F_3. Following PCR amplification of products, 5 µL aliquots of each PCR reaction was taken and added to a digest mixture containing 3.75 µL of dH_2O, 1 µL of 10x CutSmart Buffer and 0.25 µL of restriction enzyme. For *AO1*, *Dra1* (20,000 U/ mL [5 U per reaction]) was used to cut the wild type band (190 bp) to produce bands of 120 and 70 bp. For *Lip1*, *Psi1* (5,000 U/ mL [1.25 U per reaction]) was used to cut the wild type band (1100 bp) to produce bands of 700 and 500 bp. In both cases, the *bushy* allele was uncut and heterozygotes were identified by the presence of the full-length band as well as the two smaller bands.

6.2.5 Mapping and identification of candidate genes

Two linkage maps were produced, based on F_2 and F_3 populations generated from a cross of *bushy* and L1794. Maps were generated with the specialist software JOINMAP (Kyazma) using a LOD score of at least 3 for both populations. The first linkage map, generated from the F_2 population spanned the region thought to contain *bushy* and contained all markers

except *Lip1*, which produced inconclusive melts and could not be scored. The second map, produced from a segregating F_3 generation, provided a higher resolution map and incorporated the *Lip1* marker. The low efficiency of the *Lip1* marker in the F2 generation is unclear. The *NIN* maker was not amplified consistently across the F_3 population and produced ambiguous melt profiles. This marker was omitted from the analysis, resulting in the absence of a molecular marker on the other side of the *bushy* phenotypic marker. The *FRLb* marker was not scored for the F_3 population.

6.2.6 AO Sequencing

Messenger RNA for sequencing was obtained from imbibed seeds following overnight submersion in dH_2O. cDNA was synthesised by reverse transcription as described in Chapter 2.9.The three pea *AOs* were amplified from *bushy*, L1794 and L5839 using primers flanking the CDS (Chapter 2.12) and raw PCR product for each was cleaned and sequenced by Macrogen (Korea). Sequences were compared using Sequencher (Gene Codes Corp.). All primers used in this chapter are presented previously (Chapter 2.12).

6.3 Results

The map generated from the F_2 generation shows that the *bushy* locus is present at the top of pea linkage group 1 (Figure 6.1a). However, in this map the molecular markers *MYB2* and *AS2* are inverted relative to their positions in *Medicago*, suggesting that the resolution of this map is poor. It has been shown that marker positions in the pea and *Medicago* genomes are highly conserved in this region, despite significant differences in other linkage groups (Aubert et al, 2006). It is suggested that this discrepancy might be attributable to the small number of individuals in the F_2 population (n=67).

The second map is more congruent with marker positioning compared to the *Medicago* linkage group V (Figure 6.1b). While lacking a molecular marker below the *bushy* locus, the positions of all other molecular markers are strongly similar to their positions in the *Medicago* genome. The estimated map distance (cM) between each marker strongly correlates with the physical distance (bp) in *Medicago* (R^2=0.99).

Additionally, closer inspection of the raw data used to produce the linkage map shows that in the population there were several recombination events between the *AO1* marker and the *bushy* phenotype (Table 6.1). The occurrence of these recombinants excludes the *AOs* as candidates for *bushy*. In an attempt to obtain further evidence that none of the *AOs* corresponds to *bushy*, cDNA from both 297M and 1794 was sequenced (Macrogen) using an array of primers (Chapter 2.12). However, the sequences obtained for these lines were of too poor quality to identify any clear polymorphisms. Further work on sequencing these genes is required.

6.3.1 *Medicago* genome analysis and candidate selection

The candidate region between *AO1* and *NIN* spans approximately 5.75mbp in *Medicago* and contains several hundred protein-encoding genes. Based on the two linkage maps (Figure 6.1), this entire region was scanned for gene annotations relating to auxin. Primary candidate selection identified around fifty candidates that are associated with auxin perception/ signalling in some way. Amino acid sequences of each candidate were then used to identify annotated homologs in *Arabidopsis* using the TAIR portal.

While most candidates shared clear homology with *Arabidopsis*, the majority were identified as F-BOX disease resistance/ defence response proteins. There are approximately 700 members of the F-Box superfamily in *Arabidopsis* (Quint and Gray, 2006), although only components of the $SCF^{TIR1/\ AFB}$ complex have been implicated in auxin signalling (Quint and Gray, 2006). Following the exclusion of the disease resistance proteins, the candidate list was reduced to 11 genes (Table 6.2) distributed across *Medicago* linkage group V (Figure 6.1c).

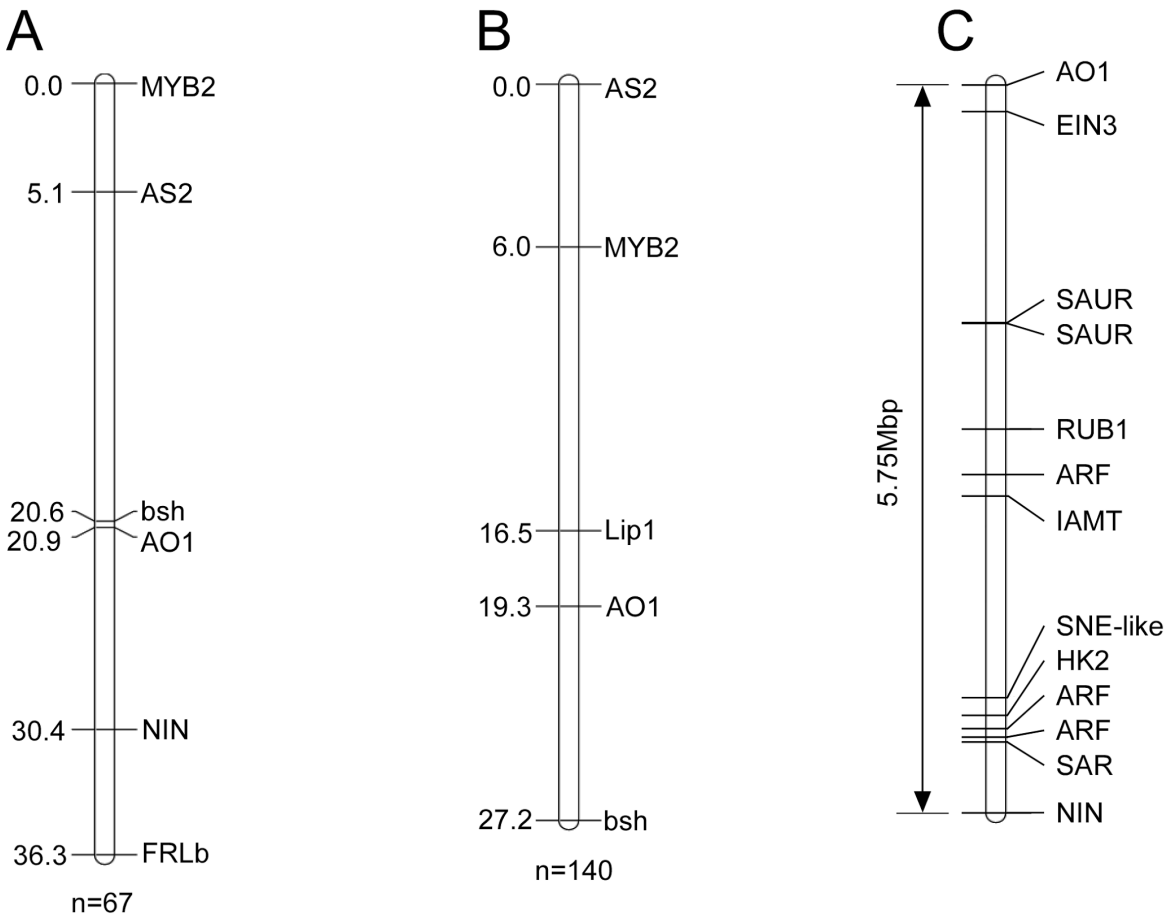

Figure 6.1 Generated marker maps in pea showing A: linkage relationships in the F_2 generation of a cross between L1794 and *bushy* (n=67), B: linkage relationships from the F_3 generation of self-fertilised heterozygous individuals from the F_2 generation (n=140) and C: the distribution of auxin related candidates between *AO1* and *NIN* molecular markers in *Medicago truncatula* (jcvi.org/Medicago/). Annotations for candidates are presented in Table 6.2.

Table 6.1 Recombination events between the *AO1* marker and the *bushy* phenotype as well as genotypes for other markers in the F_3 population. Genotypes from 1794 are coloured blue (A), 297m in red (B) and heterozygous in green (H). Markers are presented in linear order

Marker	17	30	31	47	50	53	55	56	88	95	107	113	121	123	125	126	130
AS2	A	B	H	B	A	A	H	.	H	H	H	H	H	A	H	H	H
MYB2	A	B	H	B	A	A	H	A	H	H	H	H	H	A	H	H	H
Lip1	H	B	H	B	A	A	H	H	H	H	H	H	H	H	H	H	H
AO1	H	B	H	B	H	H	H	H	H	H	H	B	B	H	H	H	H
bushy	B	H	B	H	A	B	B	A	B	B	B	H	H	B	A	A	A

Table 6.2. List of *bushy* candidates showing accession numbers and annotations for *Medicago truncatula* (JCVI; MtV4.0), accession numbers for pea homologs (pea genome atlas), as well as accessions and gene designations from *Arabidopsis* (At) homologous (TAIR; release V10).

***Medicago* Loci**	**Locus annotation**	**Pea homolog**	***At* homolog**
Medtr5g087790	ethylene insensitive transcription factor	PsCam033741	AT3G20770 (EIN3)
Medtr5g091070	SAUR-like auxin-responsive family protein	PsCam027983	-
Medtr5g091090	SAUR-like auxin-responsive family protein	PsCam027983	-
Medtr5g092700	ubiquitin-NEDD8 RUB1-like protein	PsCam052971	AT1G31340 (RUB1)
Medtr5g093520	auxin-responsive family protein	PsCam046085	AT3G25290 (ARF)
Medtr5g093900	indole-3-acetate O-methyltransferase-like protein	PsCam038419	AT5G55250 (IAMT1)
Medtr5g097150	F-box SNE-like protein	PsCam040443	AT5G48170 (SLY2)
Medtr5g097410	cytokinin receptor histidine kinase	PsCam044840	AT5G35750 (HK2)
Medtr5g097620	auxin-responsive family protein	PsCam033960	AT2G04850 (ARF)
Medtr5g097810	auxin-responsive family protein	PsCam043201	AT3G25290 (ARF)
Medtr5g097890	suppressor OF AUXIN resistance protein	PsCam049143	AT1G80680 (SAR3)

6.3.2 IPyA content is reduced in *bushy*

Similar to previous findings, the level of IAA was reduced in the *bushy* mutant (Figure 6.2b)(Symons et al, 2002; Quittenden, 2011). A novel finding is that the level of IPyA, the main intermediate in IAA biosynthesis, was also reduced (Figure 6.2a). This indicates an alteration to IAA biosynthesis in the *bushy* mutant, potentially occurring upstream of the YUCCA enzymes.

In line with this inhibition, the level of the precursor Trp accumulated in the *bushy* mutant, contrary to a previous finding (Quittenden, 2011). However, this elevation was restricted to the internode, and Trp levels were normal in leaves and apical portions (Table 6.3). Additionally, in this experiment the levels of total IAA (endogenous plus ester and amide bound IAA) were not reduced in the *bushy* mutant (Table 6.3), in contrast to a previous finding (Symons et al, 2002).

6.3.3 PAA biosynthesis and conjugation are altered in *bushy*

Despite large reductions in the levels of IAA, the levels of endogenous PAA were not significantly altered in the *bushy* mutant (Figure 6.3b). However, quantification of precursor levels shows that the phenylpyruvate content was reduced in *bushy* (Figure 6.3a), similar to IPyA (Figure 6.2a). It is interesting to note that following TAZ-labelling, the levels of (TAZ-) phenylpyruvate are substantially higher than determined earlier, in the absence of derivatization (Chapter 3). This may indicate degradation of phenylpyruvate during the workup procedure.

The levels of Phe were elevated in *bushy* (Table 6.3). However, like Trp, this was tissue specific and was only detected in apical portions. Also, the levels of bound PAA were normal in the *bushy* mutant (Table 6.3). This is unsurprising, as the levels of the endogenous hormone were also normal in these experiments.

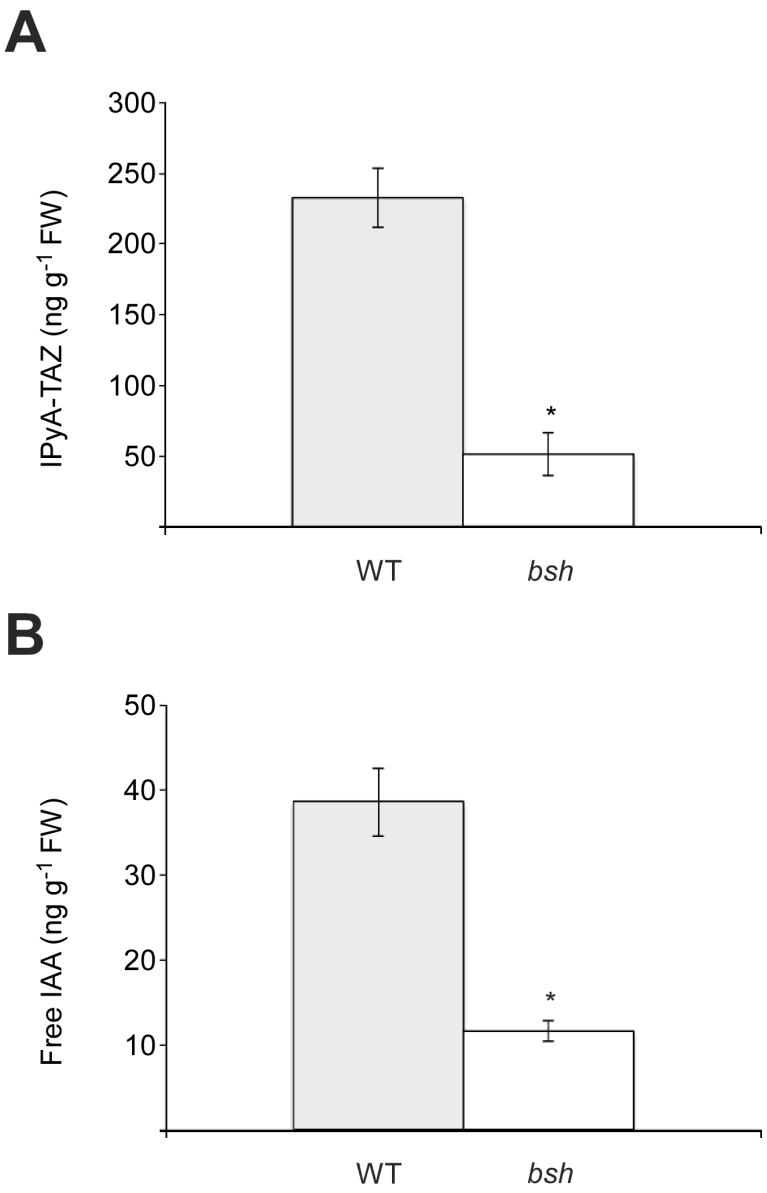

Figure 6.2 Effects of the *bushy* mutation on the levels of (A) IPyA (TAZ-labelled) and (B) free IAA in 5-week-old apical portions compared with the corresponding WT. Data are means ± SE (ng g^{-1} fresh weight [FW], n=5). '*' Indicates a significant difference at the 0.05 level.

Table 6.3. Trp and Phe levels in internode, leaf and apical portions, as well as total IAA and PAA from 2-week-old *bushy* and its WT. Values are endogenous levels (ng g^{-1}) ± SE. '*' Indicates a P value of ($P<0.05$, n=3), ns = not significant.

Endogenous compound	Tissue	Genotype	
		WT	*bushy*
Tryptophan (ng g^{-1})	Apex	17314 ± 1480	17762 ± 1883^{ns}
	Internode	3694 ± 475	76627 ± 10884*
	Leaf	13213 ± 2197	15025 ± 1942^{ns}
Phenylalanine (ng g^{-1})	Apex	91398 ± 15727	214960 ± 6850*
	Internode	43391 ± 4106	75115 ± 26225^{ns}
	Leaf	180319 ± 11864	216735 ± 62034^{ns}
Total IAA (ng g^{-1})	Whole shoot	314 ± 2	1199 ± 608^{ns}
Total PAA (ng g^{-1})	Whole shoot	97 ± 5	353 ± 113^{ns}

6.3.4 Application of Trp and Phe restores WT IAA levels

Metabolism experiments on apical portions of *bushy* and its WT show that in the presence of 100 µM D_5 Trp, the levels of endogenous IAA are restored (Figure 6.4). However, despite the restoration of IAA, the levels of deuterium labelled (D_5) IPyA are still reduced (Figure 6.5), even in the presence of massive amounts of precursor. Unexpectedly, in identical reactions containing 100 µM D_5 Phe, the levels of endogenous IAA are also completely restored (Figure 6.4). The reason for this is not clear at present.

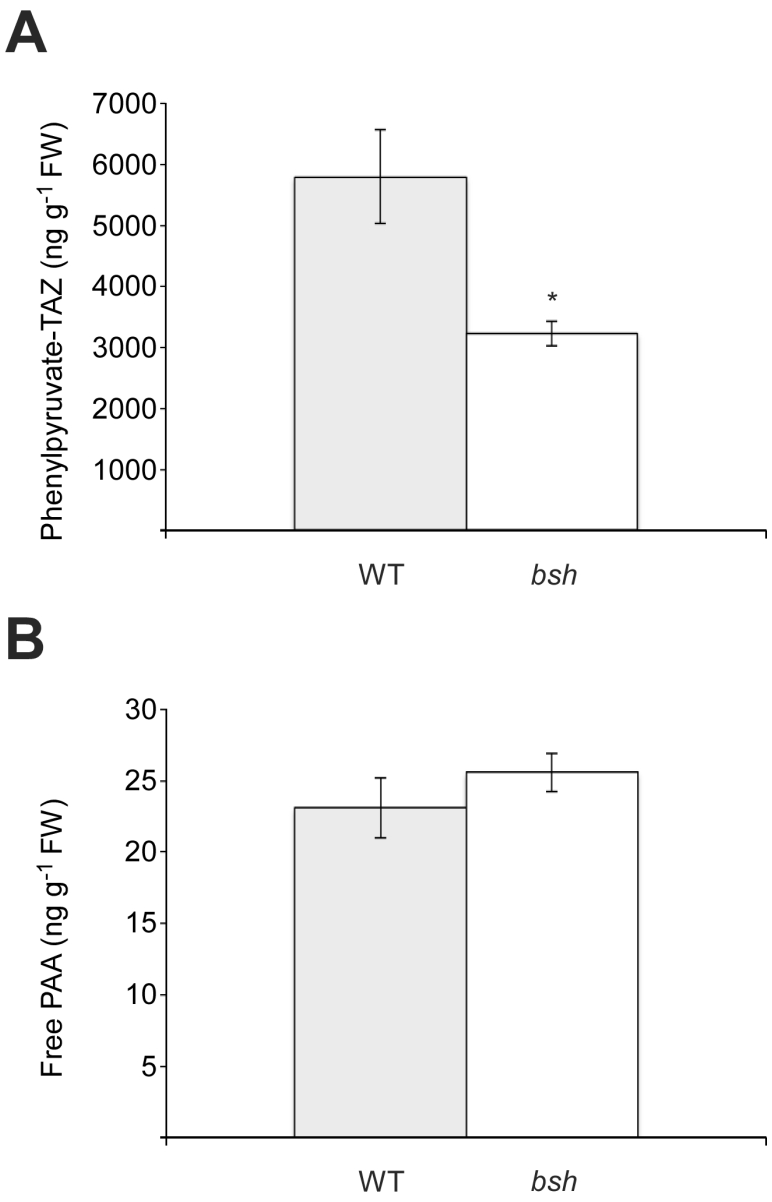

Figure 6.3 Effects of the *bushy* mutation on the levels of (A) phenylpyruvate (TAZ-labelled) and (B) free PAA in 5-week-old apical portions compared with the corresponding WT. Data are means ± SE (ng g^{-1} fresh weight [FW], n=5). '*' Indicates a significant difference at the 0.05 level.

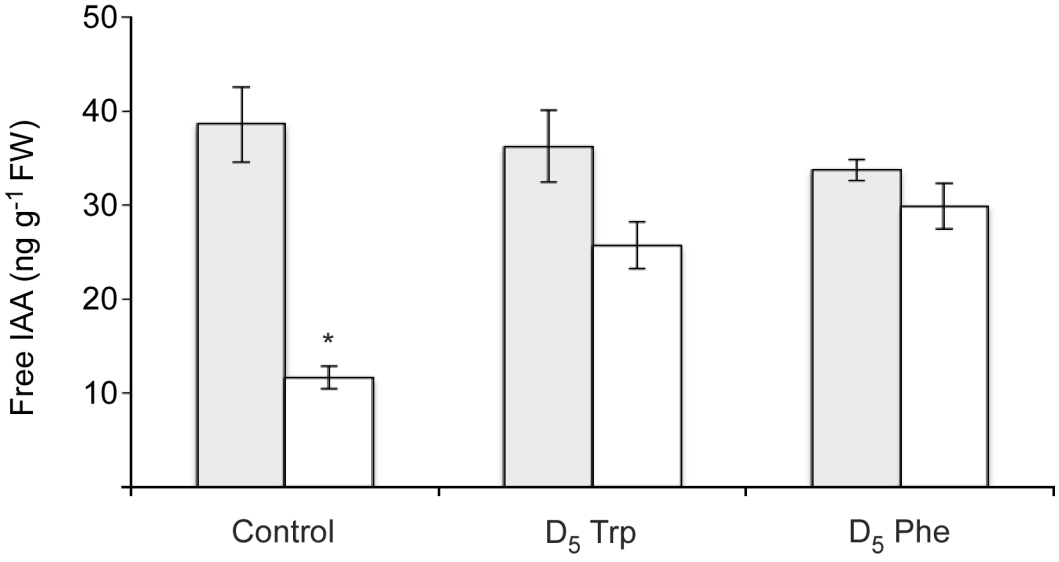

Figure 6.4 Metabolism experiments show restoration of WT IAA levels in 5-week-old apical portions of *bushy* (white) and its WT (grey) when incubated for 16 hours with 100 µM D_5 Trp and D_5 Phe compared with control reactions. Data are means ± SE (ng g^{-1} fresh weight [FW], n=5). '*' Indicates a significant difference at the 0.05 level.

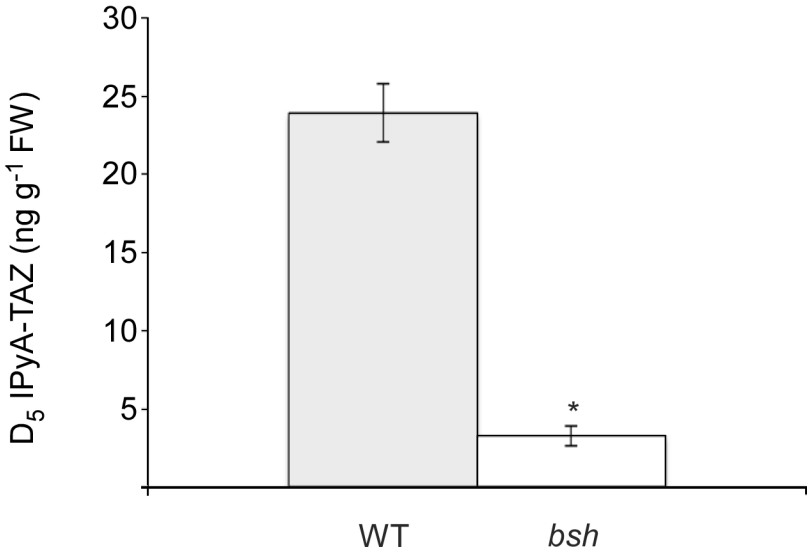

Figure 6.5 Metabolism experiments show that D_5 IPyA (TAZ labelled) levels are reduced in 5-week-old apical portions of *bushy* (white) and its WT (grey) following a 16-hour incubation. Data are means ± SE (ng g^{-1} fresh weight [FW], n=5). '*' Indicates a significant difference at the 0.05 level.

6.4 Discussion

6.4.1 The *bushy* loci is located on pea linkage group I

The mapping of the *bushy* loci reported here has revealed strong linkage to several molecular markers known to be located at the top of pea linkage group I (Aubert et al, 2006). The initial map also provided evidence that *bushy* is located between the molecular markers *NIN* and *AS2*. However, the analysis of the F_2 generation lacked power due to a small population size and marker positioning displayed poor synteny with the *Medicago* linkage group map (Aubert et al, 2006). A second analysis of the F_3 generation shows that *bushy* is located below the *AO1* marker, although in this case both the *NIN* and *FRLb* markers did not produce adequate melt profiles and were excluded.

It was previously suggested that the *bushy* phenotype might be caused by a mutation in an *aldehyde oxidase* (*AO*) gene in pea (Quittenden, 2011), based on the accumulation of IAAld in *bushy* mutants. However, preliminary analysis on the 4480 mutant line (*Psao1*) suggests that a loss of AO1 function does not produce an obvious phenotype, unlike that of *bushy* (Adj Prof. J.J. Ross; pers. comm.). This finding is supported by genetic evidence (Table 6.1) that demonstrates recombination events between the *AO1* molecular marker and the *bushy* phenotype. This combination of phenotypic and genetic evidence here largely excludes *AO1* as a candidate for *bushy*. However, this does not exclude the possibility that the expression of the *AOs* is affected in these mutants.

6.4.2 Auxin biosynthesis and metabolism is altered in the *bushy* mutant

Understanding the chemical profile of the *bushy* mutant is not only important in elucidating and eliminating candidates, but also in understanding how a mutation in these genes may affect the growth and development of mutant plants. The reduced IAA in *bushy* has been published previously (Symons et

al, 2002), but the cause of this reduction remains elusive. The *TAR* gene family has been extensively tested and members are known to catalyse the transamination of Trp to IPyA (Chapter 3)(Stepanova et al, 2008; Tao et al, 2008; Tivendale et al, 2012; Sugawara et al, 2015). As such, the reduction in IPyA levels (Figure 6.2) and the accumulation of Trp (Table 6.3) in *bushy* internodes suggests that the *TAR* gene family may be negatively regulated in this mutant.

Consistent with the findings in other chapters it was important to investigate the effect of the *bushy* mutant on the biosynthesis of PAA. While the levels of the endogenous hormone were not altered in the *bushy* mutant (Figure 6.3), the levels of phenylpyruvate were reduced (Figure 6.3), similar to IPyA (Figure 6.2). Additionally, the levels of the precursor Phe were elevated in some tissue types, similar to Trp. However, this elevation is manifest only in apical portions. The reduced levels of IPyA and phenylpyruvate suggest that the *bushy* mutation affects the biosynthesis of both IAA and PAA.

These results could be interpreted as evidence for a shared biosynthetic pathway catalysed by the same enzymes, as reported previously (Sugawara et al, 2015). However, as discussed earlier (Chapters 3 and 4), it is unlikely that Phe is a competitive substrate for the TAR enzymes in the first place, given its low K_m (Tao et al, 2008). As such, a blockage at this step in both pathways is likely to be caused by a common control mechanism. This control mechanism would regulate both phenylalanine aminotransferases as well as the tryptophan aminotransferases.

It is interesting that the levels of endogenous PAA are not reduced in *bushy*, despite a reduction in the level of phenylpyruvate. A blockage of transaminase function (i.e. Trp → IPyA, and Phe → phenylpyruvate) should have a similar effect on the levels of both IAA and PAA. However, a previous suggestion is that the biosynthesis of PAA can be independent of Phe (i.e. prephenate → phenylpyruvate → PAA, Chapter 3) and that an aromatic aminotransferase is not absolutely required for its biosynthesis. It is also possible that phenylpyruvate is compartmentalized and only a small pool of

this intermediate is destined for PAA. As such a reduction of phenylpyruvate from a separate pool may not affect the levels of PAA to any great extent.

IAA biosynthesis is altered in *bushy*, although WT IAA levels can be restored with an overnight incubation with large amounts of Trp (Figure 6.4). It is unclear how the addition of this precursor restores WT levels, since in the same experiments, the levels of the key intermediate in IAA biosynthesis, IPyA, were still reduced (Figure 6.5). This may suggest that an alternate Trp dependent pathway is functioning in pea.

It is possible given the previous findings of elevated IAAld in *bushy* (Quittenden, 2011) that this mutation is redirecting flux towards IAAld. This may explain the reduced IPyA and IAA levels. However, the mechanism behind such a redirection is unclear. It is entirely possible that an alternative pathway may be functioning (i.e. the tryptamine pathway), although this pathway has not been definitively characterised in pea and the levels of tryptamine are not altered in *bushy* (Quittenden, 2011).

6.4.3 Candidates for the *bushy* mutant

Despite further characterisation of the *bushy* mutant presented here, the exact gene involved remains elusive. The mapping conducted in this chapter has identified 11 candidates for the *bushy* mutant. It is important to compare the effect of mutations in the identified candidates from other species. However, it is unclear how each of these would manifest in pea.

6.4.3.1 IAMT

IAMTs are a group of SAM (*S*-adenosyl methionine) dependent methyl-transferases belonging to the SABATH family, which contains 24 members in *Arabidopsis* and 41 in rice (Zubieta et al, 2003; Qin et al, 2005; Zhao et al, 2008). Initial classification of this gene family described their role in the methylation of both salicylic acid (SA) and jasmonic acid (JA) (Zubieta et al, 2003). Similarly, the gene products of *AtIAMT1* (IAA methyltransferase) and its rice homolog (*OsIAMT1*) have been shown to convert IAA to its methyl ester, IAAme, in vitro (Zubieta et al, 2003; Zhao et al, 2008). The repression

of *AtIAMT* in RNAi lines, results in plants that are phenotypically similar to *bushy* (Qin et al, 2005). However, *bushy* is possibly a “gain-of-function” semi-dominant mutation and overexpression of the IAMT1 gene (as in the *iamt1-D* T-DNA line) results in reductions in auxin response and fewer lateral roots (Qin et al, 2005), phenotypes also presented in the *bushy* mutant (Symons et al, 1999).

6.4.3.2 AUXIN RESPONSE FACTORS

Auxin response factors (*ARFs*) are components of the auxin signalling/ transduction pathway. They bind specifically to TGTCTC auxin response elements (*AuxREs*), present in promoter regions of auxin inducible genes (Ulmasov et al, 1999). ARFs function in tandem with Aux/ IAA (auxin/ indoleacetic acid) proteins to promote or repress gene transcription (Ulmasov et al, 1999; Tiwari et al, 2003; Guilfoyle and Hagen, 2007). Interestingly, despite having an integral role in the regulation of auxin response, loss of function mutations in any single *ARF* does not appear to produce a distinct phenotype (Okushima et al, 2005).

The overexpression of ARF proteins in *Arabidopsis* results in a dramatic plant phenotype (Tian et al, 2004; Okushima et al, 2005). These plants can be dwarf in stature and possess altered leaves, reduced reproductive capacity and hypocotyl development. However, a brief inspection of the pea and *Medicago* ARFs from the candidate region show that these enzymes lack the DNA binding domain that recognises the TGTCTC motif, similar to ARF23 from *Arabidopsis*. It has been suggested that since ARF23 cannot recognise the binding motif, it may only be able to interfere with the function of other ARFs (Li et al 2004, Tian et al 2004). It is possible that *bushy* is caused though a faulty ARF. and the absence of the TGTCTC motif in these enzymes warrants further investigation.

6.4.3.3 RUB1

RUB1, or RELATED-TO-UBIQUITIN 1 (NEDD8 in mammalian systems) is responsible for the ubiquitination of substrates for the SCF^{TIR1} complex (Dharmasiri and Estelle, 2004). There are three members of the RUB protein

family in *Arabidopsis* (Rao-Naik et al, 1998; Bostick et al, 2004), two of which modify the CULLIN1 protein (CUL1) within the SCF^{TIR1} complex in an RBX1 (RING-BOX1) dependent manner (Gray et al, 2002). The conjugation of RUB proteins to the SCF^{TIR1} complex is regulated by many factors including *AXR1* (*Auxin Resistant 1*), *ECR1* (*E1-Conjugating Enzyme Related*), and *RCE1* (*Rub1 Conjugating Enzyme*) (Estelle and Somerville, 1987; Del Pozo et al, 1998; Del Pozo and Estelle, 1999; Del Pozo et al, 2002; Dharmasiri et al, 2003).

However, while mutations in these regulators can produce striking developmental defects due to altered auxin sensitivity (Del Pozo et al, 1998; Del Pozo et al, 2002; Woodward and Bartel, 2005), at least one functional RUB protein is absolutely required for the development of the plant system (Bostick et al, 2004). Therefore, mutations in *RUB* genes in other species do not produce obvious phenotypes due to the functional redundancy of these enzymes (Bostick et al, 2004). In the pea gene atlas, there is only one similar sequence to the *Medicago RUB* candidate (Alves-Carvalho et al, 2015). As such it is difficult to see that a mutation in this *RUB* gene, even through “gain-of-function” is responsible for *bushy*.

6.4.3.4 SMALL AUXIN UP RNAs

SMALL AUXIN UP RNAs or SAURs are an extensive family of early auxin response genes (McClure and Guilfoyle, 1987; Hagen and Guilfoyle, 2002). SAURs are up regulated in the presence of auxin and become abundant within minutes following exogenous application of this phytohormone (Hagen and Guilfoyle, 2002). The SAUR proteins have recently been identified as positive regulators of cell expansion (Chae et al, 2012; Spartz et al, 2012). *bushy* epidermal cell length is about one third of the WT, suggesting reduced cellular expansion in *bushy* mutants (Symons et al, 1999). However, while repressed or altered *SAUR* activity may explain the reduced apical dominance, there is no evidence that *SAUR* mutations alter the auxin content of cells (although it is possible that this has not yet been tested). Therefore, it is unlikely that the *SAURs* are the cause of the *bushy* mutation in pea.

6.4.3.5 SLY2

The *Medicago* F-box SNE-like is a homolog of the *Arabidopsis SNEEZY* (*SNE/ SLY2*), a positive regulator of GA signalling (McGinnis et al, 2003; Strader et al, 2004). *SNE/ SLY2* functions as component of the E3 SCF^{SNE} ubiquitination complex, by targeting DELLA proteins in the presence of GA (Strader et al, 2004; Ariizumi et al, 2011). SNE-like is appealing as a candidate for *bushy*, as mutations in *SNE/ SLY2*, may result in the accumulation of DELLA proteins and significantly reduced growth, similar to that of the *Arabidopsis sly1-10* mutant (Strader et al, 2004). However, there is extensive functional redundancy between *SLY1* and *SNE* (Itoh et al, 2003; McGinnis et al, 2003; Strader et al, 2004) and the *sly1-10* mutant does not possess a branching phenotype.

A model where SNE is over- or constitutively expressed may explain *bushy* through saturation of the SCF complex with the SNE F-Box protein. If SLY targets particular DELLA proteins for degradation and is replaced by the less effective SNE, due to its high abundance, these DELLAs would continue to repress transcription. This may also explain why bushy deviates from typical GA phenotypes, as repression of some, but not all DELLAs would conceivably produce novel deviations from WT growth. Yet in this case, one would also expect the homeostatic elevation of GA levels to repress the DELLAs. However, GAs are reduced in *bushy* (Symons, 2000).

6.4.3.6 AHK

AHK2 is a histidine kinase (*HKs/ AHKs*) belonging to the *CRE* gene family, named after the mutant *cre1* (*cytokinin response1, ahk1*) (Inoue et al, 2001). These kinases are integral to the perception of cytokinins (CKs), and *cre1* mutants possess altered cell division, chlorophyll development and shoot formation (Inoue et al, 2001; Ueguchi et al, 2001). However, no dramatic shoot phenotype has been observed for *ahk1* or any single loss of function mutant in this gene family (Higuchi et al, 2004). Additionally, over- or constitutive expression of the histidine kinases would result in hypersensitivity to cytokinin. This would result in a reduction in the levels of

endogenous CKs. However, the CK levels in *bushy* are elevated approximately 6-fold (Symons, 2000).

6.4.3.7 SAR3

SUPPRESSOR OF AUXIN RESISTANCE 1 (*SAR1*) was initially characterised in a mutant screen for suppressors of the *axr1* mutant (Cernac et al, 1997). Both *SAR1* and *SAR3* encode nucleoporins that are responsible for the translocation of Aux/ IAAs into the nucleus (Parry et al, 2006). A mutation in *SAR3* may explain the *bushy* phenotype if this gene were constitutively expressed, resulting in an accumulation of Aux/ IAAs in the nucleus (Parry et al, 2006). This would overburden the SCF^{TIR1} complex and thus repress the transcription of auxin responsive genes (AuxREs). However, the *sar3* mutant in *Arabidopsis* does not confer a branching phenotype and largely retains apical dominance, unlike that of *bushy*.

6.4.3.8 EIN3

The eth*ylene insensitive mutant 3* (*EIN3*) is an integral component of the ethylene signalling mechanism (Chao et al, 1997; Guo and Ecker, 2003; Potuschak et al, 2003). Interestingly, while though most other hormone signalling complexes are positive regulators of signalling, and promote this through degradation of repressors, the ethylene SCF^{EBF1} complex acts antagonistically to transcription, by degrading the EIN3 protein , in an as yet unknown manner. However, *EIN3* transcripts are not increased by excess ethylene (Chao et al, 1997) .

Recently it has been shown that EIN3 is capable of up regulating members of the *TAR* gene family (He et al, 2011). This is interesting as in the *bushy* mutant, the levels of IPyA are reduced (Figure 6.2), and Trp accumulates in internode tissue (Table 6.3). However, unlike the semi-dominant nature of the *bushy* mutation, *ein3* in *Arabidopsis* is recessive (Kieber et al, 1993). The *ein3* mutant also retains apical dominance, and does not have a distinct branching phenotype (An et al, 2010), unlike that of *bushy*.

6.5 Conclusion

The *bushy* mutant is curious in that it is a semi-dominant mutation that results in a substantial reduction in IAA content (Symons et al, 2002; Quittenden, 2011). The mutant is characterised by severe dwarfism, extensive branching and reduced reproductive capacity. Because the levels of several additional hormones are also altered in this mutant, it is difficult to determine if these phenotypes are caused by the direct or indirect influence of the mutation. This chapter attempts to expand upon previous work through further characterisation of the *bushy* mutant and its effects on PAA (and IAA) biosynthesis, as well as by mapping the *bushy* locus.

Here it is shown that the *bushy* locus is linked to several known genetic markers present at the top of pea linkage group 1 (Aubert et al, 2006). It is now clear that the *bushy* mutation is not caused by an *AO*, although previous findings of elevated IAAld levels (Quittenden, 2011) suggest that their expression may be altered. With the exclusion of the AOs as candidates for *bushy*, the rough mapping of the *bushy* locus presented in this chapter, has uncovered several additional candidates. While it is difficult to compare the effects of mutations in these genes across species, several of these candidates produce phenotypes similar to that of bushy. However, additional genetic analysis is required in order to identify the gene associated with the *bushy* phenotype. The further sequencing of the identified candidates as well as fine mapping of this region will be essential to identify the exact cause of the *bushy* mutation.

It is interesting to compare previous evidence with the results presented here, as a reduction in IPyA and an accumulation of Trp suggests that IAA biosynthesis (specifically TAR activity) may be reduced. To better understand the influence of bushy on the *TAA1/TARs*, future work should investigate the expression of these biosynthetic genes. The accumulation of IAAld demonstrated previously (Quittenden, 2011) also suggests that flux is being directed towards IAAld. However, whether this is directly from IPyA, or via the tryptamine pathway remains to be determined.

The reduced levels of phenylpyruvate show that *bushy* also affects the biosynthesis pathway leading to PAA, although the levels of free hormone are not reduced in this mutant. These levels data suggest that the transamination of Phe to phenylpyruvate may not contribute significantly to the PAA pool. This further supports the independence of the IPyA and phenylpyruvate pathways. However, it also suggests that these two pathways may share a common control mechanism.

Chapter 7: Concluding Discussion

7.1 Overview of previous knowledge

At the outset of this study, little was known about the biosynthesis of phenylacetic acid (PAA). However, shortly after, it was proposed that PAA is synthesized via a two-step pathway utilizing the TAA1/ TAR and YUC enzymes, identical to the IPyA pathway (Sugawara et al, 2015). The TAA1/TARs were suggested to catalyse the transamination of the amino acid Phe to phenylpyruvate and the YUCs would then catalyse the oxidative decarboxylation of phenylpyruvate to PAA.

It has been demonstrated previously that the TAA1/ TAR enzymes are capable of utilizing Phe as a substrate, although far less efficiently than Trp (Tao et al, 2008). Similarly the YUC enzymes can utilize phenylpyruvate as a substrate in addition to IPyA (Mashiguchi et al, 2011; Dai et al, 2013). These in vitro findings are supported by experiments that show an accumulation of both IAA and PAA conjugates when particular YUC enzymes are overexpressed in *Arabidopsis* (Sugawara et al, 2015). However, the proposed intermediate, phenylpyruvate, was not identified or quantified in any experiments conducted by Sugawara et al (2015). An in vivo demonstration of the conversion of Phe to phenylpyruvate to PAA was also absent in these studies.

The metabolism of PAA is also largely unknown although it may be similar to that of IAA. On the other hand, it is pointed out here that the theoretical ‘PAAox’ may not/ cannot be produced. PAA-Asp and PAA-Glu are amide conjugates of PAA in *Arabidopsis* and the levels of these two compounds are elevated in lines overexpressing GH3.9 (Sugawara et al, 2015). PAA can also be a substrate for the *Arabidopsis* UGTs, at least those with function on IAA (Jackson et al, 2001; Douglas Grubb et al, 2004). However, while these enzymes may function on both IAA and PAA, there is limited published

evidence on the distribution of auxin metabolic enzymes outside of the angiosperms.

The balance between biosynthesis and metabolism controls the endogenous auxin levels. An added level of regulation is present in the signalling/ perception of auxins by extensive regulatory machinery (Quint and Gray, 2006). The *bushy* mutant of pea is only partially characterized; although it is likely to be a signalling/ perception mutant, given its semi-dominant nature. Since *bushy* also contains less IAA than the WT (Symons et al, 1999; Symons, 2000), this mutant is appealing for investigations into auxin regulation.

This thesis investigates the similarities and differences in the biosynthesis of IAA and PAA. The findings presented here are augmented by an evolutionary comparison on the biosynthesis of these two auxins and investigations on the distribution of the enzymes involved, as well as by further studies on IAA-related mutants of pea. The research presented provides a more complete understanding of the biosynthesis of PAA.

7.2 PAA is not synthesized by the same enzymes that catalyse the IPyA pathway

It is discussed in this thesis that the IPyA pathway is not responsible for the biosynthesis of PAA (Chapter 3). While the chemical conversions of Trp to IPyA, and Phe to phenylpyruvate may be similar (Sugawara et al, 2015), the enzymes involved in these processes are unlikely to be the same. Despite the ability of the TAA1/ TAR enzymes to utilize Phe as a substrate in vitro (Tao et al, 2008), analyses on the *tar2-1* mutant in pea demonstrate no reduction in the endogenous levels of PAA in mutant seeds (Chapter 3), despite a clear reduction in both IAA and 4-Cl-IAA levels in the same tissue (Tivendale et al, 2012). This result is augmented by in vitro studies on the substrate preferences of PsTAR1 (Chapter 3), which suggests that the tryptophan aminotransferases are not strongly involved in PAA biosynthesis. Instead, it is proposed that the conversion of Phe to phenylpyruvate is

catalysed by the aromatic aminotransferases (ArATs). These enzymes have been shown to catalyse the reversible transamination of Phe to phenylpyruvate in *Petunia hybrida* (Yoo et al, 2013), *Cucumis melo* (Gonda et al, 2010) and in *Arabidopsis* (Prabhu and Hudson, 2010).

Importantly, here it is definitively demonstrated that in pea, deuterium labelled Phe can be metabolised to both phenylpyruvate and PAA, consistent with the pathway suggested by Sugawara et al (2015). Of equal importance is the demonstration that D_5 phenylpyruvate, which was commissioned for these experiments, was converted to PAA, as well as back to Phe (Chapter 3). While phenylpyruvate has previously been implicated in Phe biosynthesis (Yoo et al, 2013), the findings from these metabolism experiments are the first to directly demonstrate that phenylpyruvate is a common intermediate in both Phe and PAA biosynthesis. Similarly, these metabolism experiments are the first to demonstrate the conversion of labelled Trp to labelled IPyA in plants.

Similar to the pea *tar2-1* mutant, the maize *de18* mutant (*ZmYUC1*) also displays heavily reduced levels of IAA in developing endosperm tissue (Bernardi et al, 2012). However, analyses here show that the levels of PAA are normal in mutant endosperm (Chapter 3). It is also noted here that similar YUC enzymes are not expressed to any great extent in endosperm tissue (Sekhon et al, 2011). The conversion of phenylpyruvate to PAA is similarly unaltered in the pea *crispoid-4* (*crd-4*) mutant (Chapter 4). In fact, of all loss-of-function YUC mutants, including those from pea and *Arabidopsis*, not a single one has altered levels of PAA. While both IAA and PAA levels were normal in whole *crd-4* mutant seedlings, the precursor IPyA, but not phenylpyruvate, was elevated in mutant apical tissue.

The ArATs are a logical alternative to the TAA1/ TARs in PAA biosynthesis, yet it is unclear by what mechanism phenylpyruvate is converted to PAA. It is suggested here that plant PAA biosynthesis may be similar to that of bacteria and fungi (Kishore et al, 1976; Somers et al, 2005; Spaepen et al, 2007). In this case, phenylpyruvate is converted to phenylacetaldehyde (PAAld) by a

(phenyl) pyruvate decarboxylase, which would then converted to PAA by an aldehyde oxidase. Alternatively, it is also proposed that phenylpyruvate may be converted to PAA via a non-YUC flavin monooxygenase.

7.3 Evolutionary aspects of auxin biosynthesis and metabolism

In order to investigate auxin biosynthesis from an evolutionary perspective, the capacity of a range of plants to convert the precursors Trp and Phe to their respective auxins was tested. However, the techniques for the in vivo metabolism experiments conducted in Chapter 3, which relied on the capacity of the plant to transport the applied substrate, were not suitable for the plant divisions that lack vascular tissue, since the transport or uptake of labelled precursors would most likely not be consistent in all species. In order to better compare between the major evolutionary divisions, metabolism experiment techniques were developed (Chapter 5) that use homogenized tissue incubated with labelled precursors (D_5 Phe and D_5 Trp). While this process may break down natural cellular compartments (i.e. cytosol and plastids), these experiments were used to demonstrate the presence or absence of enzymes from the IPyA/ phenylpyruvate pathways (Chapter 5), regardless of compartmentalisation.

The results presented in this thesis show that the IPyA pathway is functional in most major divisions of land plants (Chapter 5). Deuterium labelled Trp was converted to D_5 IAA in all representatives and the endogenous IPyA pool was diluted in most cases. The IPyA pathway in these lineages is further supported through the demonstration that both the TAA1/ TARs and YUCs are present in all representative species.

In addition to the IPyA pathway, the phenylpyruvate pathway also appears functional throughout the land plants (Chapter 5). Labelled Phe was converted to D_5 PAA in all cases and D_5 phenylpyruvate was detected in most divisions. Interestingly, the lycophyte representative, *Selaginella*

moellendorfii, does not contain an ArAT homolog in its published genome. This absence is correlated with a massive accumulation of PAA (Chapter 5). Apart from the lack of an ArAT in *S. moellendorfii*, these enzymes are present in representative species from all other major divisions.

Sequence analyses in Chapter 5 demonstrate that in terms of sequence similarity, the DAO motif identified previously (Zhang et al, 2016) quickly breaks down outside of the angiosperms, although oxIAA, the end product of this conversion has been detected in most evolutionary divisions (Sztein et al, 1995; Sztein et al, 1999). The basal DAO enzymes still retain key residues required for 2OG Fe (II) oxygenase and dioxygenase function (Zhang et al, 2016). It is possible that the DAO motif is not essential for the oxidation of IAA or that this process may occur through an additional mechanism in the basal lineages. Given the chemical structure of PAA, it is unclear whether the DAOs, or indeed, oxidation is a mechanism by which this auxin is broken down.

Amide conjugation by the GH3s is widespread in the land plants with all representative species possessing a GH3 enzyme (Chapter 5). The GH3s in the angiosperms form clear groups that contain different substrate preferences and sensitivities to endogenous auxin. However, the basal GH3s may utilize numerous amino acids as substrates (Ludwig-Müller et al, 2009). Given that overexpression of GH3.9 in *Arabidopsis* results in an accumulation of both PAA-Asp and PAA-Glu (Sugawara et al, 2015), it is likely that similar GH3 enzymes utilize both IAA and PAA.

7.4 Auxin biosynthesis is altered in the *bushy* mutant

The *bushy* mutant is an important mutant related to auxin physiology in some as yet unknown way. It is demonstrated here that the *bushy* locus is present at the top of pea linkage group I. It is further demonstrated that *bushy* is (closely) linked to, and therefore not the same as, the *aldehyde oxidase* (*AO*)

genes. Based on population maps generated herein (Chapter 6), several candidates have been identified that may explain the extreme *bushy* phenotype.

The *bushy* mutant is also further characterized and similar to other auxin mutants, PAA levels are normal despite a reduction in endogenous IAA. It is demonstrated that the biosynthesis of IAA is compromised in the *bushy* mutant as the main precursor, IPyA, is also reduced. This suggests that the effect of the *bushy* mutation may occur upstream of the YUCCA enzymes. Curiously, the levels of phenylpyruvate are also reduced in the bushy mutant.

7.5 Conclusions

Based on the mutant analyses presented in this thesis, it is clear that IAA biosynthetic mutants do not greatly affect the biosynthesis of PAA. While PAA can be synthesized by transamination/ oxidative decarboxylation, the same chemical conversions required for IAA, it appears that the enzymes that catalyse these reactions are not the same for the two auxins. In fact, in the wider literature there is only circumstantial evidence that supports a role for TAA1/ TAR and YUC in the biosynthesis of PAA. This is evidence is limited to in vitro functional assays and overexpression lines, which, it could be argued, do not necessarily represent natural systems.

The findings from the mutant analyses in this thesis are further supported by evolutionary comparisons, which show that a functioning phenylpyruvate pathway and the ArATs are present in almost all major evolutionary divisions. The exception to this is *Selaginella moellendorfii*, which lacks an ArAT but contains heavily altered levels of PAA (and seemingly normal IAA). The elevation of PAA in this species indicates that PAA biosynthesis may not always be Phe dependent. While the metabolism experiments in this thesis show that Phe can be converted to PAA in vivo, it must be remembered that phenylpyruvate exists as both a precursor and a metabolite of the amino acid Phe. This represents an important difference between the IPyA and phenylpyruvate pathways, since IPyA has never been considered a

precursor to Trp, nor has it been implicated as a precursor to other endogenous compounds besides IAA (and possibly indole-3-acetaldehyde, Chapter 3).

An important observation is that plants often contain several enzymes that share functional similarities despite structural divergence. Both the TAA1/ TARs and the ArATs are class II aminotransferases and both can utilize Trp and Phe as substrates. However the TAA1/ TARs prefer Trp>Phe (Tao et al, 2008), whereas the ArATs have preference for Phe>Trp (Prabhu and Hudson, 2010; Bedewitz et al, 2014). The substrate preference of these enzymes means that Phe cannot compete with Trp for transamination by the TAA1/ TARs, and that Trp cannot compete for transamination by the ArATs. Hence, in the plant there is a large degree of specificity of these enzymes.

The work presented in this thesis supports the well-accepted idea that enzymes may be specific for particular substrates. The presence of both ArATs and TAA1/ TARs implies two separate pathways, one responsible for IAA biosynthesis and another that modulates the biosynthesis of Phe/ PAA. It is possible, indeed likely, that each amino acid may have its own aminotransferase, although an exception might be Tyr and Phe, which are chemically very similar.

Auxin biosynthetic genes are present in most land plants and the number of enzymes belonging to these families is typically higher in the angiosperms than the basal lineages (Chapter 5). This is also seen in enzymes responsible for IAA metabolism and indicates increased control over these two processes in higher plants. The large gene families in higher plants allows for particular substrate preferences and unique expression patterns. Conversely, enzymes from basal species, which are typically fewer in number, contain broad substrate preferences and given their simple body plans, do not necessarily require extensive tissue specific expression of these enzymes.

The evidence presented in this thesis clearly shows that the IPyA pathway does not contribute significantly to the biosynthesis of PAA. It is further shown that the ArATs are conserved in the majority of land plants. This suggests that an alternative mechanism for PAA biosynthesis is also conserved. It is important in moving forward that we do not assume that, in terms of biosynthesis, PAA is identical to IAA. However, the decades of research on IAA should serve to guide future investigations. Perhaps the most important question is, what role does PAA play in plants? And subsequently, how does PAA interact with IAA and other plant signalling molecules?

Bibliography

Abe H, Uchiyama M, Sato R (1974) Isolation of Phenylacetic Acid and its p-Hydroxy Derivative as Auxin-Like Substances From *Undaria pinnatifida*. Agricultural and Biological Chemistry **38:** 897-898

Abu-Zaitoon YM, Bennett K, Normanly J, Nonhebel HM (2012) A Large Increase in IAA During Development of Rice Grains Correlates With the Expression of Tryptophan Aminotransferase *OsTAR1* and a Grain‐Specific *YUCCA*. Physiologia Plantarum **146:** 487-499

Alves-Carvalho S, Aubert G, Carrère S, Cruaud C, Brochot AL, Jacquin F, Klein A, Martin C, Boucherot K, Kreplak J (2015) Full‐Length *de novo* Assembly of RNA‐Seq Data in Pea (*Pisum sativum* L.) Provides a Gene Expression Atlas and Gives Insights Into Root Nodulation in This Species. The Plant Journal **84:** 1-19

An F, Zhao Q, Ji Y, Li W, Jiang Z, Yu X, Zhang C, Han Y, He W, Liu Y (2010) Ethylene-Induced Stabilization of ETHYLENE INSENSITIVE3 and EIN3-LIKE1 is Mediated by Proteasomal Degradation of EIN3 Binding F-box 1 and 2 That Requires EIN2 in *Arabidopsis*. The Plant Cell **22:** 2384-2401

Ariizumi T, Lawrence PK, Steber CM (2011) The Role of Two F-Box Proteins, SLEEPY1 and SNEEZY, in *Arabidopsis* Gibberellin Signaling. Plant physiology **155:** 765-775

Arumingtyas E, Floyd R, Gregory M, Mufert I (1992) Branching in *Pisum*: Inheritance and Allelism Tests With 17 Ramosus Mutants. *In*,

Ashen JB, Cohen JD, Goff LJ (1999) GC-SIM-MS Detection and Quantification of Free Indole-3-Acetic Acid in Bacterial Galls on the Marine Alga *Prionitis lanceolata* (Rhodophyta). Journal of phycology **35:** 493-500

Aubert G, Morin J, Jacquin F, Loridon K, Quillet M, Petit A, Rameau C, Lejeune-Hénaut I, Huguet T, Burstin J (2006) Functional Mapping in Pea, as an Aid to the Candidate Gene Selection and for Investigating Synteny With the Model Legume *Medicago truncatula*. Theoretical and Applied Genetics **112:** 1024-1041

Bajguz A, Piotrowska A (2009) Conjugates of Auxin and Cytokinin. Phytochemistry **70:** 957-969

Bak S, Tax FE, Feldmann KA, Galbraith DW, Feyereisen R (2001) CYP83B1, a Cytochrome P450 at the Metabolic Branch Point in Auxin

and Indole Glucosinolate Biosynthesis in *Arabidopsis*. The Plant Cell Online **13:** 101-111

Baldi BG, Maher BR, Slovin JP, Cohen JD (1991) Stable Isotope Labeling, *in vivo*, of D-and L-Tryptophan Pools in *Lemna gibba* and the Low Incorporation of Label Into Indole-3-Acetic Acid. Plant physiology **95:** 1203-1208

Bandurski RS, Cohen JD, Slovin JP, Reinecke DM (1995) Auxin Biosynthesis and Metabolism. *In* Plant hormones. Springer, pp 39-65

Barlier I, Kowalczyk M, Marchant A, Ljung K, Bhalerao R, Bennett M, Sandberg G, Bellini C (2000) The *SUR2* Gene of *Arabidopsis thaliana* Encodes the Cytochrome P450 CYP83B1, a Modulator of Auxin Homeostasis. Proceedings of the National Academy of Sciences **97:** 14819-14824

Bedewitz MA, Góngora-Castillo E, Uebler JB, Gonzales-Vigil E, Wiegert-Rininger KE, Childs KL, Hamilton JP, Vaillancourt B, Yeo Y-S, Chappell J (2014) A Root-Expressed L-Phenylalanine: 4-Hydroxyphenylpyruvate Aminotransferase Is Required for Tropane Alkaloid Biosynthesis in *Atropa belladonna*. The Plant Cell Online **26:** 3745-3762

Berger BJ, English S, Chan G, Knodel MH (2003) Methionine Regeneration and Aminotransferases in *Bacillus subtilis*, *Bacillus cereus*, and *Bacillus anthracis*. Journal of bacteriology **185:** 2418-2431

Bernardi J, Lanubile A, Li Q-B, Kumar D, Kladnik A, Cook SD, Ross JJ, Marocco A, Chourey PS (2012) Impaired Auxin Biosynthesis in the *defective endosperm18* Mutant is Due to Mutational Loss of Expression in the *ZmYuc1* Gene Encoding Endosperm-Specific YUCCA1 Protein in Maize. Plant physiology **160:** 1318-1328

Beveridge CA, Kyozuka J (2010) New Genes in the Strigolactone-Related Shoot Branching Pathway. Current opinion in plant biology **13:** 34-39

Beveridge CA, Ross JJ, Murfet IC (1994) Branching Mutant *rms-2* in *Pisum sativum*: Grafting Studies and Endogenous Indole-3-Acetic Acid Levels. Plant Physiology **104:** 953-959

Beveridge CA, Ross JJ, Murfet IC (1996) Branching in Pea: Action of Genes *Rms3* and *Rms4*. Plant Physiology **110:** 859-865

Beveridge CA, Symons GM, Murfet IC, Ross JJ, Rameau C (1997) The *rms1* Mutant of Pea has Elevated Indole-3-Acetic Acid Levels and

Reduced Root-Sap Zeatin Riboside Content but Increased Branching Controlled by Graft-Transmissible Signal (s). Plant Physiology **115:** 1251

Bierfreund NM, Tintelnot S, Reski R, Decker EL (2004) Loss of *GH3* Function Does Not Affect Phytochrome-Mediated Development in a Moss, *Physcomitrella patens*. Journal of plant physiology **161:** 823-835

Blankenfeldt W, Montemartini‐Kalisz M, Kalisz HM, Hecht HJ, Nowicki C (1999) Crystal Structure of *Trypanosoma cruzi* Tyrosine Aminotransferase: Substrate Specificity is Influenced by Cofactor Binding Mode. Protein Science **8:** 2406-2417

Boatright J, Negre F, Chen X, Kish CM, Wood B, Peel G, Orlova I, Gang D, Rhodes D, Dudareva N (2004) Understanding *in vivo* Benzenoid Metabolism in Petunia Petal Tissue. Plant Physiology **135:** 1993-2011

Bostick M, Lochhead SR, Honda A, Palmer S, Callis J (2004) Related to Ubiquitin 1 and 2 are Redundant and Essential and Regulate Vegetative Growth, Auxin Signaling, and Ethylene Production in *Arabidopsis*. The Plant Cell **16:** 2418-2432

Cai X, Dong F, Edelmann RE, Makaroff CA (2003) The *Arabidopsis* SYN1 Cohesin Protein is Required for Sister Chromatid Arm Cohesion and Homologous Chromosome Pairing. Journal of Cell Science **116:** 2999-3007

Cernac A, Lincoln C, Lammer D, Estelle M (1997) The *SAR1* Gene of *Arabidopsis* Acts Downstream of the *AXR1* Gene in Auxin Response. Development **124:** 1583-1591

Chae K, Isaacs CG, Reeves PH, Maloney GS, Muday GK, Nagpal P, Reed JW (2012) *Arabidopsis SMALL AUXIN UP RNA63* Promotes Hypocotyl and Stamen Filament Elongation. The Plant Journal **71:** 684-697

Chao Q, Rothenberg M, Solano R, Roman G, Terzaghi W, Ecker JR (1997) Activation of the Ethylene Gas Response Pathway in *Arabidopsis* by the Nuclear Protein ETHYLENE-INSENSITIVE3 and Related Proteins. Cell **89:** 1133-1144

Chen Q, Westfall CS, Hicks LM, Wang S, Jez JM (2010) Kinetic Basis for the Conjugation of Auxin by a GH3 Family Indole-Acetic Acid-Amido Synthetase. Journal of Biological Chemistry **285:** 29780-29786

Cheng Y, Dai X, Zhao Y (2006) Auxin Biosynthesis by the YUCCA Flavin Monooxygenases Controls the Formation of Floral Organs and Vascular Tissues in *Arabidopsis*. Genes & Development **20:** 1790-1799

Cheng Y, Dai X, Zhao Y (2007) Auxin Synthesized by the YUCCA Flavin Monooxygenases is Essential for Embryogenesis and Leaf Formation in *Arabidopsis*. The Plant Cell Online **19:** 2430-2439

Cho M-H, Corea OR, Yang H, Bedgar DL, Laskar DD, Anterola AM, Moog-Anterola FA, Hood RL, Kohalmi SE, Bernards MA (2007) Phenylalanine Biosynthesis in *Arabidopsis thaliana:* Identification and Characterization of Arogenate Dehydratases. Journal of Biological Chemistry **282:** 30827-30835

Chourey PS, Li Q-B, Kumar D (2010) Sugar–Hormone Cross-Talk in Seed Development: Two Redundant Pathways of IAA Biosynthesis are Regulated Differentially in the Invertase-Deficient *miniature1* (*mn1*) Seed Mutant in Maize. Molecular Plant **3:** 1026-1036

Cohen JD, Bandurski RS (1982) Chemistry and Physiology of the Bound Auxins. Annual Review of Plant Physiology **33:** 403-430

Cook SD (2012) Auxin synthesis genes in seeds of maize and pea. University of Tasmania

Cook SD, Nichols DS, Smith J, Chourey PS, McAdam EL, Quittenden L, Ross JJ (2016) Auxin Biosynthesis: Are the Indole-3-Acetic Acid and Phenylacetic Acid Biosynthesis Pathways Mirror Images? Plant physiology **171:** 1230-1241

Cooke TJ, Poli D, Sztein AE, Cohen JD (2002) Evolutionary Patterns in Auxin Action. *In* Auxin Molecular Biology. Springer, pp 319-338

Cooney TP, Nonhebel HM (1991) Biosynthesis of Indole-3-Acetic Acid in Tomato Shoots: Measurement, Mass-Spectral Identification and incorporation of− 2H From− 2H2O Into Indole-3-Acetic Acid, D-and L-Tryptophan, Indole-3-Pyruvate and Tryptamine. Planta **184:** 368-376

Dai X, Mashiguchi K, Chen Q, Kasahara H, Kamiya Y, Ojha S, DuBois J, Ballou D, Zhao Y (2013) The Biochemical Mechanism of Auxin Biosynthesis by an *Arabidopsis* YUCCA Flavin-Containing Monooxygenase. Journal of Biological Chemistry **288:** 1448-1457

Dalmais M, Schmidt J, Le Signor C, Moussy F, Burstin J, Savois V, Aubert G, Brunaud V, de Oliveira Y, Guichard C (2008) UTILLdb, a

Pisum sativum in silico Forward and Reverse Genetics Tool. Genome Biol **9:** R43

Davies PJ (1995) The Plant Hormone Concept: Concentration, Sensitivity and Transport. *In* Plant hormones. Springer, pp 13-38

Del Pozo JC, Dharmasiri S, Hellmann H, Walker L, Gray WM, Estelle M (2002) AXR1-ECR1–Dependent Conjugation of RUB1 to the *Arabidopsis* Cullin AtCUL1 is Required for Auxin Response. The Plant Cell **14:** 421-433

Del Pozo JC, Estelle M (1999) The *Arabidopsis* Cullin AtCUL1 is Modified by the Ubiquitin-Related Protein RUB1. Proceedings of the National Academy of Sciences **96:** 15342-15347

Del Pozo JC, Timpte C, Tan S, Callis J, Estelle M (1998) The Ubiquitin-Related Protein RUB1 and Auxin Response in *Arabidopsis*. Science **280:** 1760-1763

Delarue M, Prinsen E, Va H, Onckelen, Caboche M, Bellini C (1998) *Sur2* Mutations of *Arabidopsis thaliana* Define a New Locus Involved in the Control of Auxin Homeostasis. The Plant Journal **14:** 603-611

Dharmasiri N, Dharmasiri S, Estelle M (2005) The F-Box Protein TIR1 is an Auxin Receptor. Nature **435:** 441-445

Dharmasiri N, Estelle M (2004) Auxin Signaling and Regulated Protein Degradation. Trends in plant science **9:** 302-308

Dharmasiri S, Dharmasiri N, Hellmann H, Estelle M (2003) The RUB/Nedd8 Conjugation Pathway is Required for Early Development in *Arabidopsis*. The EMBO journal **22:** 1762-1770

Douglas Grubb C, Zipp BJ, Ludwig-Müller J, Masuno MN, Molinski TF, Abel S (2004) *Arabidopsis* Glucosyltransferase UGT74B1 Functions in Glucosinolate Biosynthesis and Auxin Homeostasis. The Plant Journal **40:** 893-908

Drábková LZ, Dobrev PI, Motyka V (2015) Phytohormone Profiling Across the Bryophytes. PloS one **10:** e0125411

Eklund DM, Ishizaki K, Flores-Sandoval E, Kikuchi S, Takebayashi Y, Tsukamoto S, Hirakawa Y, Nonomura M, Kato H, Kouno M (2015) Auxin Produced by the Indole-3-Pyruvic Acid Pathway Regulates Development and Gemmae Dormancy in the Liverwort *Marchantia polymorpha*. The Plant Cell **27:** 1650-1669

Epstein E, Cohen JD, Slovin JP (2002) The Biosynthetic Pathway for Indole-3-Acetic Acid Changes During Tomato Fruit Development. Plant Growth Regulation **38:** 15-20

Ernstsen A, Sandberg G, Lundström K (1987) Identification of Oxindole-3-Acetic Acid, and Metabolic Conversion of Indole-3-Acetic Acid to Oxindole-3-Acetic Acid in *Pinus sylvestris* Seeds. Planta **172:** 47-52

Estelle MA, Somerville C (1987) Auxin-Resistant Mutants of *Arabidopsis thaliana* with an Altered Morphology. Molecular and General Genetics MGG **206:** 200-206

Expósito-Rodríguez M, Borges AA, Borges-Pérez A, Hernández M, Pérez JA (2007) Cloning and Biochemical Characterization of *ToFZY*, a Tomato Gene Encoding a Flavin Monooxygenase Involved in a Tryptophan-Dependent Auxin Biosynthesis Pathway. Journal of Plant Growth Regulation **26:** 329-340

Ferreira GC, Neame PJ, Dailey HA (1993) Heme Biosynthesis in Mammalian Systems: Evidence of a Schiff Base Linkage Between the Pyridoxal 5′ ‐Phosphate Cofactor and a Lysine Residue in 5 ‐Aminolevulinate Synthase. Protein Science **2:** 1959-1965

Foo E (2013) Auxin Influences Strigolactones in Pea Mycorrhizal Symbiosis. Journal of Plant Physiology **170:** 523-528

Fries L, Āberg S (1978) Morphogenetic Effects of Phenylacetic and p-OH-Phenylacetic Acid on the Green Alga *Enteromorpha compressa* (L.) Grev. in Axenic Culture. Zeitschrift für Pflanzenphysiologie **88:** 383-388

Gallavotti A, Barazesh S, Malcomber S, Hall D, Jackson D, Schmidt RJ, McSteen P (2008) *sparse inflorescence1* Encodes a Monocot-Specific YUCCA-Like Gene Required for Vegetative and Reproductive Development in Maize. Proceedings of the National Academy of Sciences **105:** 15196-15201

Gonda I, Bar E, Portnoy V, Lev S, Burger J, Schaffer AA, Tadmor Ya, Gepstein S, Giovannoni JJ, Katzir N, Lewinsohn E (2010) Branched-Chain and Aromatic Amino Acid Catabolism into Aroma Volatiles in *Cucumis melo* L. Fruit. Journal of Experimental Botany **61:** 1111-1123

Gray WM, Hellmann H, Dharmasiri S, Estelle M (2002) Role of the *Arabidopsis* RING-H2 Protein RBX1 in RUB Modification and SCF Function. The Plant Cell **14:** 2137-2144

Gray WM, Kepinski S, Rouse D, Leyser O, Estelle M (2001) Auxin Regulates SCFTIR1-Dependent Degradation of AUX/IAA Proteins. Nature **414:** 271-276

Groot MNN, de Bont JA (1998) Conversion of Phenylalanine to Benzaldehyde Initiated by an Aminotransferase in *Lactobacillus plantarum*. Applied and environmental microbiology **64:** 3009-3013

Guilfoyle TJ, Hagen G (2007) Auxin Response Factors. Current opinion in plant biology **10:** 453-460

Guo H, Ecker JR (2003) Plant Responses to Ethylene Gas are Mediated by SCF EBF1/EBF2-Dependent Proteolysis of EIN3 Transcription Factor. Cell **115:** 667-677

Hagen G, Guilfoyle T (2002) Auxin-Responsive Gene Expression: Genes, Promoters and Regulatory Factors. Plant molecular biology **49:** 373-385

Hagen G, Guilfoyle TJ (1985) Rapid Induction of Selective Transcription by Auxins. Molecular and cellular biology **5:** 1197-1203

Hagen G, Kleinschmidt A, Guilfoyle T (1984) Auxin-Regulated Gene Expression in Intact Soybean Hypocotyl and Excised Hypocotyl Sections. Planta **162:** 147-153

Hayward A, Stirnberg P, Beveridge C, Leyser O (2009) Interactions Between Auxin and Strigolactone in Shoot Branching Control. Plant physiology **151:** 400-412

He W, Brumos J, Li H, Ji Y, Ke M, Gong X, Zeng Q, Li W, Zhang X, An F, Wen X, Li P, Chu J, Sun X, Yan C, Yan N, Xie D-Y, Raikhel N, Yang Z, Stepanova AN, Alonso JM, Guo H (2011) A Small-Molecule Screen Identifies l-Kynurenine as a Competitive Inhibitor of TAA1/TAR Activity in Ethylene-Directed Auxin Biosynthesis and Root Growth in *Arabidopsis*. The Plant Cell Online **23:** 3944-3960

Helmlinger J, Rausch T, Hilgenberg W (1985) Metabolism of 14C-Indole-3-Acetaldoxime by Hypocotyls of Chinese Cabbage. Phytochemistry **24:** 2497-2502

Hermes JD, Tipton PA, Fisher MA, O'Leary M, Morrison J, Cleland W (1984) Mechanisms of Enzymatic and Acid-Catalyzed Decarboxylations of Prephenate. Biochemistry **23:** 6263-6275

Herrmann KM, Weaver LM (1999) The Shikimate Pathway. Annual review of plant biology **50:** 473-503

Higuchi M, Pischke MS, Mähönen AP, Miyawaki K, Hashimoto Y, Seki M, Kobayashi M, Shinozaki K, Kato T, Tabata S, Helariutta Y, Sussman MR, Kakimoto T (2004) *In planta* Functions of the *Arabidopsis* Cytokinin Receptor Family. Proceedings of the National Academy of Sciences of the United States of America **101:** 8821-8826

Hou X, Liu S, Pierri F, Dai X, Qu L-J, Zhao Y (2011) Allelic Analyses of the *Arabidopsis YUC1* Locus Reveal Residues and Domains Essential for the Functions of YUC Family of Flavin Monooxygenases. Journal of Integrative Plant Biology **53:** 54-62

Huang J, Yue J, Hu X (2014) Origin of Plant Auxin Biosynthesis in Charophyte Algae: a Reply to Wang et al. Trends in plant science **19:** 743

Hull AK, Vij R, Celenza JL (2000) *Arabidopsis* Cytochrome P450s that Catalyze the First Step of Tryptophan-Dependent Indole-3-Acetic Acid Biosynthesis. Proceedings of the National Academy of Sciences **97:** 2379-2384

Hwang BK, Lim SW, Kim BS, Lee JY, Moon SS (2001) Isolation and *in vivo* and *in vitro* Antifungal Activity of Phenylacetic Acid and Sodium Phenylacetate from *Streptomyces humidus*. Applied and environmental microbiology **67:** 3739-3745

Inoue T, Higuchi M, Hashimoto Y, Seki M, Kobayashi M, Kato T, Tabata S, Shinozaki K, Kakimoto T (2001) Identification of CRE1 as a Cytokinin Receptor from *Arabidopsis*. Nature **409:** 1060-1063

Itoh H, Matsuoka M, Steber CM (2003) A Role for the Ubiquitin–26S-Proteasome Pathway in Gibberellin Signaling. Trends in plant science **8:** 492-497

Jackson RG, Kowalczyk M, Li Y, Higgins G, Ross J, Sandberg G, Bowles DJ (2002) Over‐Expression of an *Arabidopsis* Gene Encoding a Glucosyltransferase of Indole‐3‐Acetic Acid: Phenotypic Characterisation of Transgenic Lines. The Plant Journal **32:** 573-583

Jackson RG, Lim E-K, Li Y, Kowalczyk M, Sandberg G, Hoggett J, Ashford DA, Bowles DJ (2001) Identification and Biochemical Characterization of an *Arabidopsis* Indole-3-Acetic Acid Glucosyltransferase. Journal of Biological Chemistry **276:** 4350-4356

Jayaswal RK, Johri MM (1985) Occurrence and Biosynthesis of Auxin in Protonema of the Moss *Funaria hygrometrica*. Phytochemistry **24:** 1211-1214

Jensen RA, Gu W (1996) Evolutionary Recruitment of Biochemically Specialized Subdivisions of Family I Within the Protein Superfamily of Aminotransferases. Journal of bacteriology **178:** 2161

Jin S-H, Ma X-M, Han P, Wang B, Sun Y-G, Zhang G-Z, Li Y-J, Hou B-K (2013) UGT74D1 Is a Novel Auxin Glycosyltransferase from *Arabidopsis thaliana*. PLOS ONE **8:** e61705

Jones DT, Taylor WR, Thornton JM (1992) The Rapid Generation of Mutation Data Matrices from Protein Sequences. Computer applications in the biosciences: CABIOS **8:** 275-282

Jones PR, Manabe T, Awazuhara M, Saito K (2003) A New Member of Plant CS-lyases: A Cystine Lyase from *Arabidopsis thaliana*. Journal of Biological Chemistry **278:** 10291-10296

Kai K, Horita J, Wakasa K, Miyagawa H (2007) Three Oxidative Metabolites of Indole-3-Acetic Acid from *Arabidopsis thaliana*. Phytochemistry **68:** 1651-1663

Karol KG, McCourt RM, Cimino MT, Delwiche CF (2001) The Closest Living Relatives of Land Plants. Science **294:** 2351-2353

Kepinski S, Leyser O (2005) The *Arabidopsis* F-Box Protein TIR1 is an Auxin Receptor. Nature **435:** 446-451

Kieber JJ, Rothenberg M, Roman G, Feldmann KA, Ecker JR (1993) *CTR1*, a Negative Regulator of the Ethylene Response Pathway in *Arabidopsis*, Encodes a Member of the Raf Family of Protein Kinases. Cell **72:** 427-441

Kilpatrick K, Pajak A, Hagel JM, Sumarah MW, Lewinsohn E, Facchini PJ, Marsolais F (2016) Characterization of Aromatic Aminotransferases from *Ephedra sinica* Stapf. Amino acids **48:** 1209-1220

Kim Y, Cho J-Y, Kuk J-H, Moon J-H, Cho J-I, Kim Y-C, Park K-H (2004) Identification and Antimicrobial Activity of Phenylacetic Acid Produced by *Bacillus licheniformis* Isolated from Fermented Soybean, Chungkook-Jang. Current microbiology **48:** 312-317

Kishore G, Sugumaran M, Vaidyanathan CS (1976) Metabolism of DL-(+/-)-Phenylalanine by *Aspergillus niger*. Journal of Bacteriology **128:** 182-191

Korasick DA, Enders TA, Strader LC (2013) Auxin Biosynthesis and Storage Forms. Journal of Experimental Botany

Koshiba T, Saito E, Ono N, Yamamoto N, Sato M (1996) Purification and Properties of Flavin- and Molybdenum-Containing Aldehyde Oxidase from Coleoptiles of Maize. Plant Physiology **110:** 781-789

Krings U, Hinz M, Berger RG (1996) Degradation of [2 H] Phenylalanine by the Basidiomycete *Ischnoderma benzoinum*. Journal of biotechnology **51:** 123-129

Kuettner EB, Hilgenfeld R, Weiss MS (2002) Purification, Characterization, and Crystallization of Alliinase from Garlic. Archives of Biochemistry and Biophysics **402:** 192-200

Last RL, Fink GR (1988) Tryptophan-requiring mutants of the plant *Arabidopsis thaliana*. Science **240:** 305-310

Lau S, Shao N, Bock R, Jürgens G, De Smet I (2009) Auxin Signaling in Algal Lineages: Fact or Myth? Trends in plant science **14:** 182-188

Le Bail A, Billoud B, Kowalczyk N, Kowalczyk M, Gicquel M, Le Panse S, Stewart S, Scornet D, Cock JM, Ljung K, Charrier B (2010) Auxin Metabolism and Function in the Multicellular Brown Alga *Ectocarpus siliculosus*. Plant Physiology **153:** 128-144

Le SQ, Gascuel O (2008) An Improved General Amino Acid Replacement Matrix. Molecular biology and evolution **25:** 1307-1320

LeClere S, Schmelz EA, Chourey PS (2010) Sugar Levels Regulate Tryptophan-Dependent Auxin Biosynthesis in Developing Maize Kernels. Plant Physiology **153:** 306-318

LeClere S, Tellez R, Rampey RA, Matsuda SPT, Bartel B (2002) Characterization of a Family of IAA-Amino Acid Conjugate Hydrolases from *Arabidopsis*. Journal of Biological Chemistry **277:** 20446-20452

Lee A, Stewart JD, Clardy J, Ganem B (1995) New Insight into the Catalytic Mechanism of Chorismate Mutases from Structural Studies. Chemistry & biology **2:** 195-203

Lee E-J, Facchini PJ (2011) Tyrosine Aminotransferase Contributes to Benzylisoquinoline Alkaloid Biosynthesis in Opium Poppy. Plant physiology **157:** 1067-1078

Lehmann T, Hoffmann M, Hentrich M, Pollmann S (2010) Indole-3-Acetamide-Dependent Auxin Biosynthesis: A Widely Distributed way of Indole-3-Acetic Acid Production? European journal of cell biology **89:** 895-905

Li Y, Baldauf S, Lim E-K, Bowles DJ (2001) Phylogenetic Analysis of the UDP-glycosyltransferase Multigene Family of *Arabidopsis thaliana*. Journal of Biological Chemistry **276:** 4338-4343

Liepman AH, Olsen LJ (2004) Genomic Analysis of Aminotransferases in *Arabidopsis thaliana*. Critical Reviews in Plant Sciences **23:** 73-89

Lim E-K, Doucet CJ, Li Y, Elias L, Worrall D, Spencer SP, Ross J, Bowles DJ (2002) The Activity of *Arabidopsis* Glycosyltransferases toward Salicylic Acid, 4-Hydroxybenzoic Acid, and Other Benzoates. Journal of Biological Chemistry **277:** 586-592

Liu H, Xie WF, Zhang L, Valpuesta V, Ye ZW, Gao QH, Duan K (2014) Auxin Biosynthesis by the *YUCCA6* Flavin Monooxygenase Gene in Woodland Strawberry. Journal of integrative plant biology **56:** 350-363

Liu H, Ying Y-Y, Zhang L, Gao Q-H, Li J, Zhang Z, Fang J-G, Duan K (2012) Isolation and Characterization of two *YUCCA* Flavin Monooxygenase Genes from Cultivated Strawberry (*Fragaria* × *ananassa* Duch.). Plant cell reports **31:** 1425-1435

Ljung K, Hull AK, Kowalczyk M, Marchant A, Celenza J, Cohen JD, Sandberg G (2002) Biosynthesis, Conjugation, Catabolism and Homeostasis of Indole-3-acetic acid in *Arabidopsis thaliana*. *In* Auxin Molecular Biology. Springer, pp 249-272

Lopukhina A, Dettenberg M, Weiler EW, Holländer-Czytko H (2001) Cloning and Characterization of a Coronatine-Regulated Tyrosine Aminotransferase from *Arabidopsis*. Plant physiology **126:** 1678-1687

Ludwig-Müller J (2011) Auxin Conjugates: Their Role for Plant Development and in the Evolution of Land Plants. Journal of Experimental Botany **62:** 1757-1773

Ludwig-Müller J, Cohen JD (2002) Identification and Quantification of Three Active Auxins in Different Tissues of *Tropaeolum majus*. Physiologia Plantarum **115:** 320-329

Ludwig-Müller J, Hilgenberg W (1990) Conversion of Indole-3-Acetaldoxime to Indole-3-Acetonitrile by Plasma Membranes from Chinese Cabbage. Physiologia Plantarum **79:** 311-318

Ludwig-Müller J, Jülke S, Bierfreund NM, Decker EL, Reski R (2009) Moss (*Physcomitrella patens*) GH3 Proteins Act in Auxin Homeostasis. New Phytologist **181:** 323-338

Maeda H, Shasany AK, Schnepp J, Orlova I, Taguchi G, Cooper BR, Rhodes D, Pichersky E, Dudareva N (2010) RNAi Suppression of *Arogenate Dehydratase1* Reveals that Phenylalanine is Synthesized Predominantly via the Arogenate Pathway in Petunia Petals. The Plant Cell Online **22:** 832-849

Maeda H, Yoo H, Dudareva N (2011) Prephenate Aminotransferase Directs Plant Phenylalanine Biosynthesis via Arogenate. Nature Chemical Biology **7:** 19-21

Manela N, Oliva M, Ovadia R, Sikron-Persi N, Ayenew B, Fait A, Galili G, Perl A, Weiss D, Oren-Shamir M (2015) Phenylalanine and Tyrosine Levels are Rate-limiting Factors in Production of Health Promoting Metabolites in *Vitis vinifera* cv. Gamay Red Cell Suspension. Frontiers in Plant Science **6**

Mano Y, Nemoto K (2012) The Pathway of Auxin Biosynthesis in Plants. Journal of Experimental Botany **63:** 2853-2872

Marchler-Bauer A, Derbyshire MK, Gonzales NR, Lu S, Chitsaz F, Geer LY, Geer RC, He J, Gwadz M, Hurwitz DI (2014) CDD: NCBI's Conserved Domain Database. Nucleic acids research**:** gku1221

Mashiguchi K, Tanaka K, Sakai T, Sugawara S, Kawaide H, Natsume M, Hanada A, Yaeno T, Shirasu K, Yao H (2011) The Main Auxin Biosynthesis Pathway in *Arabidopsis*. Proceedings of the National Academy of Sciences **108:** 18512-18517

McAdam EL, Meitzel T, Quittenden LJ, Davidson SE, Dalmais M, Bendahmane AI, Thompson R, Smith JJ, Nichols DS, Urquhart S (2017a) Evidence that Auxin is Required for Normal Seed Size and Starch Synthesis in Pea. New Phytologist **216:** 193-204

McAdam SA, Eléouët MP, Best M, Brodribb TJ, Murphy MC, Cook SD, Dalmais M, Dimitriou T, Gélinas-Marion A, Gill WM (2017b) Linking Auxin with Photosynthetic Rate via Leaf Venation. Plant Physiology **175:** 351-360

McClure BA, Guilfoyle T (1987) Characterization of a Class of Small Auxin-Inducible Soybean Polyadenylated RNAs. Plant molecular biology **9:** 611-623

McGinnis KM, Thomas SG, Soule JD, Strader LC, Zale JM, Sun T-p, Steber CM (2003) The *Arabidopsis SLEEPY1* Gene Encodes a Putative F-box Subunit of an SCF E3 Ubiquitin Ligase. The Plant Cell **15:** 1120-1130

McGowan RE, Muir RM (1971) Purification and Properties of Amine Oxidase from Epicotyls of *Pisum sativum*. Plant Physiology **47:** 644-648

Mellor N, Band LR, Pěnčík A, Novák O, Rashed A, Holman T, Wilson MH, Voß U, Bishopp A, King JR (2016) Dynamic Regulation of Auxin Oxidase and Conjugating Enzymes *AtDAO1* and *GH3* Modulates Auxin Homeostasis. Proceedings of the National Academy of Sciences**:** 201604458

Meßner B, Thulke O, Schäffner AR (2003) *Arabidopsis* Glucosyltransferases with Activities Toward both Endogenous and Xenobiotic Substrates. Planta **217:** 138-146

Michalczuk L, Ribnicky DM, Cooke TJ, Cohen JD (1992) Regulation of Indole-3-Acetic Acid Biosynthetic Pathways in Carrot Cell Cultures. Plant Physiology **100:** 1346-1353

Mikkelsen MD, Hansen CH, Wittstock U, Halkier BA (2000) Cytochrome P450 CYP79B2 from *Arabidopsis* Catalyzes the Conversion of Tryptophan to Indole-3-acetaldoxime, a Precursor of Indole Glucosinolates and Indole-3-Acetic Acid. Journal of Biological Chemistry **275:** 33712-33717

Mikkelsen MD, Naur P, Halkier BA (2004) *Arabidopsis* Mutants in the C–S Lyase of Glucosinolate Biosynthesis Establish a Critical Role for Indole-3-Acetaldoxime in Auxin Homeostasis. The Plant Journal **37:** 770-777

Milborrow BV, Purse JG, Wightman F (1975) On the Auxin Activity of Phenylacetic Acid. Annals of Botany **39:** 1143-1146

Miyata S, Suzuki Y, Kamisaka S, Masuda Y (1981) Indole-3-Acetaldehyde Oxidase of Pea Seedlings. Physiologia Plantarum **51:** 402-406

Murray MG, Thompson WF (1980) Rapid Isolation of High Molecular Weight Plant DNA. Nucleic acids research **8:** 4321-4326

Nafisi M, Goregaoker S, Botanga CJ, Glawischnig E, Olsen CE, Halkier BA, Glazebrook J (2007) *Arabidopsis* Cytochrome P450 Monooxygenase 71A13 Catalyzes the Conversion of Indole-3-Acetaldoxime in Camalexin Synthesis. The Plant Cell Online **19:** 2039-2052

Nakazawa M, Yabe N, Ichikawa T, Yamamoto YY, Yoshizumi T, Hasunuma K, Matsui M (2001) *DFL1*, an Auxin‐Responsive *GH3* Gene Homologue, Negatively Regulates Shoot Cell Elongation and

Lateral Root Formation, and Positively Regulates the Light Response of Hypocotyl Length. The Plant Journal **25:** 213-221

Nemhauser JL, Feldman LJ, Zambryski PC (2000) Auxin and *ETTIN* in *Arabidopsis* Gynoecium Morphogenesis. Development **127:** 3877-3888

Nonhebel HM (2015) Tryptophan-Independent IAA Synthesis: Critical Evaluation of the Evidence. Plant Physiology**:** pp. 01091.02015

Normanly J, Cohen JD, Fink GR (1993) *Arabidopsis thaliana* Auxotrophs Reveal a Tryptophan-Independent Biosynthetic Pathway for Indole-3-Acetic Acid. Proceedings of the National Academy of Sciences **90:** 10355-10359

Normanly J, Grisafi P, Fink GR, Bartel B (1997) *Arabidopsis* Mutants Resistant to the Auxin Effects of Indole-3-Acetonitrile are Defective in the Nitrilase Encoded by the *NIT1* Gene. The Plant Cell Online **9:** 1781-1790

Novák O, Hényková E, Sairanen I, Kowalczyk M, Pospíšil T, Ljung K (2012) Tissue-Specific Profiling of the *Arabidopsis thaliana* Auxin Metabolome. The Plant Journal **72:** 523-536

Okrent RA, Brooks MD, Wildermuth MC (2009) *Arabidopsis* GH3. 12 (PBS3) Conjugates Amino Acids to 4-Substituted Benzoates and is Inhibited by Salicylate. Journal of Biological Chemistry **284:** 9742-9754

Okushima Y, Overvoorde PJ, Arima K, Alonso JM, Chan A, Chang C, Ecker JR, Hughes B, Lui A, Nguyen D (2005) Functional Genomic Analysis of the *AUXIN RESPONSE FACTOR* Gene Family Members in *Arabidopsis thaliana*: Unique and Overlapping Functions of *ARF7* and *ARF19*. The Plant Cell **17:** 444-463

Östin A, Kowalyczk M, Bhalerao RP, Sandberg G (1998) Metabolism of Indole-3-Acetic Acid in *Arabidopsis*. Plant Physiology **118:** 285-296

Ouyang J, Shao X, Li J (2000) Indole-3-Glycerol Phosphate, a Branchpoint of Indole-3-Acetic Acid Biosynthesis from the Tryptophan Biosynthetic Pathway in *Arabidopsis thaliana*. The Plant Journal **24:** 327-334

Ozga JA, Yu J, Reinecke DM (2003) Pollination-, Development-, and Auxin-Specific Regulation of Gibberellin 3β-Jydroxylase Gene Expression in Pea Fruit and Seeds. Plant physiology **131:** 1137-1146

Paradis E, Claude J, Strimmer K (2004) APE: Analyses of Phylogenetics and Evolution in R Language. Bioinformatics **20:** 289-290

Parry G, Ward S, Cernac A, Dharmasiri S, Estelle M (2006) The *Arabidopsis* SUPPRESSOR OF AUXIN RESISTANCE Proteins are Nucleoporins with an Important Role in Hormone Signaling and Development. The Plant Cell **18:** 1590-1603

Peat TS, Böttcher C, Newman J, Lucent D, Cowieson N, Davies C (2012) Crystal Structure of an Indole-3-Acetic Acid Amido Synthetase from Grapevine Involved in Auxin Homeostasis. The Plant Cell Online **24:** 4525-4538

Peer WA, Blakeslee JJ, Yang H, Murphy AS (2011) Seven Things we Think we Know About Auxin Transport. Molecular Plant **4:** 487-504

Pěnčík A, Simonovik B, Petersson SV, Henyková E, Simon S, Greenham K, Zhang Y, Kowalczyk M, Estelle M, Zažímalová E, Novák O, Sandberg G, Ljung K (2013) Regulation of Auxin Homeostasis and Gradients in *Arabidopsis* Roots through the Formation of the Indole-3-Acetic Acid Catabolite 2-Oxindole-3-Acetic Acid. The Plant Cell Online

Petroski MD, Deshaies RJ (2005) Function and Regulation of Cullin–RING Ubiquitin Ligases. Nature reviews Molecular cell biology **6:** 9-20

Phillips KA, Skirpan AL, Liu X, Christensen A, Slewinski TL, Hudson C, Barazesh S, Cohen JD, Malcomber S, McSteen P (2011) *vanishing tassel2* Encodes a Grass-Specific Tryptophan Aminotransferase Required for Vegetative and Reproductive Development in Maize. The Plant Cell Online **23:** 550-566

Piotrowska-Niczyporuk A, Bajguz A (2014) The Effect of Natural and Synthetic Auxins on the Growth, Metabolite Content and Antioxidant Response of Green Alga *Chlorella vulgaris* (Trebouxiophyceae). Plant Growth Regulation **73:** 57-66

Pollmann S, Düchting P, Weiler EW (2009) Tryptophan-Dependent Indole-3-Acetic Acid Biosynthesis by 'IAA-Synthase' Proceeds via Indole-3-Acetamide. Phytochemistry **70:** 523-531

Pollmann S, Müller A, Piotrowski M, Weiler EW (2002) Occurrence and Formation of Indole-3-Acetamide in *Arabidopsis thaliana*. Planta **216:** 155-161

Pollmann S, Neu D, Lehmann T, Berkowitz O, Schäfer T, Weiler EW (2006) Subcellular Localization and Tissue Specific Expression of *amidase 1* from *Arabidopsis thaliana*. Planta **224:** 1241-1253

Pollmann S, Neu D, Weiler EW (2003) Molecular Cloning and Characterization of an Amidase From *Arabidopsis thaliana* Capable of Converting Indole-3-Acetamide Into the Plant Growth Hormone, Indole-3-Acetic Acid. Phytochemistry **62:** 293-300

Porco S, Pěnčík A, Rashed A, Voß U, Casanova-Sáez R, Bishopp A, Golebiowska A, Bhosale R, Swarup R, Swarup K (2016) Dioxygenase-Encoding *AtDAO1* Gene Controls IAA Oxidation and Homeostasis in *Arabidopsis*. Proceedings of the National Academy of Sciences **113:** 11016-11021

Potuschak T, Lechner E, Parmentier Y, Yanagisawa S, Grava S, Koncz C, Genschik P (2003) EIN3-Dependent Regulation of Plant Ethylene Hormone Signaling by Two *Arabidopsis* F box Proteins: EBF1 and EBF2. Cell **115:** 679-689

Prabhu PR, Hudson AO (2010) Identification and Partial Characterization of an L-Tyrosine Aminotransferase (TAT) from *Arabidopsis thaliana*. Biochemistry research international **2010**

Pybus MB, Wain R, Wightman F (1959) Studies on Plant Growth-Regulating Substances XIV. Chloro-Substituted Phenylacetic Acids. Annals of Applied Biology **47:** 593-599

Qin G, Gu H, Zhao Y, Ma Z, Shi G, Yang Y, Pichersky E, Chen H, Liu M, Chen Z (2005) An Indole-3-Acetic Acid Carboxyl Methyltransferase Regulates *Arabidopsis* Leaf Development. The Plant Cell **17:** 2693-2704

Quint M, Gray WM (2006) Auxin Signaling. Current opinion in plant biology **9:** 448-453

Quittenden L (2011) Auxin Biosynthesis in *Pisum sativum*: A Physico-Chemical Perspective. University of Tasmania

Quittenden LJ, Davies NW, Smith JA, Molesworth PP, Tivendale ND, Ross JJ (2009) Auxin Biosynthesis in Pea: Characterization of the Tryptamine Pathway. Plant Physiology **151:** 1130-1138

Rajagopal R, Larsen P (1972) Metabolism of Indole-3-Acetaldoxime in Plants. Planta **103:** 45-54

Rampey RA, LeClere S, Kowalczyk M, Ljung K, Sandberg G, Bartel B (2004) A Family of Auxin-Conjugate Hydrolases That Contributes to Free Indole-3-Acetic Acid Levels During *Arabidopsis* Germination. Plant Physiology **135:** 978-988

Rao-Naik C, Laplaza JM, Tan S, Callis J, Fisher AJ (1998) The Rub Family of Ubiquitin-like Proteins: Crystal Structure of *Arabidopsis* RUB1 and Expression of Multiple RUBs in *Arabidopsis* Journal of Biological Chemistry **273:** 34976-34982

Rapparini F, Cohen JD, Slovin JP (1999) Indole-3-Acetic Acid Biosynthesis in *Lemna gibba* Studied Using Stable Isotope Labeled Anthranilate and Tryptophan. Plant Growth Regulation **27:** 139-144

Ray PM (1958) Destruction of Auxin. Annual Review of Plant Physiology **9:** 81-118

Reineke G, Heinze B, Schirawski J, Buettner H, Kahmann R, Basse CW (2008) Indole‐3‐Acetic Acid (IAA) Biosynthesis in the Smut Fungus *Ustilago maydis* and its Relevance for Increased IAA Levels in Infected Tissue and Host Tumour Formation. Molecular plant pathology **9:** 339-355

Riewe D, Koohi M, Lisec J, Pfeiffer M, Lippmann R, Schmeichel J, Willmitzer L, Altmann T (2012) A Tyrosine Aminotransferase Involved in Tocopherol Synthesis in *Arabidopsis*. The Plant Journal **71:** 850-859

Rosas U, Cibrian-Jaramillo A, Ristova D, Banta JA, Gifford ML, Fan AH, Zhou RW, Kim GJ, Krouk G, Birnbaum KD (2013) Integration of Responses Within and Across *Arabidopsis* Natural Accessions Uncovers Loci Controlling Root Systems Architecture. Proceedings of the National Academy of Sciences **110:** 15133-15138

Ruegger M, Dewey E, Gray WM, Hobbie L, Turner J, Estelle M (1998) The TIR1 Protein of *Arabidopsis* Functions in Auxin Response and is Related to Human SKP2 and Yeast Grr1p. Genes & Development **12:** 198-207

Schliep KP (2011) Phangorn: Phylogenetic Analysis in R. Bioinformatics **27:** 592-593

Schmidt R-C, Müller A, Hain R, Bartling D, Weiler EW (1996) Transgenic Tobacco Plants Expressing the *Arabidopsis thaliana* Nitrilase II Enzyme. The Plant Journal **9:** 683-691

Schneider EA, Kazakoff CW, Wightman F (1985) Gas Chromatography-Mass Spectrometry Evidence for Several Endogenous Auxins in Pea Seedling Organs. Planta **165:** 232-241

Schneider EA, Wightman F (1986) Auxins of Non-Flowering Plants. I. Occurrence of 3-Indoleacetic Acid and Phenylacetic Acid in Vegetative

and Fertile Fronds of the Ostrich Fern (*Matteucia struthiopteris*). Physiologia Plantarum **68:** 396-402

Schomburg FM, Bizzell CM, Lee DJ, Zeevaart JAD, Amasino RM (2003) Overexpression of a Novel Class of Gibberellin 2-Oxidases Decreases Gibberellin Levels and Creates Dwarf Plants. The Plant Cell **15:** 151-163

Sekhon RS, Lin H, Childs KL, Hansey CN, Buell CR, de Leon N, Kaeppler SM (2011) Genome‐Wide Atlas of Transcription During Maize Development. The Plant Journal **66:** 553-563

Sekimoto H, Seo M, Kawakami N, Komano T, Desloire S, Liotenberg S, Marion-Poll A, Caboche M, Kamiya Y, Koshiba T (1998) Molecular Cloning and Characterization of Aldehyde Oxidases in *Arabidopsis thaliana*. Plant and Cell Physiology **39:** 433-442

Seo M, Akaba S, Oritani T, Delarue M, Bellini C, Caboche M, Koshiba T (1998) Higher Activity of an Aldehyde Oxidase in the Auxin-Overproducing *superroot1* Mutant of *Arabidopsis thaliana*. Plant Physiology **116:** 687-693

Seo M, Peeters AJM, Koiwai H, Oritani T, Marion-Poll A, Zeevaart JAD, Koornneef M, Kamiya Y, Koshiba T (2000) The *Arabidopsis* Aldehyde Oxidase 3 (*AAO3*) Gene Product Catalyzes the Final Step in Abscisic Acid Biosynthesis in Leaves. Proceedings of the National Academy of Sciences **97:** 12908-12913

Siehl DL, Connelly JA, Conn EE (1986) Tyrosine Biosynthesis in *Sorghum bicolor*: Characteristics of Prephenate Aminotransferase. Z. Naturforsch **41:** 79-86

Sievers F, Wilm A, Dineen D, Gibson TJ, Karplus K, Li W, Lopez R, McWilliam H, Remmert M, Söding J (2011) Fast, Scalable Generation of High‐Quality Protein Multiple Sequence Alignments Using Clustal Omega. Molecular systems biology **7:** 539

Somers E, Ptacek D, Gysegom P, Srinivasan M, Vanderleyden J (2005) *Azospirillum brasilense* Produces the Auxin-Like Phenylacetic Acid by Using the Key Enzyme for Indole-3-Acetic Acid Biosynthesis. Applied and Environmental Microbiology **71:** 1803-1810

Songstad DD, De Luca V, Brisson N, Kurz WGW, Nessler CL (1990) High Levels of Tryptamine Accumulation in Transgenic Tobacco Expressing Tryptophan Decarboxylase. Plant physiology **94:** 1410-1413

Spaepen S, Vanderleyden J, Remans R (2007) Indole-3-Acetic Acid in Microbial and Microorganism-Plant Signaling. FEMS Microbiology Reviews **31:** 425-448

Spaepen S, Versées W, Gocke D, Pohl M, Steyaert J, Vanderleyden J (2007) Characterization of Phenylpyruvate Decarboxylase, Involved in Auxin Production of *Azospirillum brasilense*. Journal of Bacteriology **189:** 7626-7633

Spartz AK, Lee SH, Wenger JP, Gonzalez N, Itoh H, Inzé D, Peer WA, Murphy AS, Overvoorde PJ, Gray WM (2012) The *SAUR19* Subfamily of *SMALL AUXIN UP RNA* Genes Promote Cell Expansion. The Plant Journal **70:** 978-990

Stafford HA, Lewis LL (1979) Conversion of L-and D-Phenylalanine to Phenylacetate via Phenylpyruvate in Sorghum Leaf Extracts. Plant physiology **64:** 176-181

Staswick PE, Serban B, Rowe M, Tiryaki I, Maldonado MT, Maldonado MC, Suza W (2005) Characterization of an *Arabidopsis* Enzyme Family That Conjugates Amino Acids to Indole-3-Acetic Acid. The Plant Cell **17:** 616-627

Staswick PE, Tiryaki I (2004) The Oxylipin Signal Jasmonic Acid is Activated by an Enzyme That Conjugates it to Isoleucine in *Arabidopsis*. The Plant Cell **16:** 2117-2127

Staswick PE, Tiryaki I, Rowe ML (2002) Jasmonate Response Locus *JAR1* and Several Related *Arabidopsis* Genes Encode Enzymes of the Firefly Luciferase Superfamily That Show Activity on Jasmonic, Salicylic, and Indole-3-Acetic Acids in an Assay for Adenylation. The Plant Cell **14:** 1405-1415

Stepanova AN, Alonso JM (2016) Auxin Catabolism Unplugged: Role of IAA Oxidation in Auxin Homeostasis. Proceedings of the National Academy of Sciences**:** 201613506

Stepanova AN, Robertson-Hoyt J, Yun J, Benavente LM, Xie D-Y, Dolezal K, Schlereth A, Jurgens G, Alonso JM (2008) TAA1-Mediated Auxin Biosynthesis Is Essential for Hormone Crosstalk and Plant Development. Cell **133:** 177-191

Stepanova AN, Yun J, Robles LM, Novak O, He W, Guo H, Ljung K, Alonso JM (2011) The *Arabidopsis YUCCA1* Flavin Monooxygenase Functions in the Indole-3-Pyruvic Acid Branch of Auxin Biosynthesis. The Plant Cell Online **23:** 3961-3973

Strader LC, Bartel B (2008) A New Path to Auxin. Nature Chemical Biology **4:** 337-339

Strader LC, Ritchie S, Soule JD, McGinnis KM, Steber CM (2004) Recessive-Interfering Mutations in the Gibberellin Signaling Gene *SLEEPY1* are Rescued by Overexpression of its Homologue, *SNEEZY*. Proceedings of the National Academy of Sciences of the United States of America **101:** 12771-12776

Sugawara S, Hishiyama S, Jikumaru Y, Hanada A, Nishimura T, Koshiba T, Zhao Y, Kamiya Y, Kasahara H (2009) Biochemical Analyses of Indole-3-Acetaldoxime-Dependent Auxin Biosynthesis in *Arabidopsis*. Proceedings of the National Academy of Sciences **106:** 5430-5435

Sugawara S, Mashiguchi K, Tanaka K, Hishiyama S, Sakai T, Hanada K, Kinoshita-Tsujimura K, Yu H, Dai X, Takebayashi Y (2015) Distinct Characteristics of Indole-3-Acetic Acid and Phenylacetic Acid, Two Common Auxins in Plants. Plant and Cell Physiology **56:** 1641-1654

Symons GM (2000) Mutational Analysis of Auxin Physiology in Pisum *sativum*. University of Tasmania

Symons GM, Murfet IC, Ross JJ, Sherriff LJ, Warkentin TD (1999) *bushy*, a Dominant Pea Mutant Characterised by Short, Thin Stems, Tiny Leaves and a Major Reduction in Apical Dominance. Physiologia Plantarum **107:** 346-352

Symons GM, Ross JJ, Murfet IC (2002) The *bushy* Pea Mutant is IAA-Deficient. Physiologia Plantarum **116:** 389-397

Szerszen JB, Szczyglowski K, Bandurski RS (1994) *iaglu*, a Gene From *Zea mays* Involved in Conjugation of Growth Hormone Indole-3-Acetic Acid. Science **265:** 1699-1701

Sztein AE, Cohen JD, Cooke TJ (2000) Evolutionary Patterns in the Auxin Metabolism of Green Plants. International Journal of Plant Sciences **161:** 849-859

Sztein AE, Cohen JD, de la Fuente IG, Cooke TJ (1999) Auxin Metabolism in Mosses and Liverworts. American Journal of Botany **86:** 1544-1555

Sztein AE, Cohen JD, Slovin JP, Cooke TJ (1995) Auxin Metabolism in Representative Land Plants. American journal of Botany**:** 1514-1521

Sztein AE, Ilić N, Cohen JD, Cooke TJ (2002) Indole-3-Acetic Acid Biosynthesis in Isolated Axes From Germinating Bean Seeds: The

Effect of Wounding on the Biosynthetic Pathway. Plant Growth Regulation **36:** 201-207

Tam YY, Epstein E, Normanly J (2000) Characterization of Auxin Conjugates in *Arabidopsis*. Low Steady-State Levels of Indole-3-Acetyl-Aspartate, Indole-3-Acetyl-Glutamate, and indole-3-Acetyl-Glucose. Plant Physiology **123:** 589-596

Tam YY, Normanly J (1998) Determination of Indole-3-Pyruvic Acid Levels in *Arabidopsis thaliana* by Gas Chromatography–Selected Ion Monitoring-Mass Spectrometry. Journal of Chromatography A **800:** 101-108

Tanaka K, Hayashi K-i, Natsume M, Kamiya Y, Sakakibara H, Kawaide H, Kasahara H (2014) UGT74D1 Catalyzes the Glucosylation of 2-Oxindole-3-Acetic Acid in the Auxin Metabolic Pathway in *Arabidopsis*. Plant and Cell Physiology **55:** 218-228

Tao Y, Ferrer J-L, Ljung K, Pojer F, Hong F, Long JA, Li L, Moreno JE, Bowman ME, Ivans LJ (2008) Rapid Synthesis of Auxin via a New Tryptophan-Dependent Pathway is Required for Shade Avoidance in Plants. Cell **133:** 164-176

Taylor DC, Wightman F (1987) Metabolism of D, L-Chloro-Phenylalanines by Phenylalanine Aminotransferase Isozymes Purified From Bushbean Shoots. Phytochemistry **26:** 1279-1288

Thomas SG, Phillips AL, Hedden P (1999) Molecular Cloning and Functional Expression of Gibberellin 2-Oxidases, Multifunctional Enzymes Involved in Gibberellin Deactivation. Proceedings of the National Academy of Sciences **96:** 4698-4703

Tian Ce, Muto H, Higuchi K, Matamura T, Tatematsu K, Koshiba T, Yamamoto KT (2004) Disruption and Overexpression of *auxin response factor 8* Gene of *Arabidopsis* Affect Hypocotyl Elongation and Root Growth Habit, Indicating its Possible Involvement in Auxin Homeostasis in Light Condition. The Plant Journal **40:** 333-343

Tian Q, Uhlir NJ, Reed JW (2002) *Arabidopsis* SHY2/IAA3 Inhibits Auxin-Regulated Gene Expression. The Plant Cell **14:** 301-319

Tieman D, Taylor M, Schauer N, Fernie AR, Hanson AD, Klee HJ (2006) Tomato Aromatic Amino Acid Decarboxylases Participate in Synthesis of the Flavor Volatiles 2-Phenylethanol and 2-Phenylacetaldehyde. Proceedings of the National Academy of Sciences **103:** 8287-8292

Tivendale ND, Davidson SE, Davies NW, Smith JA, Dalmais M, Bendahmane AI, Quittenden LJ, Sutton L, Bala RK, Le Signor C (2012) Biosynthesis of the Halogenated Auxin, 4-Chloroindole-3-Acetic Acid. Plant physiology **159:** 1055-1063

Tivendale ND, Davies NW, Molesworth PP, Davidson SE, Smith JA, Lowe EK, Reid JB, Ross JJ (2010) Reassessing the Role of N-Hydroxytryptamine in Auxin Biosynthesis. Plant Physiology **154:** 1957-1965

Tivendale ND, Ross JJ, Cohen JD (2014) The Shifting Paradigms of Auxin Biosynthesis. Trends in plant science **19:** 44-51

Tiwari SB, Hagen G, Guilfoyle T (2003) The Roles of *Auxin Response Factor* Domains in Auxin-Responsive Transcription. The Plant Cell **15:** 533-543

Tobeña-Santamaria R, Bliek M, Ljung K, Sandberg G, Mol JNM, Souer E, Koes R (2002) FLOOZY of Petunia is a Flavin Mono-Oxygenase-Like Protein Required for the Specification of Leaf and Flower Architecture. Genes & Development **16:** 753-763

Turnaev II, Gunbin KV, Afonnikov DA (2015) Plant Auxin Biosynthesis Did Not Originate in Charophytes. Trends in plant science **20:** 1-3

Tzin V, Malitsky S, Aharoni A, Galili G (2009) Expression of a Bacterial Bi‐Functional Chorismate Mutase/ Prephenate Dehydratase Modulates Primary and Secondary Metabolism Associated With Aromatic Amino Acids in *Arabidopsis*. The Plant Journal **60:** 156-167

Ueguchi C, Koizumi H, Suzuki T, Mizuno T (2001) Novel Family of Sensor Histidine Kinase Genes in *Arabidopsis thaliana*. Plant and Cell Physiology **42:** 231-235

Ulmasov T, Hagen G, Guilfoyle TJ (1999) Activation and Repression of Transcription by *Auxin-Response Factors*. Proceedings of the National Academy of Sciences **96:** 5844-5849

Ulmasov T, Hagen G, Guilfoyle TJ (1999) Dimerization and DNA Binding of *Auxin Response Factors*. The Plant Journal **19:** 309-319

Urquhart S, Foo E, Reid JB (2015) The Role of Strigolactones in Photomorphogenesis of Pea is Limited to Adventitious Rooting. Physiologia plantarum **153:** 392-402

Wang B, Chu J, Yu T, Xu Q, Sun X, Yuan J, Xiong G, Wang G, Wang Y, Li J (2015) Tryptophan-Independent Auxin Biosynthesis Contributes

to Early Embryogenesis in *Arabidopsis*. Proceedings of the National Academy of Sciences **112:** 4821-4826

Wang C, Li S-S, Han G-Z (2016) Commentary: Plant Auxin Biosynthesis Did not Originate in Charophytes. Frontiers in plant science **7**

Wang C, Liu Y, Li S-S, Han G-Z (2014) Origin of Plant Auxin Biosynthesis in Charophyte Algae. Trends Plant Sci **19:** 741-743

Wang M, Toda K, Maeda HA (2016) Biochemical Properties and Subcellular Localization of Tyrosine Aminotransferases in *Arabidopsis thaliana*. Phytochemistry **132:** 16-25

Weeden N (1998) A consensus Linkage Map for *Pisum sativum*. Pisum genetics **30:** 1-4

Westfall CS, Zubieta C, Herrmann J, Kapp U, Nanao MH, Jez JM (2012) Structural Basis for Prereceptor Modulation of Plant Hormones by GH3 Proteins. Science **336:** 1708-1711

Wickett NJ, Mirarab S, Nguyen N, Warnow T, Carpenter E, Matasci N, Ayyampalayam S, Barker MS, Burleigh JG, Gitzendanner MA (2014) Phylotranscriptomic Analysis of the Origin and Early Diversification of Land Plants. Proceedings of the National Academy of Sciences **111:** E4859-E4868

Wightman F, Lighty DL (1982) Identification of Phenylacetic Acid as a Natural Auxin in the Shoots of Higher Plants. Physiologia plantarum **55:** 17-24

Wightman F, Schneider EA, Thimann KV (1980) Hormonal Factors Controlling the Initiation and Development of Lateral Roots. Physiologia Plantarum **49:** 304-314

Won C, Shen X, Mashiguchi K, Zheng Z, Dai X, Cheng Y, Kasahara H, Kamiya Y, Chory J, Zhao Y (2011) Conversion of Tryptophan to Indole-3-Acetic Acid by TRYPTOPHAN AMINOTRANSFERASES OF ARABIDOPSIS and YUCCAs in *Arabidopsis*. Proceedings of the National Academy of Sciences **108:** 18518-18523

Woodward AW, Bartel B (2005) Auxin: Regulation, Action, and Interaction. Annals of Botany **95:** 707-735

Wright AD, Sampson MB, Neuffer MG, Michalczuk L, Slovin JP, Cohen JD (1991) Indole-3-Acetic Acid Biosynthesis in the Mutant Maize *orange pericarp*, a Tryptophan Auxotroph. Science **254:** 998-1000

Yamada T, Matsuda F, Kasai K, Fukuoka S, Kitamura K, Tozawa Y, Miyagawa H, Wakasa K (2008) Mutation of a Rice Gene Encoding a Phenylalanine Biosynthetic Enzyme Results in Accumulation of Phenylalanine and Tryptophan. The Plant Cell Online **20:** 1316-1329

Yokoya NS, Stirk WA, Van Staden J, Novák O, Turečková V, Strnad M (2010) Endogenous Cytokinina, Auxins, and Abscisic Acid in Red Algae From Brazil. Journal of Phycology **46:** 1198-1205

Yoo H, Widhalm JR, Qian Y, Maeda H, Cooper BR, Jannasch AS, Gonda I, Lewinsohn E, Rhodes D, Dudareva N (2013) An Alternative Pathway Contributes to Phenylalanine Biosynthesis in Plants via a Cytosolic Tyrosine: Phenylpyruvate Aminotransferase. Nature communications **4**

Yue J, Hu X, Huang J (2014) Origin of Plant Auxin Biosynthesis. Trends in Plant Science

Zažímalová E, Murphy AS, Yang H, Hoyerová K, Hošek P (2010) Auxin Transporters—Why So Many? Cold Spring Harbor perspectives in biology **2:** a001552

Zdunek-Zastocka E, Omarov RT, Koshiba T, Lips HS (2004) Activity and Protein Level of AO Isoforms in Pea Plants (*Pisum sativum* L.) During Vegetative Development and in Response to Stress Conditions. Journal of Experimental Botany **55:** 1361-1369

Zhang J, Lin JE, Harris C, Pereira FCM, Wu F, Blakeslee JJ, Peer WA (2016) DAO1 Catalyzes Temporal and Tissue-Specific Oxidative Inactivation of Auxin in *Arabidopsis thaliana*. Proceedings of the National Academy of Sciences**:** 201604769

Zhang S-W, Li C-H, Cao J, Zhang Y-C, Zhang S-Q, Xia Y-F, Sun D-Y, Sun Y (2009) Altered Architecture and Enhanced Drought Tolerance in Rice via the Down-Regulation of Indole-3-Acetic Acid by *TLD1/OsGH3.13* Activation. Plant physiology **151:** 1889-1901

Zhao N, Ferrer J-L, Ross J, Guan J, Yang Y, Pichersky E, Noel JP, Chen F (2008) Structural, Biochemical, and Phylogenetic Analyses Suggest That Indole-3-Acetic Acid Methyltransferase Is an Evolutionarily Ancient Member of the SABATH Family. Plant Physiology **146:** 455-467

Zhao Y (2010) Auxin Biosynthesis and its Role in Plant Development. Annual review of plant biology **61:** 49

Zhao Y (2012) Auxin biosynthesis: A Simple Two-Step Pathway Converts Tryptophan to Indole-3-Acetic Acid in Plants. Molecular plant **5:** 334-338

Zhao Y, Christensen SK, Fankhauser C, Cashman JR, Cohen JD, Weigel D, Chory J (2001) A Role for Flavin Monooxygenase-Like Enzymes in Auxin Biosynthesis. Science **291:** 306-309

Zhao Y, Hull AK, Gupta NR, Goss KA, Alonso J, Ecker JR, Normanly J, Chory J, Celenza JL (2002) Trp-Dependent Auxin Biosynthesis in *Arabidopsis*: Involvement of Cytochrome P450s CYP79B2 and CYP79B3. Genes & Development **16:** 3100-3112

Zhao Z, Zhang Y, Liu X, Zhang X, Liu S, Yu X, Ren Y, Zheng X, Zhou K, Jiang L (2013) A Role for a Dioxygenase in Auxin Metabolism and Reproductive Development in Rice. Developmental cell **27:** 113-122

Zheng N, Schulman BA, Song L, Miller JJ, Jeffrey PD, Wang P, Chu C, Koepp DM, Elledge SJ, Pagano M (2002) Structure of the Cul1–Rbx1–Skp1–F boxSkp2 SCF Ubiquitin Ligase Complex. Nature **416:** 703-709

Žižková E, Kubeš M, Dobrev PI, Přibyl P, Šimura J, Zahajská L, Záveská Drábková L, Novák O, Motyka V (2016) Control of Cytokinin and Auxin Homeostasis in Cyanobacteria and Algae. Annals of Botany

Zubieta C, Ross JR, Koscheski P, Yang Y, Pichersky E, Noel JP (2003) Structural Basis for Substrate Recognition in the Salicylic Acid Carboxyl Methyltransferase Family. The Plant Cell **15:** 1704-1716